UNIVERSITÀ DELLA CALABRIA

UNIVERSITA' DELLA CALABRIA

Dipartimento di Biologia, Ecologia e Scienze della Terra

Scuola di Dottorato

"Life Science"

Indirizzo

Biologia Vegetale
Settore strategico Polo di Innovazione regionale:
"Tecnologie per la gestione Sostenibile delle Risorse Ambientali"

Con il contributo di

POR CALABRIA FSE 2007/2013

CICLO XXVI

LEAF PROTEOMICS OF SEAGRASSES UNDER LIGHT CONDITIONS AND SALINITY

Settore Scientifico Disciplinare BIO/01-Area 5

Direttore: Ch.mo Prof. Marcello Canonaco
Firma

Supervisore: Ch.mo Prof.ssa Silvia Mazzuca
Firma

DiBEST UNICAL Dipartimento di Biologia, Ecologia e Scienze della Terra

Dottoranda: Dott.ssa Amalia Piro
Firma

"La presente tesi è cofinanziata con il sostegno della Commissione Europea, Fondo Sociale Europeo e della Regione Calabria. L'autore è il solo responsabile di questa tesi e la Commissione Europea e la Regione Calabria declinano ogni responsabilità sull'uso che potrà essere fatto delle informazioni in essa contenute".

Index

ABSTRACT (Italian)

"Analisi del proteoma foliare delle seagrasses esposte a diversi regimi luminosi e a variazioni di salinità"

Le fanerogame marine, nel nostro studio limitate alle *seagrasses*, si sono adattate per occupare vaste estensioni dei fondi litorali e hanno dovuto sviluppare diversi adattamenti per poter vivere completamente sommerse. Le *seagrasses* non possono crescere in profondità dove non arriva almeno il 10% della luce in superficie, per questo si situano sempre sul piano infralitorale. In acque molto chiare, possono essere presenti fino a 70 m di profondità, però in mari con acque più torbide non superano i 15-20 m. Per tutte queste ragioni, queste formazioni vegetali sommerse rivestono un importante ruolo nella biologia e nella dinamica costiera.
Posidonia oceanica è una specie esclusiva del mar Mediterraneo. Mentre *Cymodocea nodosa* è, dopo *Posidonia oceanica*, la seconda *seagrass* del Mediterraneo per estensione delle sue praterie ed è una specie di origine tropicale, attualmente ambientata nel Mediterraneo e nell'Atlantico nordorientale, dal sud del Portogallo fino al Senegal, includendo le isole Canarie. Rispetto a *P.oceanica* presenta una maggiore tolleranza agli aumenti di salinità. In questo lavoro è stata analizzata l'espressione proteica in *Posidonia oceanica* e *Cymodocea nodosa* sottoposte a diversi regimi luminosi e concentrazioni saline. L'analisi ha riguardato specificamente il proteoma foliare e il sub-proteoma del cloroplasto, attraverso l'estrazione delle proteine, separazione elettroforetica, analisi delle sequenze in spettrometria di massa e identificazione proteica con software bioinformatici.

L'approccio proteomico così strutturato ha consentito di rilevare proteine differenzialmente espresse in popolazioni naturali adattate a tre diverse profondità. I risultati più evidenti riguardano proteine enzimatiche correlate al sistema fotosintetico PSII che risulta maggiormente espresso nelle praterie a 30 m di profondità alle 13:00, ora di massima disponibilità di luce. Altro dato rilevante è l'aumento dell'espressione degli enzimi del pathways metabolici che portano alla biosintesi di ATP, fotosfosforilazione cloroplastica e fosforilazione ossidativa mitocondriale. Sempre alla profondità di 30 m e alle 13:00, risultano overespressi gli enzimi del ciclo di Calvin-Benson rispetto ai livelli riscontrati nelle altre due profondità alla stesso tempo. Risultano invece poco espressi gli enzimi correlati alla glicolisi che raggiungono livelli molto elevati di espressione nel controllo,

ossia alla profondità di 30 m nelle prime ore del mattino; anche le proteine correlate al PSI sono poco espresse in funzione delle profondità e raggiungono il minimo della loro espressione a 30 m nelle ore di massima illuminazione (13:00). Dato interessante e in apparente contraddizione con i dati di espressione dei gruppi funzionali correlati al processo fotosintetico, e la diminuzione dei livelli di espressione degli enzimi della via biosintetica delle clorofilla (a, b) alla profondità di 30 m associabili alla down-regolazione del fotosistema PSI.

L'analisi delle proteine organellari ha consentito di creare un primo catalogo di proteine cloroplastiche di *P. oceanica* attraverso analisi dell'omologia di sequenza di proteine cloroplastiche di *Arabidopsis* e la loro localizzazione nei tre comparti sub-organellari (AT_CHLORO DATABASE). I cloroplasti intatti di *P. oceanica* sono stati ottenuti in accordo con quanto riportato in Rolland *et al.* 2003. Sono state identificate 74 proteine a cui è stata assegnata una diversa localizzazione e un numero di accesso corrispondente al database utilizzato. Il maggior numero di proteine identificate sono localizzate nei tilacoidi e nello stroma, mentre un numero minore di proteine sono localizzate nell'envelope. Inoltre l'8% delle proteine non hanno una esatta localizzazione nei compartimenti del cloroplasto.

Infine è stato analizzato il proteoma foliare di *Cymodocea nodosa* esposta a stress salino in condizioni controllate in mesocosmo, dove la parziale inibizione della fotosintesi, mediante la down-regulation delle proteine e degli enzimi sia del PSII che del PSI, e la ridotta attività respiratoria ottenuta dall'analisi proteomica permette alle piante di adattarsi a questa grave condizione di stress, ma presumibilmente con vitalità ridotta, dal momento che alcune delle risorse interne necessarie per la crescita e il mantenimento della biomassa devono essere riassegnati per far fronte allo stress metabolico. Nei trattamenti ipersalini sia a breve che a lungo termine troviamo gravi alterazioni dei metabolismi primari. Inoltre, i risultati di una bassa espressione della RuBisCo nei campioni ipersalini, in accordo con Beer et al . (1980), suggerisce che in condizioni di stress salino il bilancio del carbonio tende a favorire una maggiore produzione di carbonio inorganico (Ci). Si verifica, poi, un aumento degli enzimi della glicolisi per controbilanciare la richiesta di energia e quindi produrre più molecole di ATP. Anche il metabolismo vacuolare è stato influenzato dal trattamento ipersalino , infatti, l'over-espressione dell'H(+)-PPasi suggerisce che i vacuoli sono coinvolti nel sequestro del Na^+. Questo potrebbe essere quindi il meccanismo

che consente a *C. nodosa* di sopravvivere a condizioni di salinità estremamente variabili e definirla così una specie tollerante.

Introduction

The context

Mediterranean seagrasses form dense monospecific meadows across a wide bathymetric gradient (from shallow subtidal for shallow species and deep species till to 50-60 m depth in areas with very clear waters) (Borum and Greve 2004). *Seagrass* beds have an important ecological roles in costal ecosystem and provide high-value ecosystem services. The large-scale loss of seagrasses that occurred worldwide (29% of the known areal has disappeared, Wycott *et al.*, 2009) had a serious effect on the ecosystem and on associated functions and services in the coastal zone (Duarte *et al.*, 2004). For example the *P. oceanica* loss, like other seagrass ecosystems, have been attributed to a broad spectrum of causes, principally of anthropogenic origin, such as eutrophication, disturbance of sedimentary dynamics and mechanical destruction of the coastal area. Reported seagrass losses have led to increased awareness of the need for seagrass protection, monitoring, management and restoration (Borum *et al.*, 2004; Orth *et al.*, 2006; Larkum *et al.*, 2006a; Boudereseque *et al.*, 2006; Björk *et al.*, 2008). common descriptor for monitoring programme are shoot density, leaf production and rhizome elongation, bathymetric position of the lower and/or upper depth limit, bottom cover, structure of the matte (see Pergent-Martini *et al.*, 2005 for a synthesis), while additional

suggested descriptors include P, N, non-structural carbohydrate content and various trace metals (Casazza *et al.*, 2006). However, these descriptors respond slowly to environmental change and don't detect alterations of the costal water quality before that the effects become evident on the plant and/or on the whole meadow. New tools in monitoring such as genetic analysis could be very important to comprehend the evolutionary potential as well as resilience and resistance capacity under various forms of stress and to guide restoration initiatives of destructed .

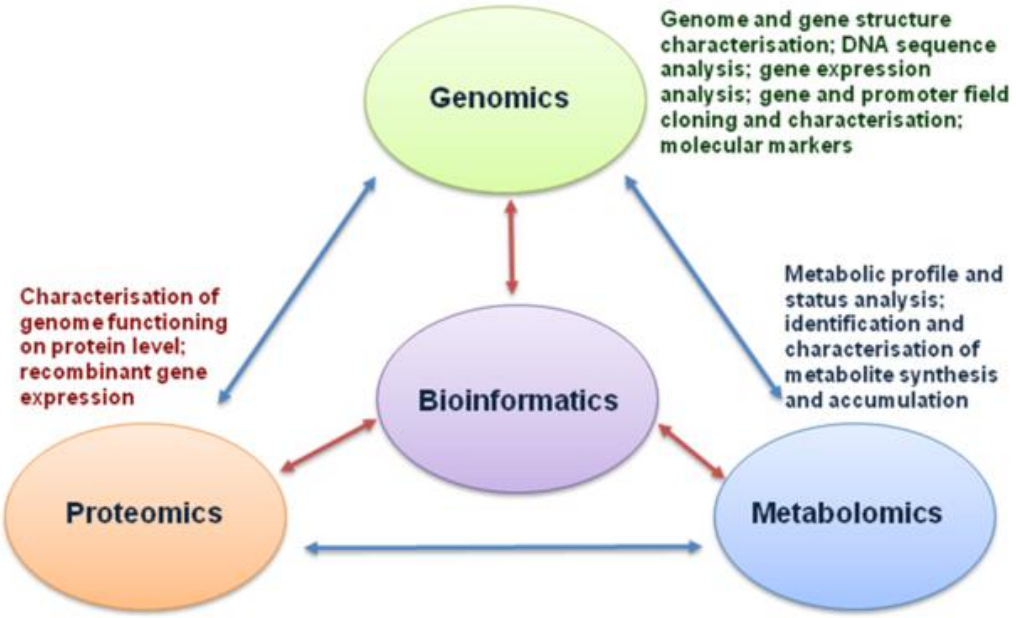

Fig.1 From genomics to proteomics. integration of information from the genome to the proteome for a better understanding of biological systems

Genomics has been the last specialty applied to study the mechanisms of acclimation of these plants to the submerged lifestyle (Wissler *et*

al., 2009; Procaccini *et al.*, 2012). Particularly the works have focused on how to incorporate the comparative gene expression studies with photosynthetic performance, carbon and nitrogen utilization and environmental adaptation, and how to combine the research related to mechanisms of carbon utilization, light requirements, temperature effects and natural

variation in pH and ocean acidification (Arnold *et al.*, 2012; Hall-Spencer *et al.*, 2008; The Royal Society, 2005).

Proteomics of marine plants is still at the early stage because of the poor information on genomics of most of the species. Among the aquatic plants, mangroves have been received attention for genomic and proteomic approaches because their constitute a model for salt-tolerant xylophytes (Huang *et al.*, 2012).

On the side of seagrasses, proteomics gave first results regarding their acclimation mechanisms under chronic low light (Mazzuca *et al.*, 2009; Serra and Mazzuca, 2011), different depths (Dattolo *et al.*, 2013) and in response to salinity stress (Serra *et al.*, 2012).

These –omics approaches have recently required to be coordinated to the research supported from the Cooperation in Science and Technology Action (COST) program of the European Science Foundation, to counteract the crisis of seagrasses conservation and their regression along the Mediterranean area. During this Action,

genomic and proteomic approaches have been integrated with ecophysiological and physical approaches with the aim of understanding changes in seagrass productivity and metabolism in different conditions, thus to apply the potential of the data that come from this synergistic approach for seagrasses.

The research activities in the current thesis have been developed within the frame of this COST Action with the aim to correlate the proteomic approach to genomics, and ecophysiology of selected seagrass ecosystems.

The submerged lifestyle imposed many limiting factors to the growth and development of seagrasses that have been adapted their gene expression and physiological machineries to the marine conditions (Wissel *et al.*, 2011). Few genes showed evidence for positive selection in seagrass branches indicating that photosynthesis, a few metabolic pathways, and ribosomes have strongly diverged after the split of the common ancestor of seagrasses from terrestrial monocots. In this context our proteomic studies have been address the following questions: how seagrasses exert their osmoregulatory capacity to tolerate high salinities, how CO_2 is fixated, how their photosynthetic apparatus has evolved for under water light harvesting.

Leave are the eligible organs to applied proteomics to seagrasses due to their abundance in meadows, their sampling is not destructive and the physiology of plant is driving by the metabolisms that take place in leaves. Moreover, since leaf protein pattern is generally well known and many proteins have been identified (Saravanan & Rose, 2004), this overcomes the lack of completeness of the gene databases for these species that generally represent the greatest obstacle in using proteomic approaches for aquatic plants. On this basis we used the adult leaves to avoid the influence of tissues differentiation on the protein expression and yield.

We applied the analysis of leaf proteome thanks to the well developed and optimized protocol for protein extraction and purification from seagrass leaves (Spadafora *et al.*, 2008) to look at the global protein expression of different species and conditions. A great challenge, working with non-model species, whose genomes are not completely sequenced, is to identify proteins by means of the classical bioinformatic engines that interrogate the public databases. To overcome this gap we used a combination of non-common software for proteomic analysis, that are easily customized, to identify much more proteins as possible against public databases and against local database of seagrasses created by the research team of University of

Calabria from the Expressed Sequence Tags and transcriptome sequences thanks to next generation sequencing approaches.

Given that photosynthesis is the primary metabolism in leaf, we deeply investigate the sub-proteome of chloroplasts and the level of the expression of proteins that are involved in this process. It is well known that chloroplast proteomics describe both the metabolisms that are drive by their own genome to synthesize proteins for specific function and also those from the nuclear-encoded proteins (Salvi *et al.*, 2007). Plant organelle proteomics should be limited mainly due to the inter-plant or inter-tissue complexity, to the difficulties in isolation of subcellular compartments and to their enrichment and purity. Despite these concerns, the field of organelle proteomics is growing in plants, such as *Arabidopsis*, *Oriza sativa* and *Zea mais*. The available data are beginning to help better understand organelles and their distinct and/or overlapping functions in different plant tissues, organs or cell types, and importantly, how protein components of organelles behave during development and with surrounding environments. As first the priority of seagrasses chloroplasts proteomics has been the isolation of organelles or sub-organellar compartments that provides a very direct method for confidently assigning proteins to specific localization, allowing to better understand known functions of the organelle or reveal novel ones. We used separation technologies in

combination with increasing amounts of plant genome sequence data, to have opened up experimental possibilities to identify a more complete set of chloroplast proteins, the seagrass chloroplast proteome catalog, as well as their expression levels (van Wijk, 2000; Ferro *et al.*, 2003; Baginsky & Gruissen, 2004; van Wijk, 2004, Rossignol *et al.*, 2006).

Research aims

One of the main purpose of the research project has been to characterize the protein composition of the chloroplast of *seagrasses* adapted to different light regimes. Organelle proteomics is one of the latest applications in both the animal and plants, and has initiated the construction of several databases dedicated that are indispensable for the study of even complex proteomes from organs of species whose genomes have in part or in nothing sequenced. This is because the organelle proteins (eg, enzymes of the Calvin - Benson cycle) have high level of homology sequence among different species whose are genetically related or not. Nowadays dedicated databases are daily updated with results from model organisms and also from species whose genomes are not sequenced yet. In particular, we identified proteins from generalist databases (NCBI) and /or against the *seagrasses*-dedicate Dr Zompo; moreover we took protein details from the AT_Chloro database that contains information on subplastidial localization of proteins from envelope, stroma and thylakoids of *Arabidobsis thaliana* chloroplasts.

Taking advantage of all the information obtained for *A. thaliana*, this research project aims to *i)* obtain purify chloroplasts from adult leaves of seagrasses starting from most common available protocols and optimize the protocol to extract and purify the proteins from the three organelle compartments, *ii)* applied the mono-dimensional electrophoresis to separate protein mixture as the first step of the gel-based proteomics and obtain protein sequences through the mass spectroscopy analysis, using different ion sources (E.S.I., S.A.C.I, Orbitrap), *iii)* identity of the corresponding proteins from peptide sequences by database searching for homology; define the protein localization within the chloroplast compartments by means of the AT_Chloro database , *iv)* build a catalog of seagrass chloroplast proteins, *v)* compare the chloroplast protein expression levels in leaves growing at shallow and deep beds during the daily cycle.

The second main purpose of the research was to applied the expression proteomics to *seagrass* plants growing in different salinity conditions to detect the proteins that are differentially expressed during the acute stress, the acclimation and resilience. In order to define the impacts of hypersaline water, experiments have been undertaken in aquaria focuses on the leaves proteome under normal and hypersaline conditions.

The research activities has been performed in collaboration with the Spanish Oceanography Institute, Oceanography Centre of Murcia, Spain, whose laboratories are well equipped for hypersaline experiments.

1.The biological systems

1.1.What are *seagrasses*?

The 60 species of seagrasses currently known in the world have had to develop different adaptations to live completely submerged, to tolerate high salinity of sea water, and to have an effective system of anchorage to the substrate and a sedimentary pollen, filamentous, capable of be transported in water (hydrophilic pollination) (Larkum *et al*., 2006).

The development of these adaptations led to a morphological model very uniform in all species of *seagrasses* , as the *habitus* that is very similar. They are rhizomatous plants (bearing a complex system of underground rhizomes) with clonal growth . The rhizomes may have a horizontal or vertical position. The former are responsible for the expansion of the bed and progressive employment space, while the latter prevents that plant has buried by sedimentation . The growth of horizontal rhizomes predominates in the edges of meadows, while the vertical development is more frequent in the central area. On the lower

part of the horizontal rhizomes a group of adventitious roots coming out, contributing to fix the plant and to absorb nutrients; on the upper part there are the short vertical rhizomes each developing a shoot with many leaves. In the rhizomes it can be distinguished nodes and internodes. Such as flowering plants, *seagrasses* can develop the inflorescence or flowers at certain times of the year, which are very noticeable and difficult to observe (Larkum *et al.*, 2006). Currently the process of flowering is quite rare in many species of *seagrasses*, dominating the vegetative reproduction by means of clonal growth of rhizomes, than sexual. This has as a consequence that the genetic diversity in bed is very low, and therefore it is assumed that these can consist of a few clones. This low genetic diversity is supposed to be one of the causes of general regression and mass mortality that affect the meadows, which are not able to develop resistance against disturbances and threats.

The *habitus* of seagrasses is that of terrestrial monocots in which the *plastocrone* interval (the time interval between the onset of leaf bud in two consecutive nodes during the growth) is really short. The pattern of stem elongation and clonal growth are relatively constant

and specie-specific. One of the factors limiting the growth of these plants is the light (as for all photosynthetic organisms). The *seagrasses* cannot grow in depth where not arrive at least 10% of the light at the surface, for this reason they are located always in the upper part of the continental shelf (infralittoral). In very clear water , as in some tropical areas , the *seagrasses* may be present up to 70 m deep, but in seas with more turbid waters do not exceed 15-20 m. The meadows of *seagrasses* worldwide covering approximately 6000000 km^2 of seabed submerged and are responsible for primary production, about 0.6 gigatons of carbon per year, and around 15% of CO_2 absorption by all marine organisms. For all these reasons, these formations submerged plants play an important role in the biology and coastal systems:

1 . The density of the leaves in the bed promotes the deposition of particles in suspension and, therefore, the transparency of the water .

2 . Its complex network of rhizomes tend to consolidate and stabilize sediments.

3 . They attenuate the marine hydrodynamics and, as a result, prevent the coastal erosion.

4 . they are responsible for high production of oxygen and organic matter .

5 . they Provide habitat for many species, a lot of which use these environments as a hideout, as a breeding place and permanence of juvenile.

Along the coasts of Europe , there are four species of *seagrasses*, *Zostera marina* Linnaeus, *Zostera noltii* Hornemann, *Cymodocea nodosa* (Ucria) Ascherson and *Posidonia oceanica* (Linnaeus) Delile. *Z. marina* is along the coasts of the north Atlantic and Pacific, and has a very localized distribution in the Mediterranean and in the Alboran Sea, while *Posidonia oceanica* is endemic in the Mediterranean. *Zostera noltii* and *Cymodocea nodosa* are living both in the Atlantic coast to the Mediterranean coast and are the only species that are found in the Canary Islands.

1.2. *Posidonia oceanica*

Posidonia oceanica, a species exclusive to the Mediterranean Sea, which is distributed in both the eastern basin than in the West, as well as in most of the islands. This seagrass lives between the surface and a depth varying, depending on water clarity. It can grow on both substrates that soft or rock. Generally, it was observed that the growth

Fig.2 Meadow of *Posidonia oceanica*

occurs on rocky seabed in shallow water and in open areas with less hydrodynamics, while large bays or deep waters, where the hydrodynamics is smaller, the growth occurs on sandy substrates. It is a plant stenoaline (i.e. unable to tolerate large variations in salinity) and cannot live with a lower salinity of 33 ‰ to 39 ‰ or higher, for this is not found in brackish or hypersaline lagoons. However, it tolerates a relatively wide temperature range from about 10°C to 28°C.

It is very sensitive to eutrophication and to the contaminants and does not tolerate high rates of sedimentation. These requirements explain his absence near the mouths of large rivers. In addition, it was

estimated that in areas with a high concentration of human activities, the *Posidonia oceanica* meadows occupy on average about 15 % of

the seabed in a bathymetric range 0-50 m, and close to 50% in a well-preserved and with very clear water. So that it can be considered an indicator of plant water clear, well-oxygenated and free from contamination.

The rhizomes of *P.oceanica* are particularly woody, can reach a thickness of about 1 cm, slightly laterally compressed and covered with scales that come from the bases of old leaves. Depart from the rhizomes some roots relatively short (normally not exceeding 10-15 cm), few in number, robust (thickness of about 2-4 mm) and that lignified very quickly. The roots have a role in anchoring the plant to the substrate and its quantity increases in the places with the most troubled waters. They form ribbon, about 1 cm in width and the length ranges from 20 to 140 cm, and they present 13-17 longitudinal veins. The growth of new leaves is a process more or less continuously over the year and their longevity varies from 4 to 11 months. The apices are rounded and they are often lost on wave action and of currents. The leaves are organized in bundles, which contain 6 or 7, with the older leaves that are outside and inside the youngest.

Leaves are divided into three categories (Fig.3):

1. Mature leaves: have a lamina with photosynthetic function and a base separated from the leaf blade from a concave structure called

ligule;

2. Intermediate leaves: they are avoid of the base; are photosynthetically active ;

3. Juvenile leaves: are conventionally length less than 50 mm, weakly pigmented.

Fig.3 Leaves of *Posidonia oceanica*

In autumn, the plant loses its mature leaves, which become brown in color and are photosynthetically inactive and the new leaves are produced during the winter. Sexual reproduction takes place by producing flowers and fruits. The flowers are hermaphrodite and grouped in an inflorescence spike-shaped, green and enclosed in floral bracts. The floral axis attaches to the rhizome in the center of the beam. The gynoecium is formed by a unilocular ovary which continues with a stylus and ends with the stigma; the androecium consists of three stamens with anthers court. The flowering is regulated by environmental factors (light and temperature) and endogenous factors (age and size of the plant) and takes place in September-October in the shallow meadows, while it is shifted of two

months in the deeper meadows. The pollen within of the anther is spherical, but it becomes filamentous soon as it is released into the water. There are not mechanisms for recognition between pollen and stigma that prevent self-fertilization. Pollination is hydrophilic and can lead to the formation of the fruit, although some abortions before its maturation after six months. Once ripe, the fruits fall off and float to the surface. The fruit, slightly fleshy and commonly called "sea olive", is similar to a drupe and has a porous and rich pericarp of an oily substance that allows the waterline. When it degenerates the seed is released, coated by a thin membrane but without a real tegument, which falls to the bottom and if it finds the suitable conditions of depth, stability and sediment type, germinates and gives rise to a new plant. To start making roots, it is necessary to find a humified substrate. The humification is produced by the degradation of plant debris, so the plant can implant in "soil" previously colonized by other plants, such as macroalgae or other seagrasses. This generates a genuine ecological succession in which *Posidonia* is the last stage of succession. Germination begins with the protrusion of a small white root from the radical pole and a leaf from the apical pole. With sexual reproduction the plant colonizes new areas, meadows spread to other areas ensuring a genetic variability. The stolonization, which allows

the expansion of meadows, it's made by plagiotropic growth of rhizomes, which grow about to 7 cm/year and colonize new areas.

A high accumulation of sediment and the decrease of the space available for the horizontal growth, stimulates the growth of the vertical rhizomes . So the vertical growth of the rhizomes leads to the formation of a structure called *matte*, consisting of a mesh of dead rhizomes and roots which remains trapped between the sediments. Only the top part of these structures is made up of alive plants. The formation of *mattes* depends mostly from the rhythms of sedimentation; the high sedimentation rate can lead to excessive silting of the rhizomes and then to their anoxia, on the contrary a too slow sedimentation can cause the weakening of the rhizomes and the regression of meadows. Since the rate of decomposition of the rhizomes is very slow they can stay inside the *matte* for millennia. The *matte* has a very slow rate of growth : its growth has been estimated at about 1 m per century. So that the meadows can accumulated organogenic structures that rise for meters above the base (Mateo *et al.*, 1997). This accumulation of organic sediments not only represents a net sink of carbon and other elements, but can also attenuate wave action. It has been estimated that the removal of 1 m^3 of *matte,* for example, can cause 20m of coastal regression (Jeudy De Grissac,

1984). Photosynthesis often depends on the light and decreases rapidly with increasing depth . Respiration, however, is independent of the light and in *Posidonia oceanica* is relatively high, since it has underground organs (roots and rhizomes) that are not photosynthetic, but have an important respiratory function. The growth dinamics and the large amount of biomass produced by *Posidonia oceanica*, are factors able to support the animal and plant communities with high biodiversity. We distinguish the community of epiphytes, ie bacteria, algae, bryozoans that colonize the surface of leaves and rhizomes, the animal communities and vagile and sessile communities of detritivore organisms.

Along the leaf there are several areas of differentiation that depend on the age of the leaf. Even epiphytic communities follow this zonation: at the base of the mature and young leaves diatoms and bacteria are implanted; incrustations algae red and brown are implanted in the central part of the leaf, while in the upper part the encrusting and filamentous algae are found.

Fig.4 *Posidonia oceanica* leaves rich in epiphytes

Epiphytic communities are preyed by Molluscs, Gastropods, Crustaceans, Polychaetes and Amphipods play a very important role in the food chain of *Posidonia oceanica* meadows. There are few organisms that can directly feed the plant tissue, which is unwelcome to most herbivores due to the high content of structural carbohydrates, high values of C and N, and for the high concentration of phenolic compounds.

The epiphytes can also cause damage of *Posidonia*. Them, in fact, increasing the weight and can cause its premature fall; they can decrease the available light and also they hinder the gaseous exchanges and the absorption of nutrients through the leaves.

The fauna associated with *Posidonia oceanica* meadows consists of sessile animals that live coated on the substrate made from the leaves and rhizomes, and vagile animals ,capable of move within the meadows. Then there are organisms, which constitute the infauna, that live inside the matte and that are primarily detritivores.

Fig.5 Denizen habitual of *Posidonia oceanica* is the bivalve *Pinna nobilis* (left)

Studies conducted by Gambi et al. in 1992 have demonstrated that approximately 70% of the total animal population of the

meadows is constituted by herbivores. Between them, the most abundant are echinoderms, in particular the *Paracentrotus lividus*, one of the few organisms able to feed directly of the leaves of the plant. The carnivores are represented by fish, molluscs, polychaetes and decapods.

Between the molluscs, habitual and nearly exclusive inhabitant of the meadows is the *Pinna nobilis*, the bivalve largest in the Mediterranean and highly threatened from fisheries and pollution.

The fish population is constituted by a small number of species, principally labrids and sparids almost all carnivores. large fish are less frequent and during the year it witness to variations the abundance specific due to the referrals and migration.

In the shallow and secluded meadows, there is an abundance of *Sarpa salpa*, which represents 40-70% of the summer fish fauna.

The detritus constituted by the litter made from the remains of fallen leaves, is colonized by microorganisms and fungi.

A particular group of detritivores are polychaetes (*Lysidice ninetta*, *Lysidice collaris* and *Nematonereis unicornis*) and isopods (*Idotea hectica, Limnoria mazzellae*), called borers that dig tunnels inside the flakes (remains of leaf bases that remain attached to the rhizome all year) to feed themselves and to expand their habitat. The leaves,

degraded by wave and microorganisms, once beached, take the name of *banquette* and they serve as shelter and food for insects, amphipods and isopods.

1.3. *Cymodocea nodosa*

Cymodocea nodosa is the second seagrasses in the Mediterranean for extension of its meadows.

Fig.6 Meadow of *Cymodocea nodosa*

The *Cymodocea nodosa* is an aquatic plant of the spermatophyte family Cymodoceaceae. *C. nodosa* is a warm water species and is widely distributed throughout the Mediterranean, around the Canary Islands and down the North African coast, it can colonize the dead matte of *Posidonia oceanica*. The species does not extend further north than the southern coasts of Portugal. *C. nodosa* can be found from shallow subtidal areas to very deep waters (50-60 m). This

species has leaf bundles consisting of 2 to 5 leaves. The leaves are 2 to 4 mm wide and from 10 to 45 cm long.

The leaves resemble those of medium sized Zostera *marina*. However, the shoots are attached to vertical rhizomes with short rhizome segments which again are attached to a horizontal rhizome with 1-6 cm long segments. The apex forms vertical rhizomes and branches to new horizontal rhizomes. The rhizome may grow several meters per year, and *C. nodosa* is considered a pioneer species which can quickly colonize bare areas of the sea floor. *C. nodosa* can easily be identified by its vertical rhizomes and the long white to pink horizontal rhizome segments. The roots are dispersed along the vertical and horizontal rhizomes. Each rhizome segment only has one root which is often strongly branched and may be up to 3 mm thick and up to 35 cm long. The individuals are either male or female plants. The female flowers have two ovaries and the two lentil-shaped seeds produced from each flower are around 8 mm long and, hence, considerably larger than the seeds of the *Zostera* species.

Only *C. nodosa* shoots older than 1 year flower, and they do so between March and June. Fruit development takes 2-3 months,

although maximum density of shoots bearing fruits is observed in July-August. Afterwards, fruits detach from the mother shoot and, because they have negative-buoyancy, they are rapidly buried into the sediment nearby the mother plant. During events of intense sediment dynamics (e.g. strong storms), however, seeds may be transported across long distances, since there are meadows separated from the closest one by more than 300 km, and seeds of *C. nodosa* can be observed, although not very often, washed on the beaches. From April til June of the following year seeds germinate. *C. nodosa* clone formation rate has been estimated to be about 0.009 clones m^{-2} yr-1in an area with intense sexual reproduction. However, clone mortality rate is about 50-70 % during the first year of life, hence, decreasing substantially the success of sexual reproduction.

Reproductive effort and success in *C. nodosa* exhibits temporal and spatial heterogeneity. Flowering intensity, for instance, has been observed to increase in response to sand burial, like in other seagrasses. In addition, seed production in *C. nodosa* should be constrained by the spatial distribution and abundance of male and female clones. The consequences of clone sex composition on reproductive success are evident when examining *C. nodosa* meadow

genetic diversity. For instance, there is almost no genetic diversity in a *C. nodosa* meadow at the Algarve (Portugal), where no female flowers have been observed. The fast growth of *C. nodosa* clones and the relatively high patch formation rate of this species, when compared with the other European seagrasses, indicate that *C. nodosa* should be able to develop a meadow within a decade, if the colonisation process were initiated, on bare sediments. The time scales for meadow recovery if not all *C. nodosa* vegetation were lost should be even shorter. The rapid occupation of space by *C. nodosa* resulting from fast clonal growth, and the relatively high patch formation rate of this species explains the pioneering role that *C. nodosa* play during succession process in the Mediterranean.

Beds of *C. nodosa* are characteristic habitats for seahorses. *C. nodosa* growth ranks amongst the fastest ones across European seagrasses. The fast clonal growth of this species allows the clones to spread across 300 m^2 after 7 years. The life span of *C. nodosa* modules and ramets is intermediate, average shoot population life-span varying between 4-22 months, and average leaf life-span ranging from 2 to 5 months. However its clones may live for at least 1 decade. The vegetative growth almost exclusively occurs during spring and

summer, exhibiting a substantial plasticity, which allows this species to survive disturbances. For instance, vertical and horizontal rhizome growth of *C. nodosa* is plastic enough for this species to colonize areas with intense sediment dynamics, such as bedforms with subaqueous dunes, with an average amplitude of 20 cm (range 7-65 cm) and wave length of 21 m (7-29 m), that migrate at average velocities of 13 m $year^{-1}$. The close relationship between the growth of the rhizome and the vertical accumulation of sediment was used to quantify the dynamics of shallow coastal sediments, impossible to be measured with conventional sedimentary techniques. *C. nodosa* also exhibits substantial plasticity in response to ambient nutrient availability.

On the side of resistance *C. nodosa* can tolerate the anoxia and the presence of hydrogen sulphide in the soil. Its leaves are home to a rich epiphytic community almost as much as that of *Posidonia*.

2. The –omics applied to seagrasses

2.1 What's "OMICS" sciences?

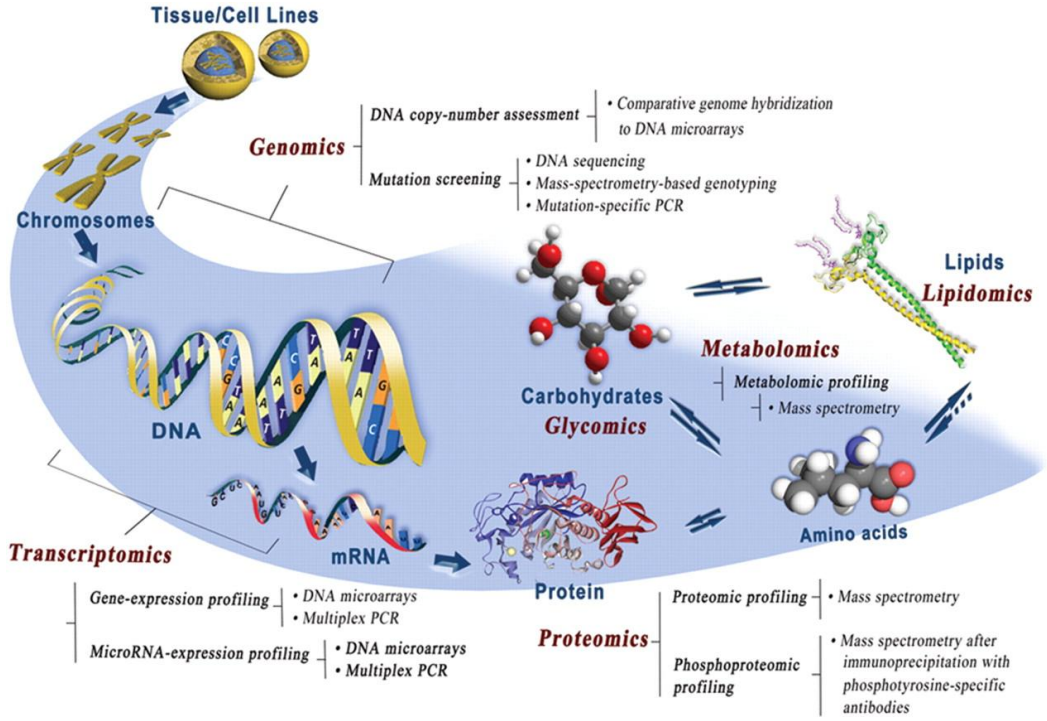

Fig.7 Omics technologies: proteomics, transcriptomics and genomics

Omics technologies such as genomics and highthroughput DNA sequencing were introduced in parallel to the Human Genome Project since 1990s. According to one etymological analysis, the suffix 'ome' is derived from the latin *omni-* ("completeness and fullness") (Lederberg and McCray, 2001). By combining 'gene' and 'ome', Hans Winkler created the term genom(e), referring to "the haploid

chromosome set, which, together with the pertinent protoplasm, specifies the material foundations of the species [...]." (Winkler *et al.*, 1920). Victor McKusick and Frank Ruddle added 'genomics' to the scientific lexicon as the title for the new journal they co-founded in 1987, with emphasis on linear gene mapping, DNA sequencing and comparison of genomes from different species (McKusick and Ruddle, 1987). Omics technologies and various neologisms that define their application contexts, however, are more than a simple play on

words. They substantially transformed both the through put and the design of scientific experiments. The omics technologies allow the generation of copious amounts of data at multiple levels of biology from gene sequence and expression to protein and metabolite patterns underlying variability in cellular networks and function of whole organ systems (Nicholson and Lindon, 2008). In fact this led to overabundance of data in biomedical experiments recently (Nicholson and Lindon, 2008). While the 1990s was named as the “decade of the brain”, we are now in the “decade of measurements”. This signals a new *era* in how we approach to scientific inquiries. In addition to amplified through put, the process of research is fundamentally altered in “omics science”. Ordinarily, scientists have accustomed to hypothesis-driven research wherein a clearly articulated scientific

question/hypothesis would be posed. Subsequently experiments would be carried out to obtain data in order to test the study hypothesis. With the omics approach, asking an initial research question is not always necessary or a pre-requisite. Genome or proteome wide data can be collected in an omics experiment without an existing hypothesis, followed by generation and testing of biological hypotheses.

During the last decades, the application of *-omics* technologies at ecological studies provided powerful tools for following the physiological acclimation in response to environmental variations (Feder and Walser, 2005; Foret *et al.*, 2007; Gracey *et al.*, 2007; Karr *et al.*, 2008), and helped researchers to correlate the differences of gene's expression profiles to changes in them a in ecological cues in many different organisms (Chevalier *et al.*, 2004; Edge *et al.*, 2008; Kassahn *et al.*, 2009; Larsen *et al.*, 2012; Richards *et al.*, 2012). Despite their high ecological value, seagrasses are poorly understood for what concerns the genetic basis behind their physiological adaptation and plasticity (Procaccini *et al.*, 2007).

It's only recently that transcriptomic approaches were implemented for few species, to correlate seagrasses gene expression with ecological factors. In particular, transcriptomic response to

temperature changes and thermal stress was studies in the two congeneric species, *Zostera marina* and *Zostera noltii* (Maathuis *et al.*, 2003; Reusch *et al.*, 2008; Massa *et al.*, 2011; Winters *et al.*, 2011), while transcriptional (Bruno *et al.*, 2010; Serra *et al.*, 2012b) and proteomic approaches (Mazzuca *et al.*, 2009) were applied to study light response in natural conditions in *Posidonia oceanica*. In *P. oceanica*, studies were hampered by the fact that available genomic and transcriptomic resources only consisted in a single Expressed Sequences Tags (EST) library, obtained from shoots collected along a depth range (from−5 to −30 m) in a single site (Wissler *et al.*, 2009), and available in Dr.Zompo, a specific seagrasses database containing both *P. oceanica* and *Z. marina* EST sequences http://drzompo.uni-muenster.de/ (Wissler *et al.*, 2009). Several approaches can be utilized for genomic studies in species for which the whole genome is not available (Hofmann *et al.*, 2005; Stapley *et al.*, 2010), most of them requiring high computational power and advanced bioinformatics resources (Morozova and Marra, 2008; Pop and Salzberg,2008; Metzker *et al.*, 2010). Among the others, Suppressive Subtractive Hybridization (SSH)–EST library (Diatchenko *et al.*, 1996) approach resulted especially powerful to identify differentially expressed genes in the presence of clear differences in physiological status (Jones *et*

al., 2006; Puthoff and Smigocki, 2007) and it was applied to study flowering (Matsumoto *et al.*, 2006), senescence (Liu *et al.*, 2008a,b), or salt-stress (Zouari *et al.*, 2007) in terrestrial plants.

Previous studies have identified some differences in transcriptional and proteomic profiles in *P. oceanica*, correlated with its bathymetric distribution, with the ultimate goal to identify the metabolic pathways involved in acclimation. They also aimed to increase genomic resources in *P. oceanica* and to present a powerful approach for studying physiological response at a molecular level in organisms for which genomic resources are limited. In order to do that, a SSH-library was built between plants growing at two different depths in the same meadow, obtaining their protein identification using the innovative USIS mass, spectrometry methodology coupled with 1D-SDS electrophoresis. On the side of search engine against genome and proteome databases it has been used for proteins identifications the Global Proteome Machine (GPM) open-source system for analyzing, storing, and validating proteomics information derived from tandem mass spectrometry (Craig *et al.*, 2004; Fenyö *et al.*, 2010) and X!Tandem software (Craig and Beavis, 2003; Craig *et al.*, 2005) that allowed to interface directly the mass spectrum data with a local database customized with the collection of each sequence stored in

the Dr.Zompo and UniProtKB databases for seagrasses and for plants among Liliopsida that are the closer terrestrial counterpart.

2.2 Proteomics

Proteomics is the large-scale study of proteins, particularly their structures and functions. Proteins are vital parts of living organisms, as they are the main components of the physiological metabolic pathways of cells. The term "proteomics" was first coined in 1997 to make an analogy with genomics, the study of the genes. The word "proteome" is a blend of "protein" and "genome", and was coined by Marc Wilkins in 1994 while working on the concept as a PhD student. The proteome is the entire complement of proteins and provides a direct measure of the quantity that are expressed in a cell at a time. Scientists are very interested in proteomics because it gives a much better understanding of an organism than genomics. First because the level of transcription of a gene gives only a rough estimate of its level of expression into a protein. An mRNA produced in abundance may be degraded rapidly or translated inefficiently, resulting in a small amount of protein. Second because , as mentioned above many proteins experience post-translational modifications that profoundly

affect their activities; for example some proteins are not active until they become phosphorylated. Third because, as it is well known the mRNA is not always translated into protein, and the amount of protein produced for a given amount of mRNA depends from the gene that it is transcribed and on the current physiological state of the cell. Even if it is studying a particular cell type, that cell may make different sets of proteins at different times, or under different conditions. Furthermore, as mentioned, any one protein can undergo a wide range of post-translational modifications. Therefore a "proteomics" study can become quite complex very quickly, even if the object of the study is very restricted.

2.3 Proteomics in seagrasses biology, ecology and threatens

Proteomics approach have been applied for the first time to *Posidonia oceanica* to understand the molecular bases of stress responses, resilience and acclimation to low light (Mazzuca *et al.*, 2009; Serra and Mazzuca, 2011). In fact, *P. oceanica* beds have recently suffered from progressive die-offs attributed to lower light availability from elevated water turbidity. In addition *P. oceanica* meadows are extremely sensitive to moderate to high disturbance, and have suffered

substantial diebacks throughout the Mediterranean Sea due to anthropogenic disturbances affecting light and temperature regimes. The adaptive low-light responses of this seagrass have been highlighted by comparing the protein expression in plants collected from turbid waters (low-light) with plants collected from pristine-clear waters (high-light). Results summarized that enzymes involved in carbohydrate cleavage (1-fructose-bisphosphate aldolase, nucleoside diphosphate kinase, and beta-amylase) were upregulated in low-light conditions. Electron microscopy studies also revealed substantial changes in the stroma lamellae/grana ratios in chloroplasts receiving lowlight, possibly as a mechanism for re-establishing optimal PSI/PSII ratios. Furthermore, under low-light conditions, four components of the ubiquitin/mediated proteolysis pathway (26 S proteasome regulatory, proteasome beta type 1, proteasome 7 D beta type, and proteasome alpha 7), and the perchloric acid soluble translation inhibitor protein, were upregulated. This suggests that, in *P. oceanica* leaves, enhanced protein turnover mediates acclimation to low-light conditions. Also, enzymes involved in defending against cellular stress (superoxide dismutase, pyridoxine, and 2-caffeic-acido-methyl transferase) were differentially expressed in low-light regime.

From this molecular approach it is possible to recognize new tools that may deserve the designation of "early-warning" markers for environmental stresses; the main goal will be to invert soon as possible the feedback mechanisms impose by stress that accelerate the decline of seagrass productivity, driving seagrass communities from autotrophic (where carbon is sequestered) to heterotrophic (where carbon is released). It is, therefore, important to understand how photosynthesis and carbon metabolism of meadows are affected by drivers of seagrass decline. The ecological status of *P. oceanica* is usually assessed by quantifying shoot densities, above-/below-ground biomass ratios, or growth rates. For example, the European Water Framework Directive (WFD, 2000/60/EC) uses seagrass taxonomic composition and abundance, determined by shoot density and spatial extent, to evaluate the ecological status of transitional or coastal water bodies. However, these descriptors respond slowly to environmental change. Once decline is apparent, it may be too late to implement a coastal management procedure that would allow an endangered meadow to recover. Therefore, early-warning indicators of seagrass health are necessary. Establishing the direct linkages between stressors and seagrass responses, and initializing the appropriate scales of spatial and temporal monitoring, will guide managers in

determining which actions are necessary to prevent further seagrass loss.

The primary cause of seagrass die-off is reductions in light due to increased turbidity and eutrophication, often attributed to anthropogenic activities along the coast (Short and Wyllie-Echeverria, 1996; Guidetti and Fabiano, 2000; Alcoverro *et al.*, 2001; Ruitz and Romero, 2003). In low-turbid pristine *P. oceanica* beds, plants can flourish at a depth of 40 m, with high shoot densities, productivities, and growth (Duarte *et al.*, 1991). Indeed, some authors have shown that, when PAR (Photosynthetically Active Radiation) lowers below 4.5%, light quality and quantity becomes insufficient to sustain the normal growth of *P.oceanica* (Zimmermann *et al.*, 2006). Others have suggested that the photosynthetic activity of *P. oceanica* is regulated by depth rather than light intensity, as seagrass can acclimate to low-light conditions (Figueroa *et al.*, 2002; Olsen *et al.*, 2002; Lorenti *et al.*, 2006). This implies that specie-specific determinants might explain differences in acclimation response. There was the need of new biomarkers, such as proteomics, to identify and quantify early alterations in the plant adaptive response. The application of proteomics in monitoring marine ecosystems is a relatively new tool focusing on gene function (Procaccini *et al.*, 2007), and can be useful

in evaluating the response of an organism to environmental conditions (Andacht and Winn, 2006). Although proteomic bio-monitoring is a sensitive tool for studying the response of aquatic animals to environmental stress, only a few studies have applied proteomics to evaluate aquatic plants (Förster *et al.*, 2006; Katz *et al.*, 2007). Even if the plant's own genome was sequenced, proteomic analyses would remain unattractive because protein sequence analysis and identification are challenging. Unlike animal tissues, *P. oceanica* tissues are rich in compounds such as polysaccharides, lipids, phenols and other secondary metabolites that interfere with protein separation and analyses, (Agostini *et al.*, 1998; Dumay *et al.*, 2004; Cozza *et al.*, 2004; Park *et al.*, 2004). Furthermore, in comparison to animal tissues, plant tissues maintain lower protein concentrations (Tsugita and Kamo,1999). To increase the quality and yield of purified proteins from plant tissues, researchers have developed a number of alternative extraction procedures (Park *et al.*, 2004; Saravan and Rose, 2004). While many of these procedures have proven useful in protein isolation and purification, newer techniques have demonstrated superior protein extraction in *P. oceanica* (Spadafora *et al.*, 2008).

2.4 Organelle proteomics: potential application in seagrasses

The organelle sub-proteomics is a new frontiers in the frame of plant proteomics (Rolland *et al.*, 2012). The characterization of proteomes in different sub-cellular locations is of prime importance for a complete understanding of plant functions, biosynthetic and signaling pathways. Sub-cellular fractionation permits simplification of the proteome and, potentially, a gain in knowledge in that the sub-cellular localization of the proteins is revealed. The quality of the biological sample analyzed is often the limiting factor in both of these aims. The classical cell fractionation procedure generally consists of two major steps: (i) disruption of the CW and membrane and (ii) fractionation of the crude homogenate to purify the organelle of interest. Cell disruption has to be controlled to avoid excessive disruption of sub-cellular compartments. Protoplast preparation is perhaps the gentlest method and is a prerequisite for the purification especially for chloroplasts (Fig.8).

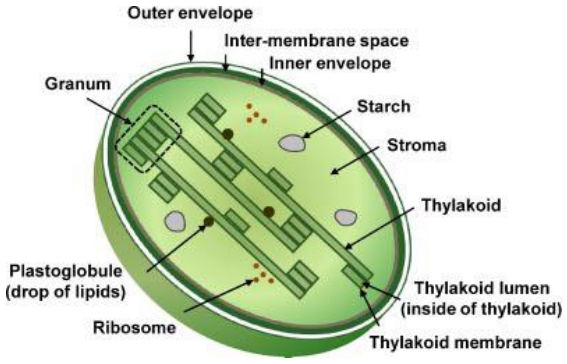

Fig. 8 The chloroplast. This plastid type is essential to the complex process of photosynthesis. Chloroplast is surrounded by a lipidbilayer composite membrane with an inter-membrane space. Moreover, it has reticulations or many infoldings that fill the inner space, the stroma. Within the stroma are stacks of thylakoids, the suborganelles that are the sites of photosynthesis. The thylakoids are arranged in stacks called granum. The chloroplast also contains plastidial DNA, plastoglobules, ribosomes and starch (in Agrawal *et al.*, 2009).

Chloroplasts are the organelle that permit the autotrophic life in plant, algae and bacteria. Assimilation of inorganic carbon (Ci) on air is promoted by diffusion of CO_2 in plant tissue, or by converting it in carbonic acid (HCO_3) by the specific enzyme Carbonic Anhydrase (CA) at plasma membrane (Ferro *et al.*, 2003). In marine plants Ci assimilation depends on the pH of water that affects sensibly the conversion of CO_2 in HCO_3; so that the relative amount of these two molecules influence the photosynthetic performance and production of organic carbon. Chloroplasts have a part in the conversion process because of a carbonic anhydrases in its envelope, whose sequences were identified in a genomic (Procaccini *et al.*,2002) and proteomic studies (Serra and Mazzuca 2011).

Understanding of chloroplast metabolisms in marine plants are essential to clarify how these plants have been able to go back to the sea twice. (Wissler *et al.*, 2011). The chloroplasts proteomics reached an advanced state of art, producing a lot of information on proteins expression and localization inside each sub-compartments. Starting from the protocol optimized for the model plants (*A. thaliana, Spinacia oleracea*) it has been evaluated the conditions that should work with aquatic or marine plants, that are living in extreme conditions of pH and salinity. In fact, the disruption medium can be

detrimental to organelle integrity and its composition is often modified for particular purposes. Thus, the osmoticum, buffering capacity, pH, ionic strength, reductant and presence of agents that protect protein structure (bovine serum albumin (BSA), polyvinylpyrrolidone (PVP) and protease inhibitors) have to be optimized. Fractionation, generally, is based on physical differences between organelles. A simple first step often involves filtration, by passing the homogenate through muslin and/or nylon mesh to remove large debris. This step is important and the pore size of the nylon mesh must be appropriate to the organelle to be isolated (usually 50 mm). A series of differential centrifugations can be used to enrich the target organelle and selectively eliminate other compartments and contaminants. The speed of centrifugation depends on size and density of the organelle to be purified. Larger and denser organelles are pelleted at lower centrifugal forces. By applying different centrifugation speeds to the cell homogenate, enriched fractions of the organelle of interest can be obtained. This enriched fraction can then be subjected to purification by density gradient centrifugation (usually on Percoll). A few protocols are schematically illustrated as examples in figure 9 that have been broadly used to purify nuclei, chloroplasts, mitochondria and vacuoles prior to proteomics characterization.

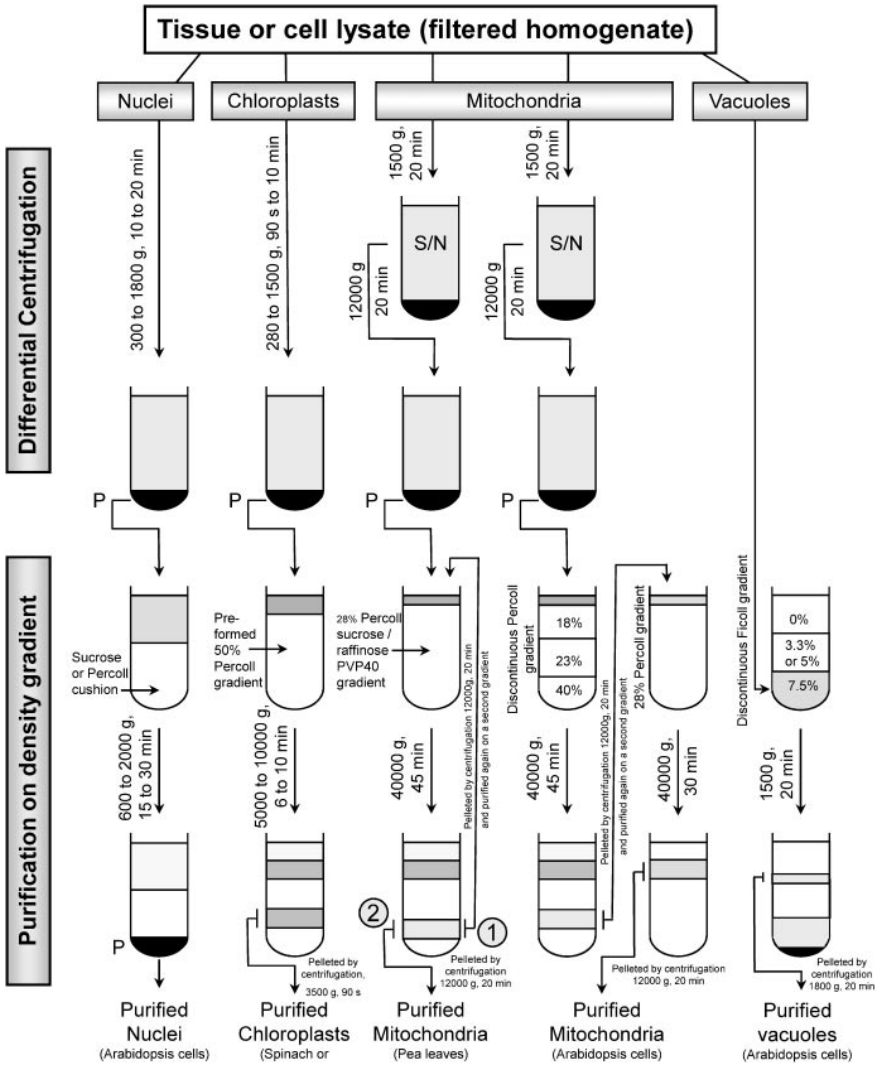

Fig.9 . Schematic representation of protocols used to isolate organelles from higher plants (in Agrawal *et al.*, 2009)

2.5 Purity of Organelle or Compartment

The current priority of organelle proteomics is to identify and characterize the protein complement of organelles and other functional compartments. There are at least three prerequisites:first, the organelle should be easily recognizable, second, the organelle can be purified, and third, the degree of enrichment can be critically assessed. The

isolation of organelles or suborganellar compartments provides a very direct method for confidently assigning proteins to specific organelles, allowing researchers to better understand known functions of an organelle or reveal novel ones. However, the level of confidence depends largely on the degree of purification and the extent to which contamination can be recognized and reduced or avoided.

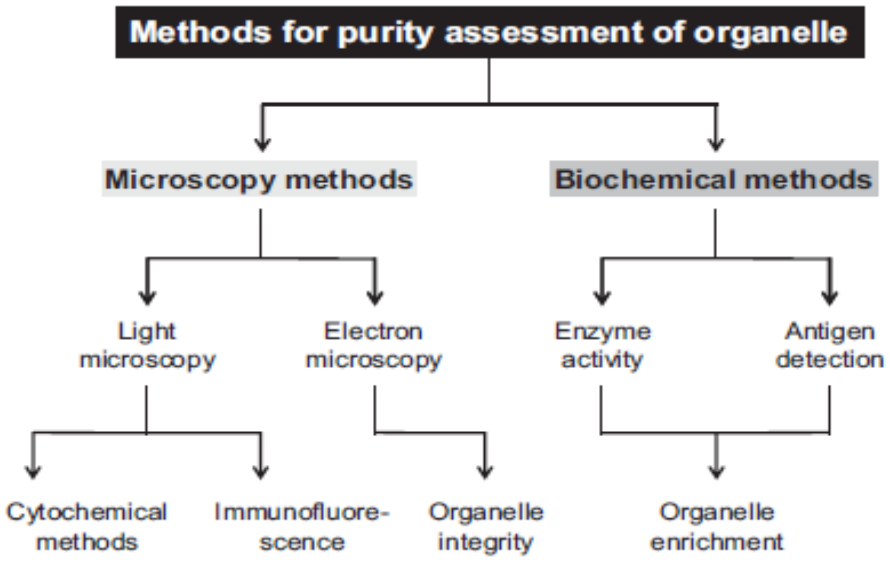

Fig.10 Schematic representation of methods used for assessing organelle purity and intactness (in Agrawal *et al.*, 2009).

Success can often depend on the sensitivity with which one can detect both the target proteins and the contamination. A variety of methods have been developed to assess different steps of the subfractionation protocol, in terms of enrichment of the target organelle as well as the

presence of contaminating proteins. A summary of these methods is given in figure 10.

2.6 Proteomics of the Chloroplast

New technologies, in combination with increasing amounts of plant genome sequence data, have opened up experimental possibilities to identify a more complete set of chloroplast proteins (the chloroplast proteome) as well as their expression levels and PTMs in a global manner (van Wijk *et al.*, 2000). Complementary with the prediction of the complete plastid proteome through analysis of targeting signals, proteomics is expected to provide many new insights into chloroplast biogenesis, adaptation, and function. Organelle purification and subfractionation is essential for cataloging proteomes (Baginsky and Gruissen, 2004; van Wijk *et al.*, 2004, Rossignol *et al.*, 2006). Furthermore, due to the limits resulting from dissimilar physicochemical properties of soluble (stroma, thylakoid lumen) or membrane (envelope or thylakoid membranes) proteins (Sun, Emanuelsson, and van Wijk, 2004), different compartments of chloroplast have been investigated using a broad range of purification and solubilization techniques. Due to the low relative abundance of

chloroplast envelope proteins (less than 1% of chloroplast proteins) compared to other plastid compartments, the envelope fraction remained poorly characterized until the availability of Arabidopsis genome information and development of proteomics-based approaches targeted to this membrane system. Transcript levels were also relatively low and corresponding ESTs for many envelope proteins were also missing from the databases. Until recently, identifying the function of chloroplast envelope proteins mostly relied on classical biochemical approaches leading to the functional characterization of a relatively low number of enzymes involved in specific metabolisms, few transporters or ion channels and some members of the Toc and Tic translocons involved in the plastid targeting of nuclear-encoded chloroplast proteins (Joyard *et al.*, 1998). One of the first efforts to develop proteomics-based analysis of the chloroplast envelope was based on classical 2-D gels. However, this study did not actually identify genuine envelope membrane proteins (Adessi *et al.*, 1997) because most of the envelope membrane proteins are now known to be highly hydrophobic and basic proteins and would not appear on 2-D gels. The first data came from the use of organic solvents to obtain a specific enrichment of intrinsic proteins from the hydrophobic core of the membrane. This treatment combined

with 1-D SDS–PAGE successfully identified these hydrophobic proteins (Seigneurin-Berny *et al.*, 1999; Ferro *et al.*, 2000) including a small number of genuine envelope proteins, some of which were novel. Based on these observations, and on the optimization of various treatments used to remove highly abundant soluble contaminants from the neighboring soluble phase (the stroma), Many envelope components were known or predicted transporters.

2.6.1 Envelope proteins - Several specific physico-chemical properties were shared by most of these experimentally identified envelope proteins: (i) a high Res/TM (ratio of the number of Residues on the number of predicted TransMembrane helices), (ii) a pI ranging from 8.8 to more than 11 and (iii) included an N-terminal extension, which was predicted as a transit peptide using the ChloroP software (Emanuelsson, Nielsen, and Von Heijne, 1999). These stringent criteria were then used to predict a total of 136 chloroplast envelope proteins, likely transporters, encoded in the Arabidopsis genome (Ferro *et al.*, 2002). At the same time, a purely theory-based in silico strategy was published that identified 541 potential inner envelope proteins (Koo and Ohlrogge, 2002). The selection criteria also relied on theprediction of chloroplast localization (3,665 proteins), the presence of transmembrane helices within the mature part of protein

(562 proteins) and the removal of 20 known thylakoid proteins (541 proteins). While excluding at least outer envelope proteins and proteins with incorrectly predicted primary sequence (lacking predicted transit peptides) and peripheral envelope membrane proteins (lacking predicted transmembrane helices), these two data sets clearly complemented proteomics based efforts in detection of minor envelope proteins or those not expressed in tissues selected for proteomics analysis (Table 1). Bioinformatics predictions were also

Model plant	Selection criteria	No. of Proteins	References
Arabidopsis genome	hydrophobic core of the inner envelope membrane (predicted basic and hydrophobic chloroplast membrane proteins)	136	Ferro et al., 2002; Rolland et al., 2003
Arabidopsis genome	inner envelope membrane (predicted chloroplast membrane proteins minus known thylakoid membrane components)	541	Koo & Ohlrogge, 2002
Arabidopsis genome	whole plant β-barrel proteome including outer envelope membrane proteins	891	Schleiff et al., 2003
Arabidopsis genome	known and predicted inner envelope membrane transporters	137	Weber, Schwacke, & Flugge, 2005
Arabidopsis genome	known and predicted outer envelope membrane proteins	24	Inoue, 2007

Tab. 1 Prediction studies targeted to the chloroplast envelope membranes (in Agrawal *et al.*, 2009)

combined with the study of tissue-specific expression of corresponding genes (Koo and Ohlrogge, 2002), thus suggesting possible functions for these putative proteins. Multiple approaches towards identification of a more exhaustive list of experimentally

determined envelope proteins were used on the chloroplast envelope from Arabidopsis. Ferro and co-workers (Ferro *et al.*, 2003) and Froehlich and co-workers (Froehlich *et al.*, 2003) developed two independent approaches, which identified more than 100 and 350 proteins, respectively. Again, the study by Ferro *et al.* (2003) was targeted to the hydrophobic core of chloroplast envelope and, various treatments (solvent, salt, and alkaline treatments) of the purified membrane fraction were performed (as reviewed in Ephritikhine; Rolland *et al.*, 2006). As a consequence, most of the identified proteins were genuine hydrophobic envelope membrane proteins. A deeper analysis revealed that the vast majority of these proteins were: (i) involved in ion and metabolite transport, (ii) components of the protein import machinery, (iii) involved in chloroplast lipid metabolism, and (iv) soluble proteins like proteases and proteins involved in carbon metabolism or in responses to oxidative stress. Almost one-third of the newly identified proteins had no known function (Rolland *et al.*, 2003). The other study (Froehlich *et al.*, 2003) was not based on pre-selection of hydrophobic envelope membrane proteins and identified three times as many proteins as Ferro *et al.*(2003). This indicates higher sensitivity since some less hydrophobic and peripheral, but genuine envelope proteins were

identified by Froehlich *et al.* (2003), but excluded from the study of Ferro *et al.* (2003). However, as a significant proportion of the 350 proteins identified by Froehlich and co-workers (Froehlich *et al.*, 2003) were known components of the stroma or the thylakoids as well as some non-chloroplast proteins (van Wijk *et al.*, 2004), the definitive subplastidial localization of these proteins would require further validation. Another study targeted the outer envelope membrane of pea chloroplasts (Schleiff *et al.*, 2003). This study combined the selection of b-barrel proteins from the complete *Arabidopsis* genome (Table 1) with protein identification from highly purified outer envelope membranes of pea chloroplasts. In addition to already known envelope components, four new proteins of the outer membrane of chloroplast envelope were identified (Schleiff *et al.*, 2003). Weber and co-workers (Weber, Schwacke, and Flugge, 2005) then published an interesting review article in which they provided an inventory of the known or predicted solute transporters of the plastid envelope membrane. Recent progress in determining the outer envelope membrane composition indicates that this envelope membrane plays an important role not only for translocation of various molecules, but also for regulation of metabolic activities and signaling processes. Inoue (2007) reviews the known outer envelope

membrane proteome, including proteins whose location has been confirmed by various methods or predicted based on their sequence similarity to known proteins. As mentioned above, proteomics analysis of the chloroplast envelope is limited by low amounts of the envelope proteins compared to stroma and thylakoid membranes. Use of the model plant, Arabidopsis, introduces additional technical problems that limit yield, particularly compared to pea or spinach. These non model plants are easily available throughout the year and remain models of choice for large-scale preparation of pure high-quality intact chloroplasts and consequently, larger amounts of envelope membranes as compared to Arabidopsis. A pea chloroplast envelope membrane proteome sample was thus analyzed using the species-specific database generated by pyrosequencing. As non-species-specific database controls, the obtained data were then compared to comprehensive cDNA databases from *M. truncatula* and A.thaliana. Applying stringent criteria, a total of 8,222 spectra were matched to 255 non-redundant (NR) proteins using a combination of pea, Arabidopsis or Medicago databases (Braütigam *et al.*,2008). Of these proteins, the pea database allowed matches of 5,012 spectra against 221 NR proteins (86% of the total), the Medicago database yielded 1,977 matched spectra on 125 proteins (49% of the total), and

only 32% or 82 proteins could be identified using the Arabidopsis database. From these data, it was concluded that low-coverage massively parallel pyrosequencing of cDNAs facilitates proteomics in non-model species (Braütigam *et al.*,2008). A quantitative proteome analysis of differentiated BS and mesophyll membranes was performed using techniques compatible with membrane proteomes and also taking advantage of a new, fast and highly accurate mass spectrometer, the LTQ Orbitrap.

As well as determining various adaptations of photosynthetic functions or metabolic machineries, the study also determined functional differentiation of envelope transporters (Majeran *et al.*, 2008). More recently, comparison of proplastid and chloroplast envelope proteomes and the corresponding transcriptomes of leaves and shoot apex was performed which allowed revealing a clearly distinct composition of the proplastid envelope especially when considering the small molecule and protein transport across proplastid envelope membranes (Braütigam and Weber, 2009). The identification and accurate localization of chloroplast envelope proteins from *Arabidopsis* was also recently revisited in *Arabidopsis*. Using a large scale and semiquantitative proteomics approach (spectral count), together with an in-depth investigation of the

literature, the envelope localization could be assessed for 300 proteins exclusively detected in the chloroplast envelope and 460 proteins when considering proteins enriched in the envelope fraction, but also shared with another chloroplast subcompartment (Ferro *et al.*, 2010). All these data provide evidence that envelope membranes are indeed one of the most complex and dynamic systems within the plant cell. Most of the available data on stromal components were derived from targeted biochemical and molecular approaches and from a global knowledge of the compartmentation of the cell metabolism, whereas envelope or thylakoid membranes were targeted in various proteomics studies (Lunn *et al.*, 2007). Proteomics data and functional annotation are available via the Plant Proteome Database (http://ppdb.tc.cornell.edu/). A major advance in the characterization of the chloroplast stroma proteome of *Arabidopsis* came from van Wijk and coworkers. Given the complexity of the stromal proteome, only a small number of stromal protein complexes in Arabidopsis had been characterized. Using highly purified chloroplasts extracted from Arabidopsis leaves, 241 proteins were identified from the stroma, representing approximately 99% of the stromal protein mass (Peltier *et al.*, 2006). Moreover, the study questioned several aspects of the stroma proteome: (i) experimental identification of the stromal

proteome with emphasis on distinguishing between paraloguous proteins, (ii) determination of approximate and relative accumulation levels of identified stromal proteins (relative protein masses and relative concentrations), (iii) identification of their native masses when present within complexes (proteins were separated by native gel electrophoresis), and (iv) collection of previously available information on plastid PPIs in higher plants. The analysis covered most known chloroplast functions, ranging from protein biogenesis and protein fate to primary and secondary metabolism, and a number of new components were identified. The stroma proteome of Arabidopsis was revisited by the same group (van Wijk *et al.*, 2004) resulting in the identification of 550 stromal proteins (Zybailov *et al.*, 2008). All these data are available within the PPDB database.

2.6.2 Thylakoid lumen - Solubility of the thylakoid lumen proteins presented the same advantages as the stromal proteins and, thus, could be also analyzed by 2-DGE. Of note, the identification of proteins present in this compartment thus preceded proteomics analyses of membrane fractions of the chloroplast. Initial study on thylakoid lumen was on spinach, where the major aim was to design a procedure for the isolation of the thylakoid lumen for characterizing luminal proteins (Kieselbach *et al.*, 1998). The same group published the

soluble luminal fraction of Arabidopsis thylakoids resolving 300 protein spots by 2-DGE, and identified two proteins, namely plastocyanin and a putative ascorbate peroxidase (Kieselbach *et al.*, 2000). In 2000, the first large-scale proteomics study was performed on the soluble and peripheral proteins of pea thylakoid membranes (Peltier *et al.*, 2000). Out of an estimated 200 proteins, more than 60 proteins were assigned with their detailed analysis of targeting signals. However, to fully utilize the benefit of the Arabidopsis genome sequence and to get deeper insight into the thylakoid lumen proteome in silico, Peltier and coworkers published a second proteomics study on its luminal and peripheral thylakoid proteome (Peltier *et al.*, 2002). A total of 81 proteins were identified using MS/MS. Importantly, they developed an approach to predict the thylakoid lumen proteome in silico by using characteristics protein parameters derived from the sequenced proteins. Detailed analysis of known or predicted proteins revealed that the main functions of the thylakoid luminal proteome are to support protein folding and proteolysis of thylakoid proteins and to protect against oxidative stress (Peltier *et al.*, 2002). The very same year Schubert and co-workers independently reported the thylakoid luminal proteome again in Arabidopsis (Schubert *et al.*, 2002). Although only 36 proteins were identified, a comparison was made

with the identified 22 spinach thylakoid lumen proteins and the luminal proteins were also predicted in silico. Based on these independent experimental and in silico analyses, the entire luminal proteome of Arabidopsis was estimated to comprise _80 proteins. As mentioned in the previous section, only one differential proteomics study was used to investigate the thylakoid lumen to reveal the presence of new lumen proteins (Goulas *et al.*, 2006). When combined, the above-cited studies yielded more than 100 proteins (Kieselbach and Schröder, 2003; van Wijk *et al.*, 2004). Interestingly, these studies have shown that chloroplast lumen proteins play an important role for the regulation of photosynthesis, but are not restricted to the generation of the pH gradient that fuels ATP synthesis. However, many of the predicted luminal proteins were found to be present at concentrations at least 10,000-fold lower than proteins of the photosynthetic apparatus (Peltier *et al.*, 2002). It is thus expected that previously unidentified/undetectable luminal proteins could be recovered during more recent studies targeted to the chloroplast (Zybailov *et al.*, 2008).

2.6.3 The thylakoid membrane - Initial MS-based studies of the thylakoid membrane proteins in spinach and pea were essentially performed on antennae or reaction-center subunits to identify the

composition of the photosynthetic complexes and to detect PTMs associated with these abundant proteins. Whitelegge and coworkers used ESI-MS to catalog intrinsic membrane proteins of the D1 and D2 reaction-center subunits from spinach thylakoids, to identify protein complexes components and to provide insights into native protein/protein interactions and their PTMs (Whitelegge, Gundersen, and Faull, 1998). Furthermore, MS analysis of tryptic peptides released from the surface of Arabidopsis thylakoid membranes was used to characterize the reversible phosphorylation of chloroplast thylakoid proteins (Vener *et al.*,2001). These studies revealed and confirmed earliest data that various subunits of the PSII and light-harvesting polypeptides LHCII are phosphorylated; some of these phosphorylation events were also found to be reversible in response to light/dark transitions. Zolla and co-workers also studied the light-harvesting proteins (LHCI or LHCII) from various monocot and dicot species and determined their intact MMs (Zolla *et al.*, 2002; Zolla *et al.*, 2003). Other than identifying the most abundant LHC proteins, the described HPLC method is very useful for comparison of the LHC proteins within a single plant or among different plant species. Whitelegge and co-workers also ESI-MS coupled with reverse-phase chromatography to catalog all detectable proteins in samples of PSII-

enriched thylakoid membrane subdomains (grana) from pea and spinach (Gomez *et al.*, 2002). Only 30 proteins were identified proteins, however, the study provided important data on the phosphorylation of several PSII subunits. One year latter, the same group reported a set of 58 nuclear encoded thylakoid membrane proteins from four plant species (Gomez *et al.*, 2003) and assigned experimentally the N-termini of all these proteins. Information thus obtained was used to test, on thylakoid membrane proteins, the various existing tools predicting plastid localization and/or cleavage sites in experimentally identified transit peptides. The first in-depth analysis of the thylakoid membrane was published by van Wijk and co-workers (Friso *et al.*, 2004), resulting in the identification of 154 proteins and the foundation of the PPDB (http://cbsusrv01.tc.cornell.edu/users/ppdb/). The same group later identified more than 240 proteins thylakoid membrane proteins, of which 86 were unknown (Peltier *et al.*, 2004). These proteins, combined with other known thylakoid or plastid envelope proteins, were assigned to functional categories and the corresponding information was also integrated in the PPDB.

2.6.4 The whole chloroplast experimental proteome - Prediction of proteins in the plastid proteome has been a matter of debate. It is the

subject of many studies that are complementary to proteomics-based data, which may even further help to define novel rules for protein import into organelles or their subcompartments (Baginsky and Gruissen, 2004; van Wijk *et al.*, 2004; Sun, Emanuelsson, and van Wijk, 2004). These analyses however converge and, ca. 3,000 proteins are estimated to be required to build a fully functional chloroplast proteome (Jarvis *et al.*, 2008). A few years ago, Baginsky and co-workers published a massive proteomics-based study targeted to the Arabidopsis chloroplast proteome with near-complete protein coverage for key chloroplast pathways, such as carbon fixation and photosynthesis (Kleffmann *et al.*, 2004). However, and despite the identification of almost 700 proteins, fewer proteins were identified from metabolic pathways that are known to be downregulated under light. These data are now completed by a huge effort performed by the same group through the proteome analysis from various plastid types. Aspecific PPDB (plprot) was created that combines proteomes information of various plastids but also data issued from plastid proteome analyses from other laboratories. This plprot database is accessible at http:// www.plprot.ethz.ch (Kleffmann *et al.*, 2006). These researchers and others also went a step further into the comprehension of the regulation of the chloroplast metabolisms and

functions in establishing PTMs of plastidial proteins, notably redox modifications in relation to day/light (Buchanan and Balmer, 2005; Baginsky and Gruissem, 2009; Lindahl and Kieselbach, 2009; Reiland *et al.*, 2009). More recently, a large-scale analysis of the purified chloroplasts from Arabidopsis leaves provided the most comprehensive chloroplast proteome to date with the identification of 1,325 proteins using nLC-Q-TOF and nLC-LTQ-Orbitrap MS (Zybailov *et al.*, 2008). Further annotation allowed identification of more than 900 proteins that could be unambiguously assigned to the chloroplast; these included some previously unknown plastid components. With this huge amount of data, an expanded PPDB (http://ppdb.tc.cornell.edu) was generated in which all MS data are projected on identified gene models (Sun *et al.*, 2009). Based on the MS-derived information and a literature survey, more than 1,500 Arabidopsis proteins were manually assigned a subcellular localization. However, the accurate subplastidial localization of many chloroplast proteins often remains hypothetical. This is especially true for envelope proteins. Ferro and co-workers recently went a step further into the knowledge of the chloroplast proteome by focusing, in the same set of experiments, on the localization of proteins in the stroma, thylakoids, and envelope membranes. LC-MS/MS-based

analyses first allowed building up the AT_CHLORO database, a comprehensive repertoire of more than 1,300 chloroplast proteins (Ferro *et al.*, 2010). The partitioning of each protein in the three chloroplast compartments was then assessed by using a semiquantitative proteomics approach (spectral count). These data, together with an in depth investigation of the literature were compiled to provide accurate subplastidial localization of previously known and newly identified chloroplast proteins (Ferro *et al.*, 2010). The spectral counting-based strategy was further used to revisit the subplastidial compartmentation of the chloroplast metabolisms and functions (Joyard *et al.*, 2009; Joyard *et al.*, 2010).

3. Environmental factors and cellular processes

The littoral coastal zone is characterized by severe environmental gradients, which mold distribution of populations and species of marine organisms. In a framework of conservation and restoration of biodiversity and in order to predict responses to environmental changes and to develop ad hoc conservation strategies, it is crucial to improve our knowledge about the limits of physiological acclimation, physiological plasticity, and intraspecific traits variation, of species living along environmental gradient (Thomas *et al.*, 2004; Schmidt *et al.*, 2008; Thomas *et al.*, 2010; Hill *et al.*, 2010). Along the coastline all over the world, excluding polar areas (Green and Short, 2003), seagrasses form among the most productive and neglected marine ecosystems, providing an high number of ecosystem's services, also in comparison to terrestrial habitats (Costanza *et al.*, 1997; McArthur and Boland, 2006). Seagrass meadows are very sensitive to disturbance and are being lost rapidly in both developed and developing parts of the world (Short and Wyllie-Echeverria, 1996; Waycott *et al.*, 2009), with only occasional efforts for mitigation and restoration. Seagrass loss has been attributed to a broad spectrum of

anthropogenic and natural causes that largely diminish their habitat, affecting their distribution and diversity (Orth *et al.*, 2006; Waycott *et al.*, 2009). For marine plants, seasonal and daily variations in light availability and temperature represent the mains factors driving their distributions along the bathymetric cline. Changes in these environmental factors, due to climatic and anthropogenic effects, can compromise the survival of these key ecosystem-engineering species (Doney *et al.*, 2002). Plasticity of *P. oceanica* long-living clones must play an important role on the persistence of the species, being able to survive changes of environmental conditions, as the ones experienced by the unstable highly-impacted Mediterranean coastline.

3.1 Variations in light and temperature

For seagrasses, seasonal and daily variations in light and temperature represent the mains factors driving their distribution along the bathymetric cline. Changes in these environmental factors, due to climatic and anthropogenic effects, can compromise their survival. In a framework of conservation and restoration, it becomes crucial to improve our knowledge about the physiological plasticity of seagrass species along environmental gradients. Here, we aimed to identify

differences in transcriptomic and proteomic profiles, involved in the acclimation along the depth gradient in the seagrass *Posidonia oceanica*, and to improve the available molecular resources in this species, which is an important requisite for the application of eco-genomic approaches. The mass spectrometry methodology has coupled with 1D-SDS electrophoresis and labeling free approach. Mass spectra were searched in the open source Global Proteome Machine (GPM) engine against plant databases and with the X!Tandem algorithm against a local Database. EST libraries had only the 3% of transcripts in common. A total of 315 peptides belonging to 64 proteins were identified by mass spectrometry. ATP synthase subunits were among the most abundant proteins in both conditions. Both approaches identified genes and proteins in pathways related to energy metabolism, transport and genetic information processing, that appear to be the most involved in depth acclimation in *P. oceanica*.

3.2 Photosynthetic processes

Light availability, both intensity and quality, influences directly and indirectly chloroplast metabolism (Jiao *et al.*, 2007). The modulation of photosynthetic machinery is critical in the short term (day by day)

and long-term (season, years) adaptation to environmental light. In photosynthetic organisms, the adaptation to different light conditions happens through adjustments of cellular homeostasis to maintain a balance between energy supply (light harvesting and electron transport) and consumption (cellular metabolism). The regulation of these mechanisms involves changes in the expression levels of both mRNA and mature proteins. During the sampling, the irradiance at the deep stand was about 1/10 of the irradiance present at the shallow stand, with values that are very close to the theoretical minimum light requirement estimated for *P. oceanica* (~9–16% of surface irradiance, Lee *et al.*, 2007). Hence, many genes and proteins belonging to the photosynthetic machinery resulted differentially regulated between stands, in order to perform photosynthesis under such different light conditions. Transcriptional and proteomic profiles showed high differentiation on Chlorophyll a-b-binding (*Cab*) proteins between the two depths. An increase of Chlorophyll concentration under low-light was reported for other seagrasses (Dennison *et al.*, 1990; Sharon *et al.*, 2011).

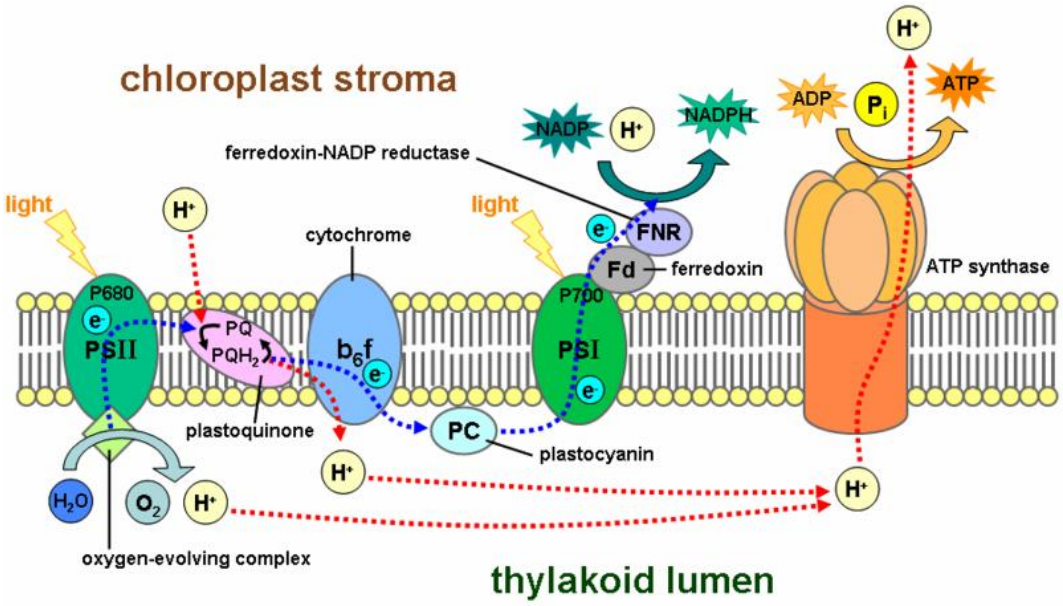

Fig.11 Light-dependent reactions of photosynthesis at the thylakoid membrane

In *P. oceanica* chlorophyll rate was reported to vary not only along the depth gradient, but also during different seasons (Pirc *et al.*, 1986). In addition, differences among *Cab* proteins identifie between depths, suggest that in *P. oceanica* different *Cab* proteins are utilized for the assembly of the antenna complex, in response to specific photo-acclimation processes. It seems that, to prevent photo-damage due to high-light, plants evolved different strategies, such as the shrinking of PSII antenna size (Escoubas *et al.*, 1995) and thermal dissipation (Elrad *et al.*, 2002). Changes in antenna pigments compositions in low- light were also suggested for *P. oceanica* and for other seagrasses by Casazza and Mazzella (2002). The relative quantity of transcripts and proteins recognized in this study also suggests an

increase in PSII and PSI transcripts in deep plants in respect to the shallow ones (especially as regards as PSI). Photosynthetic-organisms balance electron flow between the two photosystems by modulating both antenna size and photosystem stoichiometry (Chitnis *et al.*, 2001), in response to light intensity and quality. The redox status of the whole cell and of the chloroplast and the ratio between ATP and NADPH could also contribute in modulating PSI/II relative abundance (Chitnis *et al.*, 2001). PSI/II ratio was found modified across depth also in the seagrass *Halophila stipulacea* (Sharon *et al.*, 2011), in macroalgae (Fujita *et al.*, 1997; Yamazaki *et al.*, 2005) and cyanobacteria (Levitan *et al.*, 2010) as to indicate that this could be a general photoacclimatory mechanism. At the present, we are not able to explain the regulative mechanisms underlying this differential modulation between shallow and deep plants, but similar patterns of PSI/II ratio were already observed in shallow *P. oceanica* meadows growing under different light conditions (Mazzuca *et al.*, 2009). Authors reported a reorganization of the thylakoid architecture under low-light conditions, that is consistent with the rearrangement between the two photosystems, since approximately 85% of PSII is located in the apprised domains of the grana and 64% of PSI is located in the stroma lamellae. Another interesting hint suggested from our

data for the *P. oceanica* photosynthetic acclimation involves the enzyme RuBisCo. The expression pattern of this enzyme between the two light conditions was different from the expectation: we measured, in fact, a similar content of this protein between shallow and deep stations, with a slightly higher abundance in low-light, especially for what concern the large subunit. This is in contrast with previous results, where Mazzuca *et al.* (2009) showed a clear decrease of the same protein in low-light condition in *P. oceanica*. The activity of RuBisCo responds to different environmental signals including light, changes in source-sin balance, temperature and circadian rhythms (Portis *et al.*, 2003). However, regulation of RuBisCo is mediated, among others, by the activity of the chaperone Ribulose bisphosphate carboxylase/oxygenase activase A (RCA). This protein was identified in our collection as over-expressed, even if at low levels, in low-light condition. RCA is thought to have a key role in the regulation of photosynthesis under different environmental stress conditions (Portis *et al.*, 2003) and during the daily cycle (Yin *et al.*, 2010). In a recently study of Yamori *et al.* (2012) it was reported that in low-light condition, high expression of RCA contributes to maintain RuBisCo in high active state, helping in assuring high levels of CO_2 assimilation also under shade conditions. These observations open the

question regarding the real regulation mechanism of RuBisCo in *P. oceanica* in response to light, especially for what regards limiting light conditions.

3.3 Cellular energetic metabolism

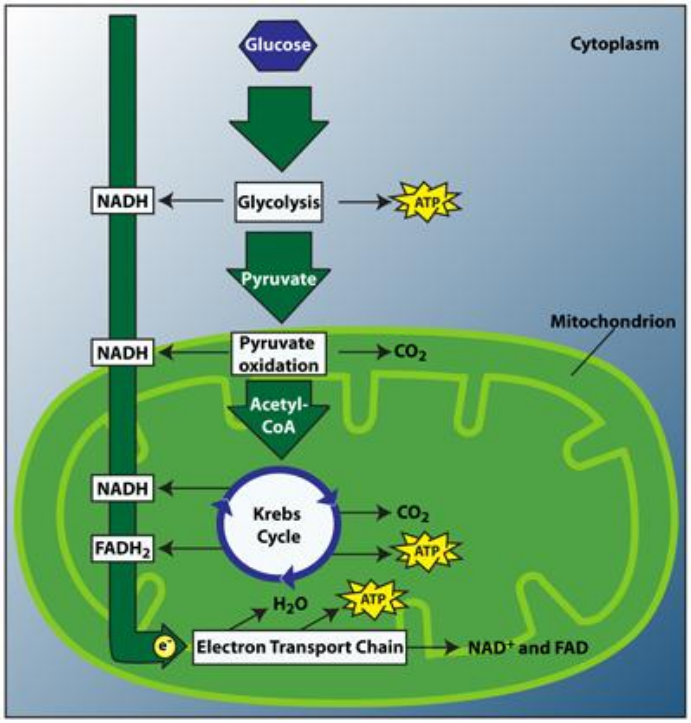

Fig.12 Cellular energetic processes

For what concerns respiration, an overall increase of related transcripts and proteins was recorded in shallow plants, probably related to the higher temperature present in respect to the deeper portion of the meadow plants (Touchette and Burkholder, 2000). Nevertheless, considering separately the regulation of each of the three main stages of the respiratory process, we see that glycolysis and

electron transport chain steps were strongly enhanced in high light, while the tricarboxylic acid (TCA) cycle was higher in low light. The understanding of the regulations of these pathways in plants is further complicated by the interactions between them and many other key elements (Fernie *et al.*, 2004). Among the putative regulatory enzymes of mitochondrial activity (Bunney *et al.*, 2001), a protein like 14-3-3 was recognized in our peptide collections. Collectively, plant 14-3-3s isoforms, which bind to phosphorylated client proteins to modulate their function, are implicated in an expanding catalogue of physiological functions and are affected by the extracellular and intracellular environment of the plant. They play a central role in the response to the plant extracellular environment, particularly environmental stress, pathogens, and light conditions (Denison *et al.*, 2011).

3.4 Adapting to changes in salinity seagrasses

P. oceanica usually grown in a salinity range between 36.5 psu (in the Alboran Sea , Ramirez *et al.* , 2005) and 39.5 psu (in the Aegean Sea; Besiktepe , 2003). Only exceptionally, this species grows in brackish water with a salinity less than 28 psu (in the Dar- danelles Strait and in the Marmara Sea ; Meinesz *et al.* , 2009) or tolerate high salinity up to

48 psu (in the costal lagoon Lagoon at Marsala ; Tomasello *et al.* , 2009), probably due to the selection of genotypes adapted to persistent stress conditions. However, in places where this species is present , meadows of *P. oceanica* are usually adapted to a very narrow range of variation of salinity , being more sensitive to the increase rather than a reduction (Fernández- Torquemada and Sánchez- Lizaso , 2005). The meadows of *Posidonia* are the subject of ocean conservation strategies and monitoring by the EU 's (the Habitats Directive , the Marine Strategy Directive), since the spread in the whole area of the Mediterranean desalination industry (Fritzmann *et al.*, 2007 ; . Boye *et al.*, 2008; Bashitialshaaer *et al.*, 2011), the concern about the effects that their hypersaline effluent (brine) perform on the ecological status and distribution of seagrass *P. oceanica* grows more and more, increasing at the same time, also the need to explore the molecular mechanisms of tolerance that this and other species of the Mediterranean to the ipersalinità induced. The combination of genomic analysis, proteomics and cytological recently provided experimental evidence on the induction of aquaporins PIP1;1 in leaf tissue of *P. oceanica* exposed to salt stress (Serra *et al.* , 2011 ; Mazzuca *et al.*, 2009). The aquaporins play an essential role in the regulation of water balance and osmotic relations in plant cells

(Cushman *et al.*, 2001) and, therefore , the study of aquaporins might be relevant to a better understanding of plant response to salt stress. In addition, some plant aquaporins can also carry physiologically important molecules such as CO_2 and H_2O_2, boron or silicon (Maurel *et al.* , 2007). Thus, the combination of molecular biology techniques and analysis of physiological responses represent an effective approach to achieve significant progress in understanding the intrinsic mechanisms of different species of marine plants to cope with stress hypersaline. While most attention has been focused on the effects of the hypersalinity on the structure, morphology and physiology of *P. oceanica* , are in reality little is known about the effects on other species of seagrasses . In order to verify this type of response , we started a collaboration with the Spanish Oceanographic Institute on the study in mesocosms of *Cymodocea nodosa*, a species that inhabits the open coastal waters with salinity stable, but also hyper-saline lagoons and estuaries . This species shows a capacity for growth and functions of the other photosynthetic higher seagrass , and is presumed to have a greater tolerance to salinity increments than *P. oceanica* . There are experiments in mesocosms in support of this hypothesis (Sandoval -Gil *et al.* , 2012) , in which photosynthesis and carbon balances are little affected by the hypersalinity than *P.*

oceanica and analysis of water relationships revealed that this marine plant is best suited to overcome salt stress conditions. Unlike *P. oceanica*, there are no studies on the response to salinity at the molecular level of *C. nodosa* until now. In order to verify the existence of a common response to all seagrasses to variations in salinity, a study was initiated in proteomic *C. nodosa* exposed to different concentrations of salinity in controlled conditions. Moreover, the need to have the availability of fresh tissue constantly and to maintain the plants in optimum conditions and controlled pushed to the choice of using plants grown in defined systems for aquariums "mesocosms". The use of naturalized populations in mesocosms provide a useful tool for the study and understanding of the complex interactions in natural populations, as individual events of stress can be played individually and monitored, so the plant's response to stress can be better understood and investigated. Last but not least mesocosm systems, large-scale, could provide useful models of prediction to certain environmental events and offer technological solutions for the conservation and management of environmental resources, such as the reforestation of *P. oceanica* to preserve the meadows of the Mediterranean. At the laboratories of Murcia Spanish Oceanographic Institute, has long housed a large facility with six

tanks each of capacity 500 L of seawater, which ensures the maintenance of the plants under controlled conditions.

The goal of this collaboration was to experimentally determine the conditions described as "stressful" and evaluate the physiological and molecular mechanisms of seagrasses in the Mediterranean such as *P. oceanica* and *C. nodosa*. The research covered the phenomena of acute response and resilience of *C. nodosa* to hypersaline stress in mesocosm in the laboratory (Fernández- Torquemada and Sánchez-Lizaso , 2005; Marín - Guirao *et al.*, 2011). The results obtained in these studies show that the increased salinity significantly influence the rate of growth of leaves, induces necrotic lesions and increases mortality. Significant changes were observed in the uptake of nutrients, such as a reduction in photosynthetic carbon assimilation, an increase in the rate of respiration and degradation of carbohydrates (Gacia *et al.* , 2007; Lizaso - Sánchez *et al.* , 2008; Ruìz *et al.*, 2009). This has led to the hypothesis that the response to salt stress persistent, through the metabolism of carbohydrates and amino acids influence on the phenomena of osmoregulation (Touchette *et al.*, 2007). Sandoval -Gil *et al.* (2012) have obtained experimental evidence of the increase in osmotic potential in leaves of *Posidonia* exposed to increasing ocean salinity and the involvement of soluble sugars and

amino acid proline in osmoregulation changes. Several experiments have already

been carried out in the field and in the laboratory (Gacia *et al.* , 2007; Ruìz *et al.*, 2009).

3.5 Adaptation of seagrasses to light changes

Studies of the physiology of photosynthesis showed that both the general layout of the equipment of photosynthetic pigments in the chloroplast of mature leaves of *Posidonia oceanica* and its response to stress following light arrangements similar to those found in terrestrial plants (Ruitz.and Romero, 2003). These studies, however, have been conducted on populations of *Posidonia* meadows of sea surface (-5m), where the share of actual solar radiation for photosynthesis (PAR) does not differ from the values needed by the emerged plants. In this sense, little or nothing is known about the adaptability of the kit of pigments and enzymes of the main metabolic pathways of chloroplast with increasing depth to which this plant goes and it can reach, in very clear waters 60 meters, where the quality and quantity of light seem theoretically incompatible with the photosynthetic activity of a higher plant. The study of the proteome is important to examine all the proteins expressed at a given time in and conditions in these

organelles. In addition to identifying the primary sequence of amino acids of chloroplastic new proteins (isoforms) or to elucidate specific sequence mutations or post-trasductional modifications that are fuctional to the acclimation of the submerged life style and in acclimation to depths.

3.6 Adaptation of seagrasses to the depths

The analysis focused specifically proteome through foliar protein extraction , electrophoresis , sequence analysis by mass spectrometry and protein identification by bioinformatics software . The results obtained allowed us to highlight proteins differentially expressed in changing light conditions related to different metabolic pathways primary and secondary structured as the proteomic approach has allowed us to detect differentially expressed proteins in natural populations adapted to three different depths.

Posidonia oceanica is the only able to adapt and colonize deep water reaching the limit of the band exceptionally photophilous in extremely clear waters . Currently there are few natural populations where environmental conditions favor the survival of the population or meadow to great depths. Among the most interesting sites of the

Mediterranean, the coast of Corsica have retained some aspects of which offer natural populations of *P. oceanica* in excellent condition and in some cases of progression. The coast facing the "Station de Recherche et Océanographiques sous- marines" (Stareso , Fig.13) was the subject of an intensive sampling and monitoring in October 2011 as part of the COST Action ES0609 "*Seagrasses productivity. From genes to ecosystem management*". During ten days, twenty researchers who represent a range of disciplines (molecular biology, physiology , botany , ecology, oceanography , underwater acoustics) analyzed in synergy the *Posidonia oceanica* which extends continuously from 5 m up to more than 40 m depth.The study of protein expression was carried out as a function of depth at 5 m, 20 m, 30 m at dawn and at noon . The proteomic data were obtained for all samples and analyzed as a function of the genomic analyzes and ecophysiological detected on the same samples by other research groups involved .

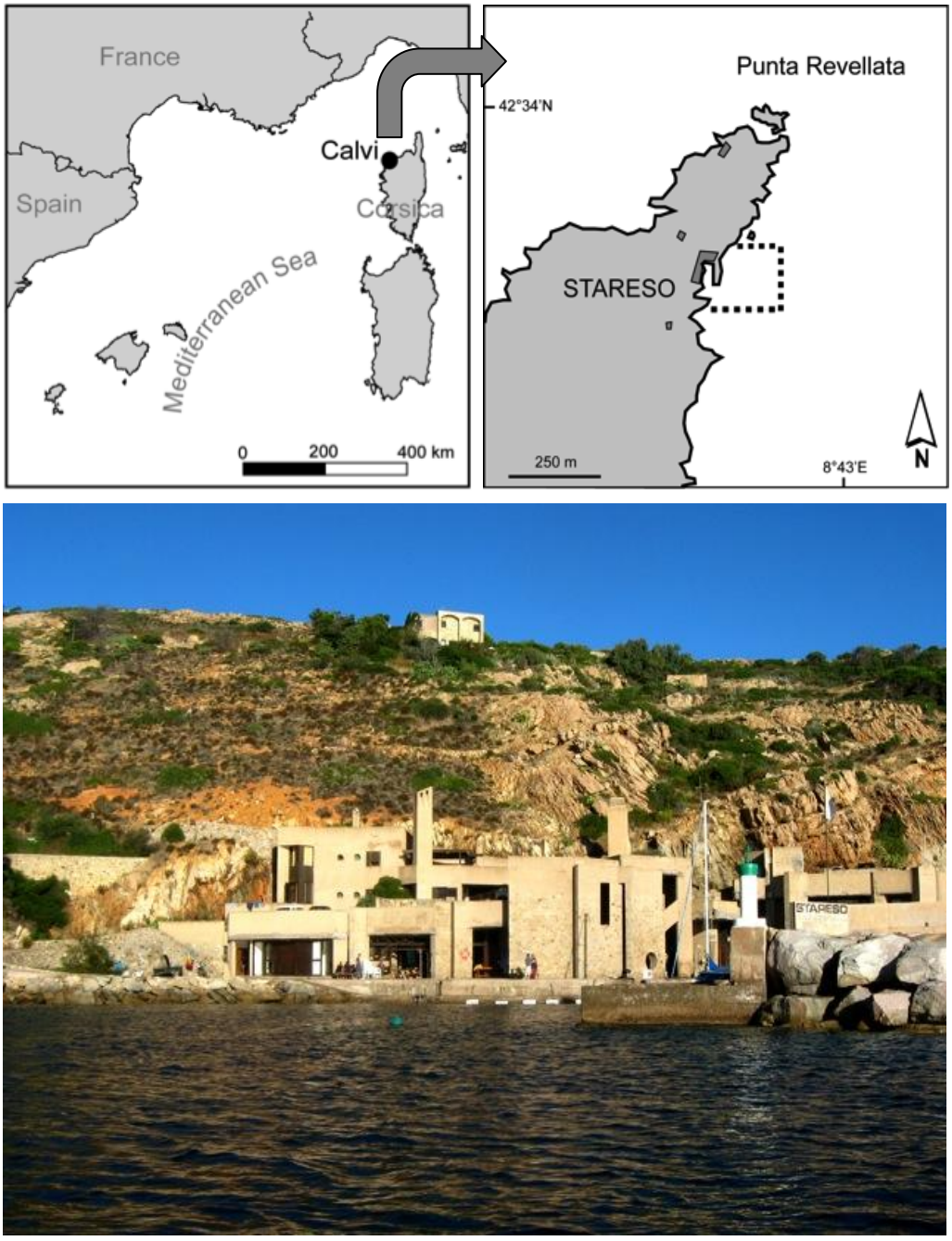

Fig.13 Location of the study area in (A) the Calvi Bay in the Mediterranean Sea of Corsica, (B) at the latitude and longitude of 8°450E, 42°350N (C) of the Station de Recherches Sous-marines et Océanographiques, STARESO.

4. Materials and methods

4.1 Culture and hypersaline treatments in the mesocosms

4.1.1 Field plant sampling – Cuttings of *Cymodocea nodosa* (no. 20 at least) were collected by SCUBA divers in July 2011 in a shallow bed (5-6 m deep) located in Isla Plana (Cartagena , Murcia, Spain). Each cuttings consisted of 10-15 shoots along a same rhizome; after cleaning, each cutting was transplanted in two separated aquaria, as described below.

Fig.14 Location of the *C. nodosa* meadow selected to collect plant material.

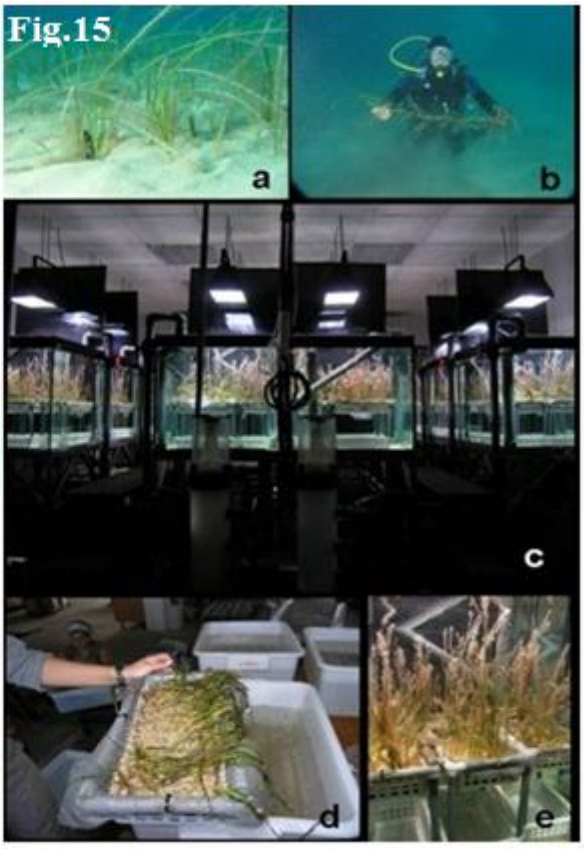

Fig.15 a) *Cymodocea nodosa* meadow at the plant collection site, b) diver during plant collection, c) aquariums of the mesocosm system, d) mounting the transplantation unit and e) detail of the transplantation units in the aquarium.

4.1.2 Mesocosm system - The mesocosm system consists of 2 glass aquaria filled with 1500 liters of sea water respectively and divided into three sections of 500 liters (sub - aquarium), each with its own source of illumination provided by a halide (Aqua Medic Aqualight - 400) at 400 W.

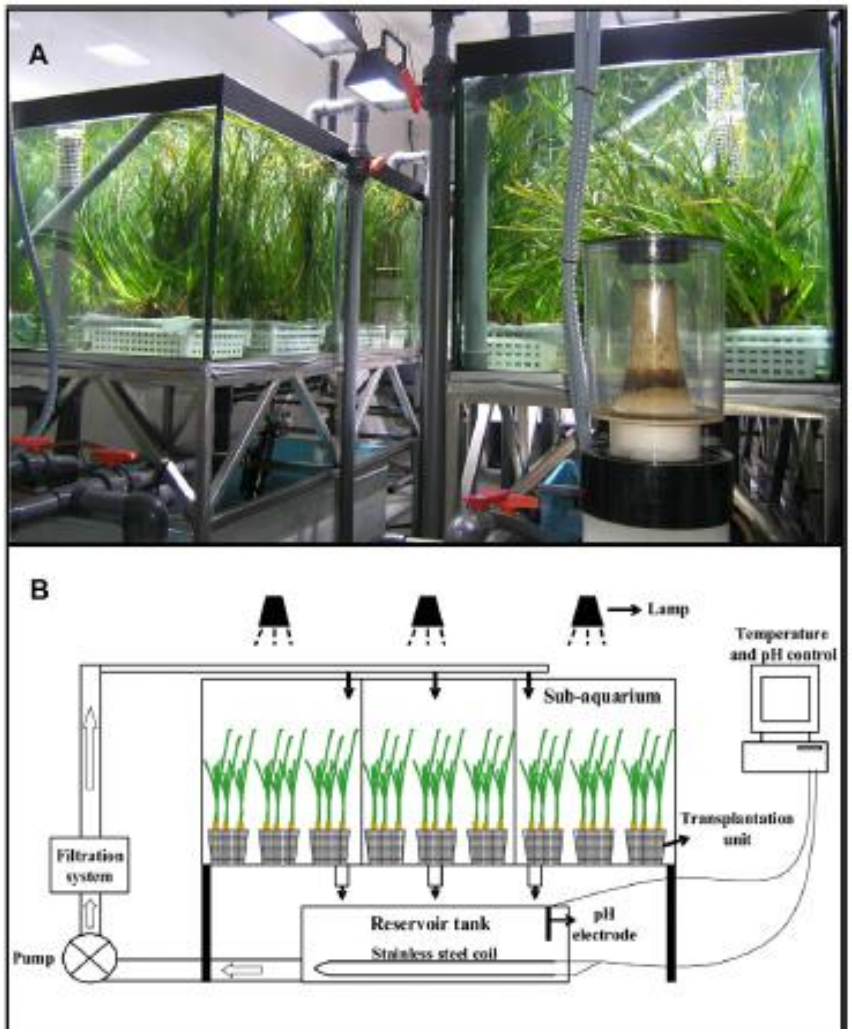

Fig. 16 (A) General view of the mesocosm system, and (B) simplified diagram of an experimental unit.

This light source is created by a highly homogeneous radiation in each sub-aquarium, measured just below the surface of sea water. Each

aquarium of 1500 liters has been integrated in a closed circuit fed with sea water from a circulating tank of 500 liters diverted to each of the three sub-tanks , and *vice versa*. This system of circulation of sea water has meant that the three sub - tanks have not been completely independent units . The sea water was circulated using a pump of 10,000 l / h^{-1}, allowing the complete replacement of the water in the system 124 times a day. Within each sub - aquarium , sea water in arrival has been diffused through a diffuser so as to create a homogenous movement of water. The water temperature was controlled by an automated high-precision (± 0.1 ° C) , designed specifically for the mesocosm system of the laboratory of the Spanish Center for Oceanography.

The quality of the sea water was controlled through a mechanical and chemical filtration continuously, checking the nitrates and phosphates every 15 days using standard colorimetric assays (Merck ®). Particular attention has been adopted for the pH of seawater, as it was found to be a critical factor in the study of physiology in marine plants. The pH was continuously recorded and monitored with a pH electrode connected to a control box (Aqua Medic AT- Control). The salinity was measured every day in each aquarium using a WTW conductivity meter (Model Cond.197i) and kept constant with the

addition of reverse osmosis water . The sea water used to fill the circuit mesocosm was selected by a nearby pristine open water area. This system is able to maintain healthy plants with survival rates at 100% for more than two months , long enough to achieve the objectives of the experiments .

4.1.3 Aquarium culture – The cuttings were immediately transported to the laboratory after their collection and used to assemble the transplant unit: cuttings were fixed onto a grid until reaching a density of leaves from 50 to 100, then they were put in a plastic box filled with clean natural sand (Fig 17).

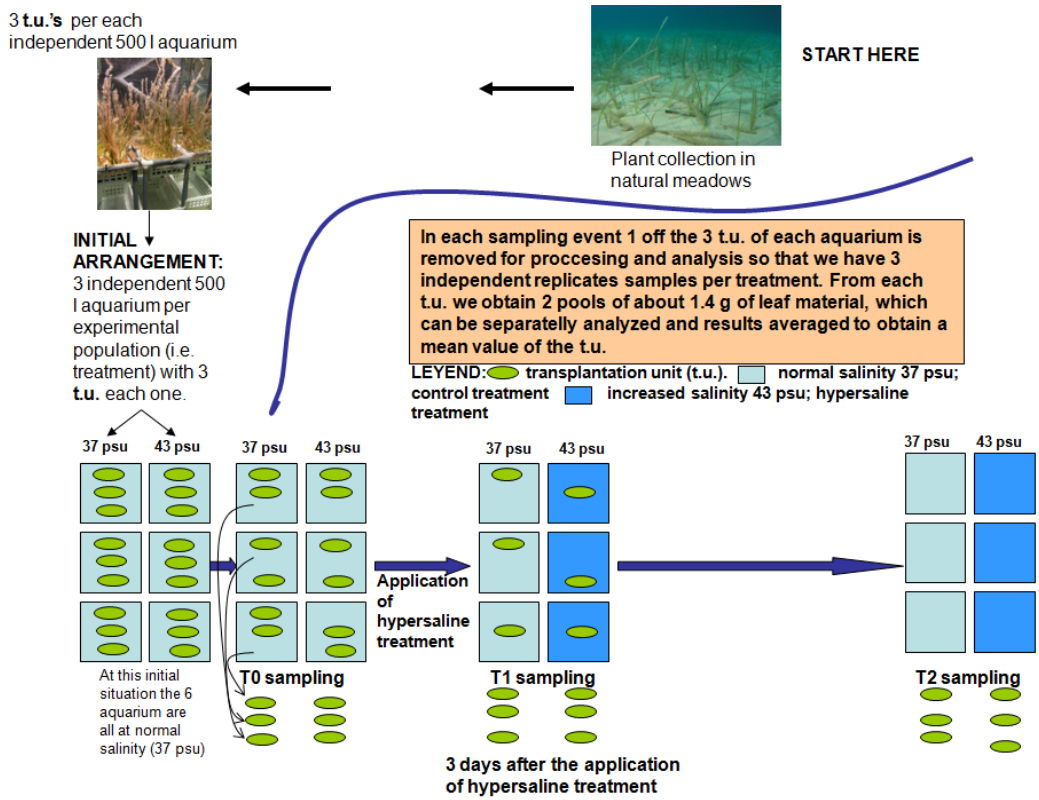

Fig. 17 Schematic representation of the experimental design

At least three transplant units were arranged in each of the six sub-aquaria. Cuttings were maintained for 7 days at 22 ºC and 37 psu for their acclimation, as control condition, with a saturating irradiance of ca. 300 □ mol quanta m^{-2} s^{-1} measured on the leaf tips on a 12 h:12 h light:dark cycle (i.e. 12.96 mol quanta m^{-2} day^{-1}). Seawater pH values of the two aquaria showed daily variations between 8.02 and 8.18, with maximum values during the light period and minimum in the dark period as a result of the photosynthetic activity of the seagrass.

After this period, 2 gr of fresh leaves were sampled randomly in the transplantation units from two acquaria, washed in sea water, frozen in liquid nitrogen and stored at -80 °C for further proteomic analysis.

4.1.4 Salinity experiment – After acclimation in aquaria, cuttings were used to perform the experiment at the short, medium and long term hypersaline stress. The salinity was increased up to 43 psu by adding sodium chloride in the circulating tank only in one aquarium to reach the hypersaline conditions; the second aquarium was maintained at 37 psu as the control. Light, temperature and pH remained unchanged. Salt concentration was monitored twice a day and eventually adjusted by adding new salt to the circulating tank or diluted with distilled water directly into the aquarium.

After 15 and 30 days under hypersaline stress leaves (2 gr) were randomly sampled in each transplantation unit; leaves were sampled also in control aquarium at same times. Tissues were washed, frozen in liquid nitrogen and stored at -80 °C. A schematic representation of the experimental design is shown in Figure 17.

At any time the transplant unit was chosen randomly in the aquarium and at the same time the measures for the PAM fluorometry and the osmolarity of the leaf were carried out. Once this extent, all the leaves were separated from the unit of transplantation for the subsequent proteomic analysis . We have chosen mature leaves avoiding the old tissue and tissue with spots, necrosis and injuries.

4.1.5 Extraction of total protein from leaf *C. nodosa* - The foliar tissue was cleaned, washed in sea water and quickly washed in distilled water to remove excess salt on the surface of the mesophyll. The samples were frozen immediately in liquid nitrogen and stored at -80 ° C. For each extraction 1.4 g of leaves were crushed in a mortar in liquid nitrogen until obtained a fine powder. This powder was aliquoted in 2 ml eppendorf; a volume of 10% TCA in acetone was added and centrifuged at 13000 rpm for 5' at 4 ° C. Subsequently, 4 washes were performed in 80% solution of acetone.

Fig. 18 Steps for extraction of total protein from leaf *C. nodosa*

After centrifugation the pellet was dried, preferably at ambient temperature. The powder was collected in an eppendorf and kept at -80 ° C for subsequent analysis or immediately processed for phenolic phase extraction.

4.1.6 Extraction and purification of proteins from the phenol phase

Approximately 0.1 g of powdered tissue was dissolved in 0.8 ml of phenol (buffered with Tris, pH 8.0 , Sigma , St. Louis , MO ml) and 0.8 ml of SDS buffer (30 % sucrose, 2 % SDS, 0.1MTris -HCl, pH 8.0, 5 % 2 - mercaptoetanol) in a 2 ml microtube . The samples were vortexed for 30 s and centrifuged at 13000 rpm for 5 min. The phenolic phase were added 5 volumes of 0.1 M Ammonium Acetate in cold methanol , and the mixture was stored at -20 ° C for 30 min. By centrifugation at 13000 rpm for 5 min proteins were precipitated. Two washes were performed with 0.1 M ammonium acetate in cold methanol, and two with cold 80% acetone, and centrifuged at 13000

RPM for 7 min. The final pellet was dried and dissolved in Laemmli 1DE buffer separation over-night.

4.1.7 Electrophoresis of leaf proteins of *C. nodosa* - It was prepared a gel at a concentration of 10 % acrylamide/bisacrylamide, according to the method of Laemmli (1970). The ratio of acrylamide/bisacrylamide is 12.5 % in the " running gel" and 6% in the "stacking gel". The samples were activated for 5' at 100°C before being loaded on the gel. The electrophoretic run was carried out at 60 mA for running in the "Stacking gel" and 120 mA in the "running gel" at constant power of 200 V. The electrophoresis had an average of 1 hour and 15 min duration. The gel was stained with Coomassie Blue over-night and subsequently destained with several changes in destaining solution (45 % methanol, 10% acetic acid).

As shown in Fig.23 , samples were loaded as follow: in the lane M) standard protein (Biorad range of molecular weights 250 kD -10 kD); lane 1) the control sample kept in the aquarium for 7 days acclimatization ; lanes 2 and 3) the samples at 37 psu (salinity control) and samples at 43 psu (hypersalinity) kept in mesocom for 15 days respectively; and finally lanes 4 and 5) the samples at 37 psu and 43 psu maintained in mesocosms for 30 days respectively.

4.1.8 In-gel digestion , mass spectrometry, bioinformatics analysis and identification of proteins of *C.nodosa* - After separation by SDS-PAGE , the bands for each lane at various conditions were manually excised from the gel, cut, S-alkylated and digested overnight at 37 ° C with trypsin (Wilm el al, 1996). Digested peptides were extracted from the gel with 25 mM NH_4HCO_3/ACN 1:1 (v/v) and the peptide mixtures were concentrated by evaporation in a vacuum centrifuge. The gel pieces were then treated with 5% (v / v) of formic acid and acetonitrile. After drying, the tryptic peptides were analyzed by tandem mass spectrometry by means of liquid chromatography (LC-MS/MS) using a mass spectrometer at high resolution (LTQ - Orbitrap XL). The chromatographic separations were carried out on a Waters XBridge C18 column (300 µM ID × 100 mm in length and 3.5 m per particle size) using a linear gradient of 5 to 90% ACN containing 0.1% formic acid with a flow of 4 µl/min, including the regeneration phase, a run lasted about 70 min. The acquisitions were made in scanning mode data-dependent MS/MS (with full scan range of 250-1800 m/z). Spectra acquired by LC-MS/MS were used to identify peptide sequences using the open-source system GPM software against the GPM plant database (http://plant.thegpm.org/ tandem/thegpmtandem.html).

Since the GPM plant database considers only a few species belonging to *Liliopsida*, excluding seagrasses, this procedure can lead to a loss of peptide identification by mass spectrometry. Thus, spectra acquired by LC-MS/MS were also used to identify peptide sequences using X!Tandem software (http://www.thegpm.org/tandem/index.html). X!Tandem is a search engine for identifying proteins by searching sequence collections in selected databases, including database built with a collection of sequences from many databases (Fenyö *et al.*, 2010).

To do this sequences from seagrasses and other species belonging to *Liliopsida* available in the UniprotKB database and the amino acid sequences of *P. oceanica* and *Z. marina* deduced from five ESTs libraries (Pooc_A, Pooc_B, Zoma_A, Zoma_B and Zoma_C) collected in the Dr.Zompo database (Wissler et al., 2009, http://drzompo.uni-muenster.de/) were included.

In the last case, it has been necessary first to create a protein database from the nucleotide sequences. The translation of each nucleotide sequence was performed using a translation tool available at http://www.ebi.ac.uk/Tools/st/emboss_transeq/5. For this, the most basic procedure is listing all possible ORFs from the six reading frames; the resulting list contains a large majority of protein sequences

that are unlikely to be real, but MS/MS data allow to discriminate between real and false polypeptide sequences (Armengaud, 2009). The use of all possible reading frames has allowed to optimize the peptide identifications (for details see Dattolo *et al.*, 2013).

4.1.9 Semi- quantitative analysis of proteins - The quantization of the proteins was performed by the method of spectral counting. The spectral count, is defined as the total number of spectra identified for a protein. This method is widely accepted (Zhang *et al.*, 2010). It is associated with the label-free method, and is based on the relative abundance of the proteins of interest. The quantization is obtained by dividing the number of mass spectra assigned to a given peptide of a specific protein by the total number of spectra allocated to all the peptides identified in each sample.

4.2 Purification of chloroplasts and organelle sub-fractionation

4.2.1 Field plant sampling - Leaf samples of *Posidonia oceanica* were collected by SCUBA divers in a shallow meadows (5-6 m deep) located in the area of San Lucido (CS) . Each cutting consists of shoot with 4-6 leaves attached to the intact rhizome. Cuttings were bring to

the lab as soon as possible and processed for the chloroplasts extraction and purification.

Fig.19 Location of the *P.oceanica* meadow selected to collect plant material.

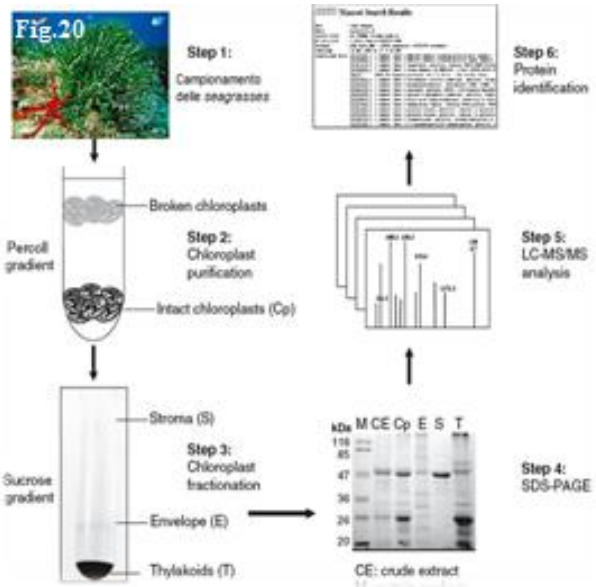

Fig. 20 Experimental design

4.2.2 Purification of chloroplasts- All procedures were performed in agreement with those reported in Rolland *et al.* 2003 (with subsequent modifications). Solutions and materials are listed in the Annex 1 to this chapter. The leaf tissue (10 g fresh weigth) was homogenated in the grinding buffer an d loaded on 60% Percoll gradients and centrifugated at 13300 g for 10 min. The intact chloroplasts were recovered at the level of dark green broadband at the bottom of the test tube and washed several times in washing buffer by centrifugation at 2070 g for 5 min at 4°C. The structural integrity of chloroplasts was assessed by observation under a fluorescence microscope (Fig 21).

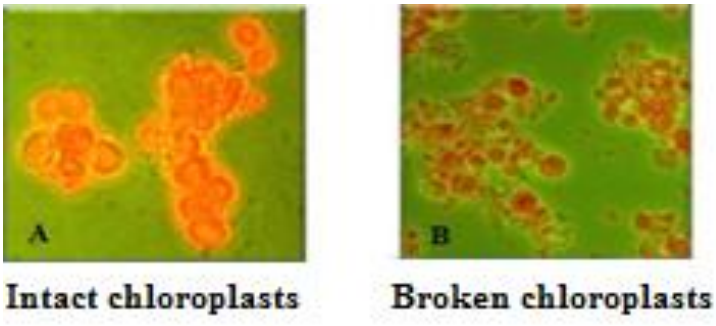

Fig.21 Intact and broken chloroplasts from P.*oceanica* shown by fluorescence microscopy

4.2.3 Electrophoresis of chloroplastic proteins on polyacrylamide gel with SDS (SDS -PAGE) - It was prepared a gel at a concentration of 10 % acrylamide/bisacrylamide, according to the method of Laemmli (1970). The ratio of acrylamide/bisacrylamide is 12.5 % in the " running gel" and 6% in the "stacking gel". The samples were activated for 5' at 100°C before being loaded on the gel. The electrophoretic run was carried out at 60 mA for running in the "stacking gel" and 120 mA in the "running gel" at constant power of 200 V. The electrophoresis had an average of 1 hour and 30 min duration. The gel is stained with Coomassie Blue over-night and subsequently destained with several changes in destaining solution (45 % methanol, 10% acetic acid). In the first lane we loaded the protein extract from foliar tissue , in the second the protein extract from intact chloroplasts, in the third the protein extract from broken chloroplasts and the last marker protein (Biorad 250 kd to 10 kD) (Fig .27).

4.2.4 Mass spectrometry , protein identification and sub-organellar localization - After SDS -PAGE , bands were excised with a scalpel as close to the edge of the band as possible, because it is important to reduce the volume of gel "background". The gel pieces, once that the bands were excised into cubes (ca. 1x1mm), were transferred into microcentrifuge tube. The gel pieces was washed with 100-150 µl of distilled water for 5 min. Acetonitrile was added for 10-15 min until the gel pieces dehydrated and became white.

After removing the liquid, the gel pieces were rehydrated in 10 mM dithiotreitol/0.1M NH_4HCO_3, incubated for 30 min at 56°C; thereafter the proteins were reduced by adding the acetonitrile. The acetonitrile was replaced with 55 mM iodoacetamide/0.1M NH_4HCO_3 and incubated for 20 min at room temperature in the dark. The iodoacetamide solution was removed and 100 µl of Acetonitrile were added; the gel particles were washed with 150-200 µl of 0.1M NH_4HCO_3 for 15 min at 37°C. The supernatant was removed with a vacuum centrifuge at each step. The gel particles were rehydrated in the digestion buffer containing 50 mM NH_4HCO_3, 5 mM $CaCl_2$ and 12.5 ng/µl of trypsin (Sigma) at 4°C for 30-45 min and removing the remaining supernatant; 5-25 µl of the same buffer but without trypsin were added and digested at 37°C overnight.

The tryptic peptides should be extracted from the gel particles with 25 mM NH_4HCO_3/ACN 1:1 at 37°C for 15 min with shaking and peptide mixtures were concentrated to be suitable for nanoLC-ESI-IT-MS/MS analyses. Then, the gel pieces were treated with 5% (v/v) of formic acid and acetonitrile. After drying, the tryptic peptides were resuspended in 0.5% aqueous trifluoroacetic acid. The samples were purified by the use of ZipTip C18 . The peptides thus obtained were analyzed by using nLC-ESI-IT-MS/MS HPLC-Chip/MS (Agilent Technologies , Santa Clara CA , USA) , equipped with an Agilent 1200 Series HPLC with μ - wellplate sampler , capillary pump , HPLC-chip cube interface and LC/MSD Trap XCT Ultra. The chromatographic separation used a gradient of solution A (3% water, 97% acetonitrile, 0.1 % formic acid) and solution B (3% acetonitrile, 97% water, 0.1% acid formic acid) over 70 min at a flow rate of 200 nl/min. The MS and MS/MS data were acquired and processed automatically using Spectrum Mill MS Proteomics software. Database search was performed using mainly NCBI and the local database built as described in the section 4.1.8.

The identified proteins were searched in AT_Chloro Database (http://www.grenoble.prabi.fr/at_chloro/) to find their putative sub-organelle localization and the function related to them.

4.3 Study of protein expression as a function of depth

4.3.1 Field plant sampling – Cutting of *P. oceanica* (n = 5) were sampled at depths of 5 m, 20 m and 30 m at 7:00 and at 13:00 on the meadow in proximity of Stareso (Corse, France) with SCUBA diving as shown in Table 2.

TIME AND PLACE			DEVICES IN FIELD							SAMPLING OF LEAVES FOR LAB						
Days	Depth	Time	Shutter Fluorometers /PAM	Classic Fluorometers	Diving-PAM	RLCs sensors	Minilog TR recorders	O_2 acustic sensors	CO_2 Incubation chambers	Pigments	Epiphyte community (after ^{13}C incubation)	O_2 electrodes	Genetics	RT-qPCR	Illumina RNAseq	1-DE free-label proteomics
from 12th to 17th October 2011	5m	6:00	↓	↓	↓	every 15 minutes	↓	↓		3 biological replicates		↓		3 biological replicates		
		7:00								↓				↓		2 biological replicates
		9:00				every 15 minutes							20 samples			2 biological replicates
		12:00				every 15 minutes									pulled leaves	
		13:00									10 biological replicates					2 biological replicates
		15:00				every 15 minutes										2 biological replicates
		18:30				every 15 minutes									pulled leaves	
		0:00								↓				↓		
	20m	6:00	↓	↓		every 15 minutes	↓	↓		3 biological replicates		↓		3 biological replicates		
		7:00								↓				↓		2 biological replicates
		9:00				every 15 minutes							20 samples			2 biological replicates
		12:00													pulled leaves	
		13:00									10 biological replicates					2 biological replicates
		15:00				every 15 minutes										2 biological replicates
		18:30				every 15 minutes									pulled leaves	
		0:00								↓				↓		2 biological replicates
	30m	6:00	↓	↓	↓	every 15 minutes	↓					↓				
		7:00								3 biological replicates				3 biological replicates		2 biological replicates
		9:00				every 15 minutes										
		12:00				every 15 minutes										
		13:00								3 biological replicates	10 biological replicates			3 biological replicates		2 biological replicates
		15:00				every 15 minutes										
		18:30				every 15 minutes	↓					↓				
		0:00														

Table 2 | Days, sampling time, sea depths, and suitable devices and tools for field measurement at seagrasses beads and for laboratory analyses on leaf biological replicates.

where were selected and cleaned; same leaves from an individual were

used both for genomic analysis, proteomics and physiological analyses as shown in Fig.22.

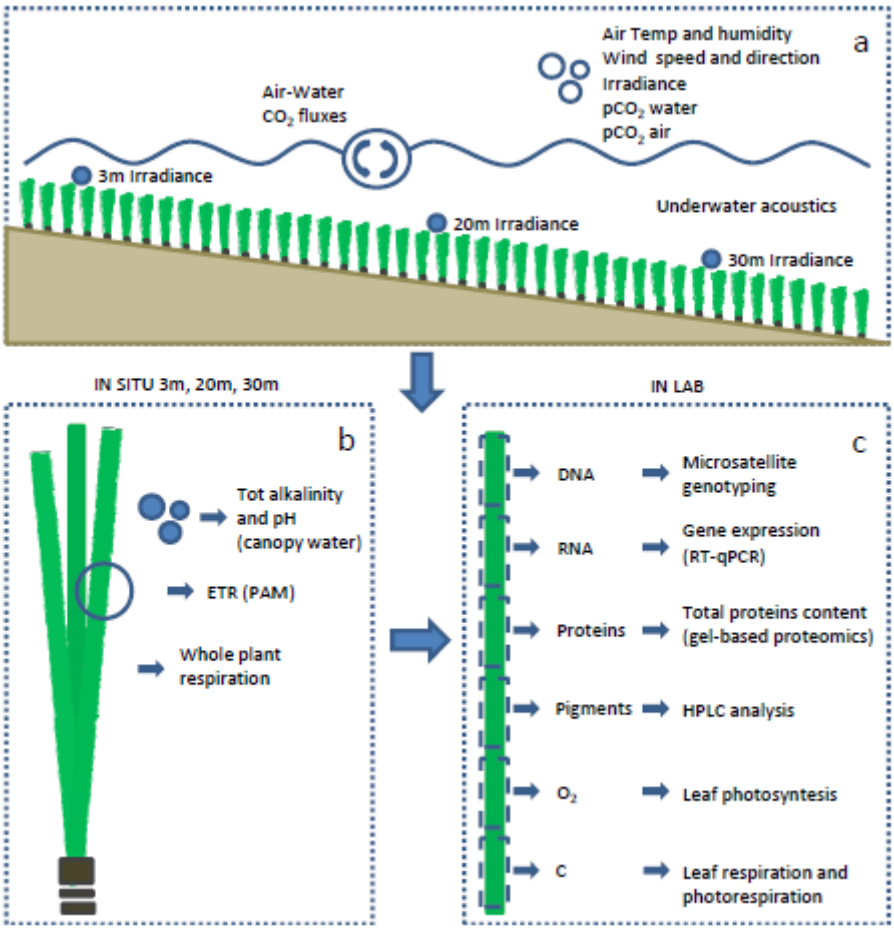

Fig.22 | Summary of methodological approaches performed *in situ* at community level (A) and at plant level (B). Replicate shoots were collected for
each depth for physiological and molecular analyses that were performed all on the same leaf (C).

4.3.2 Extraction of leaf protein of *P. oceanica* –

For proteomic analysis leaf tissue was weighed, frozen in liquid nitrogen and processed for the extraction of proteins till to the stage of tissues powder, adding the powder of quartz. The tissue were washed several times in 20% aqueous TCA + 1% PMSF and then in 80% cold

acetone till the pellet became white. The pellet was dried under a hood at room temperature in a clean mortar.

At this stage samples were transferred in a microtube and maintained refrigerated at temperatures from -4 ° C to 0 ° C during the transport to the molecular biology laboratory.

Thereafter the samples were processed as described in the previous sections 4.1.6 and 4.1.7 of this chapter.

After the SDS -PAGE , the proteins were processed for proteomic analysis as reported in sections 4.1.8 and 4.1.9.

5. Results

5.1 Analysis of the leaf proteome of *Cymodocea nodosa* under salt stress

In Fig 23 the electrophoretic profiles of leaf proteins under different salinity conditions of maintenance in mesocom are shown. The SDS-PAGE pattern in the control plants revealed high number polypeptide bands demonstrating the efficient protein extraction and purity (lane 1;see the fig legend).

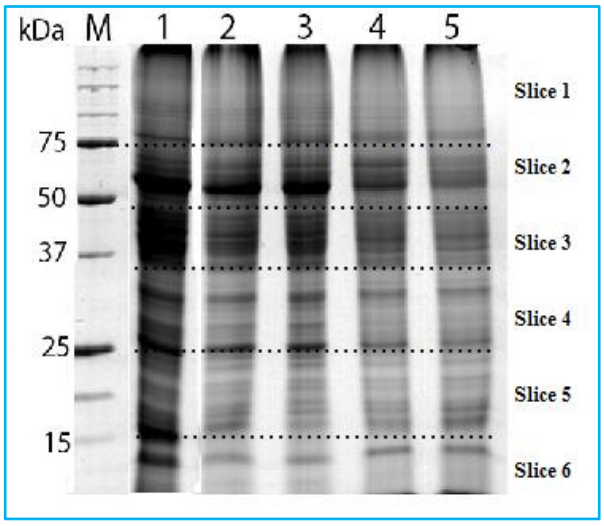

Fig.23 SDS-PAGE of proteins extracted from leaf tissue of *C.nodosa* under hypersaline stress. In lane M) was loaded the mix proteins standard (Bio-Rad range from 10 kDa to 250 kDa in molecular weight), in the lane 1) is loaded, the control sample kept in the aquarium for 7 days of acclimation, in 2) and 3) lanes, respectively, the samples at 37 psu (salinity control) and samples at 43 psu (ipersalinità) maintained in mesocosm for 15 days, and finally, in 4) and 5) lanes were loaded, respectively, the samples at 37 psu and the samples at 43 psu maintained in mesocosm for 30 days.

The most expressed band is that containing the large subunit of Rubisco (Ribulose-1,5-bisphosphate carboxylase oxygenase) with a molecular weight of 55 kDa; this protein is considered the landmarker of the leaf proteome. This enzyme is, in fact, the key enzyme in the

Calvin - Benson cycle by catalyzing the carboxylation/oxydation of organic substrates also in marine plants (Touchette and Burkholder, 2000)

Each lane in the gels has been divided in six pieces (slices 1 to 6) along a molecular weight gradient; this allowed to compare the protein expression with the same molecular weight among different samples labeled from "*1*" to "*5*". For mass spectrometry, slices were analyses in pair among treatment and duration. The samples grown in normal salinity condition after 7 days acclimation are used as referred samples. After 15 days culture in the mesocosm under normal salinity condition, the pattern of protein expression seems to be not altered in plants (lane 2) in respect to the controls at 7 days. Hypersaline treatment after 15 days do not show main changes in the leaf electrophoretic pattern (lane 3). A considerable reduction of the band corresponding to the large RuBisCo subunit occured in the sample under 43 psu hypersaline after 30 days (lane 5); a slight decrease of this band is also in the control after 30 days , suggesting a decrease in the expression of this protein due to the growing conditions in the aquarium.

The mass spectrometry analysis has allowed us to identify the leaf proteins and their changes under hypersaline conditions (Fig.24).

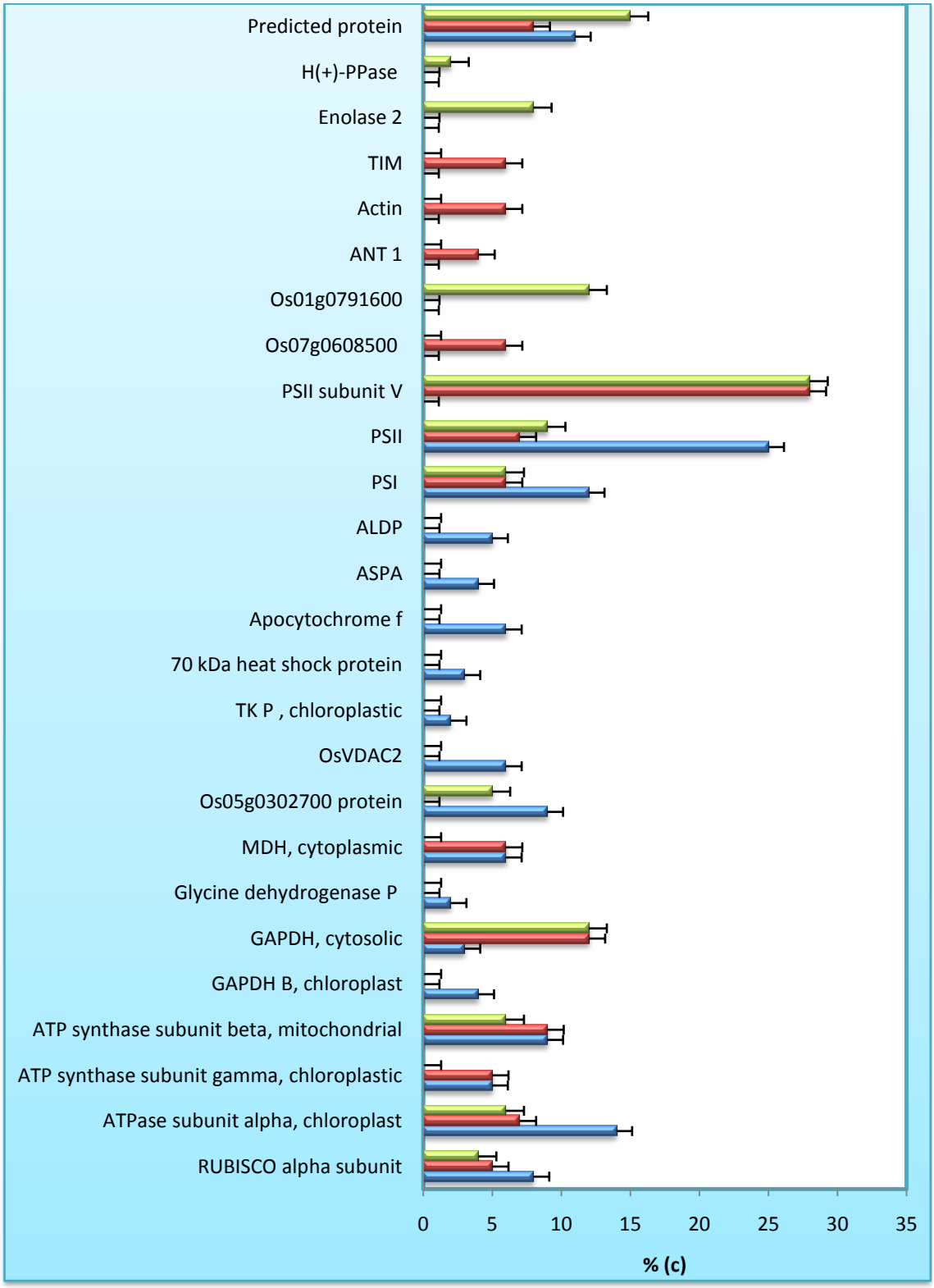

Fig.24 Results of protein expression in *C.nodosa* subjected to different hypersaline treatment times (43 psu). In blue are represented the control samples at 37 psu for 7 days of acclimation, the red ones 43 psu after 15 days of treatment and those in green to 43 psu after 30 days

Proteins quantization was made by the spectral counting method (4.1.9) among the control plants after 7 days culture in mesocoms and plants after 15 and 30 days hypersaline treatments. We identified 30 differentially expressed proteins among the samples analyzed divide into, i) *proteins highly expressed in the control and down-regulated after hypersaline treatments*: the PSII subunit PsbS, the PSI reaction center subunit II (PSI 20 kDa subunit, chloroplastic), the mitonchondrial ATP synthase alfa and beta subunits, the chloroplastic ATP synthase subunit gamma , the Rubisco large subunit and Rubisco alfa subunit; these proteins were drastically down-regulated after 15 days, except for the mitonchondrial ATP synthase beta subunit and the chloroplastic ATP synthase subunit gamma. Down-regulation of all proteins are mainly appreciated after 30 days of hypersaline treatment and the chloroplastic ATP synthase subunit gamma and the mitonchondrial ATP synthase alfa subunit have been not detected in samples; ii) *Proteins that are expressed only in the control*: the chloroplastic glyceraldehydes-3-phosphate dehydrogenase B, glycine dehydrogenase P protein, mitochondrial outer membrane protein porin 2 (OsVDAC2), chloroplastic transketolase P (TK-P), 70 kDa heat shock protein, Apocytochrome f, chloroplastic fructose-bisphosphate aldolase (ALDP), cytoplasmic Aspartate

aminotransferase A (ASPA); *iii) proteins that are highly expressed in hypersaline treatment respect to the control:* the cytosolic glyceraldehyde-3-phopsphate dehydrogenase and three putative oxidoreductase isoforms*; iv) proteins that are expressed only in the hypersaline treatment:* the cytochrome b559 subunit alpha (PSII subunit V), the Enolase 2, a putative 40 S ribosomal protein (Os07g0608500), the ATP–ADP translocase 1 (ANT 1), the Actin, a cytosolic Triose-phosphate isomerase (TIM); a tonoplastic intrinsic protein pyrophosphate-energized inorganic pyrophosphatase (H(+)-PPase).

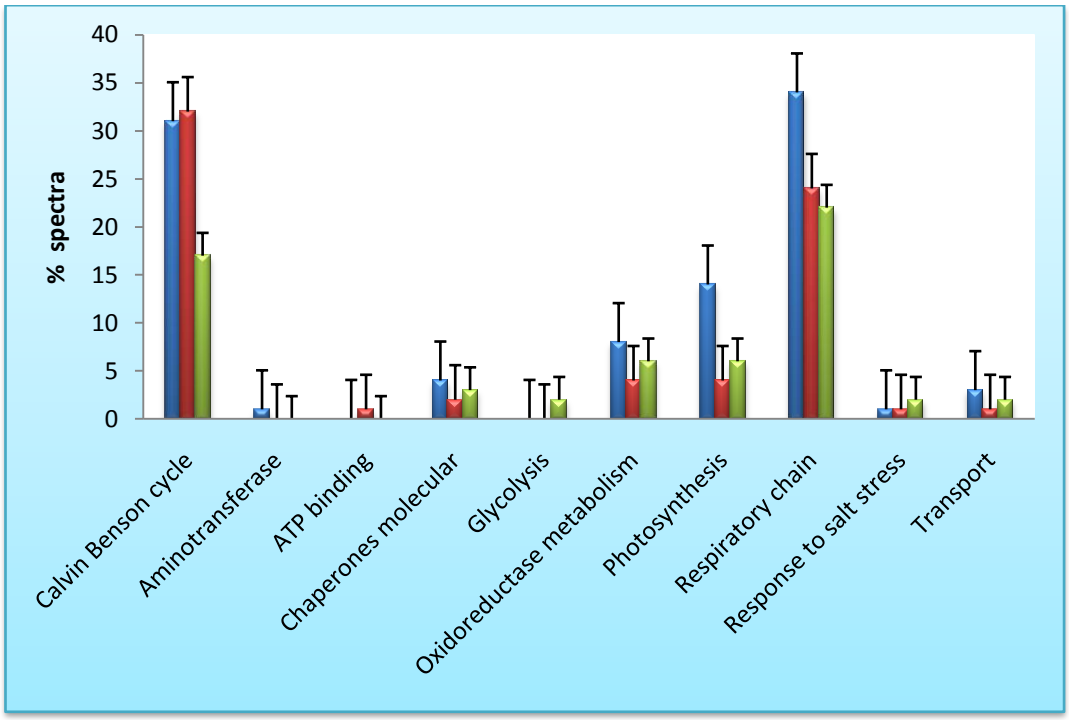

Fig.25 Results of protein expression in *C.nodosa* subjected to different hypersaline treatment times (43 psu) suddivided for metabolisms. In blue are represented the control samples at 37 psu for 7 days of acclimation, the red ones 43 psu after 15 days of treatment and those in green to 43 psu after 30 days

In the figure 25 the percentages of spectra assigned to each identified protein are reported as functional groups. In control plants the main metabolisms are those of the enzyme belonging the Calvin-Benson cycle and the respiratory chain that reached the 60 % of total identified proteins; hypersaline treatments affect both metabolism with a down-regulation of the overall proteins that have an important decrease after the long-lasting treatment (30 days). The photosynthesis metabolism are also drastically down-regulated by the hypersaline treatment just after 15 days. Also the oxidoreductase metabolism and expression of the membrane transporters are down-regulated by the treatment. An up-regulation has been found of enzyme involved in the salt stress response and glycolisis. No significant differences are detected for other metabolisms.

Statistical parameters of protein identification of control and treated plants are reported in the Annex 2 to this chapter. Single peptide sequence assigned to each identified protein and their related accession numbers are reported in the Annex 3.

5.2 Extraction of chloroplasts and organelle sub-fractionation

5.2.1 Extraction of intact chloroplasts – In the Fig 26, a tube containing the percoll gradient after centrifugation of the crude chloroplast from *P. oceanica* leaves is shown; the intact chloroplasts fraction is concentrated in a specific dark green band at bottom of the tube (see arrow). Broken chloroplast and other cytoplasmic contaminants are concentrated in a upper weakly band in the upper part of the gradient (see arrow). A sample of intact an been observed under a light and fluorescen chloroplasts are well structured and shown a strong chlorophyll fluorescence localized inside the envelope (Fig 21a). On the contrary the broken chloroplasts are disorganized in structure with thylakoid membranes diffused in the medium with a weak fluorescence (Fig. 21b). This result allowed us to extract proteins exclusively from the intact chloroplast fraction for the proteomic analysis.

Fig.26 Percoll gradients to 60% for the extraction of intact chloroplasts of *P.oceanica*

5.2.2 Extraction of the chloroplast proteins on SDS -PAGE - A 1-D representative gel with electrophoretic patterns of proteins extracted from leaves, intact chloroplasts and broken chloroplasts is reported in Figure 27; the lane 1) shown the typical pattern of proteins from leaf tissue with the main band at 55 kDa corresponding to the RuBisCo large subunit (LB- RuBisCo) expressed in the stroma of the chloroplasts; at 25 kDa the prominent band is the LHCP a complex of intrinsic proteins of the thylacoid membranes. Intact chloroplast pattern of proteins shown an enrichment of both proteins (LB-RuBisCo and LHCP) in spite of the decrease of overall bands; that means chloroplasts were really intact when they were activated in the loading buffer, because they maintained the stromal proteins (lane 2), whereas the pattern of the broken chloroplasts do not show LB- RuBisCo band, because it was solubilized in the extraction buffer; the LHCP band is still concentrated because this protein is insoluble and fixed to the thylakoid membranes (Fig. 27, lane 3).

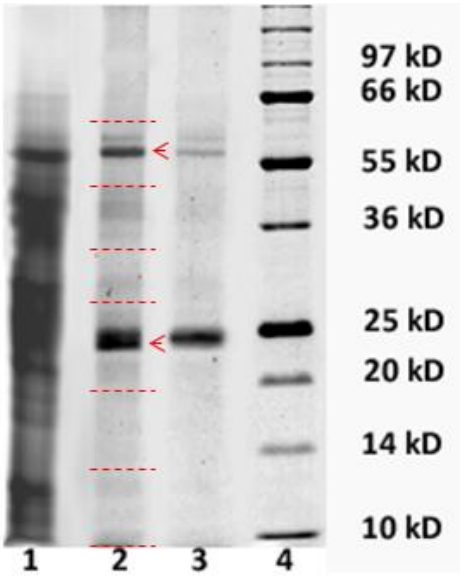

Fig.27 SDS PAGE of leaf proteins and of chloroplasts of P.oceanica: 1) the protein extract from leaf tissue, 2) the protein extract from intact chloroplasts, 3) the protein extract from broken chloroplasts, 4) the marker protein (Biorad from 250 kDa to 10 kDa)

Mass spectrometry of proteins from intact chloroplasts by nLC-ESI-IT-MS/MS followed by the analyses with Spectrum Mill MS Proteomics software returned more than ten thousand filtered spectra from the six gel slices, although only small percentage of spectra (on average 6%) deserved validation and implied the identification of proteins (Tab.3), most probably due to the partial genomic information available for seagrasses.

Molecular mass range (kDa)	MS/MS filtered spectra[a]	MS/MS spectra interpreted and validated[b]	Interpretation Yield (%)[c]
Slice 1 (65-50)	2064	129	6,3
Slice 2 (50-35)	2336	208	8,9
Slice 3 (35-30)	2545	176	6,9
Slice 4 (30-20)	2306	120	5,2
Slice 5 (20-15)	1355	77	5,7
Slice 6 (15-10)	2290	36	1,6
All slices	12896	746	34,6

a: spectra number after the filtering out extraneous noise peaks
b: spectra number after the robust statistical methods to validate peptide assignments to MS/MS spectra
c : percentage ratio between the number of interpreted spectra and number of filtered spectra for each molecular mass range

Table 3. Number of filtered and validated spectra collected from the digested proteins of intact chloroplasts in each gel slice.

In Ann 4 the assigned function of the 74 identified proteins are reported. Each protein is denoted by the accession number corresponding to the database in which best identification scores were found. Peptide sequences assigned to each protein, number of spectra

for each peptide statistical parameters for protein identification are reported in the Annex 5 and 6.

The sub-localization of each protein was based on BLAST searching of FASTA peptide sequences of identified proteins against the AT_CHLORO database. The largest number of identified proteins are localized in the thylakoid and stroma compartments, while less number of proteins are localized in the envelope (Figure 28).

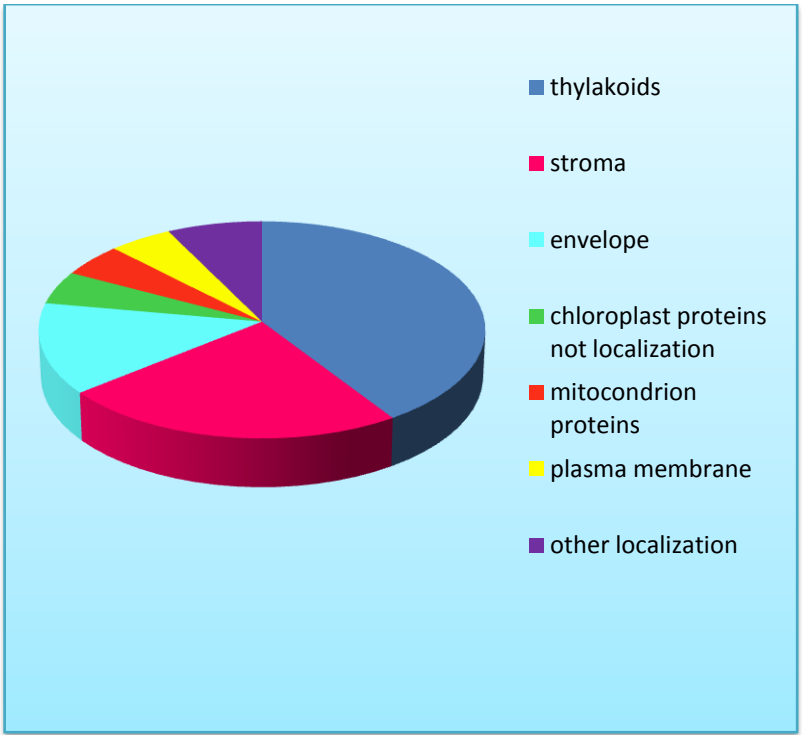

Fig. 28 Mass spectrometry.analysis . Schematic representation of the chloroplast proteins divided in different compartment

Besides these, 8 % of proteins have not a unique localization in chloroplast compartments but are shared between envelope/thylakoids or stroma/thylakoids or envelope/stroma. In the intact chloroplast

fraction proteins from the cytosol and mitochondrion have been found, representing the 5% of total identified proteins (GDP-mannose 3,5-epimerase 1, Prohibitin-2, Universal stress protein A-like protein, Plasma membrane ATPase 4, putative plasma membrane intrinsic protein, S-norcoclaurine synthase, ATP synthase subunit alpha, mitochondrial).

5.3 Protein expression as a function of depth

In the Figure 29 (A) the 1D electrophoretic patterns of proteins extracted from *Posidonia* leaves at three depths at times of the day (see figure legend for details) are shown.

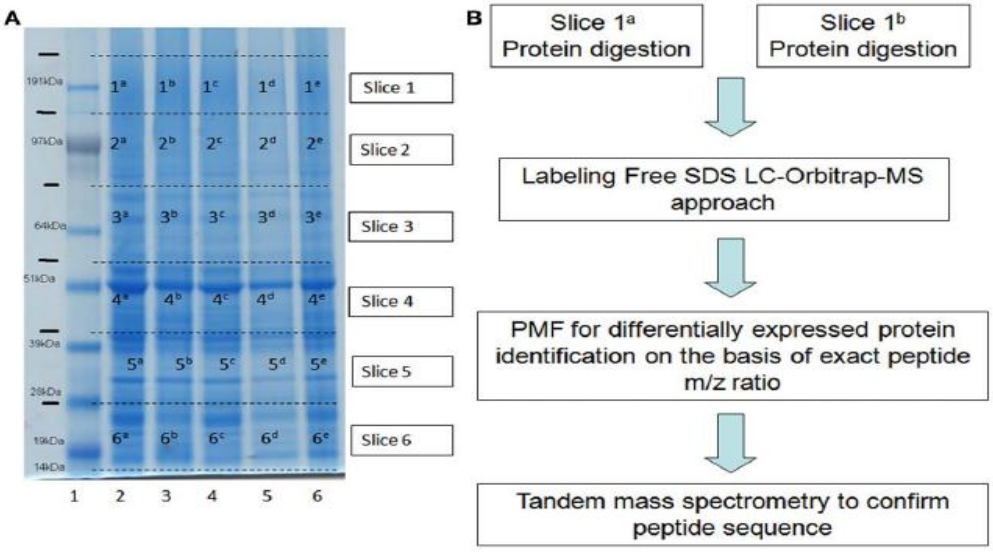

Fig. 29 (A) 1-DE gel electrophoresis of leaf protein extracts from three depths. Dotted lines indicate each gel slice analyzed by labeling-free approach; Lane (1) markers; lane (2) 8.00 h, 3m depth; lane (3) 8.00 h, 30m depth; lane (4) 13.00 h, 3m depth: lane (5) 13.00 h, 20m depth; lane (6) 13.00 h, 30m depth. **(B)** Experimental workflow applied to each pair of gel slices.

Each lane has been divided in six pieces (slices 1 to 6) along a molecular weight gradient; this allowed to compare the protein expression with the same molecular weight among different samples labeled from "*a*" to "*e*". For mass spectrometry, slices were analyses in pair according to the experimental workflow reported in Fig. 29(B). We selected as the referred samples the pattern of proteins expressed in leaves at 8:00 hours at the depth of 30 m (lane b) because at that time plants receive the lowest light intensity (PAR = 0 µE $m^{-2}s^{-1}$) and they showed the lowest expression level of the selected genes that are involved in the primary metabolisms (see discussion section for details); to evaluated the proteins differentially expressed we compared the referred samples with those at 3 m depth (lane c), 20 m depth (lane d), 30 m depth (lane e) at 13:00 hours, the time of the day with the maximum light intensity measured at meadows (PAR_{3m} = 302 µE $m^{-2}s^{-1}$; PAR_{20m}= 70,65 µE $m^{-2}s^{-1}$; PAR_{30m}= 96 µE $m^{-2}s^{-1}$).

The complete mass spectrometry analyses gave approximately four thousand validated MS/MS spectra that recorded more than 500 identified proteins. Statistical parameters, number of spectra, accession number of the identified proteins and the functional groups are reported in the Annex 5 to this chapter.

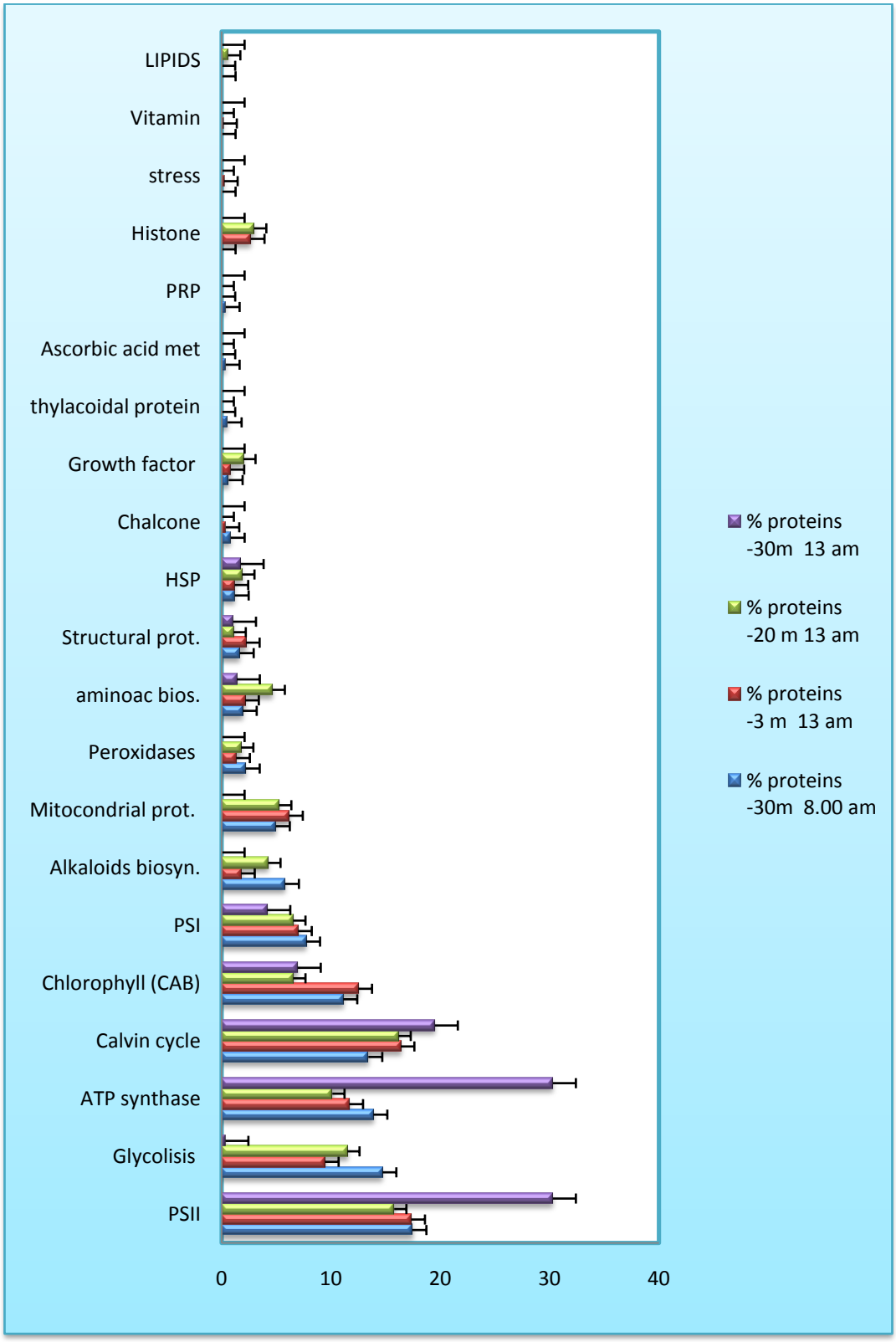

Fig. 30 Results of protein expression in *P.oceanica* to 3 different depths

In the Fig 30 the values of spectral counting obtained for the proteins expressed at three depths, organized into functional groups are shown. Functional groups are analyzed as *i) protein and enzyme system-related to PSII:* these are up regulated only in the samples at 13:00 h at 30 m depth compared to the referred samples; *ii) enzyme and proteins among the glycolis metabolism:* in the referred samples the enzymes belonging this metabolism correspond to the 15% of total proteins identified in the samples, at 13:00 h the proteins expression decreases in samples at 3 m and 20 m depth of about the 8% and 10% respectively and has ten-fold down regulation in the samples at 30 m depth; *iii) enzymes and proteins associated to the ATP synthase metabolisms (both mitochondrial and chloroplastic):* these proteins are highly expressed in samples at 13:00 h to 30 m depth related to the referred samples and also respect to the samples at 3 m and 20 m depths ; *iv) key enzymes of the Calvin-Benson cycle:* it show an increase of 6 percentage points in the samples at -30 m at 13:00 h compared to referred one. A moderate up-regulation of this metabolism is found also in samples at -3 m and -20 m at 13:00 h; *v) proteins of the chlorophyll metabolism:* samples at 3 m depth at 13:00 shown any variation respect to the referred samples, while a strong down regulation occurred in the samples at 20 m and 30 m depths at

13:00 h; *vi) protein and enzyme system-related to PSI:* the proteins that belong to this metabolism does not have high variations in protein expression in the samples at 3 m and 20 m depth at 13:00 h, however, proteins and enzymes associated to PSI are down-regulated in the samples at 30 m depth at 13:00 compared to the referred one; *vii) proteins among the alkaloids biosynthesis:* these class of enzymes has been down-regulated in the samples at 3 m and 20 m depths at 13:00 h, but their expression levels are not revealed in the samples at 30 m depth at 13:00 h; *viii) mitochondrial proteins (oxidative metabolism):* the expression levels of proteins and enzymes related to the mitochondrial metabolisms does not change significantly at 3 m and 20 m depths in respect to the referred samples, but their expression is not detected in the deepest 30 m samples at 13:00 h.

Regarding the remaining metabolisms, the class of enzyme belong the peroxide metabolisms are down-regulated at 3 m and 20 m depth at 13:00, but their expression levels are not detected at 30 m, 13:00 h; for the amino acid biosynthesis it has strongly up-regulated at 20 m depth but it is down-regulated at 30 m, 13:00 h. The aldolase, an enzymes of glycolisis, and histone proteins expression have been revealed only in the samples at 3 m and 20 m depths, while their expression are not revealed in the samples at 30 m depth at 8:00 and 13:00 hours.

6. Discussion

Phylogenetic analysis of seagrasses, based on the plastid gene encoding for RuBisCO large subunit (Les DH *et al.*, 1997), indicates that the return into the sea occurred at least three times independently through parallel evolution from a common aquatic-freshwater ancestor of terrestrial origin. Living submerged in an aqueous environment poses many challenges requiring physiological and morphological adaptations that are distinctive from terrestrial angiosperms. One factor contributing to these high light requirements is the reducing sediments to which seagrasses are rooted. These sediments challenge seagrass root tissues with anaerobic conditions since marine sediments are often oxygen deficient. When the internal transport of oxygen from shoot to root tissues is not sufficient, seagrasses can be forced to resort to fermentative metabolism (Terrados *et al.*, 1999; Touchette *et al.*, 2000). Submergence also exposes organisms to the forces of wave action and tidal currents that effects reproductive functions and reduces the availability of carbon dioxide (CO_2). Specific to marine environments, seagrasses are often exposed to high salt levels and short-term salinity fluctuations in the coastal and estuarine system

(Barbour *et al.*, 1970; Walker *et al.*, 1990). Identifying genes and cellular processes that may have adaptive contributions to submerged fully marine habitats is therefore of particular interest. In general, such phenotypic changes can be caused by both changes in gene expression and the primary sequence of encoded proteins. Protein sequences can be strongly conserved whereas changes in their expression pattern can be adaptive (Holloway *et al.*, 2007; Fraser *et al.*,2010). In this study we develop a proteomic approach to investigate the response to environmental conditions that naturally occurred at meadows. Growing along a depth gradient is quite usual for the seagrass *Posidonia oceanica* demanding adaptation to varying condition in quality and quantity of light, whereas *Cymodocea nodosa* habit infrallitoral environment with varied condition in salinity as main factor affecting response to acute stress, resilience and acclimation. Finally application of sub-proteomics at the autotrophic organelle, the chloroplasts, allow us to obtain an initial catalog of proteins that are expressed and/or allocated in the three sub-compartments as the first step to the deeper investigation of submerged-life style of seagrasses.

Expression proteomics of *Cymodocea nodosa* under salt stress

Extraction and purification of leaf proteins have been applied in *Posidonia oceanica* previously, starting the application of proteomic approaches in the study of seagrasses biology and physiology under various conditions (Spadafora *et al.*, 2008; Mazzuca *et al.*, 2009). The application of protocol suitable for *P. oceanica* and other recalcitrant plants, just with few modifications, to *Cymodocea nodosa* gave also high efficiency and quality of proteins extraction from leaves (Saravan and Rose, 2004; Wang *et al.*, 2003). Proteins were extracted from intermediate and adult leaves to avoid the influence of tissues differentiation on the protein yield and patterns. The highest protein yield was obtained with the initial 10 % trichloroacetic acid (TCA) in acetone in spite of 20% TCA used for *P. oceanica* tissue (Spadafora *et al.*, 2008). The TCA is used to solubilize the phenols that are stably kept in the vacuole of mesophyll cells; the lower amount of TCA is necessary to remove polyphenols the lower is its concentration in tissue (Spadafora *et al.*, 2008). It means that *C. nodosa* has a lower capability to synthesized and /or to store polyphenols in tissue in respect to *P. oceanica*.

As well known, polyphenols in tissues strongly interfere with the proteins extraction and their removal is essential to obtained a suitable

protein samples for electrophoretic separation and for a gel-based proteomic approach. It is essential, for that, to monitor protein yield under varying external conditions that should affect the biosynthesis of secondary metabolites (Cozza *et al.*, 2004; Dumay *et al.*, 2004; Ruiz *et al.*, 2003). The extraction protocol optimized in this work gave high quality proteins from *C. nodosa* leaves well resolved in 1-DE polypeptide; in addition the good reproducibility of protein patterns has indicated this method as a powerful tool to explore changes in protein expression in response to altered environment conditions.

Accurate controlled conditions in trials with natural populations are quite impossible to realize and unforeseen events are very probable to occur. Therefore we decide to use the mesocosm system that is an experimental tool that brings ecologically relevant components of the natural environment under controlled conditions. In this way mesocosms are a bridge between controlled laboratory experiments and the more variable and uncontrolled field environment. Under our conditions, mesocosms possess sufficient biological complexity to be realistic relative to the natural environment being modelled, possess biological and statistical sensitivity, and are long enough in duration to address the question of interest. Here, the mesocosm has been used to evaluate how *C. nodosa* might modulate the protein expression in

response to environmental change through deliberate manipulation of salinity. Salinity is a critical environmental factor determining the abundance and distribution of seagrass communities (Montague and Ley, 1993; Adams and Bate, 1994). The physiological capacity of seagrasses to tolerate increases in salinity is species specific and closely related to the salinity characteristics of the environments in which they grow. *C. nodosa*, as a euryhaline species, is considered to be tolerant to changes in this parameter because is able to grow in a broader range of coastal habitats, including lagoon, with widely different salinity levels (Tyerman *et al.*, 1989; Kuo and Den Hartog, 2000; Koch *et al.*, 2007; Touchette *et al.*, 2007; Procaccini *et al.*, 2003; Boudouresque *et al.*, 2009).

The acquisition of particular adaptations in order to maintain osmotic equilibrium (e.g., osmoregulation) and key physiological functions (e.g. photosynthesis) is one of the basic properties enabling seagrasses to successfully evolve in marine environments (Arber *et al.*, 1920; Kuo and Den Hartog, 2000), but far to be well understood, especially at molecular level. Our results shown that the hypersaline treatment induces a significant alteration of the photosynthetic physiology of the *Cymodocea nodosa* by means of the down-regulation of the structural proteins and enzyme of both the PSII and the PSI. This finding is in

agreement with previous evidences in which photosynthesis rate was inhibited in *C. nodosa* (Sandoval *et al.*, 2012) and in other seagrass species (Fernández-Torquemada *et al.*, 2005; Kahn and Durako, 2006; Koch *et al.*, 2007), when exposed to hypersaline stress. Interestingly we found an over-expression of the cytochrome b559 alpha subunit in hypersaline treatment. A number of analyses have indicated that the PSII initial complex probably consisting of D2 and cytochrome b559 and it serves as a receptor for other PSII core proteins during the biogenesis or the PSII repair process (Adir *et al.*, 1990; van Wijk *et al.*, 1997; Müller and Eichacker, 1999; Zhang *et al.*, 1999; Zhang and Aro, 2002). Both process should be enhanced after the hypersaline treatment to maintain the PSII basal activity. Again, the respiration rates significantly decreased, in the strong hypersaline condition (43 psu), compared with the control mean values (Sandoval *et al.*, 2012). Confirming these finding, proteomics analyses revealed an overall down-regulation of both mitochondrial and chloroplastic ATP synthases, suggesting a reduction of the oxidative and photoxidative phosphorilation process that are directly related to respiration and photosynthesis rates. This causes a lowered net photosynthesis in the long lasting saline treatment. The lower expression level of carbon-fixing enzyme RuBisCo detected in hypersaline samples in respect to

the normal condition. This finding is in agreement with Beer *et al.* (1980) who provided some experimental evidence that the activity of the RuBisCo in the epidermis of *Halodule uninervis* was gradually inhibited by increasing NaCl concentrations in *in vitro* assays. This suggested that under NaCl stress condition the carbon balance switch to favor the inorganic carbon (Ci) increase in tissue as a response of the decrease in respiration and photosynthesis rates. Proteomics results strongly suggests, in fact, that in *C. nodosa* the photosynthetic inhibition occurred as a consequence of decreased photophosphorylation activity, low electron transport rate and down-regulation of enzymes involved in carbon assimilation, as has been demonstrated in terrestrial plants and macroalgae exposed to hypersaline stress (Athar and Ashraf, 2005; Huchzermeyer and Koyro, 2005).

On the other hand, carbon reduction seems to be enhanced by the hypersaline treatment because the key enzymes of the glycolisis, the cytosolic glyceraldehyde-3-phopsphate dehydrogenase, has higher expression level after 15 and 30 days treatments; higher expression of the further enzymes of the glycolisis such as enolase 2 and Triose-phosphate isomerase suggested an overall up-regulation of the glucose reduction in the leaf cells. Here, we suggested that in this frame, the

glycolisis may balance the request of energy by producing the ATP molecules in the reduction steps of the 1,3- diphosphoglycerate to phosphoglycerate and from phosphoenolpyruvate to pyruvate.

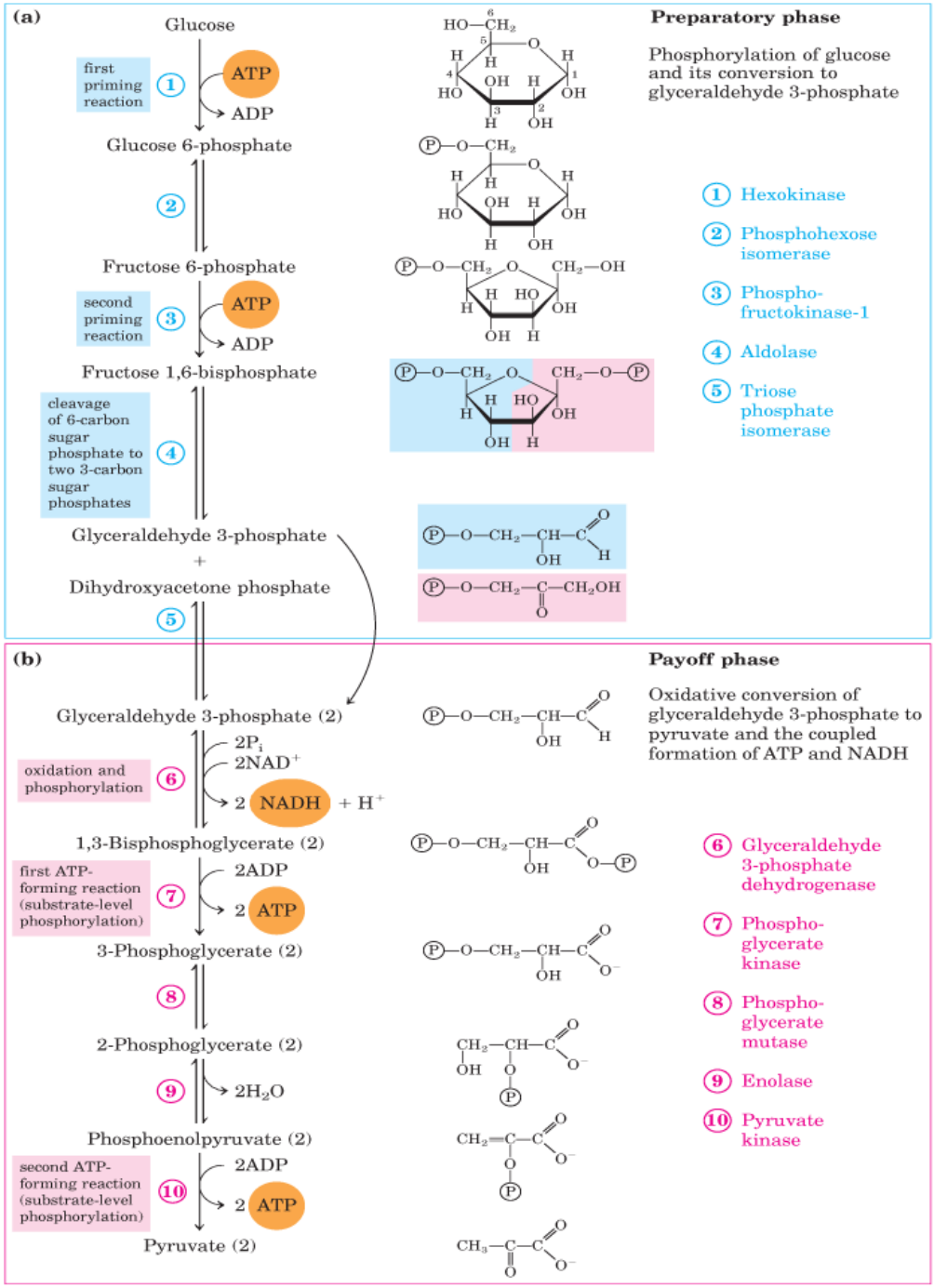

Fig.31 The glycolytic pathway (Nelson, 2004)

As expected the vacuolar metabolism has been affected by the hypersaline treatment; in fact, the overexpression of the tonoplast specific intrinsic protein pyrophosphate-energized inorganic pyrophosphatase (H(+)-PPase) suggests that vacuoles are engaged in Na+ sequestration accordingly with a high capacity of proton pumping and Na+ uptake via the Na+/H+-antiporter; this evidence has been previously reported in Arabidopsis thaliana under hypersaline stress with NaCl (Svetlana Epimashko *et al.*, 2006).

In conclusion, the partial inhibition of photosynthesis and the reduced respiratory activity reported from 43psu salinity treatment enables plants to adapt in this severe stress condition, but presumably with reduced vitality, since some of the internal resources required for growth and biomass maintenance must be reallocated to cope with stress metabolism (Lichtenthaler, 1996). A leaf loss was reported in this experiment for *C. nodosa* shoots consisting with such a situation (Sandoval-Gil *et al.*, 2012). Obviously, this tolerance threshold is only valid for *C. nodosa* populations native from the Spanish Mediterranean Sea with a mean constant salinity of 37 e 38 psu.

We find severe changes in the leaf primary metabolisms due to hypersaline both at short and long-lasting treatments. These drastic rearrangements in the carbon balance did not cause the death of plants

in the mesocosm, where conditions of extreme salinity have been persistent for more than one month. A similar hypersaline treatment was done with *Posidonia* and results indicated that photosynthesis of *P. oceanica* is highly sensitive to hypersaline stress and that it likely account for the decline in leaf growth and shoot survival in response to even small increments of the ambient salinity (Marin Guirao *et al.*, 2011). As it is well known, *C. nodosa* adapts to marine infralittoral environments with instable salinity whereas *P. oceanica* is generally considered to be a stenohaline seagrass species inhabiting infralittoral open coast environments and is not usually present in estuaries and coastal lagoons (Boudouresque *et al.*, 2009; but see Pergent *et al.*, 2002). Overall, proteomics revealed that the physiological tolerance of *C. nodosa* to sudden and chronic increases in external salinity is mediated by its capacity to modulate the primary metabolisms resulting in a new carbon balance and to carry out the efficient Na+ sequestration in the vacuole of the mesophyll cells.

Acclimation to the depth of *Posidonia oceanica*: a proteomic view

First combine genomic and proteomic study was made in meadows growing at two depths in Lacco Ameno (Ischia island, Italy) reporting

changes in the expression of genes and proteins related to the photosynthetic processes, cellular energetic metabolism, stress response and protein turnover (Dattolo *et al.*, 2013). For the authors, acclimation to the depth of *P. oceanica* is carried out by high differentiation on Chlorophyll a-b-binding (*Cab*) proteins between the two depths, suggesting that in *P. oceanica* different *Cab* proteins are utilized for the assembly of the antenna complex, in response to specific photo-acclimation processes. The relative quantity of transcripts and proteins recognized by Dattolo *et al.* (2013) also suggests an increase in PSII and PSI transcripts in deep plants in respect to the shallow ones (especially as regards as PSI). Similar patterns of PSI/II ratio were already observed in shallow *P. oceanica* meadows growing in high-light and low-light conditions (Mazzuca *et al.*, 2009). Accordingly with these finding in our study, plants growing at 30m depth showed a strong up-regulation of proteins associate to the PSII, when the plant receives the maximum quantum yield of the day (PAR_{30m}= 96 $\mu E\ m^{-2}s^{-1}$). This allow us to affirm that over expression of PSII complex is a result of *P. oceanica* acclimation to low light and so that the main metabolic way to acclimate to depth. Conversely the proteins related to the PSI complex are slightly down-regulated in deep plants; this behavior should be a further example of

photosystem arrangements to maintain the best PSI/PSII ratio (Albertsson and Andreasson, 2004). It is now that a calculation of the total number of Chl associated with PSI and PSII suggested that more Chl (approximately 10%) are associated with PSI than with PSII, in agreement with results showing that PSI absorbs approximately 20% more photons than PSII (Nelson and Yocum, 2006). According to this we found a decrease of chlorophyll binding proteins (CAB) in the deep plant respect to the shallow at the maximum PAR values at each depth. Both results are not in agreement with those the reported from Dattolo *et al.* (2013), in which deep plant showed increases in PSI and CAB proteins respected to the shallow one; therefore this aspect of the photosynthesis physiology requires further investigation to be elucidated and correlated with acclimation to the depth of seagrasses.

Another interesting hint revealed in Dattolo *et al.* (2013) is that *P. oceanica* photosynthetic changes involve the enzyme RuBisCo. The expression patterns of the mRNA and the large subunit protein of this enzyme has been found slightly higher in deep plants. On the proteomic side this is in agreement for RuBisCo large subunit that is over expressed in plants growing at 20 and 30 m depth in respect to the shallow one. This allow us to state that the increasing of expression of the key enzyme of the Calvin-Benson cycle seems to be

related to the acclimation to depth in two independent studies carried out in genetically unrelated natural populations.

On the side of the cellular energetic metabolism, considering separately the regulation of each of the three main stages of the respiratory process, we see that glycolysis and the tricarboxylic acid (TCA) cycle were strongly inhibited in low light; this could be the reason way the level of the chloroplastic ATP synthase appears to be up-regulated as function of depth, to maintain energy balance within the cells. As a general rule, the up-regulation of ATP synthesis normally occurs in physiological conditions when intracellular ATP levels are too low.

Several transcripts encoding for proteins associated with stress response and plant defense were detected in low-light. Amongst these, S-norcoclaurine synthase, glutathione S-transferase, 2-cys peroxiredoxin, two heat shock proteins, the stress protein A-like, GDP-mannose 3,5-epimerase 1 and polyphenol oxidase. Most of these protein are involved in detoxification from alkaloids, peroxides and stress responses mediated by phenols. All these elements suggest that plants living in the deep stands are more sensitive to oxidative stress than plants growing in shallow stands, due to the higher investment by the former in maintaining basal metabolism and the consequent lower

resources available for cell defense and repair. In addition, deep plants could also respond to exogenous oxidative stress due to the local distribution of stressing factors, which seem to be more important in the area of the bay where the deep stand is growing.

In conclusion, all of these physiological rearrangement are mostly appreciated in plant growing at 30 m depth in respect those growing at 20 m depth suggesting that this last depth represents the "deep-cline" for *Posidonia oceanica* to acclimate to the depth by drastically rebalance of the photosynthesis processes especially those related to the redox potential maintenance and carbon balance from Ci and gluconeogenesis.

Does *Posidonia oceanica* is a model plant for chloroplast sub-organelle proteomics in seagrasses?

Organelle proteomics is the emergent approach to investigate the specific expression of proteins inside the sub-cellular compartments but also to assign the proper localization of single protein species, elucidate the proteins trafficking in cytoplasm and highlighted the cross-talking among organelles inside a cell (Agrawal et al, 2012). Proteomics of the chloroplast have been initiated the last decade in

model plant *Arabidopsis thaliana* with the aim to sequence all proteins that are synthesized and/or translocated in this organelle (Rolland *et al.*, 2003; Ferro *et al.*, 2003). This goal was reached by Ferro *et al.* (2010) with the built of AT_CHLORO, a comprehensive chloroplast proteome database with subplastidial localization and curated information on envelope proteins.

From this date the chloroplast proteomics became easier than the past.

The sampling for sub-organelle proteomics does not constitute a threat for *P. oceanica* meadows and chloroplast from *P. oceanica* is the excellent candidate to be the model organelle for investigation of photosynthesis in seagrasses for many reasons; first, *P. oceanica* meadows have higher leaf density that other seagrasses; second, the chloroplast from *P. oceanica* has the size and density very similar to those of terrestrial plants; third, take the leaf from the meadows is now less invasive thanks to the conservative new technique of sampling that leaves the shoots on place, then they produce new leaves faster than uncut shoots of the same meadow (Gobert *et al.*, 2006.); fourth, the amount of leaf tissue needed to obtain a purified chloroplast fraction suitable for proteomics is really small in weight, just 10 g, corresponding to fifty leaves collected from 10-12 shoots.

For completeness of information, the chloroplast purification protocol was applied also to *Zostera noltii* leaves, but with disappointing results because of the great contamination of green fraction probably due to low density and small size of *Z. noltii* chloroplasts which migrate at same gradient zone than cyanobacteria and mitochondrion (data not shown); this allowed the isopycnic separation not applicable to this seagrass.

The yield of chloroplast protein identification was not satisfactory at this time, because few proteins received their proper function and subplastidial localization. In details we identified a large percentage of proteins localized in the thylakoids (41%) respect to the other compartments; because the proteins localized in thylacoids correspond to the 8,5 % of total chloroplast proteins (see AT_CHLORO database web site) our finding is surprisingly high. It have to be considered that protein identification starting from MS/MS spectra undergo the robust statistical methods to validate peptide assignments and that first of this, peptide validation depends on the quantity and quality of genomic resources available in databases. So that, the reason way the high identification of the thylakoids proteins occurs is because more genomics information is available in databases in respect to envelope and stroma, in terms of gene and protein sequence items.

On the other hand the organelle proteomics gave, at this time, a large data-set of validated MS/MS spectra that are still waiting for an identification as new genomic information will coming from seagrass species, in particular, and from other non-model plants in general. This resource is much richer in information when it consider that over 95% of the MS/MS spectra have not received they validation due to the lacks of genomic data.

The answer to the question "does *Posidonia oceanica* is a model plant for chloroplast sub-organelle proteomics in seagrasses ?" is, without a doubt, yes it is ! The chloroplast drive the development and differentiation of the leaves, as well as is involved in the stress response and the acclimations investigated in this work but also in all the other aspects of the physiology of seagrasses. What is missing in the development of this new branch of molecular biology of seagrasses is the effort in implementing a research consortium that collects the collaborations of those groups that are actually engaged in sequencing the genomes of seagrasses.

References

Adessi C, Miege C, Albrieux C, Rabilloud T .Two-dimensional electrophoresis of membrane proteins: a current challenge for immobilized pH gradients. Electrophoresis.1997 Jan;18(1):127-35.

Agostini, S., Desjobert, J.M., Pergent, G., 1998. Distribution of phenolic compounds in the seagrass Posidonia oceanica. Phytochemistry 48, 611–617.

Agrawal ,GK; and Rakwa, R. Rice proteomics: a cornerstone for cereal food crop proteomes. Mass Spectrom. Review, 2005, 25, 1–53.

Aguilar, R., Pastor, X., de Pablo, MJ. 2006. Hábitats en peligro. OCEANA-Fundación Biodiversidad.

Alcoverro, T; Cerbian, E; Ballesteros, E. The photosynthetic capacity of theseagrass Posidonia oceanica: influence of nitrogen and light. Journal of Experimental Marine Biology and Ecology, 2001, 261, 107–120.

Andacht, TM; & Winn, RN. Incorporating proteomics into aquatic toxicology. Marine Environmental Research., 2006,62, 156–186.

Arnold, T., Mealey, C., Leahey, H., Whitman Miller, A., Hall-Spencer, J. M., Marco Milazzo, M., et al. (2012). Ocean acidification and the loss of phenolic substances in marine plants. PLoS ONE 7:e35107. doi: 10.1371 /journal. pone.0035107

Aula del mar de Málaga (1998). Praderas de fanerógamas marinas en el litoral andaluz. Consejería de Medio Ambiente de la Junta de Andalucía.

Baginsky S. and Gruissem W., Chloroplast proteomics: potentials and challenges. J Exp Bot. 2004 May;55(400):1213-20. Epub 2004 Mar 12. Review.

Baginsky S. and GruissemW. The chloroplast kinase network: new insights from large-scale phosphoproteome profiling. Mol Plant.2009,1141-53.

Bashitialshaaer R, Persson KM, Aljaradin M (2011) Estimated future salinity in the Arabian Gulf, the Mediterranean Sea and the Red Sea consequences of brine discharge from desalination. Int J of Academic Res 3:133–140

Besiktepe S.T., 2003, Density currents in the two-layer flow: an example of Dardanelles outflow. Oceanol. Acta 26, 243- 253.

Björk, Mats et al. , Managing Seagrasses for Resilience to Climate Change. - IUCN, Gland, Switzerland, 2008.

Borde, A.B., O´Rourke, L.K., Thom, R.M., Williams, G.W. (2004). National Review of Innovative and Successful Coastal Habitat Restoration. Battelle Memorial Institute.

Borum, J., Duarte, CM, Krause-Jensen, D. & Greve, TM. 2004. European seagrasses: an introduction to monitoring and management. The M&MS project, Copenhagen.

Bouderesque C. F., Meinesz A., Ledoyer M. & P. Vitello (1994). Les herbiers á phanerogames marines 98- 118. In Les biocénoses marines et litorales de Méditerranée synthése, menaces et perspectivas (Bellan- Santini D., Lacaz J. C. & C. Poizat) Muséum Nacional d´Histoire Naturelle, Paris.

Boudouresque C, Bernard G, Bonhomme P, Charbonnel E, DiviaccoG, Meinesz A, Pergent G, Pergent-Martini C, Ruitton S, Tunesi L (2006) Pre´servation et conservation des herbiers a` Posidonia oceanica. Ramonge pub: 1-202. ISBN 2-905540-30-3. www.ramonge.org

Boudouresque FC, Bernard G, Shili A, Verlaque M (2009) Regression of Mediterranean seagrasses caused by natural processes and anthropogenic disturbances and stress: a critical review. Bot Mar 52:395-418

Boye´ H (2008) Water, energy, desalination and climate change in the Mediterranean. http://www.planbleu.org/publications/Regional study_desalination_EN.pdf

Braütigam A, Hofmann-Benning S, Weber AP. 2008. Comparative proteomics of chloroplast envelopes from C3 and C4 plants reveals specific adaptations of the plastid envelope to C4 photosynthesis and candidate proteins required for maintaining C4 metabolite fluxes. Plant Physiol 148:568–579.

Braütigam A, Weber AP. 2009. Proteomic analysis of the proplastid envelope membrane provides novel insights into small molecule and protein transport across proplastid membranes. Mol Plant 2:1247–1261.

Bruno, A., Bruno, L., Chiappetta, A., Giannino, D., and Bitonti, M. B. (2010). PoCHL P expression pattern in Posidonia oceanica is related to critical light conditions. Mar. Ecol. Prog. Ser. 415, 61–71.Buchanan and Balmer, 2005;

Buia M. C. & I. Mazzella (1991). Reproductive phenology of the Mediterranean seagrasses Posidonia oceanica (L.) Delile, Cymodocea nodosa (Ucria) Aschers, and Zostera noltii Hornem. Aquat. Bot., 40: 343- 362.

Bunney, T. D., Van Walraven, H. S., and De Boer, aH. (2001). 14-3-3 protein is a regulator of the mitochondrial and chloroplast ATP

synthase. Proc. Natl. Acad. Sci. U.S.A. 98, 4249–4254. doi: 10.1073/pnas. 061437498

Cancemi G., Buia M. C. & L. Mazzella (2002). Structure and growth dynamics of Cymodocea nodosa meadows: Sci. Mar., 66 (4): 365-373.

Casazza, G., and Mazzella, L. (2002). Photosynthetic pigment composition of marine angiosperms: preliminary characterization of Mediterranean seagrasses.. Bull. Sci. Mar. 71, 1171–1181.

Casazza, G; Lopez Royo, C; Silvestri, C. Seagrasses as key coastal ecosystems: an overview of the recent EU WFD requirements and current applications. Biologia Marina Mediterranea, 2006,13, 189–193.

Caye, G. and Meinesz, A., 1986. Experimental study of seed germination in the seagrass Cymodocea nodosa. Aquat. Bot., 26: 79--87.

Chevalier, F., Martin, O., Rofidal, V., Devauchelle, A.-D., Barteau, S., Sommerer, N., et al. (2004). Proteomic investigation of natural variation between Arabidopsis ecotypes. Proteomics 4, 1372–1381. doi: 10.1002/pmic.200300750Chitnis et al., 2001

Chitnis, P. R. (2001). PHOTOSYSTEM I: function and physiology. Annu. Rev. Plant Physiol. Plant Mol. Biol. 52, 593–626. doi: 10.1146/annurev.arplant.52.1.593

Costanza R., d'Arget R., de Groot R. et al. The value of the world's ecosystem services and natural capital // Nature. – 1997.

Cozza, R., Chiappetta, A., Petrarulo, M., Salimonti, A., Rende, F., Bitonti, M.B., Innocenti, A.M., 2004. Cytophisiological features of Posidonia oceanica as putative markers of environmental conditions. Chemistry and Ecology 20, 215–223.

Craig, R., and Beavis, R. C. (2003). A method for reducing the time required to match protein sequences with tandem mass spectra. Rapid Commun. Mass Spectrom. 17, 2310–2316. doi: 10.1002/rcm.1198

Craig, R., Cortens, J. P., and Beavis, R. C. (2004). Open source system for analyzing, validating, and storing protein identification data. J. Proteome Res. 3, 1234–1242. doi: 10.1021/pr049882h

Craig, R., Cortens, J. P., and Beavis, R. C. (2005). The use of proteotypic peptide libraries for protein identification. Rapid Commun. Mass Spectrom. 19, 1844–1850. doi: 10.1002/rcm.1992

Cunha, A. (2008). Projecto BIOMARES LIFE 06/NAT/P/000192. Relatório não técnico. Centro de Ciencias do Mar.

Curiel, D., Scarton, F., Rismondo, A., & Mrzocchi, M. (2003) Transplanting seagrasses in the Lagoon of Venice: Results and perspectives. Proceedings of the Sixth International Conference

on the Mediterranean Coastal Environment, MEDCOAST 03, E. Özhan (Editor), 7-11 October 2003, Ravenna, Italy. Vol 2: 853-864

Cushman, J., 2001. Osmoregulation in plants: implications for agriculture. Am. Zool. 41, 758–769.

Dattolo E, Jenny Gu, Philipp E. Bayer, Silvia Mazzuca, Ilia A. Serra,Antonia Spadafora, Letizia Bernardo, Lucia Natali, Andrea Cavallini and Gabriele Procaccini .Acclimation to different depths by the marine angiosperm Posidonia oceanica: transcriptomic and proteomic profiles. 2013 Frontiers in Plant Sciences

Denison, F. C., Paul, A.-L., Zupanska, A. K., and Ferl, R. J. (2011). 14-3-3 proteins in plant physiology. Semin. Cell Dev. Biol. 22, 720–727. doi: 10.1016/j.semcdb.2011.08.006

Dennison, W. C. (1990). "Chlorophyll content," in Seagrass Research Methods, eds R. C. Phillips and C. P. McRoy (UNESCO), 83–85.

Diatchenko, L., Laut, Y. C., Campbellt, A. P., Chenchik, A., Moqadam, F., Huang, B., et al. (1996). Suppression subtractive hybridization: a method for generating differentially regulated or tissuespecific cDNA probes. Proc. Natl. Acad. Sci. U.S.A. 93, 6025–6030. doi: 10.1073/pnas.93.12.6025

Doney, S. C., Ruckelshaus, M., Emmett Duffy, J., Barry, J. P., Chan, F., English, C. A., et al. (2002). Climate change impacts on marine ecosystems.Estuaries 25, 149–164. doi:10.1007/BF02691304

Douce, R., and Joyard, J. (1982) Purification of the chloroplast envelope. In Methods in Chloroplast Molecular Biology (Edelman, M., Hallick, R., and Chua, N.H., eds.), Elsevier/North-Holland, Amsterdam, pp. 139--256.

Duarte C, Marba` N, Santos R (2004) What may cause loss of seagrasses? In: Borum J, Duarte CM, Krause-Jensen D, Greve TM (eds) European seagrasses: an introduction to monitoring and management. The MandMS project, Hillerød, pp 19–23. ISBN: 87-89143-21-3

Duarte C. M. & K. Sand- Jensen (1990). Seagrass colonization: patch formation and patch growth in Cymodocea nodosa. Mar. Ecol. Prog. Ser., 65: 193- 200.

Duarte C. M. & K. Sand- Jensen (1990). Seagrass colonization: biomass development and shoot demography in Cymodocea nodosa patches. Mar. Ecol. Prog. Ser. 67: 97- 103.

Duarte, C.M., 1991. Seagrass depth limits. Aquatic Botany 40, 363–377.

Duarte, C.M., 2002. The future of seagrass meadows. Environmental Conservation, 29:2. Cambridge University Press , pp. 192–206.

Dumay, O., Costa, J., Desjobert, J.M., Pergent, G., 2004. Variations in the concentration of phenolic compounds in the seagrass Posidonia oceanica under conditions of competition. Phytochemistry 65 (24), 3211–3220.

Edge, S. E., Morgan, M. B., and Snell, T. W. (2008). Temporal analysis of gene expression in a field population of the Scleractinian coral Montastraea faveolata. J. Exp.Mar. Biol. Ecol. 355, 114–124. doi: 10.1016/j.jembe.2007.12.004Elrad et al., 2002

Emanuelsson O, Nielsen H, von Heijne G. 1999. ChloroP, a neural networkbased method for predicting chloroplast transit peptides and their cleavage sites. Protein Sci 8:978–984.

Escoubas, J. M., Lomas, M., LaRoche, J., and Falkowski, P. G. (1995). Light intensity regulation of cab gene transcription is signaled by the redox state of the plastoquinone pool. Proc. Natl. Acad. Sci. U.S.A. 92, 10237–10241. doi: 10.1073/pnas.92.22.10237Feder and Walser, 2005;

Fenyö, D., Eriksson, J., and Beavis, R. (2010). "Mass spectrometric protein identification using the global proteome machine," in Computational Biology, Methods in Molecular Biology, Vol. 673, ed D. Fenyö (New York, NY: The Rockefeller University), 189–202. doi: 10.1007/978-1-60761-842-3_11

Fernández-Torquemada Y, Sánchez-Lizaso JL (2005) Effects of salinity on leaf growth and survival of the Mediterranean seagrass Posidonia oceanica (L.) Delile. J Exp Mar Biol Ecol 320:57-63

Fernie, A. R., Carrari, F., and Sweetlove, L. J. (2004). Respiratory metabolism: glycolysis, the TCA cycle and mitochondrial electron transport. Curr. Opin. Plant Biol. 7, 254–261. doi: 10.1016/j.pbi.2004.03.007Ferro et al., 2000

Ferro M, Brugiere S, Salvi D, Seigneurin-Berny D, Court M, Moyet L, Ramus C, Miras S, Mellal M, Le Gall S, Kieffer-Jaquinod S, Bruley C, Garin J, Joyard J, Masselon C and Rolland N AT_CHLORO: A comprehensive chloroplast proteome database with subplastidiallocalization and curated information on envelope proteins. Molecular and Cellular Proteomics, 2010, 9(1): 1063-1084

Ferro, M., Salvi, D., Brugière, S., Miras, S., Kowalski, S., Louwagie, M., Garin, J., Joyard, J.,and Rolland, N. (2003) Proteomics of the chloroplast envelope membranes from Arabidopsis thaliana. Mol. Cell Proteomics 2, 325--345.

Ferro, M., Salvi, D., Rivière-Rolland, H., Vermat, T., Seigneurin-Berny, D., Grunwald, D.,Garin J., Joyard, J., and Rolland, N. (2002) Integral membrane proteins of the chloroplast envelope:

identification and subcellular localization of new transporters. Proc. Natl. Acad.Sci. U.S.A. 99, 11487—11492.

Ferro, M., Seigneurin-Berny, D. Rolland, N., Chapel, A., Salvi, D., Garin, J., and Joyard, J.(2002) Organic solvent extraction as a versatile procedure to identify hydrophobic chloroplast membrane proteins. Electrophoresis 21, 3517--3526.

Figueroa, F.L., Jimenez, C., Vinegla, B., Perez-Rodriguez, E., Aguilera, J., Flores Moya, A., Altamirano, M., Lebert, M., Haeder, D.P., 2002. Effects of solar UV radiation on photosynthesis of marine angiosperme Posidonia ocenica from southern Spain. Mar. Ecol. Prog. Ser. 230, 59–70.

Fonseca, M. S., Denworthy, W. J., Cheap, K. M., Currin, C. A., and Thayer, G. W. 1984. "A low-cost transplanting technique for shoalgrass (Halodule wrightii) and manatee grass (Syringodium filiforme)", Instruction Report EL-84-1, US Army Engineer Waterways Experiment Station, Vickburg, Miss., prepared by National Marine Fisheries Service under contract to Envieronmental Laboratory.

Fonseca, Mark S., et al. 1998. Guidelines for the Conservation and Restoration of Seagrasses in the United States and Adjacent Waters. NOAA Coastal Ocean Program Decision Analysis Series No. 12. NOAA Coastal Ocean Office, Silver Spring, MD. 222 pp.

Foret, S., Kassahn, K. S., Grasso, L. C., Hayward, D. C., Iguchi, A., Ball, E. E., et al. (2007). Genomic and microarray approaches to coral reef conservation biology. Coral Reefs 26, 475–486. doi: 10.1007/s00338- 007-0206-1Förster et al., 2006;

Friso G, Giacomelli L, Ytterberg AJ, Peltier JB, Rudella A, Sun Q, Wijk KJ. 2004. In-depth analysis of the thylakoid membrane proteome of Arabidopsis thaliana chloroplasts: New proteins, new functions, and a plastid proteome database. Plant Cell 16:478–499.

Fritzmann C. , J. Löwenberg, T. Wintgens, T. Melin State-of-the-art of reverse osmosis desalination Desalination Volume 216, Issues 1–3, 5 October 2007, Pages 1–76

Froehlich JE, Wilkerson CG, Ray WK, McAndrew RS, Osteryoung KW, Gage DA, Phinney BS. 2003. Proteomic study of the Arabidopsis thaliana chloroplastic envelope membrane utilizing alternatives to traditional two-dimensional electrophoresis. J Proteome Res 2:413-425.

Fujita, Y. (1997). A study on the dynamic features of photosystem stoichiometry: accomplishments and problems for future studies. Photosynth. Res. 53, 83–93. doi:10.1023/A:1005870301868

Gacia E, Invers O, Manzanera M, Ballesteros E, Romero J (2007) Impact of the brine from a desalination plant on a shallow seagrass (Posidonia oceanica) meadow. Estuar Coast Shelf S 72:579-590

Ganassin, C. and Gibbs, P.J., 2007. A review of seagrass planting as a means of habitat compensation following loss of seagrass meadow. NSW Department of Primary Industries – Fisheries Final Report Series No. 96. 41pp. ISSN 1449-9967.

Genomics 92, 255–264. doi: 10.1016/j.ygeno.2008.07.001

Gomez SM, Bil KY, Aguilera R, Nishio JN, Faull KF, Whitelegge JP. 2003. Transit peptide cleavage sites of integral thylakoid membrane proteins.Mol Cell Proteomics 2:1068–1085.

Gomez SM, Nishio JN, Faull KF, Whitelegge JP. 2002. The chloroplast grana proteome defined by intact mass measurements from liquid chromatography mass spectrometry. Mol Cell Proteomics 1:46–59.

Goulas E, Schubert M, Kieselbach T, Kleczkowski LA, Gardestrom P,Schroder W, Hurry V. 2006. The chloroplast lumen and stromal proteomes of Arabidopsis thaliana showdifferential sensitivity to shortand long-term exposure to low temperature. Plant J 47:720–734

Gracey AY.Interpreting physiological responses to environmental change through gene expression profiling.J Exp Biol. 2007 May;210(Pt 9):1584-92.

Green EP, Short FT, eds. 2003. World Atlas of Seagrasses. Berkeley: University of California Press.

Greenpeace. Trasplante Letal. 2008. La destrucción legalizada de Posidonia oceanica pradera submarina del Mediterráneo en el ámbito de la UE

*Guidetti P, Fabiano M. 2000. The use of lepidochronology to assess the impact of terrigenous discharges on the primary leaf production of the Mediterranean seagrass Posidonia oceanica. Marine Pollution Bulletin **40**(5): 449-453.*

Hall-Spencer,J.M.,Rodolfo-Metalpa, R.,Martin,S.,Ransome,E.,Fine,M., Turner,S.M.,etal.(2008).Volcanic carbondioxideventsshowecosys-temeffectsofoceanacidification. Nature 454, 96–99.

Hill, J. K., Griffiths, H. M., and Thomas, C. D. (2010). "Climate change and evolutionary adaptations at species' range margins," in Annual Review of Entomology, Vol. 56, eds M. R. Berenbaum, R. T. Carde, and G. E. Robinson, 143–159. doi: 10.1146/annurevento- 120709-144746

Hofmann, G. E., Burnaford, J. L., and Fielman, K. T. (2005). Genomicsfueled approaches to current challenges in marine

ecology. Trends Ecol. Evol. 20, 305–311. doi: 10.1016/j.tree.2005.03.006

Huang J, Lu X, Yan H, Chen S, Zhang W, Huang R, Zheng Y.Transcriptome characterization and sequencing-based identification of salt-responsive genes in Millettia pinnata, a semi-mangrove plant.DNA Res. 2012 Apr;19(2):195-207. doi: 10.1093/dnares/dss004. Epub 2012 Feb 19.

Inoue T. 2007. The chloroplast outer envelope membrane: The edge of light and excitement. J Integr Plant Biol 49:1100–1111.

Jarvis P. 2008. Targeting of nucleus-encoded proteins to chloroplasts in plants. New Phytol 179:257–285.

Jiao, Y., Lau, O. S., and Deng, X. W. (2007). Light-regulated transcriptional networks in higher plants. Nat. Rev. Genet. 8, 217–230. doi: 10.1038/nrg2049

Jones, H., Ostrowski, M., and Scanlan, D. J. (2006). A suppression subtractive hybridization approach reveals niche-specific genes that may beinvolved in predator avoidance in marine Synechococcus isolates. Proc. Nat. Acad. Sci. U.S.A. 72, 2730–2737. doi: 10.1128/AEM.72.4. 2730-2737.2006

Joyard J, Ferro M, Masselon C, Seigneurin-Berny D, Salvi D, Garin J,Rolland N. 2009. Chloroplast proteomics and the compartmentation of plastidial isoprenoid biosynthetic pathways. Mol Plant 2:1154– 1180.

Joyard J, Teyssier E, Miege C, Berny-Seigneurin D, Marechal E, Block MA, Dorne AJ, Rolland N, Ajlani G, Douce R. 1998. The biochemical machinery of plastid envelope membranes. Plant Physiol 118:715–723.

Joyard J, Ferro M, Masselon C, Seigneurin-Berny D, Salvi D, Garin J, Rolland N. Chloroplast proteomics highlights the subcellular compartmentation of lipid metabolism. Prog Lipid Res. 2010 Apr;49(2):128-58. doi: 10.1016/j.plipres.2009.10.003. Epub 2009 Oct 30. Review.

Karr, T. L. (2008). Application of proteomics to ecology and population biology. Heredity 100, 200–206. doi: 10.1038/sj.hdy.6801008

Kassahn, K. S., Crozier, R. H., Poertner, H. O., and Caley, M. J. (2009). Animal performance and stress: responses and tolerance limitsat different levels of biological organisation. Biol. Rev. 84, 277–292. doi: 10.1111/j.1469-185X.2008. 00073.x

Katz A,Waridel P, Shevchenko A, Pick U. 2007. Salt-induced changes in the plasma membrane proteome of the halotolerant alga

Dunaliella salina as revealed by blue native gel electrophoresis and nano-LC-MS/MS analysis. Mol Cell Proteomics 6:1459–1472.

Kieselbach T, Bystedt M, Hynds P, Robinson C, Schro¨der WP. 2000. A peroxidase homologue and novel plastocyanin located by proteomics to the Arabidopsis chloroplast thylakoid lumen. FEBS Lett 480:271–276

Kieselbach T, Hagman A, Andersson B, Schro¨der WP. 1998. The thylakoid lumen of chloroplasts. Isolation and characterization. J Biol Chem 273:6710–6716

Kieselbach T, Schro¨der WP. 2003. The proteome of the chloroplast lumen of higher plants. Photosynth Res 78:249–264.

Kleffmann T, Hirsch-Hoffmann M, GruissemW, Baginsky S. 2006. plprot: A comprehensive proteome database for different plastid types. Plant Cell Physiol 47:432–436

Kleffmann T, Russenberger D, von Zychlinski A, Christopher W, Sjolander K, Gruissem W, Baginsky S. 2004. The Arabidopsis thaliana chloroplast proteome reveals pathway abundance and novel protein functions. Curr Biol 14:354–362.

Kleffmann T, von Zychlinski A, Russenberger D, Hirsch-Hoffmann M, Gehrig P, Gruissem W, Baginsky S. 2007. Proteome dynamics during plastid differentiation in rice. Plant Physiol 143:912–923.

Koo AJ, Ohlrogge JB. 2002. The predicted candidates of Arabidopsis plastid inner envelope membrane proteins and their expression profiles. Plant Physiol 130:823–836.

*Larkum, AWD; Drew, EA; Ralph, PJ**.** Photosynthesis in seagrasses**.** In Seagrasses: Biology, Ecology and Conservation**,** Larkum AWD**,** Orth RJ. and Duarte C. (Eds.). Springer, Dordrecht; 2006 b; 323-345*

Larkum, WD; Orth, RJ; Duarte, CM (Eds.). Seagrasses: Biology, Ecology and Conservation. Springer, Dordrecht; 2006 a; 691 pp.

Larsen, P. F., Nielsen, E. E., Meier, K., Olsvik, P. A., Hansen, M. M., and Loeschcke, V. (2012). Differences in salinity tolerance and gene expression between two populations of Atlantic cod (Gadus morhua) in response to salinity stress. Biochem. Genet. 50, 454–466. doi: 10.1007/s10528-011-9490-0

Lederberg, J; McCray, AT 'Ome sweet 'omics - A genealogical treasury of words. SCIENTIST 2001 15(7): 8-8

Lee, K.-S., Park, S. R., and Kim, Y. K. (2007). Effects of irradiance, temperature, and nutrients on growth dynamics of seagrasses: a review. www.frontiersin.org June 2013 | Volume 4 | Article 195 | 13

Levitan, O., Kranz, S. A., Spungin, D., Prásil, O., Rost, B., and Berman-Frank, I. (2010). Combined effects of CO2 and light on the N2-fixing cyanobacterium Trichodesmium IMS101: a mechanistic view. Plant Physiol. 154, 346–356. doi: 10.1104/pp.110.159285

Lindahl M, Kieselbach T (2009) Disulphide proteomes and interactions with thioredoxin on the track towards understanding redox regulation in chloroplasts and cyanobacteria. Journal of Proteomics 72: 416-438

Liu, L., Zhou, Y., Zhou, G., Ye, R., Zhao, L., Li, X., et al. (2008a). Identification of early senescenceassociated genes in rice flag leaves. Plant Mol. Biol. 67, 37–55. doi: 10.1007/s11103-008-9300-1

Liu, X., Zhang, M., Duan, J., and Wu, K. (2008b). Gene expression analysis of germinating rice seeds responding to high hydrostatic pressure. J. Plant Physiol. 165, 1855–1864. doi: 10.1016/j.jplph. 2008.05.004

Lorenti , Dappiano and Gambi , 2006 Occurrence and ecology of Mesanthura (Crustacea: Isopoda: Anthuridea) in two Italian harbours. Marine Biodiversity Records, page 1 of 5. #2009 Marine Biological Association of the United Kingdom doi:10.1017/S1755267209000153;

Luque A. A. & J. Templado (Coords,) (2004). Praderas y bosques marinos de Andalucía. Consejería de Medio Ambiente, Junta de Andalucía. Sevilla, 336pp.

Maathuis, F. J.M., Filatov, V., Herzyk, P. C., Krijger, G. B., Axelsen, K., Chen, S., et al. (2003). Transcriptome analysis of root transporters reveals participation of multiple gene families in the response to cation stress. Plant J. 35, 675–692. doi: 10.1046/j.1365-313X.2003.01839.x

MajeranW, Zybailov B, Ytterberg J, Dunsmore J, Sun Q, vanWijk KJ. 2008.Consequences of C4 differentiation for chloroplast membrane proteomes in maize mesophyll and bundle sheath cells. Mol Cell Proteomics 7:1609–1638

Marín-Guirao L, Sandoval-Gil JM, Ruiz JM, Sánchez-Lizaso JL (2011) Photosynthesis, growth and survival of the Mediterranean seagrass Posidonia oceanica in response to simulated salinity increases in a

laboratory mesocosm system. Estuar Coast Shelf S. doi:10.1016/j.ecss.2011.01.003

Massa, S. I., Pearson, G. A., Aires, T., Kube, M., Olsen, J. L., Reinhardt, R., et al. (2011). Expressed sequence tags from heat-shocked seagrass Zostera noltii (Hornemann) from its southern distribution range. Mar. Genomics 4, 181–188. doi: 10.1016/j.margen.2011.04.003

Matsumoto, T. K. (2006). Genes uniquely expressed in vegetative and potassium chlorate induced floral buds of Dimocarpus longan. Plant Sci. 170, 500–510. doi 10.1016/j.plantsci.2005.09.016

Mazzuca S., Cozza, R., Pangaro, T., 2009. Tissue expression pattern of two aquaporin-encoding genes in different organs of the seagrass Posidonia oceanica. Aquat. Bot. 91, 117–121

McArthur, L. C., and Boland, J. W. (2006). The economic contribution of seagrass to secondary production in South Australia. Ecol. Model. 196, 163–172. doi: 10.1016/j.ecolmodel.2006.02.030

Meinesz, A; Cirik, S; Akcali, B; Javel, F; Migliaccio, M; Thibaut, T; Yuksek, A; Procaccini, G. Posidonia oceanica in the Marmara Sea. Aquatic Botany, 2009,90, 18-22

Metzker, M. L. (2010). Sequencing technologies – the next generation. Nat. Rev. Genet. 11, 31–46. doi: 10.1038/nrg2626

Moreno, D., Guirado, J., 2006. Nuevos datos sobre la floración, fructificación y germinación de fanerógamas marinas en Andalucía. Acta Botanica Malacitana 31, 51-72.

Morozova, O., and Marra, M. A. (2008). Applications of next-generation sequencing technologies in functional genomics.

*Nicholson and Lindon, 2008; Systems biology: MetabonomicsNature **455**, 1054-1056 (23 October 2008) | doi:10.1038/4551054a; Published online 22 October 2008*

Olesen, B., Enríquez, S., Duarte, C., Sand-Jensen, K., 2002. Depth-acclimation of pho-tosynthesis, morphology and demography of Posidonia oceanica and Cymodoceanodosa in the Spanish Mediterranean Sea. Mar. Ecol. Prog. Ser. 236, 89–97.

Olsen, J.L. , Sadowski, G., Stam, W.T., Veldsink, J.H. & Jones, K., 2002. Characterization of microsatellite loci in the marine seaweed Ascophyllum nodosum (Phaeophyceae; Fucales). Molecular Ecology Notes 2:33-34. 2002-OlsenMolEcolN.pdf

Orth, R. J., M. C. Harwell, E. M. Bailey, A. Bartholomew, J. T. Jawad, A. V. Lombana, K. A. Moore, J. M. Rhode, H. E. Woods. 2000. A

review of issues in seagrass seed dormancy and germination: Implications for conversation and restoration. Mar. Ecol. Prog. Ser. 200:277-288.

Orth, R., S. Marion, S. Granger, and M. Traber. 2008. Restoring eelgrass (Zostera marina) from seed: A comparison of planting methods for large-scale projects. SAV Technical Notes Collection. ERDC/TN SAV-08-1. Vicksburg, MS: U.S. Army Engineer Research and Development Center.

Orth, R.J., T.J.B. Carruthers, W.C. Dennison, C.M. Duarte, J.W. Fourqurean, W. James, H.K. Heck Jr, A.R. Hughes, G.A. Kendrick, W.J. Kenworthy, and others. 2006. A global crisis for seagrass ecosystems. Bioscience 56:987–996.

Park, O.K., 2004. Proteomic studies in plants. J. Biochem. Mol. Ecol 37, 133–138.

Pastor, X., Aguilar, R. & de Pablo, M. J., 2007. Praderas sumergidas. OCEANA-Fundación Santander Central Hispano.

Pavón- Salas N., Garrido M. & R. Haroun (1998). Distribution and structure of seagrass meadows in Las Canteras Beach, Las Palmas, Canary Islands (Spain) Bol. Mus. Mun. Funchal., 50 (289): 107- 115.

Pearce D (1998) Auditing the Earth. The value of World's ecosystem services and natural capital. Environment 40: 23-28

Peltier JB, Cai Y, Sun Q, Zabrouskov V, Giacomelli L, Rudella A, Ytterberg AJ, Rutschow H, van Wijk KJ. 2006. The oligomeric stromal proteome of Arabidopsis thaliana chloroplasts. Mol Cell Proteomics 5:114–133.

Peltier JB, Emanuelsson O, Kalume DE, Ytterberg J, Friso G, Rudella A, Liberles DA, Soderberg L, Roepstorff P, von Heijne G, van Wijk KJ. 2002. Central functions of the lumenal and peripheral thylakoid proteome of Arabidopsis determined by experimentation and genomewide prediction. Plant Cell 14:211–236.

Peltier JB, Friso G, Kalume DE, Roepstorff P, Nilsson F, Adamska I, vanWijk KJ. 2000. Proteomics of the chloroplast: Systematic identification and targeting analysis of lumenal and peripheral thylakoid proteins. Plant Cell 12:319–341.

Peltier JB, Ytterberg AJ, Sun Q, van Wijk KJ. 2004. New functions of the thylakoid membrane proteome of Arabidopsis thaliana revealed by a simple, fast, and versatile fractionation strategy. J Biol Chem 279:49367–49383.

Pergent-Martini, C; Leoni, V; Pasqualini, V; Ardizzone, GD; and 35 others. Descriptors of Posidonia oceanica meadows: use and application. Ecological Indicators, 2005,5, 213–230.

Pirhc H., Buia M. C. & L. Mazzella (1986). Germination and seed development of Cymodocea nodosa (Ucria) Ascherson under laboratory conditions and "in situ". Aquatic Botany, 26: 181- 188.

Pop, M., and Salzberg, S. L. (2008). Bioinformatics challenges of new sequencing technology. Trends Genet. 24, 142–149. doi: 10.1016/j.tig.2007.12.006

Portis, A. R. (2003). Rubisco activase – Rubisco's catalytic chaperone. Photosynth. Res. 75, 11–27. doi: 10.1023/A:1022458108678

Procaccini G. , Beer S. , Björk M. , Olsen J. , Mazzuca S. , Santos R. , " Seagrass ecophysiology meets ecological genomics: Are we ready?". Marine Biology, 2012, pp. 1-6.

Procaccini G., Olsen J.L., Reusch T.B.H. (2007) Contribution of genetics and genomics to seagrass biology and conservation. Journal of Experimental Marine Biology and Ecology,350, 234–259.

Proccaccini G, Buia MC, Gambi MC, Perez M, Pergent G, Pergent-Martini C, Romero J (2003) Seagrasses of the western mediterranean. In: Green EP, Short FT (eds) World Atlas of Seagrasses. University of California Press, Berkeley, pp 48-58

Puthoff DP, Smigocki AC. Insect feeding-induced differential expression of Beta vulgaris root genes and their regulation by defense-associated signals. Plant Cell Rep. 2007 Jan;26(1):71-84. Epub 2006 Jul 21.

Ramirez Ramirez, T., Cortes, D., Mercado, J.M., Vargas-Yanez, M., Sebastian, M., Liger, E., 2005. Seasonal dynamics of inorganic nutrients and phytoplankton biomass in the NW Alboran Sea. Estuar. Coast. Shelf Sci. 65, 654–670.

Reiland S, Messerli G, Baerenfaller K, Gerrits B, Endler A, Grossmann J, Gruissem W, Baginsky S. Large-scale Arabidopsis

phosphoproteome profiling reveals novel chloroplast kinase substrates and phosphorylation networks. Plant Physiol. 2009 Jun;150(2):889-903. doi: 10.1104/pp.109.138677. Epub 2009 Apr 17.

Reusch,T.B.H.,Veron,A.,andPreuss, C., Weiner,J.,Wissler,L.,Beck,A., etal.(2008).Comparativeanaly- sis ofexpressedsequenceTag(EST) librariesintheseagrass Zostera marina subjectedtotemperature stress. Mar.Biotechnol.(N.Y.) 10, 297–309.

Reyes J. & M. Sansón (1994). Morfología y anatomía de Cymodocea nodosa (Cymodoceaceae, Magnoliophyta) en praderas de El Médano (Tenerife, Islas Canarias), Vieraea, 23: 43- 64.

Reyes J., Sansón M. & J. Afonso- Carrillo (1995). Distribution and reproductive phenology of the seagrass Cymodocea nodosa (Ucria) Ascherson in the Canary Islands. Aquatic Botany 50: 171-180.

Richards, C. L., Rosas, U., Banta, J., Bhambhra, N., and Purugganan, M. D. (2012). Genome-wide patterns of Arabidopsis gene expression in nature. PLoS Genet. 8, 482–495. doi:10.1371/journal.pgen.1002662

Rismondo A., Curiel D., Marzocchi M. & M. Scattolin (1997). Seasonal pattern of Cymodocea nodosa biomass and production in the lagoon of Venice. Aquatic Botany

Rolland N, Ferro M, Ephritikhine G, Marmagne A, Ramus C, Brugière S, Salvi D, Seigneurin-Berny D, Bourguignon J, Barbier-Brygoo H, Joyard J, Garin J. A versatile method for deciphering plant membrane proteomes. J Exp Bot. 2006;57(7):1579-89. Epub 2006 Apr 4.

Rolland N, Ferro M, Seigneurin-Berny D, Garin J, Douce R, Joyard J. 2003. Proteomics of chloroplast envelope membranes. Photosynth Res 78:205–230.

Rossignoll, M; Peltier, J-B; Mock, H-P; Matros, A; Maldonado, AM; Jorrín, JV. Plant proteome analysis: A 2004–2006 update. Proteomics 2006, 6, 5529–5548

Ruitz, J.M., Romero, J., 2003. Effects of disturbances caused by coastal constructions on spatial structure growth dynamics and photosynthesis of the seagrass Posidonia

Ruiz de la Rosa, M., García, N., Zarranz, M., Manent, P., Domínguez, R., Gritón, M., Louzara, G., González, N. (2006). Preliminary results of experimental evaluation about different methods of transplanting Cymocodea nodosa in the Canary Islands. Bio. Mar. Medti. (2006), 13 (4): 267-271

Ruiz JM, Marín-Guirao L, Sandoval-Gil JM (2009) Responses of the Mediterranean seagrass Posidonia oceanica to in situ simulated salinity increase. Bot Mar 52:459-470

Salvi Daniel, Norbert Rolland, Jacques Joyard, and Myriam Ferro(2007) Purification and Proteomic Analysis of Chloroplasts and their Sub-Organellar Compartments. In Methods in Molecular Biology, vol. 432: Organelle Proteomics

Sandoval-Gil, J.M., L. Marín-Guirao[1], J.M. Ruiz. (2012) Tolerance of - Mediterranean seagrasses (Posidonia oceanica and Cymodocea nodosa) to hypersaline stress: water relations and osmolyte concentrations.

Saravanan, R.S., Rose, J.K.C., 2004. Acritical evaluation of sample extraction techniques for enhanced proteomic analysis of recalcitrant plant tissues. Proteomics 4, 2522–2532

Schleiff E, Eichacker LA, Eckart K, Becker T, Mirus O, Stahl T, Soll J. 2003. Prediction of the plant beta-barrel proteome: A case study of the chloroplast outer envelope. Protein Sci 12:748–759.

Schmidt, P. S., Serrao, E. A., Pearson, G. A., Riginos, C., Rawson, P. D., Hilbish, T. J., et al. (2008). Ecological genetics in the north Atlantic: environmental gradients and adaptation at specific loci. Ecology 89, S91–S107. doi:10.1890/07-1162.1

Schubert M, Petersson UA, Haas BJ, Funk C, Schroder WP, Kieselbach T. 2002. Proteome map of the chloroplast lumen of Arabidopsis thaliana. J Biol Chem 277:8354–8365.

Seddon S (2004) Going with the flow: Facilitating seagrass rehabilitation. Ecological Management & Restoration 5, 167-176.

Seigneurin-Berny D, Rolland N, Garin J, Joyard J. 1999. Technical advance: Differential extraction of hydrophobic proteins from chloroplast envelope membranes: A subcellular-specific proteomic approach to identify rare intrinsic membrane proteins. Plant J 19:217–228.

Serra and Mazzuca, 2011 Posidonia oceanica: from ecological status to genetic and proteomics resourses.

Serra I. A. , Nicastro S. , Mazzuca S. , Natali L. , Cavallini A. , Innocenti A. M. , " Response to salt stress in seagrasses: PIP1;1 aquaporin antibody localization in". Aquatic Botany, 2011, pp. x-x

Serra,I.A.,Lauritano,C.,Dattolo,E., Puoti,A.,Nicastro,S.,Innocenti,A. M., etal.(2012).Referencegenes assessmentfortheseagrass Posido- nia oceanica in differentsalinity,pH and lightconditions. Mar.Biol. 159, 1269–1282.

Sharon, Y., Levitan, O., Spungin, D., Berman-Frank, I., and Beer, S. (2011). Photoacclimation of the seagrass Halophila stipulacea to the dim irradiance at its 48-meter depth limit. Limnol. Oceanogr. 56, 357–362. doi: 10.4319/lo.2011.56.1.0357

Shevchenko, A., Wilm, M., Vorm, O., Jensen, O.N., Podtelejnikov, A.V., Neubauer, G.,Shevchenko, A., Mortensen, P., Mann, M., 1996. A strategy for identifying gelseparated proteins in sequence databases by MS alone. Biochem. Soc. Trans 24 (3), 893–896

Short, F. T., and Wyllie-Echeverria, S. (1996). Natural and humaninduced disturbance of seagrasses. Environ. Conserv. 23, 17–27. doi: 10.1017/S0376892900038212

Spadafora,A.,Filadoro,D.,Mazzuca,S., Bracale,M.,Marsoni,M.,Cardilio, M., etal.(2008).2-DEpolypep-tide mapping of Posidonia oceanica leaves, a molecular tool for marine environment studies. Plant Biosyst. 142, 213–218.

Stapley J, Reger J, Feulner PG, Smadja C, Galindo J, Ekblom R, Bennison C, Ball AD, Beckerman AP, Slate J. Adaptation genomics: the next generation. Trends Ecol Evol. 2010 Dec;25(12):705-12. doi: 10.1016/j.tree.2010.09.002. Epub 2010 Oct 16.

Sun Q, Emanuelsson O, van Wijk KJ. 2004. Analysis of curated and predicted plastid subproteomes of Arabidopsis. Subcellular compartmentalization leads to distinctive proteome properties. Plant Physiol 135:723–734.

Sun, Q; Zybailov, B; Majeran, W; Friso, G; Olinares, PDB; van Wijk, KJ. PPDB, the Plant Proteomics Database at Cornell. Nucleic Acids Research 2009, 37, 969-974.

Terrados J (1991) La vegetación sumergida del Mar Menor: 64-72, en Ramírez L et al., La Región de Murcia y su Naturaleza. Vol. I. Ed. La Opinión de Murcia, S.A. Murcia.

The Royal Society. (2005). Ocean Acidification due to Increasing Atmospheric Carbon Dioxide. Policy Document 12/05. London: The Royal Society.

Thomas, C. D. (2010). Climate, climate change and range boundaries. Diversity Distrib. 16, 488–495. doi: 10.1111/j.1472-4642.2010.00642.x

Thomas, C. D., Cameron, A., Green, R. E., Bakkenes, M., Beaumont, L. J., Collingham, Y. C., et al. (2004). Extinction risk from climate change. Nature 427, 145–148. doi:10.1038/nature02121

Tomasello A, Di Maida G, Calvo S, Pirrotta M, Borra M, Procaccini G (2009) Seagrass meadows at the extreme of environmental tolerance: the case of Posidonia oceanica in a semi-enclosed coastal lagoon. Mar Ecol 30:288-300

Touchette BW (2007) Seagrass-salinity interactions: Physiological mechanisms used by submersed marine angiosperms for a life at sea. J Exp Mar Biol Ecol 350:194-215

Touchette, B., and Burkholder, J. (2000). Overview of the physiological ecology of carbon metabolism in seagrasses. J. Exp. Mar. Biol. Ecol. 250, 169–205. doi: 10.1016/S0022-0981(00)00196-9

Tuya, F., Martín, J. A., Luque A. (2007). Ciclo estacional de una pradera marina de Cymodocea nodosa y la ictiofauna asociada en Playa Dorada (Lanzarote, Islas Canarias, Atlántico oriental).

van Wijk KJ. 2000. Proteomics of the chloroplast: Experimentation and prediction. Trends Plant Sci 5:420–425.

van Wijk KJ. 2001. Challenges and prospects of plant proteomics. Plant Physiol 126:501–508.

vanWijk KJ. 2004. Plastid proteomics. Plant Physiol Biochem 42:963–977.

Vener AV, Harms A, Sussman MR, Vierstra RD. 2001. Mass spectrometric resolution of reversible protein phosphorylation in photosynthetic membranes of Arabidopsis thaliana. J Biol Chem 276:6959–6966.

Virnstein, R. W. and L. J. Morris. 1996. Seagrass preservation and restoration: a diagnostic plan for the Indian River Lagoon. St. Johns River Water Management District, Palatka, FL, USA. Technical Memorandum 14.

Waycott,M., Duarte, C.M., Carruthers, T. J. B., Orth, R. J., Dennison, W. C., Olyarnik, S., et al. (2009). Accelerating loss of seagrasses across the globe threatens coastal ecosystems. Proc. Natl. Acad. Sci. U.S.A. 106, 12377–12381. doi: 10.1073/pnas.0905620106

Wear, R. J. (2006) Recent advances in research into seagrass restoration. Prepared for the Coastal Protection Branch, Department for Environment and Heritage. SARDI Aquatic Sciences Publications No. RD04/0038-4. SARDI Aquatic Sciences, Adelaide.

Weber AP, Schwacke R, Flugge UI. 2005. Solute transporters of the plastid envelope membrane. Annu Rev Plant Biol 56:133–164.

Whitelegge JP, Gundersen CB, Faull KF. 1998. Electrospray-ionization mass spectrometry of intact intrinsic membrane proteins. Protein Sci 7:1423– 1430.

Winters, G., Nelle, P., Fricke, B., Rauch, G., and Reusch, T. B. H. (2011). Effects of a simulated heat wave on photophysiology and gene expression of high- and low-latitude populations of Zostera marina. Mar. Ecol. Prog. Ser. 435, 83–95. doi: 10.3354/meps09213

Wissler, L., Dattolo, E., Moore, A. D., Reusch, T. B. H., Olsen, J. L., Migliaccio, M., et al. (2009). Dr. Zompo: an online data repository for Zostera marinaand Posidonia oceanica ESTs. Database (Oxford) 2009:bap009. doi: 10.1093/database/bap009

Wissler,L.,Codoñer,F.M.,Reusch,T. B.H.,Olsen,J.L.,Procaccini,G., and Bornberg-Bauer,E.(2011).Back totheSeatwice:identifyingcandi-dateplantgenesformolecularevo- lutiontomarinelife. BMC Evol. Biol. 11:8. doi:10.1186/1471-2148- 11-8

Yamazaki, J.-Y., Suzuki, T., Maruta, E., and Kamimura, Y. (2005). The stoichiometry and antenna size of the two photosystems in marine green algae, Bryopsis maxima and Ulva pertusa, in relation to the light environment of their natural habitat. J. Exp. Bot. 56, 1517–1523. doi: 10.1093/jxb/eri147

Yamori, W., Masumoto, C., Fukayama, H., and Makino, A. (2012). Rubisco activase is a key regulator of nonsteady- state photosynthesis at any leaf temperature and, to a lesser extent, of steady-state photosynthesis at high temperature. Plant J. 71, 871–880. doi: 10.1111/j.1365-313X.2012.05041.x

Yin, Z., Meng, F., Song, H., Wang, X., Xu, X., and Yu, D. (2010). Expression quantitative trait loci analysis of two genes encodingrubisco activase in soybean. Plant Physiol. 152, 1625–1637. doi: 10.1104/pp.109.148312

Zimmerman, RC. Light and photosynthesis in seagrass meadows. In: Larkum,WD; Orth, RJ; Duarte CM, (Ed.), Seagrasses: biology, ecology and conservation. Springer, Netherlands; 2006; pp. 303-321.

Zolla L, Rinalducci S, Timperio AM, Huber CG. 2002. Proteomics of lightharvesting proteins in different plant species. Analysis and comparison by liquid chromatography-electrospray ionization mass spectrometry. Photosystem I. Plant Physiol 130:1938–1950.

Zolla L, Rinalducci S, Timperio AM. 2007. Proteomic analysis of photosystem I components from different plant species. Proteomics 7:1866–1876.

Zolla L, Timperio AM, Walcher W, Huber CG. 2003. Proteomics of lightharvesting proteins in different plant species. Analysis and comparison by liquid chromatography-electrospray ionization mass spectrometry. Photosystem II. Plant Physiol 131:198–214.

Zouari, N., Ben Saad, R., Legavre, T., Azaza, J., Sabau, X., Jaoua, M., et al. (2007). Identification and sequencing of ESTs from the halophyte grass Aeluropus littoralis. Gene 404, 61–69. doi: 10.1016/j.gene.2007.08.021

Zybailov B, Rutschow H, Friso G, Rudella A, Emanuelsson O, Sun Q, van Wijk KJ. 2008. Sorting signals, N-terminal modifications and abundance of the chloroplast proteome. PLoS ONE 3(4):e1994.

Svetlana Epimashko, Elke Fischer-Schliebs, Anna-Luise Christian, Gerhard Thiel and Ulrich Lüttge Planta Vol. 224, No. 4 (2006), pp. 944-951

Albertsson and Andreasson, 2004

Nathan Nelson and Charles F. Yocum. Structure and Function of Photosystems I and II Annu. Rev. Plant Biol. 2006. 57:521–65

Gobert, S.,Cambridge, M. L.,Velimirov, B., Pergent, G., Lepoint, G., Bouquegneau, J. M., et al. (2006). "Biology of Posidonia," in Seagrasses: Biology, Ecology and Conservation, eds A. W. D. Larkum, R. J. Orth, and C. M. Duarte (Berlin: Springer Verlag), 387–408

Annex 1: *Materials and buffers for chloroplast*

Material for chloroplast:

1. Muslin or cheesecloth, 80 cm large
2. Nylon blutex (50 μm aperture)
3. Beakers (500 ml, 1 liter, 5 liters)
4. Ice and ice buckets
5. Pipettes (1 ml, 10 ml)
6. Percoll (Sigma)
7. Motor-driven blendor, 3 speed, 1 gallon (3.785 liters) (Waring blendor)
8. Superspeed refrigerated centrifuge (Kontron), with the following rotor (and
corresponding tubes in polypropylene) swinging bucket rotor (6 x 30 ml)
9. Preparative refrigerated ultracentrifuge (Eppendorf)

Buffer:

1. Leaf grinding medium: 0.45 M sorbitol, 20 mM Tricine-KOH, pH 8.4, 10 mM EDTA, 10 mM NaHCO3, 0.1 bovine serum albumin (Sigma)

2. Chloroplast isolation and washing medium: 0.30 M sorbitol, 20 mM Tricine-KOH, pH 7.6,5 mM MgCl2, 2.5 mM EDTA

3. Sorbitol solution: 0.60 M sorbitol, 40 mM Tricine-KOH, pH 7.6, 10 mM MgCl2, 5 mM EDTA

4. Solution for Percoll gradients: 60% Percoll / 0.36 M sorbitol solution

Annex 2: *Table of proteins from Cymodocea nodosa under salt stress*

A = referred sample
B= hypersaline after 15 days
C= hypersaline after 30 days

A

rank	log (e)	log (I)	% (m)	% (c)	unique	total	Mr	Accession	Description
1	-8	6,9	4,2	9	2	3	50,4	tr|Q6L9Z6|Q6L9Z6_9LILI	RuBisCO large subunit;
2	-3,9	5,6	2,1	3	1	1	74	tr|Q2QV45|Q2QV45_ORYSJ	70 kDa heat shock protein; Os12g0244100 protein;
3	-3,5	6,2	4,3	5	1	3	33,2	sp|P08477|G3PC_HORVU	Glyceraldehyde-3-phosphate dehydrogenase, cytosolic;
4	-1,8	5,9	1,6	2	1	1	72,9	sp|Q7SIC9|TKTC_MAIZE	Transketolase:p , chloroplastic; TK; EC 2.2.1.1;
5	-1,7	5,6	1,5	2	1	1	111,4	tr|Q6V9T1|Q6V9T1_ORYSJ	Glycine dehydrogenase P protein; Os01g0711400 protein;
1	-54	7,4	17	21	6	13	53,6	tr|H2CPP4|H2CPP4_COLES	EC 3.6.3.14; ATP synthase F1 sector subunit beta;
2	-44	7,3	3,2	3	1	1	59,1	tr|Q4FGI4|Q4FGI4_TYPLA	ATP synthase subunit beta; EC 3.6.3.14;
3	-42	7,3	2	2	1	2	55,3	sp|Q95AD6|ATPB_WHIBI	EC 3.6.3.14; ATP synthase F1 sector subunit beta;
4	-38	7,2	12	21	5	8	55,3	sp|A9LYH0|ATPA_ACOAM	EC 3.6.3.14; ATP synthase F1 sector subunit alpha;
5	-36	7,4	11	24	5	8	50,4	tr|Q6L9Z6|Q6L9Z6_9LILI	RuBisCO large subunit;
6	-28	7,1	2	2	1	1	55,3	sp|P62626|ATPB_AEGCO	EC 3.6.3.14; ATP synthase F1 sector subunit beta;
7	-19	6,9	2,3	2	1	1	50,4	tr|C6G4V9|C6G4V9_9ASPA	Ribulose-1:p,5-bisphosphate carboxylase/oxygenase large subunit;
8	-19	6,2	6,3	8	3	3	59,1	sp|P19023|ATPBM_MAIZE	ATP synthase subunit beta, mitochondrial; EC 3.6.3.14;
9	-9,3	5,9	4,6	6	2	2	61,4	tr|Q7X9A7|Q7X9A7_ORYSJ	60 kDa chaperonin alpha subunit; Putative rubisco subunit binding-protein alpha subunit;
10	-5,1	5,2	4,1	6	1	1	55,1	sp|P05494|ATPAM_MAIZE	ATP synthase subunit alpha, mitochondrial;
1	-22	6,8	10	15	3	5	42,7	tr|F2D714|F2D714_HORVD	Predicted protein;
2	-22	6,7	7,9	9	3	4	50	tr|Q1ENY9|Q1ENY9_MUSAC	Phosphoglycerate kinase, chloroplast,

									putative; EC 2.7.2.3;
3	-21	6,6	3,5	4	1	1	0	sp|P12782|PGKH_WHEAT	no protein information available
4	-20	6,7	1,9	2	1	1	50	tr|B6STH5|B6STH5_MAIZE	Phosphoglycerate kinase; EC 2.7.2.3; EC 3.6.3.14; ATP synthase F1 sector subunit beta;
5	-18	6,3	7,8	10	3	3	53,6	sp|Q3V527|ATPB_ACOCL	Phosphoglycerate kinase; EC 2.7.2.3;
6	-11	6,3	5,4	6	1	1	31,4	tr|C1JYE2|C1JYE2_9POAL	no protein information available
7	-7,4	6,1	5	12	2	2	48,9	tr|O78641|O78641_9ASPA	no protein information available
8	-4,7	5,7	4,2	6	1	1	47,2	sp|Q42450|RCAB_HORVU	ATP synthase subunit gamma, chloroplastic; F-ATPase gamma subunit;
9	-3,7	6,4	3,3	5	1	2	39,8	sp|P0C1M0|ATPG_MAIZE	Peroxidase 1; EC 1.11.1.7; Glyceraldehyde-3-phosphate dehydrogenase B, chloroplast
10	-3,5	6,1	5,1	8	1	1	33	sp|P27337|PER1_HORVU	Fructose-bisphosphate aldolase, chloroplastic; ALDP; EC 4.1.2.13;
11	-3,4	5,7	2,9	4	1	1	47,1	tr|Q9SNK3|Q9SNK3_ORYSJ	Apocytochrome f; Aspartate aminotransferase, cytoplasmic; EC 2.6.1.1; Transaminase A;
12	-3,1	5,4	3,4	5	1	1	42	sp|Q40677|ALFC_ORYSJ	Malate dehydrogenase, cytoplasmic; EC 1.1.1.37; Os05g0302700 protein; cDNA clone:001-036-B04, full insert sequence; Ribulose-bisphosphate carboxylase large subunit;
13	-2,7	5,7	4,7	6	1	1	35,2	sp|A6MMM0|CYF_DIOEL	Phosphoglycerate kinase 2; EC 2.7.2.3; Mitochondrial outer membrane protein porin 2; OsVDAC2; 60 kDa chaperonin beta subunit; Os02g0102900 protein;
15	-2,1	5,8	3,2	4	1	1	44,5	sp|P37833|AATC_ORYSJ	Predicted protein;
19	-1,3	6,7	3,3	5	1	3	35,6	sp|Q08062|MDHC_MAIZE	Putative chlorophyll a/b binding protein;
1	-11	6,2	6,1	9	2	2	41	tr|Q0DJC0|Q0DJC0_ORYSJ	Photosystem II subunit PsbS
2	-8,2	6,2	5	12	2	2	49,2	tr|Q8WL39|Q8WL39_9ASPA	Photosystem I reaction center subunit II, chloroplastic; Photosystem I 20 kDa subunit;
3	-2,5	5,5	3	3	1	1	42,3	tr|Q1EPF8|Q1EPF8_MUSAC	Glyceraldehyde-3-phosphate dehydrogenase, cytosolic; EC 1.2.1.12;
4	-2,5	5,7	3,9	6	1	1	29,6	sp|Q6L5I5|VDAC2_ORYSJ	
5	-2,4	5,4	2	2	1	1	63,8	tr|Q6ZFJ9|Q6ZFJ9_ORYSJ	
6	-2	6,1	4,9	6	1	2	34,4	tr|F2CRK1|F2CRK1_HORVD	
9	-1,5	5,8	5,7	8	1	2	29,8	tr|G0YLW6|G0YLW6_9ARAE	
1	-23	6,7	15	25	3	10	27,7	tr|Q6WFB1|Q6WFB1_MAIZE	
2	-4	5,5	6,8	12	1	1	21,9	sp|P36213|PSAD_HORVU	
7	-1,4	5,7	4,3	5	1	1	33,2	sp|P08477|G3PC_HORVU	

1	-1,9	5,7	13	14	1	1	9,3	tr|I1IWU7|I1IWU7_BRADI	Uncharacterized protein;
2	-1,8	5,8	13	28	1	1	9,4	sp|A1EA25|PSBE_AGRST	no protein information available

B

rank	log(e)	log(I)	% (measured)	% (corrected)	unique	total	Mr	Accession	Description
1	-37	6,8	11	24	5	8	50,4	tr|Q6L9Z6|Q6L9Z6_9LILI	RuBisCO large subunit;
2	-3,3	5,2	2,6	7	1	1	56	sp|A9LYC6|PSBB_ACOAM	Photosystem II CP47 chlorophyll apoprotein;
3	-2,3	5,4	2	3	1	1	71,5	tr|C5YWM8|C5YWM8_SORBI	no protein information available
4	-2,2	5,7	4,3	5	1	1	33,2	sp|P08477|G3PC_HORVU	Glyceraldehyde-3-phosphate dehydrogenase, cytosolic; EC 1.2.1.12;
5	-1,8	5,7	3	5	1	1	55,3	sp|A9LYH0|ATPA_ACOAM	EC 3.6.3.14; ATP synthase F1 sector subunit alpha; F-ATPase subunit alpha;
1	-46	6,8	14	17	5	9	53,6	tr|H2CPP4|H2CPP4_COLES	EC 3.6.3.14; ATP synthase F1 sector subunit beta; F-ATPase subunit beta;
2	-43	6,8	5	5	1	1	59,1	tr|H6THB0|H6THB0_9LILI	ATP synthase subunit beta; EC 3.6.3.14;
3	-38	6,8	7	16	5	9	49	tr|B5RHG8|B5RHG8_9ASPA	Ribulose-bisphosphate carboxylase large subunit;
4	-32	6,8	9,7	18	4	6	55,3	sp|A9LYH0|ATPA_ACOAM	EC 3.6.3.14; ATP synthase F1 sector subunit alpha; F-ATPase subunit alpha;
5	-29	6,7	4,7	11	2	2	51,6	tr|B0B735|B0B735_9POAL	Ribulose-1:p,5-bisphosphate carboxylase/oxygenase large subunit; EC 4.1.1.39;
6	-29	6,6	2,2	2	1	1	0	tr|F8RS97|F8RS97_JUNEF	ATP synthase subunit alpha
7	-29	7,1	2,2	2	1	3	0	tr|Q6L9Z6|Q6L9Z6_9LILI	RuBisCO large subunit;
8	-20	6,7	2	2	1	1	0	sp|P62626|ATPB_AEGCO	EC 3.6.3.14; ATP synthase F1 sector subunit beta;
9	-18	6,2	7,4	9	3	4	59,1	sp|P19023|ATPBM_MAIZE	ATP synthase subunit beta, mitochondrial; EC 3.6.3.14;
10	-6,1	5,9	2	2	1	2	63,8	tr|Q6ZFJ9|Q6ZFJ9_ORYSJ	60 kDa chaperonin beta subunit; Os02g0102900 protein;
1	-22	6,5	7,9	9	3	3	50	tr|Q1ENY9|Q1ENY9_MUSAC	Phosphoglycerate kinase, chloroplast, putative; EC 2.7.2.3;
2	-20	6,4	3,3	3	1	1	50	tr|B6STH5|B6STH5_MAIZE	Phosphoglycerate kinase; EC 2.7.2.3;

3	-9,8	6,6	14	19	2	3	20,8	tr|F8UCA0|F8UCA0_9LILI	Glyceraldehyde-3-phosphate dehydrogenase; EC 1.2.1.12;
4	-9	6,5	6,7	10	2	2	42,7	tr|F2D714|F2D714_HORVD	Predicted protein;
5	-2,8	5,4	5,3	6	1	1	31,5	tr|G3FBL3|G3FBL3_9LILI	Actin; Flags: Fragment
7	-1,6	5,6	5,1	6	1	1	37	tr|Q7XZW5|Q7XZW5_ORYSJ	Malate dehydrogenase; EC 1.1.1.37
12	-1,2	5,8	3,3	5	1	1	39,8	sp|P0C1M0|ATPG_MAIZE	ATP synthase subunit gamma, chloroplastic; F-ATPase gamma subunit;
1	-3,5	5,5	4,3	6	1	1	26,7	sp|P34937|TPIS_HORVU	Triosephosphate isomerase, cytosolic; TIM; Triose-phosphate isomerase; EC 5.3.1.1
2	-2,4	5,8	4,9	6	1	2	34,4	tr|F2CRK1|F2CRK1_HORVD	Predicted protein;
3	-1,9	5,2	5,2	6	1	1	26	tr|Q6YTY2|Q6YTY2_ORYSJ	Os07g0608500 protein; Putative 40S ribosomal protein;
4	-1,6	5,6	2,8	4	1	1	42,4	sp|P04709|ADT1_MAIZE	ADP:p ,ATP carrier protein 1, mitochondrial; ADP/ATP translocase 1;
1	-3,8	5,8	3,8	6	1	1	24,8	sp|P13192|PSAF_HORVU	Light-harvesting complex I 17 kDa protein;
1	-2,3	5,7	13	28	1	2	9,4	sp|A1EA25|PSBE_AGRST	Cytochrome b559 subunit alpha; PSII reaction center subunit V;

C

rank	log(e)	log(I)	% (measured)	% (corrected)	unique	total	Mr	Accession	Description
1	-18	6,3	8,2	12	3	3	41,7	tr|C7IWD0|C7IWD0_ORYSJ	Os01g0791600 protein;
2	-9,3	6,2	4,3	8	2	3	55,3	sp|A9LYH0|ATPA_ACOAM	EC 3.6.3.14; ATP synthase F1 sector subunit alpha; F-ATPase subunit alpha;
3	-7,7	6,4	2,2	2	1	2	0	tr|Q6L9Z6|Q6L9Z6_9LILI	RuBisCO large subunit;
4	-4,3	5,4	3,8	4	1	1	48,1	sp|P42895|ENO2_MAIZE	no protein information available
6	-2,4	5,5	1,5	2	1	1	104,8	sp|Q7XPY2|PMA1_ORYSJ	no protein information available
7	-2,2	5,5	3,5	11	1	1	50,8	tr|G1C6J9|G1C6J9_9LILI	no protein information available
10	-1,8	5,5	1,3	2	1	1	79,5	sp|Q06572|AVP_HORVU	EC 3.6.1.1; Pyrophosphate-energized inorganic pyrophosphatase;
1	-54	6,9	18	22	6	10	53,6	sp|A9L9A3|ATPB_LEMMI	EC 3.6.3.14; ATP synthase F1 sector subunit beta; F-

									ATPase subunit beta;
2	-52	6,9	3,2	3	1	1	0	tr|H2CPP4|H2CPP4_COLES	EC 3.6.3.14; ATP synthase F1 sector subunit beta; F-ATPase subunit beta;
3	-32	6,7	9,7	18	4	5	55,3	sp|A9LYH0|ATPA_ACOAM	EC 3.6.3.14; ATP synthase F1 sector subunit alpha; F-ATPase subunit alpha;
4	-12	5,8	7	8	2	2	48,1	sp|P42895|ENO2_MAIZE	Enolase 2; EC 4.2.1.11; 2-phospho-D-glycerate hydro-lyase 2;
5	-10	6,3	4,7	6	2	3	59,1	sp|P19023|ATPBM_MAIZE	ATP synthase subunit beta, mitochondrial; EC 3.6.3.14;
6	-9,5	6,6	4,4	10	2	3	50,4	tr|Q6L9Z6|Q6L9Z6_9LILI	RuBisCO large subunit;
7	-3,5	5,7	2	2	1	2	63,8	tr|Q6ZFJ9|Q6ZFJ9_ORYSJ	60 kDa chaperonin beta subunit; Os02g0102900 protein;
12	-1,5	5,3	2,1	3	1	1	61,4	tr|Q7X9A7|Q7X9A7_ORYSJ	60 kDa chaperonin alpha subunit;
1	-23	6,3	8,8	11	3	4	49,8	tr|B6STH5|B6STH5_MAIZE	Phosphoglycerate kinase; EC 2.7.2.3;
2	-21	6,3	2,5	3	1	1	0	tr|Q1ENY9|Q1ENY9_MUSAC	Phosphoglycerate kinase, chloroplast, putative; EC 2.7.2.3;
3	-11	6,1	4	4	1	1	0	tr|Q655T1|Q655T1_ORYSJ	no protein information available
4	-11	6,7	14	19	2	3	20,8	tr|F8UCA0|F8UCA0_9LILI	Glyceraldehyde-3-phosphate dehydrogenase; EC 1.2.1.12;
5	-9,9	6,7	3,9	4	1	1	0	tr|Q7FAH2|Q7FAH2_ORYSJ	Glyceraldehyde-3-phosphate dehydrogenase 2, cytosolic; EC 1.2.1.12
6	-2,9	6,1	5,1	8	1	1	33	sp|P27337|PER1_HORVU	Peroxidase 1; EC 1.11.1.7;
7	-2,1	5,4	3,2	5	1	1	42,7	tr|F2D714|F2D714_HORVD	Predicted protein;
11	-1,5	5,9	3,3	8	1	2	50,1	sp|P25776|ORYA_ORYSJ	no protein information available
1	-9,4	6,2	9,8	12	2	4	34,4	tr|F2CRK1|F2CRK1_HORVD	Predicted protein;
2	-4,9	5,9	3,2	5	1	1	41	tr|Q0DJC0|Q0DJC0_ORYSJ	Os05g0302700 protein;
3	-4,6	5,6	8,5	12	1	1	24,7	tr|F2DTJ2|F2DTJ2_HORVD	Predicted protein
4	-3,4	5,8	5,1	8	1	1	33	sp|P27337|PER1_HORVU	Peroxidase 1; EC 1.11.1.7;
7	-2	5,7	5,4	7	1	1	29,8	tr|G0YLW6|G0YLW6_9ARAE	Putative chlorophyll a/b binding protein;
1	-2,7	6,2	3,8	6	1	2	24,8	sp|P13192|PSAF_HORVU	Light-harvesting complex I 17 kDa protein; PSI-F;
2	-2,4	5,4	5,7	9	1	1	27,7	tr|Q6WFB1|Q6WFB1_MAIZE	Photosystem II subunit PsbS;
1	-1,5	5,5	13	28	1	2	9,4	sp|A1EA25|PSBE_AGRST	Cytochrome b559 subunit alpha; PSII reaction center subunit V;

Annex 3: *Table of peptides from Cymodocea nodosa under salt stress*

A = referred sample
B= hypersaline after 15 days
C= hypersaline after 30 days

A

Rank	log (e)	log (I)	% (m)	% (c)	unique	tot	Mr	Accession	Description
1	**-8**	**6,91**	**4,2**	**9**	**2**	**3**	**50,4**	**tr|Q6L9Z6|Q6L9Z6_9LILI**	**RuBisCO large subunit;**
spectrum	log(e)	log(I)	m+h	delta	z	zeta	pre	start	Sequence
1036	-1,1	6,16	1261,65	1,499	2	1	wrdr	211	FLFCAEALYK
624	-1,9	6,56	1230,63	0,594	2	1	negr	429	DLATEGNEIIR
619	-1,8	6,49	1230,63	0,903	2	1	negr	429	DLATEGNEIIR
2	**-3,9**	**5,61**	**2,1**	**3**	**1**	**1**	**74**	**tr|Q2QV45|Q2QV45_ORYSJ**	**70 kDa heat shock protein; Os12g0244100 protein;**
spectrum	log(e)	log(I)	m+h	delta	z	zeta	pre	start	sequence
922	-3,9	5,61	1723,89	1,311	2	1	evlr	227	IINEPTAASLAYGFEK
3	**-3,5**	**6,23**	**4,3**	**5**	**1**	**3**	**33,2**	**sp|P08477|G3PC_HORVU**	**Glyceraldehyde-3-phosphate dehydrogenase, cytosolic; EC 1.2.1.12;**
spectrum	log(e)	log(I)	m+h	delta	z	zeta	pre	start	sequence
988	-3,5	5,88	1498,85	-0,16	2	1	mafr	205	VPTVDVSVVDLTVR
983	-2,3	5,71	1498,85	-0,49	2	1	mafr	205	VPTVDVSVVDLTVR
981	-1,1	5,64	1498,85	1,335	2	1	mafr	205	VPTVDVSVVDLTVR
4	**-1,8**	**5,92**	**1,6**	**2**	**1**	**1**	**72,9**	**sp|Q7SIC9|TKTC_MAIZE**	**Transketolase:p , chloroplastic; TK; EC 2.2.1.1;**
spectrum	log(e)	log(I)	m+h	delta	z	zeta	pre	start	sequence
450	-1,8	5,92	1182,62	2,042	2	1	gidk	648	FGASAPAGTIYK

5	**-1,7**	**5,56**	**1,5**	**2**		**1**	**1**	**111**	**tr|Q6V9T1|Q6V9T1_ORYSJ**	**Glycine dehydrogenase P protein; Os01g0711400 protein;**
spectrum	log(e)	log(I)	m+h	delta	z		zeta	pre	start	sequence
1282	-1,7	5,56	1793,97	0,267		2	1	glkk	439	LGTVTVQELPFFDTVK

1	**-54**	**7,36**	**17**	**21**		**6**	**13**	**53,6**	**tr|H2CPP4|H2CPP4_COLES**	**EC 3.6.3.14; ATP synthase F1 sector subunit beta;**
spectrum	log(e)	log(I)	m+h	delta	z		zeta	pre	start	sequence
1271	-4,1	6,05	1735,02	1,479		2	1	nlgr	23	IAQIIGPVLDVAFPPGK
1305	-3,1	5,82	1735,02	0,942		2	1	nlgr	23	IAQIIGPVLDVAFPPGK
1113	-6,9	6,44	1955,02	0,504		2	1	tlgr	110	IFNVLGEPVDNLGPVDTR
1117	-6,4	6,35	1955,02	0,3		2	1	tlgr	110	IFNVLGEPVDNLGPVDTR
1118	-5	6,24	1955,02	1,063		2	1	tlgr	110	IFNVLGEPVDNLGPVDTR
1669	-1,2	5,77	1471,86	0,89		2	1	gvgk	179	TVLIMELINNIAK
1679	-1,2	6,04	1471,86	1,342		2	1	gvgk	179	TVLIMELINNIAK
1456	-1,1	5,66	1487,85	1,285		2	1	gvgk	179	TVLIMELINNIAK
387	-2,2	6,21	1517,75	0,924		2	1	memk	218	ESGVINEQNIAESK
392	-1,8	5,89	1517,75	0,644		2	1	memk	218	ESGVINEQNIAESK
475	-2,2	5,69	1617,8	1,76		2	1	aesk	232	VALVYGQMNEPPGAR
984	-3,2	6,65	1433,78	0,909		2	1	nifr	278	FVQAGSEVSALLGR
986	-2,1	6,7	1433,78	0,324		2	1	nifr	278	FVQAGSEVSALLGR

2	**-44**	**7,29**	**3,2**	**3**		**1**	**1**	**0**	**tr|Q4FGI4|Q4FGI4_TYPLA**	**ATP synthase subunit beta; EC 3.6.3.14;**
spectrum	log(e)	log(I)	m+h	delta	z		zeta	pre	start	sequence
1311	-4,1	5,62	1735,02	1,258		2	1	nlgr	23	IAQIIGPVLDAVFPPGK
1113	-6,9	6,44	1955,02	0,504		2	1	tlgr	110	IFNVLGEPVDNLGPVDTR
1117	-6,4	6,35	1955,02	0,3		2	1	tlgr	110	IFNVLGEPVDNLGPVDTR

1118	-5	6,24	1955,02	1,063		2	1	tlgr	110	IFNVLGEPVDNLGPVDTR
1669	-1,2	5,77	1471,86	0,89		2	1	gvgk	179	TVLIMELINNIAK
1679	-1,2	6,04	1471,86	1,342		2	1	gvgk	179	TVLIMELINNIAK
1456	-1,1	5,66	1487,85	1,285		2	1	gvgk	179	TVLIMELINNIAK
475	-2,2	5,69	1617,8	1,76		2	1	aesk	232	VALVYGQMNEPPGAR
984	-3,2	6,65	1433,78	0,909		2	1	nifr	278	FVQAGSEVSALLGR
986	-2,1	6,7	1433,78	0,324		2	1	nifr	278	FVQAGSEVSALLGR

3	**-42**	**7,34**	**2**	**2**		**1**	**2**	**0**	**sp|Q95AD6|ATPB_WHIBI**	**EC 3.6.3.14; ATP synthase F1 sector subunit beta;**
spectrum	log(e)	log(I)	m+h	delta	z		zeta	pre	start	sequence
1036	-1,6	6,22	1262,66	0,629		2	1	plgk	40	MPNNYNALVVK
1030	-1,3	6,17	1262,66	-0,01		2	1	plgk	40	MPNNYNALVVK
1113	-6,9	6,44	1955,02	0,504		2	1	tlgr	110	IFNVLGEPVDNLGPVDTR
1117	-6,4	6,35	1955,02	0,3		2	1	tlgr	110	IFNVLGEPVDNLGPVDTR
1118	-5	6,24	1955,02	1,063		2	1	tlgr	110	IFNVLGEPVDNLGPVDTR
1669	-1,2	5,77	1471,86	0,89		2	1	gvgk	179	TVLIMELINNIAK
1679	-1,2	6,04	1471,86	1,342		2	1	gvgk	179	TVLIMELINNIAK
1456	-1,1	5,66	1487,85	1,285		2	1	gvgk	179	TVLIMELINNIAK
475	-2,2	5,69	1617,8	1,76		2	1	aesk	232	VALVYGQMNEPPGAR
984	-3,2	6,65	1433,78	0,909		2	1	nifr	278	FVQAGSEVSALLGR
986	-2,1	6,7	1433,78	0,324		2	1	nifr	278	FVQAGSEVSALLGR

4	**-38**	**7,22**	**12**	**21**		**5**	**8**	**55,3**	**sp|A9LYH0|ATPA_ACOAM**	**EC 3.6.3.14; ATP synthase F1 sector subunit alpha;**
spectrum	log(e)	log(I)	m+h	delta	z		zeta	pre	start	sequence
793	-3,9	6,18	1598,89	0,871		2	1	revk	26	VVNTGTVLQVGDGIAR
791	-3,1	6,31	1598,89	0,478		2	1	revk	26	VVNTGTVLQVGDGIAR
707	-1,3	5,74	1598,89	2,201		2	1	revk	26	VVNTGTVLQVGDGIAR
787	-2,1	6,59	1416,79	0,717		2	1	atgr	95	IAQIPVSEAYLGR

652	-2,7	6,55	1252,73	0,451		2	1	sefr	129	LIESPAPGIISR
659	-1,6	6,18	1252,73	0,787		2	1	sefr	129	LIESPAPGIISR
498	-1,4	5,83	1274,7	-0,13		2	1	qtgk	177	TAVATDTILNQK
1062	-1,3	6,46	1251,65	1,345		2	1	sstk	481	TFTEEAEALLK

5	**-36**	**7,35**	**11**	**24**		**5**	**8**	**50,4**	**tr|Q6L9Z6|Q6L9Z6_9LILI**	**RuBisCO large subunit;**
spectrum	log(e)	log(I)	m+h	delta	z		zeta	pre	start	sequence
560	-1,6	6,98	1407,67	0,915		2	1	kdyk	15	LTYYTPEYETK
581	-1	5,83	1407,67	1,601		2	1	kdyk	15	LTYYTPEYETK
471	-2,1	6,15	1465,76	0,991		2	1	ayik	140	TFQGPPHGIQVER
1058	-1,1	6,54	1261,65	0,969		2	1	wrdr	211	FLFCAEALYK
369	-2,4	6,52	1116,6	0,077		2	1	vanr	415	VALEACVQAR
360	-1,4	5,95	1116,6	0,272		2	1	vanr	415	VALEACVQAR
528	-2,3	6,06	1230,63	1,746		2	1	negr	429	DLATEGNEIIR
658	-1,2	6,31	1230,63	1,369		2	1	negr	429	DLATEGNEIIR

6	**-28**	**7,13**	**2**	**2**		**1**	**1**	**0**	**sp|P62626|ATPB_AEGCO**	**EC 3.6.3.14; ATP synthase F1 sector subunit beta;**
spectrum	log(e)	log(I)	m+h	delta	z		zeta	pre	start	sequence
782	-2,1	6,12	1191,63	0,404		2	1	pihr	135	SAPAFIELDTK
1669	-1,2	5,77	1471,86	0,89		2	1	gvgk	179	TVLIMELINNIAK
1679	-1,2	6,04	1471,86	1,342		2	1	gvgk	179	TVLIMELINNIAK
1456	-1,1	5,66	1487,85	1,285		2	1	gvgk	179	TVLIMELINNIAK
475	-2,2	5,69	1617,8	1,76		2	1	eesk	232	VALVYGQMNEPPGAR
984	-3,2	6,65	1433,78	0,909		2	1	nifr	278	FVQAGSEVSALLGR
986	-2,1	6,7	1433,78	0,324		2	1	nifr	278	FVQAGSEVSALLGR

7	**-19**	**6,87**	**2,3**	**2**	**1**	**1**	**0**	**tr|C6G4V9|C6G4V9_9ASPA**		**Ribulose-1:p,5-bisphosphate carboxylase/oxygenase large subunit;**
spectrum	log(e)	log(I)	m+h	delta	z	zeta	pre	Start		sequence
471	-2,1	6,15	1465,76	0,991	2	1	sysk		140	TFQGPPHGIQVER
1392	-2,2	6,27	1292,7	2,441	2	1	eger		333	QMTLGFVDLLR
369	-2,4	6,52	1116,6	0,077	2	1	vanr		415	VALEACVQAR
360	-1,4	5,95	1116,6	0,272	2	1	vanr		415	VALEACVQAR

8	**-19**	**6,18**	**6,3**	**8**	**3**	**3**	**59,1**	**sp|P19023|ATPBM_MAIZE**		**ATP synthase subunit beta, mitochondrial; EC 3.6.3.14;**
spectrum	log(e)	log(I)	m+h	delta	z	zeta	pre	Start		sequence
430	-1,7	5,56	1278,63	2,452	2	1	nmvr		132	TIAMDGTEGLVR
1544	-2,2	5,73	1457,84	1,993	2	1	gvgk		235	TVLIMELINNVAK
895	-2,6	5,79	1399,77	0,159	2	1	arar		306	VGLTGLTVAEHFR

9	**-9,3**	**5,93**	**4,6**	**6**	**2**	**2**	**61,4**	**tr|Q7X9A7|Q7X9A7_ORYSJ**		**60 kDa chaperonin alpha subunit;**
spectrum	log(e)	log(I)	m+h	delta	z	zeta	pre	Start		sequence
998	-2	5,63	1555,91	-0,73	2	1	eiik		142	LGLLSVTSGANPVSIK
697	-2,3	5,63	1479,75	1,552	2	1	eidr		238	GYISPQFVTNPEK

10	**-5,1**	**5,2**	**4,1**	**6**	**1**	**1**	**55,1**	**sp|P05494|ATPAM_MAIZE**		**ATP synthase subunit alpha, mitochondrial;**
spectrum	log(e)	log(I)	m+h	delta	z	zeta	pre	Start		sequence
1661	-5,1	5,2	2308,16	1,114	2	1	aqyr		402	EVAAFAQFGSDLDAATQALLNR

1	**-22**	**6,77**	**10**	**15**	**3**	**5**	**42,7**	**tr|F2D714|F2D714_HORVD**		**Predicted protein;**
spectrum	log(e)	log(I)	m+h	delta	z	zeta	pre	Start		sequence
969	-4,6	6,38	1443,7	1,292	2	1	hllk		113	YDSTLGIFDADVK
977	-1,2	5,91	1443,7	-0,45	2	1	hllk		113	YDSTLGIFDADVK

1218	-1,8	5,93	1780,02	0,478		2	1	ialr	300	VPTPNVSVVDLVVQVSK
998	-3,6	6,04	1786,82	1,162		2	1	dmvk	375	VIAWYDNEWGYSQR
1008	-1,7	5,85	1786,82	0,411		2	1	dmvk	375	VIAWYDNEWGYSQR

2	**-22**	**6,67**	**7,9**	**9**		**3**	**4**	**50**	**tr|Q1ENY9|Q1ENY9_MUSAC**	**Phosphoglycerate kinase, chloroplast, putative; EC 2.7.2.3;**
spectrum	log(e)	log(I)	m+h	delta	z		zeta	pre	Start	sequence
785	-3	6,16	1404,74	0,698		2	1	llqk	252	ELDYLVGAVSNPK
443	-2,5	5,96	1102,64	1,237		2	1	snpk	265	RPFAAIVGGSK
664	-4,2	6,3	1573,84	1,904		2	1	lsgk	423	GVTTIIGGGDSVAAVEK
644	-1,9	5,55	1573,84	0,156		2	1	lsgk	423	GVTTIIGGGDSVAAVEK

3	**-21**	**6,57**	**3,5**	**4**		**1**	**1**	**0**	**sp|P12782|PGKH_WHEAT**	**no protein information available**
spectrum	log(e)	log(I)	m+h	delta	z		zeta	pre	Start	sequence
668	-2,6	5,7	2028,95	1,629		2	1	vlvr	95	ADLNVPLDDNQNITDDTR
443	-2,5	5,96	1102,64	1,237		2	1	snpk	263	RPFAAIVGGSK
664	-4,2	6,3	1573,84	1,904		2	1	lskk	421	GVTTIIGGGDSVAAVEK
644	-1,9	5,55	1573,84	0,156		2	1	lskk	421	GVTTIIGGGDSVAAVEK

4	**-20**	**6,65**	**1,9**	**2**		**1**	**1**	**0**	**tr|B6STH5|B6STH5_MAIZE**	**Phosphoglycerate kinase; EC 2.7.2.3;**
spectrum	log(e)	log(I)	m+h	delta	z		zeta	pre	Start	sequence
443	-2,5	5,96	1102,64	1,237		2	1	sspk	266	RPFAAIVGGSK
345	-1,4	6,08	992,542	1,542		2	1	efdk	406	FAVGTEAVAK
664	-4,2	6,3	1573,84	1,904		2	1	lsgk	424	GVTTIIGGGDSVAAVEK
644	-1,9	5,55	1573,84	0,156		2	1	lsgk	424	GVTTIIGGGDSVAAVEK

5	**-18**	**6,32**	**7,8**	**10**		**3**	**3**	**53,6**	**sp|Q3V527|ATPB_ACOCL**	**EC 3.6.3.14; ATP synthase F1 sector subunit beta;**
spectrum	log(e)	log(I)	m+h	delta	z		zeta	pre	Start	sequence
1646	-2,3	5,48	1471,86	0,231		2	1	gvgk	179	TVLIMELINNIAK
615	-1,9	5,54	1601,81	-0,06		2	1	eesk	232	VALVYGQMNEPPGAR

954	-2,3	6,15	1433,78	0,699		2	1	nifr	278	FVQAGSEVSALLGR
6	**-11**	**6,26**	**5,4**	**6**		**1**	**1**	**31,4**	**tr|C1JYE2|C1JYE2_9POAL**	**Phosphoglycerate kinase; EC 2.7.2.3;**
spectrum	log(e)	log(I)	m+h	delta	z		zeta	pre	Start	sequence
443	-2,5	5,96	1102,64	1,237		2	1	snpk	118	RPFAAIVGGSK
660	-3,2	5,96	1574,8	1,707		2	1	lskk	276	GVTTNIGGGDSVAAVEK
7	**-7,4**	**6,07**	**5**	**12**		**2**	**2**	**48,9**	**tr|O78641|O78641_9ASPA**	**no protein information available**
spectrum	log(e)	log(I)	m+h	delta	z		zeta	pre	Start	sequence
438	-1,4	5,68	1465,76	1,384		2	1	sysk	139	TFQGPPHGIQVER
1353	-1,2	5,84	1295,66	2,341		2	1	eger	332	DMTLGFVDLLR
8	**-4,7**	**5,7**	**4,2**	**6**		**1**	**1**	**47,2**	**sp|Q42450|RCAB_HORVU**	**no protein information available**
spectrum	log(e)	log(I)	m+h	delta	z		zeta	pre	Start	sequence
1322	-4,7	5,7	2089,17	0,82		2	1	enpr	265	VPIIVTGNDFSTLYAPLIR
9	**-3,7**	**6,35**	**3,3**	**5**		**1**	**2**	**39,8**	**sp|P0C1M0|ATPG_MAIZE**	**F-ATPase gamma subunit;**
spectrum	log(e)	log(I)	m+h	delta	z		zeta	pre	Start	sequence
783	-3,7	5,88	1358,73	-0,41		2	1	qilr	301	ALQESLASELAAR
776	-1,7	6,17	1358,73	0,258		2	1	qilr	301	ALQESLASELAAR
10	**-3,5**	**6,09**	**5,1**	**8**		**1**	**1**	**33**	**sp|P27337|PER1_HORVU**	**Peroxidase 1; EC 1.11.1.7;**
spectrum	log(e)	log(I)	m+h	delta	z		zeta	pre	Start	sequence
1054	-3,5	6,09	1710,92	0,553		2	1	vaar	123	DSVVALGGPSWTVPLGR
11	**-3,4**	**5,65**	**2,9**	**4**		**1**	**1**	**47,1**	**tr|Q9SNK3|Q9SNK3_ORYSJ**	**Glyceraldehyde-3-phosphate dehydrogenase B; Os03g0129300 protein;**
spectrum	log(e)	log(I)	m+h	delta	z		zeta	pre	Start	sequence
950	-3,4	5,65	1772,8	0,985		2	1	dmvk	389	VVAWYDNEWGYSQR

12	**-3,1**	**5,35**	**3,4**	**5**	**1**	**1**	**42**	**sp|Q40677|ALFC_ORYSJ**		**Fructose-bisphosphate aldolase, chloroplastic; ALDP; EC 4.1.2.13;**
spectrum	log(e)	log(I)	m+h	delta	z	zeta	pre	Start		sequence
292	-3,1	5,35	1482,67	0,439	2	1	spgr		58	GILAMDESNATCGK
13	**-2,7**	**5,7**	**4,7**	**6**	**1**	**1**	**35,2**	**sp|A6MMM0|CYF_DIOEL**		**Apocytochrome f;**
spectrum	log(e)	log(I)	m+h	delta	z	zeta	pre	Start		sequence
448	-2,7	5,7	1625,81	-0,04	2	1	dgsk		201	SNNTVYNATSAGIVSK
15	**-2,1**	**5,75**	**3,2**	**4**	**1**	**1**	**44,5**	**sp|P37833|AATC_ORYSJ**		**Aspartate aminotransferase, cytoplasmic; EC 2.6.1.1;**
spectrum	log(e)	log(I)	m+h	delta	z	zeta	pre	Start		sequence
512	-2,1	5,75	1448,77	-0,85	2	1	qenr		101	VATVQCLSGTGSLR
19	**-1,3**	**6,68**	**3,3**	**5**	**1**	**3**	**35,6**	**sp|Q08062|MDHC_MAIZE**		**Malate dehydrogenase, cytoplasmic; EC 1.1.1.37;**
spectrum	log(e)	log(I)	m+h	delta	z	zeta	pre	Start		sequence
1319	-1,3	5,9	1346,74	0,094	2	1	ngvk		56	MELVDAAFPLLK
1168	-1,3	6,13	1362,73	0,175	2	1	ngvk		56	MELVDAAFPLLK
1307	-1,1	6,42	1346,74	0,573	2	1	ngvk		56	MELVDAAFPLLK
1	**-11**	**6,23**	**6,1**	**9**	**2**	**2**	**41**	**tr|Q0DJC0|Q0DJC0_ORYSJ**		**Os05g0302700 protein;**
spectrum	log(e)	log(I)	m+h	delta	z	zeta	pre	Start		sequence
1107	-2,6	5,86	1446,74	0,124	2	1	nvir		154	YFPTQALNFAFK
491	-3,6	5,98	1191,64	0,394	2	1	nilr		353	AVAGAGVLAGYDK
2	**-8,2**	**6,2**	**5**	**12**	**2**	**2**	**49,2**	**tr|Q8WL39|Q8WL39_9ASPA**		**Ribulose-bisphosphate carboxylase large subunit;**
spectrum	log(e)	log(I)	m+h	delta	z	zeta	pre	Start		sequence
470	-1,4	6,14	1407,67	0,581	2	1	kdyr		15	LTYYTPEYETK
362	-1,9	5,27	1466,74	2,189	2	1	aysk		140	TFEGPPHGIQVER

3	**-2,5**	**5,54**	**3**	**3**	**1**	**1**	**42,3**	**tr|Q1EPF8|Q1EPF8_MUSAC**		**Phosphoglycerate kinase 2; EC 2.7.2.3;**
spectrum	log(e)	log(I)	m+h	delta	z	zeta	pre	Start		sequence
728	-2,5	5,54	1404,74	0,78	2	1	lmqk	179		ELDYLVGAVSNPK
4	**-2,5**	**5,66**	**3,9**	**6**	**1**	**1**	**29,6**	**sp|Q6L5I5|VDAC2_ORYSJ**		**Voltage-dependent anion-selective channel protein 2; OsVDAC2**
spectrum	log(e)	log(I)	m+h	delta	z	zeta	pre	Start		sequence
725	-2,5	5,66	1292,7	0,437	2	1	frpk	253		SLVTISTEVDTK
5	**-2,4**	**5,37**	**2**	**2**	**1**	**1**	**63,8**	**tr|Q6ZFJ9|Q6ZFJ9_ORYSJ**		**60 kDa chaperonin beta subunit; Os02g0102900 protein;**
spectrum	log(e)	log(I)	m+h	delta	z	zeta	pre	Start		sequence
323	-2,4	5,37	1295,74	-0,02	2	1	egvk	158		VVAAGANPVQITR
6	**-2**	**6,13**	**4,9**	**6**	**1**	**2**	**34,4**	**tr|F2CRK1|F2CRK1_HORVD**		**Predicted protein;**
spectrum	log(e)	log(I)	m+h	delta	z	zeta	pre	Start		sequence
392	-2	5,89	1562,76	1,227	2	1	pkgr	242		GGSTGYDNAVALPAGGR
400	-1,3	5,76	1562,76	1,103	2	1	pkgr	242		GGSTGYDNAVALPAGGR
9	**-1,5**	**5,78**	**5,7**	**8**	**1**	**2**	**29,8**	**tr|G0YLW6|G0YLW6_9ARAE**		**Putative chlorophyll a/b binding protein;**
spectrum	log(e)	log(I)	m+h	delta	z	zeta	pre	Start		sequence
1386	-1,5	5,55	1835,95	1,07	2	1	ihar	119		WAMLGAAGFIIPEAFNK
1378	-1,2	5,4	1835,95	0,957	2	1	ihar	119		WAMLGAAGFIIPEAFNK
1	**-23**	**6,71**	**15**	**25**	**3**	**10**	**27,7**	**tr|Q6WFB1|Q6WFB1_MAIZE**		**Photosystem II subunit PsbS;**
spectrum	log(e)	log(I)	m+h	delta	z	zeta	pre	Start		sequence
1006	-4,4	5,65	1584,79	0,427	2	1	pkpk	73		VEDGIFGTSGGIGFTK
1009	-2,2	5,61	1584,79	1,345	2	1	pkpk	73		VEDGIFGTSGGIGFTK

991	-1,3	5,43	1584,79	0,117	2	1	pkpk		73	VEDGIFGTSGGIGFTK
1835	-5	5,58	1748,96	1,991	2	1	fvgr		97	VAMLGFAASLLGEAITGK
1500	-4,5	5,9	1764,95	1,692	2	1	fvgr		97	VAMLGFAASLLGEAITGK
1516	-4,4	5,26	1764,95	1,257	2	1	fvgr		97	VAMLGFAASLLGEAITGK
1837	-4	5,48	1748,96	0,934	2	1	fvgr		97	VAMLGFAASLLGEAITGK
1819	-3,5	5,25	1748,96	1,322	2	1	fvgr		97	VAMLGFAASLLGEAITGK
1491	-3	5,38	1764,95	2,188	2	1	fvgr		97	VAMLGFAASLLGEAITGK
922	-1,1	6,29	1052,54	1,075	2	1	lgls		183	EGGPLFGFTK
2	**-4**	**5,5**	**6,8**	**12**	**1**	**1**	**21,9**	**sp|P36213|PSAD_HORVU**		**Photosystem I 20 kDa subunit;**
spectrum	log(e)	log(I)	m+h	delta	z		zeta	pre	Start	sequence
542	-4	5,5	1668,76	-0,13	2	1	tspk		104	EQVFEMPTGGAAIMR
7	**-1,4**	**5,66**	**4,3**	**5**	**1**	**1**	**33,2**	**sp|P08477|G3PC_HORVU**		**Glyceraldehyde-3-phosphate dehydrogenase, cytosolic; EC 1.2.1.12;**
spectrum	log(e)	log(I)	m+h	delta	z		zeta	pre	Start	sequence
1023	-1,4	5,66	1498,85	0,647	2	1	mafr		205	VPTVDVSVVDLTVR
1	**-1,9**	**5,69**	**13**	**14**	**1**	**1**	**9,3**	**tr|I1IWU7|I1IWU7_BRADI**		**Uncharacterized protein;**
spectrum	log(e)	log(I)	m+h	delta	z		zeta	pre	Start	sequence
982	-1,9	5,69	1484,7	1,58	2	1	itdr		69	FNSLEQLDEFSR
2	**-1,8**	**5,75**	**13**	**28**	**1**	**1**	**9,4**	**sp|A1EA25|PSBE_AGRST**		**no protein information available**
spectrum	log(e)	log(I)	m+h	delta	z		zeta	pre	Start	sequence
981	-1,8	5,75	1485,69	0,71	2	1	itdr		70	FDSLEQLDEFSR

B

rank	log (e)	log (I)	% (m)	% (c)	unique	tot	Mr	Accession	Description
1	**-37**	**6,8**	**11**	**24**	**5**	**8**	**50,4**	**tr|Q6L9Z6|Q6L9Z6_9LILI**	**RuBisCO large subunit;**

spectrum	log(e)	log(I)	m+h	delta	z	zeta	pre	start	sequence
578	-2	6,06	1407,7	0,072	2	1	kdyk	15	LTYYTPEYETK
471	-2	5,54	1465,8	0,223	2	0,667	ayik	140	TFQGPPHGIQVER
486	-2	5,34	1465,8	0,71	2	0,667	ayik	140	TFQGPPHGIQVER
1063	-1	6,06	1261,6	0,195	2	1	wrdr	211	FLFCAEALYK
368	-2	6,08	1116,6	0,633	2	1	vanr	415	VALEACVQAR
370	-2	6,11	1116,6	0,973	2	1	vanr	415	VALEACVQAR
532	-2	5,77	1230,6	0,603	2	1	negr	429	DLATEGNEIIR
523	-2	5,63	1230,6	2,142	2	1	negr	429	DLATEGNEIIR

2	**-3**	**5,24**	**2,6**	**7**	**1**	**1**	**56**	**sp|A9LYC6|PSBB_ACOAM**	**Photosystem II CP47 chlorophyll apoprotein;**

spectrum	log(e)	log(I)	m+h	delta	z	zeta	pre	start	sequence
1028	-3	5,24	1923,9	-0,712	2	1	gptr	273	YQWDQGYFQQEIYR

3	**-2**	**5,36**	**2**	**3**	**1**	**1**	**71,5**	**tr|C5YWM8|C5YWM8_SORBI**	**no protein information available**

spectrum	log(e)	log(I)	m+h	delta	z	zeta	pre	start	sequence
786	-2	5,36	1287,6	0,559	2	1	sssk	335	DISAAAAAGAGGAER

4	**-2**	**5,73**	**4,3**	**5**	**1**	**1**	**33,2**	**sp|P08477|G3PC_HORVU**	**Glyceraldehyde-3-phosphate dehydrogenase, cytosolic; EC 1.2.1.12;**

spectrum	log(e)	log(I)	m+h	delta	z	zeta	pre	start	sequence
1016	-2	5,73	1498,8	1,516	2	1	mafr	205	VPTVDVSVVDLTVR

5	**-2**	**5,69**	**3**	**5**	**1**	**1**	**55,3**	**sp|A9LYH0|ATPA_ACOAM**	**EC 3.6.3.14; ATP synthase F1 sector subunit alpha;**

spectrum	log(e)	log(I)	m+h	delta	z	zeta	pre	start	sequence
798	-2	5,69	1598,9	0,594	2	1	revk	26	VVNTGTVLQVGDGIAR

1	**-46**	**6,83**	**14**	**17**	**5**	**9**	**53,6**	**tr|H2CPP4|H2CPP4_COLES**	**EC 3.6.3.14; ATP synthase F1 sector subunit beta;**

spectrum	log(e)	log(I)	m+h	delta	z	zeta	pre	start	sequence
1254	-5	5,73	1735	-0,001	2	1	nlgr	23	IAQIIGPVLDVAFPPGK
1288	-4	5,49	1735	0,627	2	1	nlgr	23	IAQIIGPVLDVAFPPGK
1072	-5	5,59	1955	0,53	2	1	tlgr	110	IFNVLGEPVDNLGPVDTR
1078	-4	5,48	1955	2,437	2	1	tlgr	110	IFNVLGEPVDNLGPVDTR
390	-3	5,9	1517,7	1,701	2	1	memk	218	ESGVINEQNIAESK
385	-1	5,93	1517,7	1,203	2	1	memk	218	ESGVINEQNIAESK
1040	-2	5,54	1487,8	0,891	2	1	armr	249	VGLTALTMAEYFR
1275	-2	6,39	1471,8	0,774	2	1	armr	249	VGLTALTMAEYFR
972	-3	5,94	1433,8	1,092	2	1	nifr	278	FVQAGSEVSALLGR

2	**-43**	**6,79**	**5**	**5**	**1**	**1**	**0**	**tr|H6THB0|H6THB0_9LILI**	**ATP synthase subunit beta; EC 3.6.3.14;**

spectrum	log(e)	log(I)	m+h	delta	z	zeta	pre	start	sequence
840	-2	5,38	2099,1	-0,614	2	1	gltr	18	GMEVVDTGAPLSVPVGGATLGR
1072	-5	5,59	1955	0,53	2	1	tlgr	40	IFNVLGEPVDNLGPVDTR
1078	-4	5,48	1955	2,437	2	1	tlgr	40	IFNVLGEPVDNLGPVDTR

390	-3	5,9	1517,7	1,701	2	1	memk		148	ESGVINEQNIAESK
385	-1	5,93	1517,7	1,203	2	1	memk		148	ESGVINEQNIAESK
1040	-2	5,54	1487,8	0,891	2	1	armr		179	VGLTALTMAEYFR
1275	-2	6,39	1471,8	0,774	2	1	armr		179	VGLTALTMAEYFR
972	-3	5,94	1433,8	1,092	2	1	nifr		208	FVQAGSEVSALLGR

3	**-38**	**6,79**	**7**	**16**	**5**	**9**	**49**	**tr|B5RHG8|B5RHG8_9ASPA**	**Ribulose-bisphosphate carboxylase large subunit;**

spectrum	log(e)	log(I)	m+h	delta	z	zeta	pre	start	sequence
478	-4	5,58	1466,7	-0,371	2	0,667	aysk	143	TFEGPPHGIQVER
464	-4	5,76	1466,7	-0,702	2	0,667	aysk	143	TFEGPPHGIQVER
476	-1	5,6	1466,7	0,175	2	0,667	aysk	143	TFEGPPHGIQVER
468	-1	5,39	1365,7	-0,245	2	0,667	yskt	144	FEGPPHGIQVER
465	-2	5,39	1200,6	0,567	2	0,667	sktf	145	EGPPHGIQVER
471	-1	5,81	1218,6	-0,624	2	0,667	sktf	145	EGPPHGIQVER
461	-1	5,8	1218,6	0,854	2	0,667	sktf	145	EGPPHGIQVER
1362	-1	6,23	1293,7	1,3	2	1	eger	336	EMTLGFVDLLR
370	-2	6,14	1116,6	0,99	2	1	vanr	418	VALEACVQAR

4	**-32**	**6,81**	**9,7**	**18**	**4**	**6**	**55,3**	**sp|A9LYH0|ATPA_ACOAM**	**EC 3.6.3.14; ATP synthase F1 sector subunit alpha;**

spectrum	log(e)	log(I)	m+h	delta	z	zeta	pre	start	sequence
778	-5	6,08	1598,9	-0,195	2	1	revk	26	VVNTGTVLQVGDGIAR
782	-4	6,09	1598,9	1,189	2	1	revk	26	VVNTGTVLQVGDGIAR
785	-5	6,07	1416,8	0,816	2	1	atgr	95	IAQIPVSEAYLGR
776	-3	6,13	1416,8	0,917	2	1	atgr	95	IAQIPVSEAYLGR
655	-2	5,91	1252,7	-0,159	2	1	sefr	129	LIESPAPGIISR
486	-1	5,85	1274,7	-0,427	2	1	qtgk	177	TAVATDTILNQK

5	**-29**	**6,74**	**4,7**	**11**	**2**	**2**	**51,6**	**tr|B0B735|B0B735_9POAL**	**Ribulose-1:p,5-bisphosphate carboxylase/oxygenase large subunit; EC 4.1.1.39;**

spectrum	log(e)	log(I)	m+h	delta	z	zeta	pre	start	sequence
466	-4	5,81	1465,8	1,327	2	0,667	tysk	138	TFQGPPHGIQVER
370	-2	6,14	1116,6	0,99	2	1	aanr	413	VALEACVQAR

6	**-29**	**6,64**	**2,2**	**2**	**1**	**1**	**0**	**tr|F8RS97|F8RS97_JUNEF**	**ATP synthase subunit alpha**

spectrum	log(e)	log(I)	m+h	delta	z	zeta	pre	start	sequence
785	-5	6,07	1416,8	0,816	2	1	atgr	95	IAQIPVSEAYLGR
776	-3	6,13	1416,8	0,917	2	1	atgr	95	IAQIPVSEAYLGR
452	-2	5,43	1266,7	0,525	2	1	ylgr	108	VINALAQPIDGR
655	-2	5,91	1252,7	-0,159	2	1	sesr	129	LIESPAPGIISR
486	-1	5,85	1274,7	-0,427	2	1	qtgk	177	TAVATDTILNQK

7	**-29**	**7,05**	**2,2**	**2**	**1**	**3**	**0**	**tr|Q6L9Z6|Q6L9Z6_9LILI**	**RuBisCO large subunit;**

spectrum	log(e)	log(I)	m+h	delta	z	zeta	pre	start	sequence
466	-4	5,81	1465,8	1,327	2	0,667	ayik	140	TFQGPPHGIQVER

370	-2	6,14	1116,6	0,99	2	1	vanr		415	VALEACVQAR
650	-2	6,64	1230,6	0,109	2	1	negr		429	DLATEGNEIIR
657	-1	6,03	1230,6	1,676	2	1	negr		429	DLATEGNEIIR
652	-1	6,55	1230,6	0,621	2	1	negr		429	DLATEGNEIIR

8	**-20**	**6,69**	**2**	**2**	**1**	**1**	**0**	**sp|P62626|ATPB_AEGCO**	**EC 3.6.3.14; ATP synthase F1 sector subunit beta;**

spectrum	log(e)	log(I)	m+h	delta	z	zeta	pre	start	sequence
774	-2	6,08	1191,6	1,017	2	1	pihr	135	SAPAFIELDTK
1040	-2	5,54	1487,8	0,891	2	1	armr	249	VGLTALTMAEYFR
1275	-2	6,39	1471,8	0,774	2	1	armr	249	VGLTALTMAEYFR
972	-3	5,94	1433,8	1,092	2	1	nifr	278	FVQAGSEVSALLGR

9	**-18**	**6,24**	**7,4**	**9**	**3**	**4**	**59,1**	**sp|P19023|ATPBM_MAIZE**	**ATP synthase subunit beta, mitochondrial; EC 3.6.3.14;**

spectrum	log(e)	log(I)	m+h	delta	z	zeta	pre	start	sequence
639	-1	5,7	1262,6	1,181	2	1	nmvr	132	TIAMDGTEGLVR
1522	-3	5,7	1457,8	0,751	2	1	gvgk	235	TVLIMELINNVAK
1525	-2	5,43	1457,8	1,93	2	1	gvgk	235	TVLIMELINNVAK
1044	-2	5,67	2061,1	1,166	2	1	vlsr	412	QISELGIYPAVDPLDSTSR

10	**-6**	**5,94**	**2**	**2**	**1**	**2**	**63,8**	**tr|Q6ZFJ9|Q6ZFJ9_ORYSJ**	**60 kDa chaperonin beta subunit; Os02g0102900 protein;**

spectrum	log(e)	log(I)	m+h	delta	z	zeta	pre	start	sequence
409	-6	5,75	1295,7	-0,556	2	1	egvk	158	VVAAGANPVQITR
419	-3	5,5	1295,7	-0,644	2	1	egvk	158	VVAAGANPVQITR

1	**-22**	**6,45**	**7,9**	**9**	**3**	**3**	**50**	**tr|Q1ENY9|Q1ENY9_MUSAC**	**Phosphoglycerate kinase, chloroplast, putative; EC 2.7.2.3;**

spectrum	log(e)	log(I)	m+h	delta	z	zeta	pre	start	sequence
782	-3	5,98	1404,7	0,667	2	1	llqk	252	ELDYLVGAVSNPK
429	-2	5,68	1102,6	0,027	2	0,667	snpk	265	RPFAAIVGGSK
651	-4	6,14	1573,8	0,624	2	1	lsgk	423	GVTTIIGGGDSVAAVEK

2	**-20**	**6,35**	**3,3**	**3**	**1**	**1**	**0**	**tr|B6STH5|B6STH5_MAIZE**	**Phosphoglycerate kinase; EC 2.7.2.3;**

spectrum	log(e)	log(I)	m+h	delta	z	zeta	pre	start	sequence
1183	-2	5,57	1748	-0,281	2	1	evek	180	LVAALPNGGVLLLENVR
429	-2	5,68	1102,6	0,027	2	0,667	sspk	266	RPFAAIVGGSK
651	-4	6,14	1573,8	0,624	2	1	lsgk	424	GVTTIIGGGDSVAAVEK

3	**-10**	**6,57**	**14**	**19**	**2**	**3**	**20,8**	**tr|F8UCA0|F8UCA0_9LILI**	**Glyceraldehyde-3-phosphate dehydrogenase; EC 1.2.1.12;**

spectrum	log(e)	log(I)	m+h	delta	z	zeta	pre	start	sequence
867	-2	5,37	1743,8	0,134	2	1	apsk	29	DAPMFVMGVNEDQYK
947	-3	6,35	1498,8	1,217	2	1	mafr	137	VPTVDVSVVDLTVR
953	-3	6,1	1498,8	1,326	2	1	mafr	137	VPTVDVSVVDLTVR

4	**-9**	**6,53**	**6,7**	**10**	**2**	**2**	**42,7**	**tr|F2D714|F2D714_HORVD**	**Predicted protein;**

spectrum	log(e)	log(I)	m+h	delta	z	zeta	pre	start	sequence
545	-2	6,48	1384,8	0,63	2	1	rrar	266	AAALNIVPTSTGAAK
971	-2	5,62	1786,8	0,21	2	1	dmvk	375	VIAWYDNEWGYSQR

5	**-3**	**5,38**	**5,3**	**6**	**1**	**1**	**31,5**	**tr|G3FBL3|G3FBL3_9LILI**	**Actin; Flags: Fragment**

spectrum	log(e)	log(I)	m+h	delta	z	zeta	pre	start	sequence
903	-3	5,38	1761,9	-0,402	2	1	siek	147	TYELPDGQVITIGAER

7	**-2**	**5,59**	**5,1**	**6**	**1**	**1**	**37**	**tr|Q7XZW5|Q7XZW5_ORYSJ**	**Malate dehydrogenase; EC 1.1.1.37**

spectrum	log(e)	log(I)	m+h	delta	z	zeta	pre	start	sequence
1121	-2	5,59	1795,1	0,244	2	1	pgfk	45	VAVLGAAGGIGQPLSLLMK

12	**-1**	**5,77**	**3,3**	**5**	**1**	**1**	**39,8**	**sp|P0C1M0|ATPG_MAIZE**	**F-ATPase gamma subunit;**

spectrum	log(e)	log(I)	m+h	delta	z	zeta	pre	start	sequence
761	-1	5,77	1358,7	1,643	2	1	qilr	301	ALQESLASELAAR

1	**-4**	**5,48**	**4,3**	**6**	**1**	**1**	**26,7**	**sp|P34937|TPIS_HORVU**	**Triose-phosphate isomerase; EC 5.3.1.1**

spectrum	log(e)	log(I)	m+h	delta	z	zeta	pre	start	sequence
483	-4	5,48	1374,7	-0,362	2	1	qglk	124	VIACVGETLEQR

2	**-2**	**5,81**	**4,9**	**6**	**1**	**2**	**34,4**	**tr|F2CRK1|F2CRK1_HORVD**	**Predicted protein;**

spectrum	log(e)	log(I)	m+h	delta	z	zeta	pre	start	sequence
401	-2	5,37	1562,8	0,425	2	1	pkgr	242	GGSTGYDNAVALPAGGR
387	-2	5,61	1562,8	-0,101	2	1	pkgr	242	GGSTGYDNAVALPAGGR

3	**-2**	**5,23**	**5,2**	**6**	**1**	**1**	**26**	**tr|Q6YTY2|Q6YTY2_ORYSJ**	**Os07g0608500 protein; Putative 40S ribosomal protein;**

spectrum	log(e)	log(I)	m+h	delta	z	zeta	pre	start	sequence
417	-2	5,23	1423,7	0,045	2	1	mltr	30	ELAEDGYSGVEVR

4	**-2**	**5,55**	**2,8**	**4**	**1**	**1**	**42,4**	**sp|P04709|ADT1_MAIZE**	**ADP:p ,ATP carrier protein 1, mitochondrial; ADP/ATP translocase 1;**

spectrum	log(e)	log(I)	m+h	delta	z	zeta	pre	start	sequence
1102	-2	5,55	1446,7	0,64	2	1	nvir	161	YFPTQALNFAFK

1	**-4**	**5,76**	**3,8**	**6**	**1**	**1**	**24,8**	**sp|P13192|PSAF_HORVU**	**Light-harvesting complex I 17 kDa protein;**

spectrum	log(e)	log(I)	m+h	delta	z	zeta	pre	start	sequence
1178	-4	5,76	1179,6	0,317	2	1	iipr	210	GFIWPVAAYR

1	**-2**	**5,68**	**13**	**28**	**1**	**2**	**9,4**	**sp|A1EA25|PSBE_AGRST**	**Cytochrome b559 subunit alpha; PSII reaction center subunit V;**

spectrum	log(e)	log(I)	m+h	delta	z	zeta	pre	start	sequence
1012	-2	5,35	1485,7	0,412	2	1	itdr	70	FDSLEQLDEFSR
1006	-1	5,41	1485,7	1,349	2	1	itdr	70	FDSLEQLDEFSR

C

rank	log (e)	log (I)	% (m)	% (c)	unique	tot	Mr	Accession	Description
1	**-18**	**6,28**	**8,2**	**12**	**3**	**3**	**41,7**	**tr|C7IWD0|C7IWD0_ORYSJ**	**Os01g0791600 protein;**

spectrum	log(e)	log(I)	m+h	delta	z	zeta	pre	start	sequence
617	-1,6	6,03	1408	1	2	1	kdyk	22	LTYYTPEYETK
787	-1,4	5,65	1228	0,2	2	1	lnlr	259	AYDFVSQEIR
853	-2,9	5,58	1548	1,5	2	1	qeir	269	AAEDPEFETFYTK

rank	log (e)	log (I)	% (m)	% (c)	unique	tot	Mr	Accession	Description
2	**-9,3**	**6,15**	**4,3**	**8**	**2**	**3**	**55,3**	**sp|A9LYH0|ATPA_ACOAM**	**EC 3.6.3.14; ATP synthase F1 sector subunit alpha;**

spectrum	log(e)	log(I)	m+h	delta	z	zeta	pre	start	sequence
698	-2,5	5,79	1253	0,4	2	1	sefr	129	LIESPAPGIISR
710	-1,4	5,69	1253	2,2	2	1	sefr	129	LIESPAPGIISR
541	-1,9	5,47	1275	0,1	2	1	qtgk	177	TAVATDTILNQK

rank	log (e)	log (I)	% (m)	% (c)	unique	tot	Mr	Accession	Description
3	**-7,7**	**6,41**	**2,2**	**2**	**1**	**2**	**0**	**tr|Q6L9Z6|Q6L9Z6_9LILI**	**RuBisCO large subunit;**

spectrum	log(e)	log(I)	m+h	delta	z	zeta	pre	start	sequence
617	-1,6	6,03	1408	1	2	1	kdyk	15	LTYYTPEYETK
692	-1,2	6,07	1231	0	2	1	negr	429	DLATEGNEIIR
575	-1,1	5,54	1231	-0,1	2	1	negr	429	DLATEGNEIIR

rank	log (e)	log (I)	% (m)	% (c)	unique	tot	Mr	Accession	Description
4	**-4,3**	**5,41**	**3,8**	**4**	**1**	**1**	**48,1**	**sp|P42895|ENO2_MAIZE**	**no protein information available**

spectrum	log(e)	log(I)	m+h	delta	z	zeta	pre	start	sequence
1018	-4,3	5,41	1791	-0,4	2	1	tfar	36	AAVPSGASTGVYEALELR

rank	log (e)	log (I)	% (m)	% (c)	unique	tot	Mr	Accession	Description
6	**-2,4**	**5,48**	**1,5**	**2**	**1**	**1**	**105**	**sp|Q7XPY2|PMA1_ORYSJ**	**no protein information available**

spectrum	log(e)	log(I)	m+h	delta	z	zeta	pre	start	sequence
821	-2,4	5,48	1430	-0,6	2	1	alkk	599	ADIGIAVADATDAAR

rank	log (e)	log (I)	% (m)	% (c)	unique	tot	Mr	Accession	Description
7	**-2,2**	**5,53**	**3,5**	**11**	**1**	**1**	**50,8**	**tr|G1C6J9|G1C6J9_9LILI**	**no protein information available**

spectrum	log(e)	log(I)	m+h	delta	z	zeta	pre	start	sequence
1055	-2,2	5,53	1762	2,1	2	1	iyrr	278	VSAGLAENLSLSEAWSK

rank	log (e)	log (I)	% (m)	% (c)	unique	tot	Mr	Accession	Description
10	**-1,8**	**5,46**	**1,3**	**2**	**1**	**1**	**79,5**	**sp|Q06572|AVP_HORVU**	**EC 3.6.1.1; Pyrophosphate-energized inorganic pyrophosphatase;**

spectrum	log(e)	log(I)	m+h	delta	z	zeta	pre	start	sequence
412	-1,8	5,46	1016	0,5	2	1	iytk	247	AADVGADLVGK

rank	log (e)	log (I)	% (m)	% (c)	unique	tot	Mr	Accession	Description
1	**-54**	**6,94**	**18**	**22**	**6**	**10**	**53,6**	**sp|A9L9A3|ATPB_LEMMI**	**ATP synthase subunit beta, chloroplastic; EC 3.6.3.14;**

spectrum	log(e)	log(I)	m+h	delta	z	zeta	pre	start	sequence
899	-4,6	5,55	2083	2	2	1	gltr	88	GMDVIDTGAPLSVPVGGATLGR
905	-3,2	5,89	2083	2	2	1	gltr	88	GMDVIDTGAPLSVPVGGATLGR
1037	-3,7	5,36	1955	1,5	2	1	tlgr	110	IFNVLGEPVDNLGPVDTR
1621	-1,6	5,63	1472	1	2	1	gvgk	179	TVLIMELINNIAK

1398	-1,3	5,6	1488	2	2	1	gvgk		179	TVLIMELINNIAK
612	-2,7	5,89	1602	2,3	2	1	tesk		232	VALVYGQMNEPPGAR
1249	-3,4	6,3	1472	1,6	2	1	armr		249	VGLTALTMAEYFR
1012	-1,5	5,65	1488	0,3	2	1	armr		249	VGLTALTMAEYFR
953	-3	6,35	1434	1	2	1	nifr		278	FVQAGSEVSALLGR
963	-2,8	6,03	1434	2	2	1	nifr		278	FVQAGSEVSALLGR

2	**-52**	**6,9**	**3,2**	**3**	**1**	**1**	**0**	**tr|H2CPP4|H2CPP4_COLES**	**EC 3.6.3.14; ATP synthase F1 sector subunit beta;**

spectrum	log(e)	log(I)	m+h	delta	z	zeta	pre	start	sequence
1231	-2,5	5,53	1735	0,9	2	1	nlgr	23	IAQIIGPVLDVAFPPGK
1037	-3,7	5,36	1955	1,5	2	1	tlgr	110	IFNVLGEPVDNLGPVDTR
1621	-1,6	5,63	1472	1	2	1	gvgk	179	TVLIMELINNIAK
1398	-1,3	5,6	1488	2	2	1	gvgk	179	TVLIMELINNIAK
612	-2,7	5,89	1602	2,3	2	1	aesk	232	VALVYGQMNEPPGAR
1249	-3,4	6,3	1472	1,6	2	1	armr	249	VGLTALTMAEYFR
1012	-1,5	5,65	1488	0,3	2	1	armr	249	VGLTALTMAEYFR
953	-3	6,35	1434	1	2	1	nifr	278	FVQAGSEVSALLGR
963	-2,8	6,03	1434	2	2	1	nifr	278	FVQAGSEVSALLGR

3	**-32**	**6,71**	**9,7**	**18**	**4**	**5**	**55,3**	**sp|A9LYH0|ATPA_ACOAM**	**EC 3.6.3.14; ATP synthase F1 sector subunit alpha;**

spectrum	log(e)	log(I)	m+h	delta	z	zeta	pre	start	sequence
758	-4,9	5,98	1599	0,9	2	1	revk	26	VVNTGTVLQVGDGIAR
760	-2,7	5,93	1599	1,1	2	1	revk	26	VVNTGTVLQVGDGIAR
762	-2,5	6,1	1417	0,6	2	1	atgr	95	IAQIPVSEAYLGR
624	-2,6	6,18	1253	1	2	1	sefr	129	LIESPAPGIISR
475	-2,1	5,75	1275	-0,9	2	1	qtgk	177	TAVATDTILNQK

4	**-12**	**5,83**	**7**	**8**	**2**	**2**	**48,1**	**sp|P42895|ENO2_MAIZE**	**EC 4.2.1.11; 2-phospho-D-glycerate hydro-lyase 2;**

spectrum	log(e)	log(I)	m+h	delta	z	zeta	pre	start	sequence
933	-5,5	5,49	1791	-0,6	2	1	tfar	36	AAVPSGASTGVYEALELR
789	-1,1	5,57	1574	-0,2	2	1	lllk	355	VNQIGSVTESIEAVK

5	**-10**	**6,29**	**4,7**	**6**	**2**	**3**	**59,1**	**sp|P19023|ATPBM_MAIZE**	**ATP synthase subunit beta, mitochondrial; EC 3.6.3.14;**

spectrum	log(e)	log(I)	m+h	delta	z	zeta	pre	start	sequence
639	-2,3	5,86	1410	0,8	2	1	rgqr	147	VLNTGSPITVPVGR
669	-2,1	5,54	1410	1,7	2	1	rgqr	147	VLNTGSPITVPVGR
872	-3,2	5,93	1493	1,5	2	1	nifr	335	FTQANSEVSALLGR

6	**-9,5**	**6,61**	**4,4**	**10**	**2**	**3**	**50,4**	**tr|Q6L9Z6|Q6L9Z6_9LILI**	**RuBisCO large subunit;**

spectrum	log(e)	log(I)	m+h	delta	z	zeta	pre	start	sequence
540	-2,6	6,06	1408	1,1	2	1	kdyk	15	LTYYTPEYETK
626	-2	6,24	1231	0,4	2	1	negr	429	DLATEGNEIIR
629	-1,2	6,09	1231	0,1	2	1	negr	429	DLATEGNEIIR

7	**-3,5**	**5,72**	**2**	**2**	**1**	**2**	**63,8**	**tr|Q6ZFJ9|Q6ZFJ9_ORYSJ**	**60 kDa chaperonin beta subunit; Os02g0102900 protein;**

spectrum	log(e)	log(I)	m+h	delta	z	zeta	pre	start	sequence
389	-3,5	5,55	1296	1,3	2	1	egvk	158	VVAAGANPVQITR
400	-2,5	5,23	1296	1,3	2	1	egvk	158	VVAAGANPVQITR

12	**-1,5**	**5,34**	**2,1**	**3**	**1**	**1**	**61,4**	**tr|Q7X9A7|Q7X9A7_ORYSJ**	**60 kDa chaperonin alpha subunit;**

spectrum	log(e)	log(I)	m+h	delta	z	zeta	pre	start	sequence
671	-1,6	5,34	1480	-0,1	2	1	eidr	238	GYISPQFVTNPEK
1	**-23**	**6,3**	**8,8**	**11**	**3**	**4**	**49,8**	**tr|B6STH5|B6STH5_MAIZE**	**Phosphoglycerate kinase; EC 2.7.2.3;**
spectrum	log(e)	log(I)	m+h	delta	z	zeta	pre	start	sequence
1156	-4,1	5,88	1748	1,5	2	1	evek	180	LVAALPNGGVLLLENVR
411	-1,8	5,52	1103	-0,2	2	1	sspk	266	RPFAAIVGGSK
408	-1,3	5,49	1103	0,6	2	1	sspk	266	RPFAAIVGGSK
631	-4,8	5,77	1574	-0,2	2	1	lsgk	424	GVTTIIGGGDSVAAVEK
2	**-21**	**6,3**	**2,5**	**3**	**1**	**1**	**0**	**tr|Q1ENY9|Q1ENY9_MUSAC**	**Phosphoglycerate kinase, chloroplast, putative; EC 2.7.2.3;**
spectrum	log(e)	log(I)	m+h	delta	z	zeta	pre	start	sequence
753	-2,5	5,88	1405	1,8	2	1	llqk	252	ELDYLVGAVSNPK
411	-1,8	5,52	1103	-0,2	2	1	snpk	265	RPFAAIVGGSK
408	-1,3	5,49	1103	0,6	2	1	snpk	265	RPFAAIVGGSK
631	-4,8	5,77	1574	-0,2	2	1	lsgk	423	GVTTIIGGGDSVAAVEK
3	**-11**	**6,12**	**4**	**4**	**1**	**1**	**0**	**tr|Q655T1|Q655T1_ORYSJ**	**no protein information available**
spectrum	log(e)	log(I)	m+h	delta	z	zeta	pre	start	sequence
1161	-1,1	5,86	1751	0,8	2	1	evqk	106	LAATLPDGGVLLLENVR
631	-4,8	5,77	1574	-0,2	2	1	itak	350	GVTTIIGGGDSVAAVEK
4	**-11**	**6,7**	**14**	**19**	**2**	**3**	**20,8**	**tr|F8UCA0|F8UCA0_9LILI**	**Glyceraldehyde-3-phosphate dehydrogenase; EC 1.2.1.12;**
spectrum	log(e)	log(I)	m+h	delta	z	zeta	pre	start	sequence
865	-2,1	5,35	1744	-0,9	2	1	apsk	29	DAPMFVMGVNEDQYK
925	-3,7	6,47	1499	1,3	2	1	mafr	137	VPTVDVSVVDLTVR
934	-3,2	6,27	1499	0,7	2	1	mafr	137	VPTVDVSVVDLTVR
5	**-9,9**	**6,73**	**3,9**	**4**	**1**	**1**	**0**	**tr|Q7FAH2|Q7FAH2_ORYSJ**	**Glyceraldehyde-3-phosphate dehydrogenase 2, cytosolic; EC 1.2.1.12**
spectrum	log(e)	log(I)	m+h	delta	z	zeta	pre	start	sequence
925	-3,7	6,47	1499	1,3	2	1	mafr	237	VPTVDVSVVDLTVR
934	-3,2	6,27	1499	0,7	2	1	mafr	237	VPTVDVSVVDLTVR
945	-1,3	5,73	1762	0,7	2	1	nfvk	312	LVSWYDNEWGYSSR
6	**-2,9**	**6,05**	**5,1**	**8**	**1**	**1**	**33**	**sp|P27337|PER1_HORVU**	**Peroxidase 1; EC 1.11.1.7;**
spectrum	log(e)	log(I)	m+h	delta	z	zeta	pre	start	sequence
1017	-2,9	6,05	1711	1,2	2	1	vaar	123	DSVVALGGPSWTVPLGR
7	**-2,1**	**5,39**	**3,2**	**5**	**1**	**1**	**42,7**	**tr|F2D714|F2D714_HORVD**	**Predicted protein;**
spectrum	log(e)	log(I)	m+h	delta	z	zeta	pre	start	sequence
959	-2,1	5,39	1787	0,6	2	1	dmvk	375	VIAWYDNEWGYSQR
11	**-1,5**	**5,86**	**3,3**	**8**	**1**	**2**	**50,1**	**sp|P25776|ORYA_ORYSJ**	**no protein information available**
spectrum	log(e)	log(I)	m+h	delta	z	zeta	pre	start	sequence

509	-1,5	5,61	1539	1,3		2	1	slqk	254	AVANQPVSVAIEAGGR
505	-1,2	5,5	1539	2,5		2	1	slqk	254	AVANQPVSVAIEAGGR

1	**-9,4**	**6,23**	**9,8**	**12**		**2**	**4**	**34,4**	**tr|F2CRK1|F2CRK1_HORVD**	**Predicted protein;**
spectrum	log(e)	log(I)	m+h	delta	z		zeta	pre	start	sequence
754	-2,3	5,68	1761	1,1		2	1	feek	186	DGIDYAAVTVQLPGGER
345	-2,2	5,87	1563	1		2	1	pkgr	242	GGSTGYDNAVALPAGGR
292	-1,8	5,35	1563	2,1		2	1	pkgr	242	GGSTGYDNAVALPAGGR
354	-1,7	5,38	1563	2,3		2	1	pkgr	242	GGSTGYDNAVALPAGGR

2	**-4,9**	**5,9**	**3,2**	**5**		**1**	**1**	**41**	**tr|Q0DJC0|Q0DJC0_ORYSJ**	**Os05g0302700 protein;**
spectrum	log(e)	log(I)	m+h	delta	z		zeta	pre	start	sequence
437	-4,9	5,9	1192	-0,4		2	1	nilr	353	AVAGAGVLAGYDK

3	**-4,6**	**5,6**	**8,5**	**12**		**1**	**1**	**24,7**	**tr|F2DTJ2|F2DTJ2_HORVD**	**Predicted protein**
spectrum	log(e)	log(I)	m+h	delta	z		zeta	pre	start	sequence
1184	-4,6	5,6	2233	1,5		2	1	flar	51	NPFGQVPVLEDGDLTLFESR

4	**-3,4**	**5,75**	**5,1**	**8**		**1**	**1**	**33**	**sp|P27337|PER1_HORVU**	**Peroxidase 1; EC 1.11.1.7;**
spectrum	log(e)	log(I)	m+h	delta	z		zeta	pre	start	sequence
918	-3,4	5,75	1711	0,5		2	1	vaar	123	DSVVALGGPSWTVPLGR

7	**-2**	**5,65**	**5,4**	**7**		**1**	**1**	**29,8**	**tr|G0YLW6|G0YLW6_9ARAE**	**Putative chlorophyll a/b binding protein;**
spectrum	log(e)	log(I)	m+h	delta	z		zeta	pre	start	sequence
974	-2	5,65	1697	-0,1		2	1	vwfk	149	TGALLLDGNTLNYFGK

1	**-2,7**	**6,22**	**3,8**	**6**		**1**	**2**	**24,8**	**sp|P13192|PSAF_HORVU**	**Light-harvesting complex I 17 kDa protein; PSI-F;**
spectrum	log(e)	log(I)	m+h	delta	z		zeta	pre	start	sequence
1152	-2,7	6,08	1180	1		2	1	iipr	210	GFIWPVAAYR
1162	-2,7	5,65	1180	0,7		2	1	iipr	210	GFIWPVAAYR

2	**-2,4**	**5,44**	**5,7**	**9**		**1**	**1**	**27,7**	**tr|Q6WFB1|Q6WFB1_MAIZE**	**Photosystem II subunit PsbS;**
spectrum	log(e)	log(I)	m+h	delta	z		zeta	pre	start	sequence
1004	-2,4	5,44	1585	1,3		2	1	pkpk	73	VEDGIFGTSGGIGFTK

1	**-1,5**	**5,48**	**13**	**28**		**1**	**2**	**9,4**	**sp|A1EA25|PSBE_AGRST**	**Cytochrome b559 subunit alpha; PSII reaction center subunit V;**
spectrum	log(e)	log(I)	m+h	delta	z		zeta	pre	start	sequence
1002	-1,5	5,05	1486	1,8		2	1	itdr	70	FDSLEQLDEFSR
997	-1,2	5,28	1486	0,5		2	1	itdr	70	FDSLEQLDEFSR

Annex 4: *Table chloroplastic proteins of P. oceanica*

ENV= envelope sub-compartment; STR= stroma sub-compartment; THY= thylakoids sub-compartment; NA= not assigned

Assigned function of the identified proteins from intact chloroplasts, their accession number according to the NCBInr and Dr.Zompo databases and protein sub-localization deduced from the AT_CHLORO database searching. The highlighted lines refer to proteins whose localization in the chloroplast is doubtful, or to chloroplast proteins whose sub-location is still unclear.

Assigned function of the identified proteins from intact chloroplasts, their accession number according to the NCBInr and Dr.Zompo databases and protein sub-localization deduced from the AT_CHLORO database searching. The highlighted lines refer to proteins whose localization in the chloroplast is doubtful, or to chloroplast proteins whose sub-location is still unclear.

Accession no.	Database	Assigned function	MW	*p*I	cell compartment	AT_CLHORO sub-localization
P21240	PA.Pooc	**40S ribosomal protein S19-3**	23888.1	9.71	CLHOROPLAST	ENV
Q8H173	PA.ZomaAB	**40S ribosomal protein Sa-2**	47139.6	4.99	CLHOROPLAST	ENV
AT1G27400.1	PA.Pooc	**60S ribosomal protein L12-3**	29642.3	9.30	CLHOROPLAST	ENV
AT2G07698.1	NCBInr.Viridiplantae ChloroplastProteins	**ATP synthase CF1 alpha subunit**	55526.8	5.33	CLHOROPLAST	ENV
I0YRB9	PA.Pooc	**DUF1118**	26628.2	8.84	CLHOROPLAST	ENV
AT5G04900.1	PA.Pooc	**GDP-mannose 3,5-epimerase**	16867.7	8.93	CLHOROPLAST	ENV
AT1G01620	PA.ZomaAB	**Outer plastidial membrane protein porin**	38993.9	9.35	CLHOROPLAST	ENV
AT4G00630.1	PA.ZomaAB	**Putative K(+)-stimulated pyrophosphate-energized sodium pump**	63226.2	6.50	CLHOROPLAST	ENV
AT1G76030.1	PA.Pooc	**V-type proton ATPase subunit B 1**	36806.0	5.06	CLHOROPLAST	ENV
AT4G38510.1	PA.ZomaAB	**V-type proton ATPase subunit B2**	69761.9	5.48	CLHOROPLAST	ENV
AT5G54190.1	PA.Pooc	**Protochlorophyllide reductase A**	14242.9	9.21	CLHOROPLAST	ENV-THY
AT1G55490.1	PA.ZomaAB	**Chaperonin 60 subunit beta 1**	77684.3	8.51	CLHOROPLAST	STR
Q40677	PA.ZomaAB	**Fructose-bisphosphate aldolase 2**	58334.4	8.20	CLHOROPLAST	STR

AT3G25660.1	PA.Pooc	**Glutamine synthetase cytosolic isozyme 1-1**	22373.8	5.49	CLHOROPLAST	STR
AT1G66200.1	PA.Pooc	**Glutamine synthetase nodule isozyme**	32989.0	5.70	CLHOROPLAST	STR
AT2G47730.1	PA.Pooc	**Glutathione S-transferase F8**	32995.2	5.74	CLHOROPLAST	STR
AT2G47730	PA.Pooc	**Glutathione S-transferase F8**	34899.8	6.70	CLHOROPLAST	STR
AT1G42970.1	NCBInr.Chloroplast ProteinsArath	**glyceraldehyde 3-phosphate dehydrogenase B subunit**	42796.2	5.60	CLHOROPLAST	STR
PF02800	PA.Pooc	**Glyceraldehyde-3-phosphate dehydrogenase**	48901.2	9.91	CLHOROPLAST	STR
AT3G26650.1	PA.Pooc	**Glyceraldehyde-3-phosphate dehydrogenase A**	17647.1	9.55	CLHOROPLAST	STR
AT1G42970.1	PA.ZomaAB	**Glyceraldehyde-3-phosphate dehydrogenase B**	73473.1	9.04	CLHOROPLAST	STR
AT5G63310.1	PA.Pooc	**Nucleoside diphosphate kinase B**	25755.9	5.46	CLHOROPLAST	STR
AT3G12780.1	PA.Pooc	**Phosphoglycerate kinase 2**	27001.7	9.46	CLHOROPLAST	STR
AT1G56190.1	PA.ZomaAB	**Phosphoglycerate kinase**	61251.3	8.76	CLHOROPLAST	STR
AT5G08280.1	PA.ZomaAB	**Porphobilinogen deaminase**	51733.8	7.11	CLHOROPLAST	STR
P19311	PA.Pooc	**Ribulose bisphosphate carboxylase small chain SSU5A**	35008.3	9.73	CLHOROPLAST	STR
AT1G140	NCBInr.Posido	**ribulose-1,5-bisphosphate**	44004.3	6.24	CLHOROPLAST	STR

30	niaceaePS	**carboxylase/oxygenase large subunit**				
AT3G55800.1	NCBInr.Chloroplast ProteinsArath	**sedoheptulose-1,7-bisphosphatase**	42414.6	6.18	CLHOROPLAST	STR
AT2G21170.1	PA.Pooc	**Triosephosphate isomerase, cytosolic**	27826.7	5.11	CLHOROPLAST	STR
AT5G20720.1	PA.Pooc	**20 kDa chaperonin**	36995.0	8.34	CLHOROPLAST	STR-ENV
AT1G53240	PA.ZomaAB	**Malate dehydrogenase 1**	46985.6	8.79	CLHOROPLAST	STR-ENV
ATCG00490	NCBInr.ViridiplantaeChloroplastProteins	**ribulose-1,5-bisphosphate carboxylase/oxygenase large subunit**	50069.2	6.10	CLHOROPLAST	STR-ENV
AT2G01140.1	PA.Pooc	**Fructose-bisphosphate aldolase**	29311.2	6.15	CLHOROPLAST	STR-THY
ATCG00480	NCBInr.PosidoniaceaePS	**ATP synthase beta subunit, partial**	51509.2	4.99	CLHOROPLAST	THY
A1E9T0	NCBInr.Chloroplast ProteinsArath	**ATP synthase epsilon chain, ATP synthase F1**	14498.8	5.83	CLHOROPLAST	THY
AT5G08670	PA.ZomaAB	**ATP synthase subunit beta**	72422.6	7.37	CLHOROPLAST	THY
ATCG00120	NCBInr.PosidoniaceaePS	**ATPase alpha subunit**	39042.1	8.34	CLHOROPLAST	THY
P00850	NCBInr.Chloroplast ProteinsArath	**ATPase beta subunit**	53934.1	5.38	CLHOROPLAST	THY

P07370	PA.Pooc	**Chlorophyll a-b binding protein 1B**	37633.2	6.35	CLHOROPLAST	THY
AT1G61520	PA.Pooc	**Chlorophyll a-b binding protein 3**	40437.5	9.16	CLHOROPLAST	THY
P27494	PA.Pooc	**Chlorophyll a-b binding protein 36**	36055.9	7.47	CLHOROPLAST	THY
P27521	PA.Pooc	**Chlorophyll a-b binding protein 4**	40884.0	9.46	CLHOROPLAST	THY
AT1G15820.1	PA.Pooc	**Chlorophyll a-b binding protein 6A**	36612.6	6.15	CLHOROPLAST	THY
P27491	PA.Pooc	**Chlorophyll a-b binding protein 7**	44111.1	8.89	CLHOROPLAST	THY
P36494	PA.Pooc	**Chlorophyll a-b binding protein CP24**	22444.5	10.09	CLHOROPLAST	THY
AT5G01530.1	PA.Pooc	**Chlorophyll a-b binding protein CP29.1**	11108.7	9.21	CLHOROPLAST	THY
AT5G01530.1	PA.Pooc	**Chlorophyll a-b binding protein CP29.2**	19473.0	9.68	CLHOROPLAST	THY
P22686	PA.Pooc	**Chlorophyll a-b binding protein of LHCII type I**	40319.1	8.93	CLHOROPLAST	THY
P27523	PA.Pooc	**Chlorophyll a-b binding protein of LHCII type III**	32917.0	5.62	CLHOROPLAST	THY
ATCG00580	NCBInr.Chloroplast ProteinsArath	**Cytochrome b559 subunit alpha. PSII reaction center subunit V**	9386.6	4.83	CLHOROPLAST	THY
AT4G03280.1	PA.ZomaAB	**Cytochrome b6-f complex iron-sulfur subunit**	42290.0	8.40	CLHOROPLAST	THY
AT1G06680	PA.Pooc	**Oxygen-evolving enhancer protein 1**	45304.2	8.91	CLHOROPLAST	THY

AT4G05180.1	PA.Pooc	**Oxygen-evolving enhancer protein 3-2**	22787.1	9.77	CLHOROPLAST	THY
AT5G13120.1	PA.Pooc	**Peptidyl-prolyl cis-trans isomerase CYP19-1**	23129.7	9.19	CLHOROPLAST	THY
AT3G26060.1	PA.Pooc	**Peroxiredoxin Q**	33083.2	9.64	CLHOROPLAST	THY
AT1G44575.1	PA.Pooc	**Photosystem II 22 kDa protein**	30030.1	9.65	CLHOROPLAST	THY
ATCG00280	NCBInr.PosidoniaceaePS	**photosystem II CP43**	45720.0	6.37	CLHOROPLAST	THY
ATCG00680	NCBInr.PosidoniaceaePS	**photosystem II CP47 protein**	54893.1	6.13	CLHOROPLAST	THY
Q85FM2	NCBInr.PosidoniaceaePS	**photosystem II D2**	34202.4	5.57	CLHOROPLAST	THY
ATCG00020	NCBInr.Chloroplast ProteinsArath	**Photosystem Q(B) protein. 32 kDa thylakoid membrane protein. Photosystem II protein D1**	38936.8	5.12	CLHOROPLAST	THY
AT1G73110.2	PA.Pooc	**Ribulose bisphosphate carboxylase/oxygenase activase 1**	22175.5	5.00	CLHOROPLAST	THY
AT1G73110.1	PA.ZomaAB	**Ribulose bisphosphate carboxylase/oxygenase activase**	60729.7	5.48	CLHOROPLAST	THY
AT4G37930.1	PA.ZomaAB	**Serine hydroxymethyltransferase 1**	63195.9	8.00	CLHOROPLAST	THY
ATCG00350	NCBInr.PosidoniaceaePS	**photosystem I P700 apoprotein A1, partial**	9428.2	10.15	CLHOROPLAST	THY-ENV
AT1G31330.1	PA.Pooc	**Photosystem I reaction center subunit III**	17283.6	5.88	CLHOROPLAST	THY-ENV

ATCG00350	NCBInr.Chloroplast ProteinsArath	**PSI P700 apoprotein A1**	83231.2	6.60	CLHOROPLAST	THY-ENV
ATCG00350	NCBInr.Chloroplast ProteinsArath	**PSI P700 apoprotein A2**	82475.7	6.89	CLHOROPLAST	THY-ENV
AT1G07660.1	PA.Pooc	**Histone H4**	24737.4	9.99	CLHOROPLAST	THY-STR
P05694	PA.ZomaAB	**homocysteine methyltransferase**	99310.3	6.65	CLHOROPLAST?	none
AT1G68010.1	PA.ZomaAB	**Glycerate dehydrogenase**	56313.6	8.25	CLHOROPLAST	none
AT5G38480.1	PA.Pooc	**general regulatory factor, a 14-3-3 gene expressed in seedling growth**	22211.9	8.42	CLHOROPLAST	none
P19358	PA.Pooc	**S-adenosylmethionine synthase 2**	31452.9	5.50	CLHOROPLAST	none
P46248	PA.ZomaAB	**Aspartate aminotransferase**	59326.2	8.20	CLHOROPLAST	STROMA ?
Q9SJ12	PA.Pooc	**ATP synthase 24 kDa subunit**	16504.2	9.42	CHLOROPLAST?	none

Annex 5. *Peptide sequences assigned to each identified chloroplast proteins*

Accession	Description	Peptide sequenze
365823909	photosystem II CP43	(R)LGANIGSAQGPTGLGK(Y) (K)ITNLTLSPSVIFGYLLK(S) (R)KITNLTLSPSVIFGYLLK(S) (K)DIQPWQER(R) (R)GPNGLDLSR(L) (R)APWLEPLRGPNGLDLSR(L)
365823609	photosystem II CP47 protein	(R)VVTGLAENLSLSEAWSK(I) (K)LAFYDYIGNNPAK(G) (R)YQWDQGYFQQEIYR(R) (R)AQLGEIFELDR(A) (R)ADVPFRR(A)
5881693	PSI P700 apoprotein A2	(K)QILIEPIFAQWIQSAHGK(T) (R)FSQGLAQDPTTR(R) (R)TPLANLIR(W) (K)DFGYSFPCDGPGR(G)
Pooc_Contig239_4	Chlorophyll a-b binding protein 36, chloroplastic	(K)NRELEVIHAR(W) (R)ELEVIHAR(W) (K)SIWYGVDRPK(Y) (K)FGEAVWFK(A)
5881694	PSI P700 apoprotein A1	(R)YNDLLDR(V) (R)SPEPEVK(I) (K)EIPLPHEFILNR(D) (R)GIQITSGFFQIWR(A) (K)DILEAHK(G)
44889035	Photosystem Q(B) protein	(R)VINTWADIINR(A) (R)FGQEEETYNIVAAHGYFGR(L) (R)ETTENESANEGYR(F)
365823908	photosystem II D2	(R)AAEDPEFETFYTK(N) (R)AYDFVSQEIR(A)

2734972	RUBISCO large subunit partial	(K)DTDILAAFR(V) (R)EITLGFVDLLR(D) (K)LTYYTPEYETK(D)
Zoma_B_i01704_4	5-methyltetrahydropteroyltriglutamate--homocysteine methyltransferase	(K)YGAGIGPGVYDIHSPR(I) (K)ALAGQKDEAFFSANAAAQASR(K)
Pooc_Contig378_6	Oxygen-evolving enhancer protein 1	(R)GGSTGYDNAVALPAGGR(G) (K)SKPQTGEVIGVFESIQPSDTDLGAK(V)
429125385	photosystem I P700 apoprotein A1 partial	(K)VAPATQPR(A) (R)ALSIVQGR(A)
Zoma_B_i16547_4	Plasma membrane ATPase 4	(K)ADIGIAVADATDAAR(S) (K)LGDIVPADAR(L)
27527694	putative plasma membrane intrinsic protein	(R)QPIGTAAQTGDDR(D) (R)SFGAAVIYNK(Q)
Zoma_C_c33689_1	Ribulose bisphosphate carboxylase large chain	(R)DLASEGNEIIR(E)
5881679	ATPase alpha subunit	(K)IAQIPVSEAYLGR(V) (R)LIESPAPGIISR(R) (R)ADEISNIIR(E)
Zoma_B_i14155_6	Putative K(+)-stimulated pyrophosphate-energized sodium pump	(K)YIEAGASEHAR(T) (K)AADVGADLVGK(V)
310109904	ATP synthase beta subunit, partial (chloroplast)	(K)TVLIMELINNIAK(A) (R)IAQIIGPVLDVAFPPGK(M) (R)AVAMSATDGLTR(G) (R)IFNVLGEPVDNLGPVDTR(T) (R)FVQAGSEVSALLGR(M) (R)VGLTALTMAEYFR(D)

		(R)GMEVIDTGAPLSVPVGGATLGR(I) (K)ESGVINEQNIAESK(V) (K)VALVYGQMNEPPGAR(M) (R)SAPAFIQLDTK(L) (K)LSIFETGIK(V) (R)MPSAVGYQPTLSTEMGSLQER(I) (K)AHGGVSVFGGVGER(T) (K)MPNIYNALAVK(G)
2734972	RuBisCO large subunit partial	(K)DTDILAAFR(V) (K)DDENVNSQPFMR(W) (K)GHYLNATAATCEEMLKR(A) (K)LTYYTPEYETK(D) (K)TFQGPPHGIQVER(D) (R)ALRLEDLR(I) (R)AMHAVIDR(Q) (R)AVYECLR(G) (R)DDYIEKDR(S) (R)EITLGFVDLLR(D) (R)EITLGFVDLLRDDYIEK(D) (R)FLFCAEAIYK(S) (R)IPPAYSK(T) (R)MSGGDHVHAGTVVGK(L)
Zoma_B_i13224_2	ATP synthase subunit beta	(R)IPSAVGYQPTLATDLGGLQER(I) (K)TVLIMELINNVAK(A) (R)VGLTGLTVAEHFR(D) (R)QISELGIYPAVDPLDSTSR(M) (R)IINVIGEPIDER(G) (R)FTQANSEVSALLGR(I) (R)VLNTGSPITVPVGR(A) (K)VVDLLAPYQK(G)
5881679	ATPase alpha subunit	(R)LIESPAPGIISR(R) (K)IAQIPVSEAYLGR(V) (R)ADEISNIIR(E) (R)SVYEPLQTGLIAIDSMIPIGR(G)
Zoma_C_c33689_1	Ribulose bisphosphate carboxylase large chain	(R)DLASEGNEIIR(E) (K)WSPELAAACEVWK(E)
149390253	ATP synthase CF1 alpha	(K)VVNTGTVLQVGDGIAR(I)

	subunit	(K)ASSVAQVVTTFQER(G)
114509222	ATPase alpha subunit	(R)GLRPAINVGLSVSR(V) (K)AVDSLVPIGR(G) (K)TAIAVDTILNQK(E)
440233610	RuBisCO large subunit partial	(R)EITLGFVDLLRDEYIEKDR(S) (R)EITLGFVDLLRDEYIEK(D)
131968 222863988	RuBisCO large subunit predicted protein	(R)DLATEGNEIIR(E) (K)TFEGPPHGIQVER(D) (K)VVIGPATVGGIQAGAFK(I) (R)AGKDLVSSLVSGLLTIGPR(F)
Zoma_C_c6123 3_6	ATP synthase subunit alpha, mitochondrial	(R)AILSTIDPQLLNELASK(G) (R)LTEVLKQPQYEPLPIEK(Q)
Pooc_Contig181 _1	V-type proton ATPase subunit B 1	(R)QIYPPINVLPSLSR(L) (R)VTLFLNLANDPTIER(I)
Zoma_B_i13386 _5	Chaperonin 60 subunit beta 1, chloroplastic	(K)LADLVGVTLGPK(G) (R)GYISPYFVTDSEK(M)
5881701	ATPase beta subunit	(K)GRDTLGQEINVTCEVQQLLG NNR(V) (K)SAPAFIELDTK(L)
Zoma_B_i11853 _4	V-type proton ATPase subunit B2	(K)AVVQVFEGTSGIDNK(Y) (R)TVSGVAGPLVILEK(V)
411031317	RuBisCO large subunit partial	(K)DDENVNSQXFMR(W) (R)GGLDFTKDDENVNSQXFMR(W)
Zoma_B_i14775 _1	Serine hydroxymethyltransferase 1	(K)NAVFGDSSALAPGGVR(I) (K)ISATSIYFESLPYK(V)
Zoma_B_i16244 _3	Ribulose bisphosphate carboxylase/oxygenase activase	(R)VPIIVTGNDFSTLYAPLIR(D)
310109904	ATP synthase beta subunit, partial (chloroplast)	(K)TVLIMELINNIAK(A) (R)FVQAGSEVSALLGR(M) (R)IFNVLGEPVDNLGPVDTR(T)

		(K)ESGVINEQNIAESK(V) (R)VGLTALTMAEYFR(D) (R)IAQIIGPVLDVAFPPGK(M) (K)IGLFGGAGVGK(T)
Pooc_B_c65_6	Glyceraldehyde-3-phosphate dehydrogenase A	(R)VPTPNVSVVDLVVQVSK(K) (K)TFAEEVNAAFR(E) (K)AVALVLPGLK(G) (K)LNGIALRVPTPNVSVVDLVVQVSK(K) (K)DILVVCDEPLVSVDFR(C)
336390	glyceraldehyde 3-phosphate dehydrogenase B subunit	(K)AVSLVLPQLK(G) (K)GTMTTTHSYTGDQR(L) (R)AAALNIVPTSTGAAK(A) (R)LLDASHR(D) (K)VAINGFGR(I) (K)GKLNGIALR(V)
Pooc_Contig14_2	Glyceraldehyde-3-phosphate dehydrogenase	(K)AGIALSENFVK(L) (K)LVSWYDNEWGYSSR(V) (K)AAGFNIIPSSTGAAK(A) (R)SSIFDAK(A) (K)SATYEQIK(A) (K)VLPALNGK(L)
Pooc_Contig222_4	Glutamine synthetase cytosolic isozyme 1-1	(R)LTGHHETASIDQFSWGVANR(G) (R)KDGGYEVIKK(A) (K)DGGYEVIKK(A) (K)EHISAYGEGNER(R) (K)GYFEDR(R)
Pooc_PC021E08_3	Phosphoglycerate kinase 2, chloroplastic	(K)ELDYLVGAVSNPK(R) (K)LVAALPDGGVLLLENVR(F) (K)LASLADLYVNDAFGTAHR(A) (K)RPFAAIVGGSK(V)
Pooc_PC053G11_2	Glyceraldehyde-3-phosphate dehydrogenase	(K)AVGNNIISVDGK(E) (K)YDSTLGIFDADVK(A) (R)VVSDRNPANLPWK(E) (K)VLITAPGK(G)

		(K)KVLITAPGK(G)
Pooc_Contig131_4	Sedoheptulose-1,7-bisphosphatase, chloroplastic	(R)LLFEVAPLGFLVEK(A) (K)VITQLDER(T) (K)GIFTNVTSPTTK(A) (R)ATFDNADYAK(L) (R)FEETLYGSSR(L)
Zoma_B_i13486_4	Malate dehydrogenase 1, mitochondrial	(R)DDLFNINAGIVK(G) (K)VAILGAAGGIGQPLSLLMK(H) (K)RTQDGGTEVVEAK(A)
Pooc_B_rp10_H5_R_5	GDP-mannose 3,5-epimerase	(K)VVGTQAPVQLGSLR(A) (K)NLPIHHIPGPEGVR(G) (K)TQGIDLSIYGTSK(V)
Pooc_PC035C04_2	Fructose-bisphosphate aldolase, chloroplastic	(R)TAAYYQQGAR(F) (K)KIVDVLVEQNIVPGIK(V) (K)IVDVLVEQNIVPGIK(V)
Pooc_Contig291_3	Glutamine synthetase nodule isozyme	(K)VFSIPEVAAEEPWYGIEQEYTLLQK(D) (R)DIVDSHYK(A) (R)TLPGPVSDPK(K)
122246696	Actin-3	(K)LAYIALDYEQELETAK(S) (R)GYSFTTTAER(E) (R)AVFPSIVGRPR(H)
Pooc_Contig341_3	Fructose-bisphosphate aldolase, chloroplastic	(K)YTSDGEAAEAK(E) (K)ANSLAQLGK(Y) (K)TWGGRPENVK(A) (K)AAQDTLLIR(A)
Pooc_PC035E06_4	Glyceraldehyde-3-phosphate dehydrogenase A	(K)VIAWYDNEWGYSQR(V) (R)VVDLADIVANNWK(*)
2734972	RuBisCO large subunit partial	(R)EITLGFVDLLR(D) (K)SQAETGEIK(G) (K)DTDILAAFR(V) (K)LTYYTPEYETK(D)
365823909	photosystem II CP43	(K)ITNLTLSPSVIFGYLLK(S)

		(K)DIQPWQER(R) (R)LGANIGSAQGPTGLGK(Y)
Zoma_B_i03673_5	40S ribosomal protein Sa-2	(R)LLILTDPR(T) (K)FAQYIGAHPIAGR(H) (R)YVDIGIPANNK(G)
Zoma_B_i11957_5	Aspartate aminotransferase, chloroplastic	(R)VATVQGLSGTGSLR(L) (K)LNLGVGAYR(T) (K)EYLPIEGLAAFNK(A)
223534945	ATP synthase gamma chain	(R)ALQESLASELAAR(M) (R)VALVVVTGDR(G)
Pooc_Contig159_2	Chlorophyll a-b binding protein of LHCII type I, chloroplastic(LHCP)	(K)SAAVSPASDELAK(W) (R)IYLPEGLLDR(S) (K)TGALLLDGNTLNYFGK(N)
222841756	predicted protein	(K)KNEEGVVVNK(F) (R)LYSIASSAIGDFGDSK(T)
Pooc_Contig205_2	S-adenosylmethionine synthase 2	(K)TIFHLNPSGR(F) (R)FVIGGPHGDAGLTGR(K) (K)TQVTVEYK(N)
Zoma_B_i10215_2	Fructose-bisphosphate aldolase 2, chloroplastic	(R)YAAISQDNGLVPIVEPEILLDGEHGIER(N) (K)EAAWGLAR(Y)
Zoma_B_i03277_2	Glycerate dehydrogenase	(R)GPVIDEAALVEHLK(A) (K)GQTVGVIGAGR(I)
Zoma_B_i11978_5	Glyceraldehyde-3-phosphate dehydrogenase B, chloroplastic	(K)GITAEDVNAAFR(K) (K)GITAEDVNAAFRK(A)
Zoma_B_i16636_5	GDP-mannose 3,5-epimerase 1	(R)ISITGAGGFIASHIAR(R) (R)SFTFIDECVEGVLR(L)
44889035	Photosystem Q(B) protein	(R)VINTWADIINR(A) (R)ETTENESANEGYR(F)
Zoma_B_i13503_1	Phosphoglycerate kinase, chloroplastic	(K)ELDYLVGAVSSPK(R)

		(K)GVTTIIGGGDSVAAVEK(V)
Zoma_B_i13108_5	Prohibitin-2	(R)VLTRPIPDQLPEIYR(T) (R)ARPHLVESTSGSR(D)
Zoma_B_i00463_2	Porphobilinogen deaminase, chloroplastic	(R)GLVASPDGTR(V) (K)ILNQPLADIGGK(G)
Pooc_B_c182_4	Protochlorophyllide reductase A, chloroplastic	(R)SASFENQLSQEASDAAK(A) (-)LAQVVIDPSLTK(S)
Pooc_Contig343_1	Ribulose bisphosphate carboxylase/oxygenase activase 1, chloroplastic	(K)DGPPDFTQPK(M) (R)VYDDEVRK(W)
786466	sedoheptulose-1,7-bisphosphatase	(R)YTGGMVPDVNQIIVK(E) (K)MFSPGNLR(A)
Pooc_Contig159_2	Chlorophyll a-b binding protein of LHCII type I, chloroplastic(LHCP)	(K)LHPGGPFDPLGLASDPDQTALLK(V) (K)SAAVSPASDELAK(W) (K)TGALLLDGNTLNYFGK(N) (K)YQAFELIHAR(W) (R)SEVPEYLNGEVPGDYGYDPFGLSK(K) (R)IYLPEGLLDR(S) (K)DKLHPGGPFDPLGLASDPDQTALLK(V)
Pooc_Contig97_6	Chlorophyll a-b binding protein 1B, chloroplastic	(R)WAMLGTLGCVFPELLSR(N) (K)NRELEVIHCR(W) (R)ELEVIHCR(W) (K)AVPGSPWYGPDRVK(Y) (K)FGEAVWFK(A) (K)AVPGSPWYGPDR(V)
Pooc_Contig239_4	Chlorophyll a-b binding protein 36, chloroplastic	(R)WAMLGTLGCVLPELLAK(N) (R)ELEVIHAR(W) (K)NRELEVIHAR(W) (K)FGEAVWFK(A) (K)SIWYGVDRPK(Y)
Pooc_Contig35_6	Chlorophyll a-b binding protein of LHCII type III,	(K)YLGPFSAQTPTYLK(G)

	chloroplastic	(K)GPLENLLDHLDNPVANNAWAYATK(F) (R)ALEVIHGR(W) (K)VQFKEPVWFK(A) (R)WAMLGTFGCITPEVLAK(W)
Pooc_Contig109_2	Triosephosphate isomerase, cytosolic	(K)DNVSPDVAASTR(I) (K)AISDKVTNWDNVVLAYEPVWAIGTGK(V) (R)EWLKDNVSPDVAASTR(I) (K)VIACVGETLEQR(E) (K)FFVGGNWK(C) (R)ALLGESNEFVGDK(V
Pooc_Contig333_3	Photosystem II 22 kDa protein, chloroplastic	(R)VAMLGFAASIFGEAITGK(G) (K)ANELFVGR(M) (R)FVDDATGLDK(A) (K)SKVEDGIFGTSGGIGFTK(Q) (K)EGGPLFGFTK(A)
Pooc_Contig378_6	Oxygen-evolving enhancer protein 1, chloroplastic	(K)DGIDYAAVTVQLPGGER(V) (R)GGSTGYDNAVALPAGGR(G) (K)SKPQTGEVIGVFESIQPSDTDLGAK(V) (K)GRGGSTGYDNAVALPAGGR(G) (R)VPFLFTIK(Q)
Pooc_Contig79_3	Chlorophyll a-b binding protein 3, chloroplastic	(R)FAMLGAAGSIAPELFGK(L) (K)GLGGSGDPAYPGGPFFNPLGFGK(D) (K)QYFLGLEK(G) (R)QLWFASK(Q)
Pooc_Contig313_2	Glutathione S-transferase F8, chloroplastic	(K)EILIKPLLGGTTDPENVETSAAK(L) (K)EIEYELVPVDLR(T) (R)VIVLLHEKEIEYELVPVDLR(T)
Pooc_B_c272_6	Chlorophyll a-b binding protein CP29.1, chloroplastic	(K)STPFQPYTEVFGLQR(F)

		(K)NNVGDLIGTR(F) (R)FETADVK(S)
Pooc_Contig94_6	Chlorophyll a-b binding protein 6A, chloroplastic	(R)LGEVPSNLER(F) (R)FKEAELIHCR(W) (K)LQEFK(V)
Pooc_Contig283_4	Chlorophyll a-b binding protein 4, chloroplastic	(K)LTGTDVGYPGGLWFDPLGWGSGSPEK(I) (R)WAMLGAAGIFVPELLTK(L)
Pooc_PC039D11_5	14-3-3-like protein C	(K)SAQDIATSDLAPTHPIR(L) (K)DAAESTLAAYK(S) (R)YLAEFK(T)
351726054	MnSOD	(K)HHQTYITNYNK(A) (K)RLVVETTANQDPLVTK(G)
44889035	Photosystem Q(B) protein	(R)VINTWADIINR(A) (R)ETTENESANEGYR(F)
Pooc_PC046B02_4	Chlorophyll a-b binding protein CP29.2, chloroplastic	(K)ATLQLAEIK(H) (K)KATLQLAEIK(H)
Pooc_B_c320_5	Chlorophyll a-b binding protein CP24, chloroplastic	(K)TAENFSNATGEQGYPGGK(F) (K)FFDPLR(V)
222845436	light-harvesting complex II protein Lhcb6	(K)TAENFANATGDQGYPGGK(F)
Pooc_Contig136_3	Glutathione S-transferase F8, chloroplastic	(K)VLDVYEAR(L) (K)NPFGQVPVLEDGDITIFESR(A)
Zoma_B_i08974_1	Outer plastidial membrane protein porin	(K)SLITLSGEVDTK(A) (K)DLIFGEIQTQIK(N)
Pooc_Contig225_1	ATP synthase 24 kDa subunit, mitochondrial	(K)ITLDPEDSTAVSQYAK(V)
Pooc_Contig338_6	20 kDa chaperonin, chloroplastic	(K)TAGGLLLTEATK(E)
		(K)YAGSELDFNEAK(H)
365823908	photosystem II D2	(R)AAEDPEFETFYTK(N)
Pooc_Contig291_3	Glutamine synthetase nodule isozyme	(K)VFSIPEVAAEEPWYGIEQEYTLLQK(D)
Pooc_PC028C07	Peptidyl-prolyl cis-trans	(K)HVVFGQIVDGIDVVR(A)

_2	isomerase CYP19-1	(R)IVMELYADVVPR(T) (K)FADENFVKK(H) (K)VFFDMTIGAAPAGR(I) (R)GNGTGGESIYGEK(F)
Pooc_Contig94_6	Chlorophyll a-b binding protein 6A, chloroplastic	(K)KYPGGAFDPLGFSK(D) (R)FKEAELIHCR(W) (R)LGEVPSNLER(F) (R)SMEKDPEKK(K) (K)LQEFK(V)
Pooc_Contig264_2	Nucleoside diphosphate kinase B	(K)IIGATNPSDAVPGTIR(G) (R)KIIGATNPSDAVPGTIR(G) (R)GDYAIDIGR(N) (R)GLVGEIIGR(F)
Pooc_B_c320_5	Chlorophyll a-b binding protein CP24, chloroplastic	(K)TAENFSNATGEQGYPGGK(F) (K)DGVYVPDGERLER(L) (K)DGVYVPDGER(L) (K)FFDPLR(V)
Pooc_Contig333_3	Photosystem II 22 kDa protein, chloroplastic	(K)SKVEDGIFGTSGGIGFTK(Q) (K)EGGPLFGFTK(A) (R)FVDDATGLDK(A) (K)ANELFVGR(M)
132270	Rubber elongation factor protein=Hev b 1	(K)DASIQVVSAIR(A) (R)SLASSLPGQTK(I)
Pooc_Contig3_2	Ribulose bisphosphate carboxylase small chain SSU5A, chloroplastic	(K)KAYPTYFAR(I) (R)QHGNTPGYYDGR(Y) (K)EIEYLLR(N)
Pooc_PC036A05_6	Oxygen-evolving enhancer protein 3, chloroplastic	(K)LGGPPPPSGGLPGTLNSDEAR(D) (R)DLDLPLTER(F)
Pooc_Contig132_3	S-norcoclaurine synthase	(K)LVPNTIEKTEIEGDGGVGTTTK(L) (K)LFFAPGIPGVK(Y)
Pooc_Contig278_3	Peroxiredoxin Q, chloroplastic	(K)GVVQLIYNNQFQPEK(H)

		(K)AGAEVVGISGDDSASHK(A)
5881724	cytochrome B6	(R)GSASVGQSTLTR(F) (R)LEIQAIADDITSK(Y)
Pooc_B_c81_2	Oxygen-evolving enhancer protein 3-2, chloroplastic	(K)ELTDAVFSSISGLDYAAK(I) (K)AWPYVQNDLR(L) (K)SAIGDLFAK(L)
Pooc_Contig244_4	60S ribosomal protein L12-3	(R)VTGGEIGAASSLAPK(I) (K)IGPLGLSPK(K)
Pooc_Contig27_3	Chlorophyll a-b binding protein 7, chloroplastic	(K)NPGCVNQDPIFK(N) (K)IGIINVPEWYDAGK(S) (K)WFVQAELQNGR(W)
Pooc_Contig78_1	Universal stress protein A-like protein	(R)KGDHLILINVQK(Q) (K)WVVENIAR(K)
Pooc_Contig327_5	Photosystem I reaction center subunit III, chloroplastic	(K)EIIIDVPLASK(L) (R)GFIWPVAAYR(E)
Zoma_B_i01620_4	Cytochrome b6-f complex iron-sulfur subunit, chloroplastic	(K)VVFVPWVETDFR(T) (R)GPAPLSLALAHADIDDGK(V)
Pooc_Contig256_3	40S ribosomal protein S19-3	(R)DLDQVAGR(I) (K)DVSPHEFVK(A)
332278159	ATP synthase epsilon chain	(K)RQTIEANLALRR(A) (R)QTIEANLALR(R)
Pooc_Contig3_2	Ribulose bisphosphate carboxylase small chain SSU5A	(R)NNWVPCIEFSADGFISR(Q) (K)KFETFSYLPPFTDEMLIK(E) (R)QHGNTPGYYDGR(Y) (R)QVQCISFIAYKPK(G) (K)KAYPTYFAR(I) (R)IIGFDNKR(Q) (K)AYPTYFAR(I)
Pooc_PC006G03_2	Histone H4	(R)DAVTYTEHAR(R) (R)DNIQGITKPAIR(R)

		(R)ISGLIYEETR(G) (K)IFLENVIR(D)
30794280	serum albumin precursor	(R)RHPEYAVSVLLR(L) (K)DAFLGSFLYEYSR(R) (K)LVVSTQTALA(-) (K)IETMREK(V)
114152861	Cytochrome b559 subunit alpha	(R)FDSLEQLDEFSR(S) (R)QGIPLITGR(F)
132270	Rubber elongation factor protein =Hev b 1	(K)DASIQVVSAIR(A) (R)SLASSLPGQTK(I)
Pooc_Contig139_1	DUF1118	(K)AGLLSAAESFGLSLSTVER(I) (K)GTTVFPLGEPGPR(E)

Annex 6: *Identified proteins from P. oceanica chloroplasts*

Number of spectra for each proteins, number of unique peptides; the of sequence coverage (%C) and mean peak intensity (MI)

Identified proteins	No. spectra	No. Unique peptides	Score	%C	MI	MW	Pi	Accession
20 kDa chaperonin, chloroplastic	3	2	22,24	6	2,05E+08	45304.4	8.34	AT5G20720.1
osomal protein S19-3	2	2	24,46	7	9,96E+07	45304.4	9.71	P21240
40S ribosomal protein Sa-2	3	3	37,37	7	2,70E+08	45304.4	4.99	Q8H173
60S ribosomal protein L12-3	3	2	27,98	8	7,20E+07	45304.4	9.30	AT1G27400.1
ATP synthase CF1 alpha subunit	2	2	32,57	5	9,83E+08	45304.4	5.33	AT2G07698.1
ATP synthase F1 sector epsilon subunit	3	2	23,92	9	8,80E+07	45304.1	5.83	A1E9T0
ATP synthase gamma chain, chloroplastic	2	2	33,45	6	5,51E+08	42438.0	6.21	AT4G04640
ATP synthase beta subunit, partial (chloroplast)	31	14	236,59	40	1,19E+09	51509.2	4.99	ATCG00480
ATP synthase subunit beta	13	8	137,32	17	8,12E+08	72422.6	7.37	AT5G08670
ATPase alpha subunit	13	7	44,24	9,5	6,07E+08	45304.3	6,765	ATCG00120
Chaperonin 60 subunit beta 1, chloroplastic	4	2	25,76	3	5,79E+08	45304.3	8.51	AT1G55490.1
Chlorophyll a-b binding protein 1B, chloroplastic	11	6	107,57	13	1,70E+09	37633.2	6.35	P07370
Chlorophyll a-b binding protein 3, chloroplastic	4	4	54,91	14	3,51E+08	45304.5	9.16	AT1G61520
Chlorophyll a-b binding protein 36,	10	5	84,37	13	1,48E+09	36055.9	7.47	P27494

chloroplastic								
Chlorophyll a-b binding protein 4, chloroplastic	2	2	37,55	11	1,27E+08	45304.1	9.46	P27521
Chlorophyll a-b binding protein 6A, chloroplastic	8	5	67,75	13	2,16E+08	36612.6	6.15	AT1G15820.1
Chlorophyll a-b binding protein 7, chloroplastic	4	3	27,95	9	1,50E+08	45304.1	8.89	P27491
Chlorophyll a-b binding protein CP24, chloroplastic	7	4	49,18	18	1,50E+08	45304.7	10.09	P36494
Chlorophyll a-b binding protein CP29.1, chloroplastic	3	3	41,23	30	6,82E+08	45304.9	9.21	AT5G01530.1
Chlorophyll a-b binding protein CP29.2, chloroplastic	3	2	29,03	5	4,20E+08	45304.1	9.68	AT5G01530.2
Chlorophyll a-b binding protein of LHCII type I, chloroplastic(LHCP)	15	7	107,93	25	3,44E+08	40319.1	8.93	P22686
Chlorophyll a-b binding protein of LHCII type III, chloroplastic	5	5	82,98	23	9,75E+08	32917.0	5.62	P27523
Cytochrome b6-f complex iron-sulfur subunit, chloroplastic	7	4	27,58	9	2,70E+08	45304.1	8.55	AT4G03280.1
DUF1118	3	2	22,14	12	1,93E+08	45304.5	8.84	I0YRB9
Fructose-bisphosphate aldolase, chloroplastic	9	7	42,495	12,5	2,43E+08	45304.3	7.715	AT2G01140.1
GDP-mannose 3,5-epimerase	5	5	74,01	32	3,86E+08	45304.4	7.78	AT5G04900.1
Glutamine	5	5	68,0	23	3,31E+	4530	5.4	AT3G256

synthetase cytosolic isozyme 1-1			7		08	4.2	9	60.1
Glutamine synthetase nodule isozyme	4	3	42,01	14	5,39E+08	45304.3	5.70	AT1G66200.1
Glutathione S-transferase F8, chloroplastic	8	5	32,23	11	3,57E+08	45304.3	6.22	AT2G47730.1
glyceraldehyde 3-phosphate dehydrogenase B subunit	8	6	74,27	15	8,45E+08	45304.2	7.04	AT1G42970.1
Glyceraldehyde-3-phosphate dehydrogenase	6	6	68,56	13	4,90E+08	45304.2	9.91	PF02800
Glyceraldehyde-3-phosphate dehydrogenase A, chloroplastic	11	7	121,02	43,5	7,21E+08	45304.2	7.30	AT3G26650.1
Histone H4	6	4	65,30	17	5,58E+08	24737.4	9.99	AT1G07660.1
light-harvesting complex II protein Lhcb6	3	1	23,75	7	4,72E+08	27309.6	6.75	A9PFP4
Malate dehydrogenase 1, mitochondrial	4	3	54,67	9	2,51E+08	45304.3	8.79	AT1G53240
Nucleoside diphosphate kinase B	6	4	55,76	14	1,23E+08	45304.3	5.46	AT5G63310.1
Outer plastidial membrane protein porin	2	2	22,86	6	1,81E+08	45304.4	9.35	AT1G01620
Oxygen-evolving enhancer protein 1, chloroplastic	7	5	63,95	16	2,65E+08	45304.2	8.91	AT1G06680
Oxygen-evolving enhancer protein 3-2, chloroplastic	3	3	29,27	18	9,51E+07	45304.1	9.77	AT4G05180.1
Peptidyl-prolyl cis-trans isomerase CYP19-1	7	5	74,16	28	1,76E+08	23129.7	9.19	AT5G13120.1

Peroxiredoxin Q, chloroplastic	3	2	31,18	10	8,56E+07	45304.1	9.64	AT3G26060.1
Phosphoglycerate kinase 2, chloroplastic	6	4	66,28	23	3,34E+08	45304.3	9.46	AT3G12780.1
Phosphoglycerate kinase, chloroplastic	2	2	27,65	5	5,07E+08	45304.3	8.76	AT1G56190.1
Photosystem I reaction center subunit III, chloroplastic	2	2	26,14	13	1,33E+08	45304.1	5.88	AT1G31330.1
Photosystem II 22 kDa protein, chloroplastic	12	5	65,72	22	3,18E+08	30030.1	9.65	AT1G44575.1
photosystem II CP43	12	6	83,72	14	4,83E+08	45720.0	6.37	ATCG00280
photosystem II CP47 protein	9	5	66,40	12	5,48E+08	54893.1	6.13	ATCG00680
photosystem II D2	4	2	38,21	7	6,08E+08	45304.1	5.57	Q85FM2
Photosystem II protein D1	7	3	44,87	12	6,71E+08	45304.8	5.12	ATCG00020
Porphobilinogen deaminase, chloroplastic	2	2	25,69	4	2,00E+08	45304.4	7.11	AT5G08280.1
predicted protein	5	4	31,55	12	7,88E+08	53689.1	8.45	AT3G43520
Protochlorophyllide reductase A, chloroplastic	2	2	22	21	1,77E+08	45304.5	9.21	AT5G54190.1
PSI P700 apoprotein A1	5	5	51,49	6	8,86E+07	45304.6	10.15	ATCG00350.1
PSI P700 apoprotein A2	5	4	55,06	6	3,52E+08	45304.4	6.89	ATCG00350.2
PSII reaction center subunit V	2	2	33,57	25	6,10E+08	45304.1	4.83	ATCG00580
Putative K(+)-stimulated pyrophosphate-energized sodium pump	2	2	20,29	3	1,30E+07	45304.5	6.50	AT4G00630.1
Ribulose	7	4	42,8	1	3,09E+	4530	7.8	ATCG004

bisphosphate carboxylase large chain			7		09	4.3	5	90
Ribulose bisphosphate carboxylase small chain SSU5A, chloroplastic	17	8	110,91	26	5,89E+08	45304.2	9.73	P19311
Ribulose bisphosphate carboxylase/oxygenase activase 1, chloroplastic	2	2	20,76	8	1,50E+08	45304.2	5.00	AT1G73110.2
Ribulose bisphosphate carboxylase/oxygenase activase, chloroplastic	3	1	21,37	3	1,90E+08	45304.2	5.48	AT1G73110.1
ribulose-1,5-bisphosphate carboxylase/oxygenase large subunit, partial	31	17	108,4	40	9,94E+08	43915,6	7.31	AT1G14030
Sedoheptulose-1,7-bisphosphatase, chloroplastic	5	5	59,85	11	2,88E+08	45304.3	6.10	AT3G55800.1
Serine hydroxymethyltransferase 1	5	2	21,44	5	6,88E+08	45304.2	8.00	AT4G37930.1
Triosephosphate isomerase, cytosolic	6	6	76,06	29	1,42E+08	45304.2	5.11	AT2G21170.1
V-type proton ATPase subunit B 1	3	2	29,66	8	4,39E+08	45304.4	5.06	AT1G76030.1
V-type proton ATPase subunit B2	2	2	23,87	4	4,03E+08	45304.4	5.48	AT4G38510.1

SN=number of spectra; PN=number of unique peptides; %C=percent of coverage; MI=mean intensity

Annex 7: *Identified proteins from P. oceanica at different depths*

Sample	log (e)	log (I)	% (m)	% (c)	unique	tot parz	tot	Mr	Metabolism	Accession	Description
8:00 am, 30m depth	-144	5,95	38	70	15	48	**89**	44	Calvin cycle	gi|2734972|gb|AAB93814.1|	rbcL , ribulose-1,5-bisphosphate carboxylase/oxygenase large subunit, partial (chloroplast) [Posidonia oceanica].
	-95,4	5,72	5,5	5	1	1	**65**	36,3	PSI	Zoma_B_i05288_5	oxygen evolving enhancer protein 1 [Litchi chinensis]
	-38,6	4,91	19	23	5	13	**63**	28,9	Alkaloids biosyn.	Pooc_Contig132_3	S-norcoclaurine synthase OS=Thalict…
	-55,7	5,13	14	39	6	16	**58**	56,1	PSII	tr|H6T014|H6T014_LILSU	Photosystem II CP47 chlorophyll apoprotein
	-187	6,05	54	67	15	57	57	45,4	ATP synthase	tr|H6THA9|H6THA9_9LILI	ATP synthase subunit beta
	-67,7	5,43	30	45	5	16	**52**	37,6	Chlorophyll	EG_Contig15_1	chlorophyll A-B binding protein (CAB), putative [Musa balbisiana]
	-74,7	5,16	15	33	8	21	**40**	51,4	Calvin cycle	tr|B5WX89|B5WX89_9ARAE	Ribulose-biphosphate carboxylase
	-102	5,69	21	37	10	29	**32**	55,3	ATP synthase	tr|H2F4C9|H2F4C9_9ASPA	ATP synthase subunit alpha
	-109	5,57	21	28	10	25	**29**	72,4	ATP synthase	Zoma_B_i13224_2	ATP synthase subunit beta
	-68,9	5,37	41	67	7	21	**29**	38,7	Chlorophyll	EG_Contig99_6	chlorophyll A-B binding protein (CAB), putative [Musa acuminata]
	-24,1	4,97	9,3	23	3	10	**27**	51,8	PSII	tr|H2CPN3|H2CPN3_COLES	Photosystem II CP43 chlorophyll apoprotein;
	-70,9	5,28	25	52	7	16	**24**	39,6	PSII	sp|Q4FFP4|PSBD_ACOAM	Photosystem II D2 protein; PSII D2 protein; EC 1.10.3.9; Photosystem Q(A) protein;
	-27,9	5,3	14	53	4	16	**23**	38,9	PSII	sp|Q3V554|PSBA_ACOCL	Photosystem Q(B) protein; EC 1.10.3.9; 32 kDa thylakoid membrane protein; Photosystem II protein D1; Flags: Precursor;
	-56,3	5,54	14	21	5	15	**22**	49	Glycolisis	Pooc_Contig14_1	Glyceraldehyde-3-phosphate dehydrogenase
	-55,5	5,45	20	30	5	19	19	40,3	Chlorophyll	EG_Contig27_6	chlorophyll A/B binding protein, putative [Ricinus communis] >gb|EEF42554.1| chlorophyll A/B binding protein, putative [Ricinus communis]
	-67,3	5,72	23	35	6	19	19	33,6	Glycolisis	tr|H9B8E3|H9B8E3_MISSI	Glyceraldehyde-3-phosphate dehydrogenase-like protein
	-63	5,16	13	17	6	15	**18**	72,4	ATP synthase	Zoma_B_i13224_2	ATP synthase subunit beta, mitochondrial
	-35,5	5,73	22	28	4	18	**18**	20,8	Glycolisis	tr|C4B8E5|C4B8E5_TULGE	Glyceraldehyde-3-phosphate dehydrogenase
	-62,1	5,59	13	35	5	17	**17**	54,6	PSII	tr|A0ARD8|A0ARD8_9LILI	Photosystem II CP47 chlorophyll apoprotein
	-22,3	4,92	1	2	1	3	**16**	158	PSII	Zoma_B_i08822_2	Photosystem II CP43 chlorophyll apo...
	-52,2	5,49	8,8	14	5	15	15	88,2	ATP synthase	Zoma_C_c61233_6	ATP synthase subunit alpha,
	-	5,4	13	17	6	15	**15**	61,	Glycolisis	Zoma_B_i13503_1	Phosphoglycerate kinase

53,2	5						2			
-9	5,08	13	23	2	6	**15**	33	Aminoacid biosynthesis	Pooc_Contig291_3	Glutamine synthetase
-46,6	4,77	16	21	6	9	**14**	53,7	ATP synthase	tr|Q4FGI4|Q4FGI4_TYPLA	ATP synthase subunit beta
-23,6	4,98	10	18	2	9	**13**	37	Peroxidase	Pooc_Contig281_1	glutathione S-transferase
-12,1	5,22	11	12	2	6	**12**	26,1	Mitochondrial	Pooc_Contig356_1	malate dehydrogenase
-82,8	5,18	3,2	3	1	3	**12**	0	PSII	tr|H6TGJ9|H6TGJ9_9LILI	Photosystem II CP47 protein
-35,2	5,08	22	26	4	11	11	27,8	Glycolisis	Pooc_Contig109_2	Triosephosphate isomerase, cytosolic
-33,4	5,23	9,8	13	4	7	**10**	56,4	Mitochondrial	Zoma_B_i02521_4	Ferredoxin--NADP reductase, chloroplastic
-22,1	5,08	2,7	3	1	3	**10**	0	Glycolisis	Zoma_B_i11422_2	Enolase 2 glycolisis)
-24,4	5,03	12	15	3	9	9	35,4	Mitochondrial	sp|Q6ENG0|CYF_ORYNI	Apocytochrome f
-14,7	5	7,8	12	2	9	9	33	Flavonoids	Pooc_Contig89_5	Chalcone--flavonone isomerase
-51,4	5,46	9,6	10	2	6	**9**	0	Glycolisis	EG_Contig109_4	chloroplast glyceraldehyde-3-phosphate dehydrogenase, partial [Chlorokybus atmophyticus]
-32,9	4,85	11	18	4	8	**8**	54,3	ATP synthase	tr|A0ZSE5|A0ZSE5_ZOSMR	Vacuolar H+-ATPase subunit B
-18	4,46	12	16	3	4	**8**	36	Glycolisis	tr|Q5PY03|Q5PY03_MUSAC	Glyceraldehyde-3-phosphate dehydrogenase
-78,3	5,23	4	4	1	5	**8**	56	PSII	tr|A0ARD7|A0ARD7_SMIRO	Photosystem II CP47 chlorophyll apoprotein; Flags: Fragment;
-19,4	4,72	1,3	2	2	6	**7**	241	PSI	Zoma_C_c64621_5	Photosystem I P700 chlorophyll a ap...
-25,1	4,86	1,4	2	4	7	**7**	212	PSI	Zoma_B_i00191_2	Photosystem I P700 chlorophyll a ap...
-20,2	4,83	5,4	7	3	7	7	80,1	HSP	sp|A2YWQ1|HSP81_ORYSI	Heat shock protein 81-1
-11,3	4,79	12	30	2	4	**7**	33,5	Growth factor	Pooc_Contig188_1	Elongation factor 1-alpha
-24,8	4,81	16	19	3	7	7	29	uncharacterized	Pooc_Contig48_2	OSIGBa0142I02-OSIGBa0101B20.20 [Oryza sativa Indica Group]
-23	5,12	6,4	8	1	3	**7**	27	Glycolisis	Pooc_PC021E08_3	Phosphoglycerate kinase
-21,1	4,88	26	41	3	5	**7**	21,4	Glycolisis	Pooc_PC016D03_2	Fructose-bisphosphate aldolase cytoplasmic isozyme
-14,7	5,18	36	43	2	7	7	11,1	chlorophyll	Pooc_B_c272_6	Chlorophyll a-b binding protein CP29.1, chloroplastic
-25,7	4,57	6,2	8	4	6	6	83,7	Aminoacid biosynthesis	tr|Q8W0Q7|Q8W0Q7_SORBI	Methionine synthase protein;
-14,3	4,67	3,7	6	2	6	6	74	HSP	tr|Q2QV45|Q2QV45_ORYSJ	70 kDa heat shock protein
-22,1	4,52	5,5	8	3	6	6	72,6	Calvin cycle	Zoma_B_i13574_3	RuBisCO large subunit-binding protein subunit alpha
-26,7	5,18	6,3	7	2	6	6	49,1	uncharacterized	tr|Q7XN85|Q7XN85_ORYSJ	OSJNBa0011F23.7 protein
-16,1	5,07	11	21	2	6	6	38,5	chlorophyll	EG_Contig11_1	type III chlorophyll a/b-binding protein [Lycoris aurea]

-19,6	4,79	24	49	3	6	6	21,7	Mitochondrial	Pooc_PC050E01_3	Mitochondrial outer membrane
-14,2	4,49	4,4	6	2	4	**5**	76,6	uncharacterized	tr|F2CYQ8|F2CYQ8_HORVD	Predicted protein
-33,4	4,53	7	9	4	5	5	63,8	Structural	tr|Q6ZFJ9|Q6ZFJ9_ORYSJ	60 kDa chaperonin beta subunit
-10,2	4,98	1,7	2	1	3	**5**	50	Glycolisis	Zoma_Contig14_1	Glyceraldehyde-3-phosphate dehydrogenase
-12,8	4,7	7,6	22	2	5	**5**	44,9	PSII	tr|H6TH78|H6TH78_9LILI	Photosystem II CP43
-25	4,77	14	16	3	5	5	41,8	Structural	sp|A2XLF2|ACT1_ORYSI	Actin-1
-13,5	4,84	10	16	2	5	5	37	Structural	Pooc_Contig338_6	20 kDa chaperonin, chloroplastic
-13,3	4,61	14	20	2	5	5	36,3	PSI	EG_Contig19_1	Oxygen-evolving enhancer protein 2, chloroplastic; photosystem II oxygen evolving complex protein 2 precursor
-8,3	4,62	7,2	8	2	5	5	32,1	Mitochondrial	Pooc_PC018F07_1	ADP,ATP carrier protein, mitochondrial
-21,7	4,76	17	25	3	5	5	22	Peroxidase	Pooc_PC040E03_2	Cationic peroxidase 1
-15,9	4,82	6,1	9	2	4	**4**	52,2	Peroxidase	Zoma_B_i12464_1	GDP-mannose 3,5-epimerase 1
-11,5	4,78	3,4	5	2	4	4	40,7	Peroxidase	EG_Contig28_2	cytosolic ascorbate peroxidase [Nicotiana tabacum]
-14,3	4,41	14	15	2	4	4	18		Pooc_B_c412_3	Basic endochitinase CHB4
-21,3	4,78	4,2	7	1	3	3	32,9	chlorophyll	Pooc_Contig35_6	Chlorophyll a-b binding protein 3
-9,3	4,72	29	68	2	3	3	16,3	chlorophyll	Zoma_C_c34012_2	Chlorophyll a-b binding protein CP29.2, chloroplastic
-14,1	4,65	2,6	3	1	3	3	0	Structural	tr|Q2QU06|Q2QU06_ORYSJ	60 kDa chaperonin alpha subunit
-64,5	5,47	0,8	1	1	3	3	0	ATP synthase	Zoma_B_i02363_1	ATP synthase CF1 alpha chain
-24,5	5,39	2,3	2	1	3	3	0	Glycolisis	tr|Q9SNK3|Q9SNK3_ORYSJ	Putative glyceraldehyde-3-phosphate dehydrogenase
-36,1	4,99	4,6	5	1	1	**3**	0	Calvin cycle	sp|P34767|RBL_ALIPL	Ribulose bisphosphate carboxylase large chain
-10,6	4,17	8,5	12	2	2	2	35,4	Mitochondrial	tr|Q94JA2|Q94JA2_ORYSJ	malate dehydrogenase
-10	4,81	2,9	3	1	2	2	0	Mitochondrial	tr|Q2THT3|Q2THT3_9LILI	Cytochrome f
-12,3	4,6	3,5	3	1	2	2	0	Glycolisis	sp|P09315|G3PA_MAIZE	Glyceraldehyde-3-phosphate dehydrogenase A, chloroplastic
-13,5	5,21	6,3	6	1	2	2	0	uncharacterized	tr|C5XIJ3|C5XIJ3_SORBI	Putative uncharacterized protein Sb03g046340
-39,1	4,92	2,6	3	1	1	**2**	0	Calvin cycle	tr|P93926|P93926_9LILI	Ribulose-1,5-bisphosphate carboxylase, large subunit
-29,3	4,48	3,2	3	1	2	2	0	Calvin cycle	Zoma_B_i13386_5	RuBisCO large subunit-binding protein subunit beta
-38,3	5,31	2,9	3	1	1	**2**	0	uncharacterized	tr|I1PWX1|I1PWX1_ORYGL	Uncharacterized protein
-9,8	4,44	1,3	2	1	1	1	91,9	Calvin cycle	Zoma_B_i14449_4	Transketolase, chloroplastic
-17,5	4,7	4,1	9	1	1	**1**	49	Calvin cycle	tr|C6G4U0|C6G4U0_9ASPA	Ribulose-1,5-bisphosphate carboxylase/oxygenase large subunit
-9,7	4,49	5,6	7	1	1	1	36,4	Glycolisis	sp|Q43247|G3PE_MAIZE	Glyceraldehyde-3-phosphate dehydrogenase, cytosolic 3

-9,4	3,94	6	9	1	1	**1**	34,9	Peroxidase	Pooc_Contig136_3	Glutathione S-transferase 6, chloroplastic
-9,4	4,4	9	11	1	1	1	24,3	Flavonoids	EG_Contig2_4	naringenin 2-oxoglutarate 3-dioxygenase [Clitoria ternatea]
-161	5,99	5,4	5	1	1	**1**	0	ATP synthase	tr|Q8WJH1|Q8WJH1_9LILI	ATP synthase subunit beta, chloroplastic
-15,7	4,46	32	32	1	1	1	0	chlorophyll	Zoma_C_c31258_4	Chlorophyll a-b binding protein 4
-10,2	4,45	7,1	7	1	1	1	0	chlorophyll	Zoma_C_c67279_1	Chlorophyll a-b binding protein 40,...
-12,6	4,26	4,4	4	1	1	1	0	uncharacterized	tr|B7ZZZ2|B7ZZZ2_MAIZE	Putative uncharacterized protein
-26,4	4,71	2,5	3	1	1	1	0	Calvin cycle	tr|Q95CF6|Q95CF6_WELCA	Ribulose 1,5-bisphosphate carboxylase large subunit
-68,5	5,58	3	3	1	1	1	0	Calvin cycle	tr|Q9MRC5|Q9MRC5_9POAL	Ribulose-bisphosphate carboxylase large subunit
-20,6	4,74	1	2	1	3	1	158	PSII	Zoma_B_i08822_2	Photosystem II CP43 chlorophyll apo...
-33,8	5,25	5,3	12	4	10	1	158	PSII	Zoma_B_i08822_2	Photosystem II CP43 chlorophyll apoprotein
-83,7	5,18	16	42	7	21	1	56	PSII	tr|H2CPH7|H2CPH7_COLES	Photosystem II CP47 chlorophyll apoprotein;
-69	5,03	16	42	7	18	1	56	PSII	tr|H2CPH7|H2CPH7_COLES	Photosystem II CP47 chlorophyll apoprotein;
-53,8	5,15	3,2	9	1	3	1	54,9	PSII	tr|H6TGJ9|H6TGJ9_9LILI	Photosystem II CP47 protein
-21,5	4,83	9,3	23	3	8	1	51,8	PSII	tr|H2CPN3|H2CPN3_COLES	Photosystem II CP43 chlorophyll apoprotein;
-22,4	4,86	6,3	15	3	7	1	51,8	PSII	tr|H2CPN3|H2CPN3_COLES	Photosystem II CP43 chlorophyll apoprotein;
-32,7	5,3	2,7	7	1	2	1	51,8	PSII	tr|H2CPN3|H2CPN3_COLES	Photosystem II CP43 chlorophyll apoprotein;
-63,2	5,37	4,5	10	2	4	1	51,4	Calvin cycle	tr|B5WX62|B5WX62_9ARAE	Ribulose-biphosphate carboxylase
-66,9	5,06	2,6	6	1	2	1	51,4	Calvin cycle	tr|B5WX89|B5WX89_9ARAE	Ribulose-biphosphate carboxylase
-9,7	4,3	4,7	7	2	3	1	49,2	Growth factor	sp|Q41803|EF1A_MAIZE	Elongation factor 1-alpha
-29,6	5,21	7,8	10	3	7	1	48,9	Glycolisis	Pooc_Contig14_2	Glyceraldehyde-3-phosphate dehydrogenase
-28,3	5,14	12	13	3	7	1	47,9	Glycolisis	tr|Q10P35|Q10P35_ORYSJ	Enolase 2, putative, expressed
-181	6,07	41	47	17	64	1	45,3	PSI	Pooc_Contig378_6	Oxygen-evolving enhancer protein 1, chloroplastic
-79,5	5,21	24	45	9	24	1	44	Calvin cycle	gi|2734972|gb|AAB93814.1|	rbcL , ribulose-1,5-bisphosphate carboxylase/oxygenase large subunit, partial (chloroplast) [Posidonia oceanica].
-69,5	5,02	24	45	8	15	1	44	Calvin cycle	gi|2734972|gb|AAB93814.1|	rbcL , ribulose-1,5-bisphosphate carboxylase/oxygenase large subunit, partial (chloroplast) [Posidonia oceanica].
-74,4	5,14	9,4	18	1	2	1	44	Calvin cycle	gi|2734972|gb|AAB93814.1|	rbcL , ribulose-1,5-bisphosphate carboxylase/oxygenase large subunit, partial (chloroplast) [Posidonia oceanica].
-29,8	4,79	14	30	4	8	1	39,6	PSII	sp|Q4FFP4|PSBD_ACOAM	Photosystem II D2 protein; PSII D2 protein; EC 1.10.3.9; Photosystem Q(A) protein;

-11,3	4,56	6,2	23	2	5	1	38,9	PSII	sp|Q3V554|PSBA_ACOCL	Photosystem Q(B) protein; EC 1.10.3.9; 32 kDa thylakoid membrane protein; Photosystem II protein D1; Flags: Precursor;
-10,1	4,27	6,2	23	2	2	1	38,9	PSII	sp|Q3V554|PSBA_ACOCL	Photosystem Q(B) protein; EC 1.10.3.9; 32 kDa thylakoid membrane protein; Photosystem II protein D1; Flags: Precursor;
-13,2	4,36	16	26	3	4	1	38,7	chlorophyll	EG_Contig99_6	chlorophyll A-B binding protein (CAB), putative [Musa acuminata]
-11	4	14	22	2	2	1	38,7	chlorophyll	EG_Contig99_6	chlorophyll A-B binding protein (CAB), putative [Musa acuminata]
-8,5	4,22	12	19	2	2	1	38,7	chlorophyll	EG_Contig99_6	chlorophyll A-B binding protein (CAB), putative [Musa acuminata]
-46,2	5,01	36	54	5	12	1	37,6	chlorophyll	EG_Contig15_1	chlorophyll A-B binding protein (CAB), putative [Musa balbisiana]
-37,2	4,99	32	49	4	10	1	37,6	chlorophyll	EG_Contig15_1	chlorophyll A-B binding protein (CAB), putative [Musa balbisiana]
-35,8	4,67	32	49	4	7	1	37,6	chlorophyll	EG_Contig15_1	chlorophyll A-B binding protein (CAB), putative [Musa balbisiana]
-24,7	5,05	22	34	3	7	1	37,6	chlorophyll	EG_Contig15_1	chlorophyll A-B binding protein (CAB), putative [Musa balbisiana]
-12,8	3,59	5,7	10	1	2	1	37	stress	Pooc_Contig281_1	Probable glutathione S-transferase
-14,5	3,72	5,7	10	1	2	1	37	stress	Pooc_Contig281_1	Probable glutathione S-transferase
-42,6	4,84	27	33	5	13	1	28,9	Alkaloids biosyn.	Pooc_Contig132_3	S-norcoclaurine synthase OS=Thalict…
-42,5	5,06	28	34	5	13	1	28,9	Alkaloids biosyn.	Pooc_Contig132_3	S-norcoclaurine synthase OS=Thalict…
-43,9	5	28	34	5	11	1	28,9	Alkaloids biosyn.	Pooc_Contig132_3	S-norcoclaurine synthase OS=Thalict…
-32,3	4,94	23	28	4	10	1	28,9	Alkaloids biosyn.	Pooc_Contig132_3	S-norcoclaurine synthase OS=Thalict…
-4,3	3,87	12	14	1	3	1	28,9	Alkaloids biosyn.	Pooc_Contig132_3	S-norcoclaurine synthase OS=Thalict…
-13,1	4,84	11	12	2	6	1	26,1	Mitochondrial	Pooc_Contig356_1	malate dehydrogenase
-12,4	4,36	12	15	2	3	1	25,1	Glycolisis	EG_Contig109_4	chloroplast glyceraldehyde-3-phosphate dehydrogenase, partial [Chlorokybus atmophyticus]
-21	4,81	21	30	3	9	1	23,9	amino acid	EG_Contig105_6	glutamine synthetase-like [Panax quinquefolius]
-98,7	5,69	2	2	1	3	1	0	ATP synthase	sp|A6MMJ2|ATPA_DIOEL	ATP synthase subunit alpha
-105	5,57	5,1	5	1	3	1	0	ATP synthase	tr|O24345|O24345_SORBI	ATP synthase subunit beta
-83,3	5,69	6,2	6	1	1	1	0	ATP synthase	tr|G1CZN3|G1CZN3_AGRST	ATP synthase subunit beta
-159	6,03	3,3	3	1	2	1	0	ATP synthase	tr|Q95FJ9|Q95FJ9_SPAAM	ATP synthase subunit beta, chloroplastic
-182	6,04	3,2	3	1	1	1	0	ATP synthase	tr|H2CPP4|H2CPP4_COLES	ATP synthase subunit beta, chloroplastic

	-174	6,01	5,6	6	1	1	1	0	ATP synthase	tr|Q8WJF3|Q8WJF3_9LILI	ATP synthase subunit beta, chloroplastic
	-163	5,99	5	5	1	1	1	0	ATP synthase	tr|H6THA8|H6THA8_9LILI	ATP synthase subunit beta, chloroplastic
	-59,4	5,19	4,2	4	1	3	1	0	ATP synthase	sp|P19023|ATPBM_MAIZE	ATP synthase subunit beta, mitochondrial
	-14,2	5,18	3	3	1	3	1	0	Mitochondrial	tr|Q8RVZ8|Q8RVZ8_WHEAT	Ferredoxin-NADP(H) oxidoreductase
	-9,9	4,5	4,7	5	1	2	1	0	Glycolisis	Zoma_ZMC13016_1	Fructose-bisphosphate aldolase, cytoplasmic isozyme
	-23,1	5,01	11	11	2	4	1	0	Glycolisis	Pooc_PC053G11_2	Glyceraldehyde-3-phosphate dehydrogenase
	-27,8	5	6,8	7	1	1	1	0	Glycolisis	tr|C9EAC1|C9EAC1_FESAR	Glyceraldehyde-3-phosphate dehydrogenase 1
	-11,4	4,84	7,1	7	1	1	1	0	Glycolisis	tr|C9EAC2|C9EAC2_FESAR	Glyceraldehyde-3-phosphate dehydrogenase 2
	-38,7	5,28	3,5	4	1	2	1	0	Mitochondrial	tr|Q1ENY9|Q1ENY9_MUSAC	Phosphoglycerate kinase
	-18,2	5,07	1,7	2	1	2	1	0	Mitochondrial	Zoma_B_i10270_3	Phosphoglycerate kinase
	-19	4,73	2,7	3	1	1	1	0	PSII	sp|A6MMK6|PSAB_DIOEL	Photosystem I P700 chlorophyll a apoprotein A2
	-56,1	5,27	1,8	2	1	3	1	0	PSII	tr|H2CPH7|H2CPH7_COLES	Photosystem II CP47 chlorophyll apoprotein;
	-61,3	5,06	4	4	1	3	1	0	PSII	tr|A0ARD7|A0ARD7_SMIRO	Photosystem II CP47 chlorophyll apoprotein; Flags: Fragment;
	-66	5,04	3,2	3	1	3	1	0	PSII	tr|H6TGJ9|H6TGJ9_9LILI	Photosystem II CP47 protein
	-61,2	5,37	3,2	3	1	3	1	0	PSII	tr|H6TGJ9|H6TGJ9_9LILI	Photosystem II CP47 protein
	-67,2	5,63	3,2	3	1	1	1	0	uncharacterized	tr|F2D714|F2D714_HORVD	Predicted protein
	-23,9	4,65	4,6	5	1	1	1	0	Calvin cycle	sp|P34767|RBL_ALIPL	Ribulose bisphosphate carboxylase large chain
	-71,6	5,58	4,6	5	1	1	1	0	Calvin cycle	sp|P34767|RBL_ALIPL	Ribulose bisphosphate carboxylase large chain
	-38,1	5,28	2,2	2	1	1	1	0	Calvin cycle	tr|H6THE9|H6THE9_9LILI	Ribulose-1,5-bisphosphate carboxylase, large subunit
	-65,8	5,2	4,5	5	2	4	1	0	Calvin cycle	tr|B5WX62|B5WX62_9ARAE	Ribulose-biphosphate carboxylase
	-115	5,98	2,2	2	1	4	1	0	Calvin cycle	tr|B5WX62|B5WX62_9ARAE	Ribulose-biphosphate carboxylase
	-63,6	5,28	2,2	2	1	3	1	0	Calvin cycle	tr|B5WX64|B5WX64_9ARAE	Ribulose-biphosphate carboxylase
	-128	5,93	2,6	3	1	2	1	0	Calvin cycle	tr|B5WX89|B5WX89_9ARAE	Ribulose-biphosphate carboxylase
	-9,6	4,43	2,8	3	1	1	1	0	uncharacterized	tr|I1QF81|I1QF81_ORYGL	Uncharacterized protein
						###	##				
13:00 am, 3 m depth	log(e)	log(I)	% (measured)	% (corrected)	unique	total parz	**total**	Mr	metabolism	Accession	Description
	-72,6	5,27	36	43	7	21	21	29	aldolase	Pooc_Contig48_2	OSIGBa0142I02-OSIGBa0101B20.20 [Oryza sativa Indica Group] >gb|EAZ31829.1|
	-87,9	5,38	48	57	9	24	24	28,9	Alkaloids biosyn.	Pooc_Contig132_3	S-norcoclaurine synthase OS=Thalict…
	-40,6	5,19	26	39	5	16	16	23,1	amino acid biosyn	Pooc_PC028C07_2	Peptidyl-prolyl cis-trans isomerase

-16,5	4,71	4,2	6	3	6	**7**	83,7	amino acid biosyn	tr|Q8W0Q7|Q8W0Q7_SORBI	Methionine synthase protein;
-5,5	4,74	13	23	2	5	**5**	33	amino acid biosyn	Pooc_Contig291_3	Glutamine synthetase root isozyme 4
-16	4,04	7,6	14	1	1	1	18,3	amino acid biosyn	sp|P21569|CYPH_MAIZE	Peptidyl-prolyl cis-trans isomerase
-131	5,68	26	46	13	40	40	55,4	ATP synthase	tr|F8RS98|F8RS98_KINAU	ATP synthase subunit alpha; Flags: Fragment;
-47,5	4,87	15	19	5	10	**42**	53,7	ATP synthase	tr|Q4FGI4|Q4FGI4_TYPLA	ATP synthase subunit beta
-209	5,88	53	69	17	51	51	51,5	ATP synthase	tr|G8A3N5|G8A3N5_9LILI	ATP synthase subunit beta
-28,6	4,51	12	20	4	8	**16**	55,3	ATP synthase	tr|H2F4C9|H2F4C9_9ASPA	ATP synthase subunit alpha, chloroplastic
-10,9	4,55	2,9	5	2	4	**4**	104	ATP synthase	tr|Q43275|Q43275_ZOSMR	Putative plasma membrane H+-ATPase
-94,8	5,38	0,8	1	1	3	3	0	ATP synthase	Zoma_B_i02363_1	ATP synthase CF1 alpha chain [Phoenix dactylifera]
-5,3	3,64	11	17	1	1	1	14,5	ATP synthase	tr|G1C6C0|G1C6C0_9LILI	ATP synthase epsilon chain, chloroplastic
-121	5,52	18	41	13	31	**63**	51,4	Calvin cycle	tr|B5WX89|B5WX89_9ARAE	Ribulose-biphosphate carboxylase
-54,5	5,52	21	27	6	23	**26**	33,7	Calvin cycle	EG_Contig1_1...	chloroplast ribulose-1,5-bisphosphate carboxylase/oxygenase small subunit
-171	5,84	41	77	17	51	**74**	44	Calvin cycle	gi|2734972|gb|AAB93814.1|	rbcL , ribulose-1,5-bisphosphate carboxylase/oxygenase large subunit, partial (chloroplast) [Posidonia oceanica].
-35,3	4,73	5,5	6	3	8	**21**	0	Calvin cycle	Zoma_B_i13574_3	RuBisCO large subunit-binding protein subunit alpha, chloroplastic
-35,5	4,93	12	16	3	7	**7**	46,3	Calvin cycle	Zoma_Contig910_2	Ribulose bisphosphate carboxylase/oxygenase activase 2, chloroplastic
-9,6	4,3	4,1	9	1	1	**5**	49	Calvin cycle	tr|C6G4U0|C6G4U0_9ASPA	Ribulose-1,5-bisphosphate carboxylase/oxygenase large subunit
-8,9	4,52	11	12	2	4	4	26,1	Calvin cycle	Pooc_Contig356_1	malate dehydrogenase
-8,3	4,76	58	58	1	4	4	3,1	Calvin cycle	sp|P84209|MDHM_IMPCY	Malate dehydrogenase, mitochondrial
-32	4,76	4,6	11	1	2	**3**	43,9	Calvin cycle	sp|P34767|RBL_ALIPL	Ribulose bisphosphate carboxylase large chain
-55,7	5,61	1,5	1	1	2	**3**	0	Calvin cycle	tr|Q9BA33|Q9BA33_BALSE	Ribulose bisphosphate carboxylase large subunit
-6,3	4,38	2,8	4	1	3	3	50,7	Calvin cycle	Pooc_Contig131_4	Sedoheptulose-1,7-bisphosphatase, chloroplastic
-12,5	4,53	1,3	2	1	3	3	91,9	Calvin cycle	Zoma_B_i14449_4	Transketolase, chloroplastic
-9	4,52	7,4	12	1	1	**1**	27,7	Calvin cycle	tr|Q6J4N8|Q6J4N8_9ARAE	Putative RuBisCo activase protein
-73,9	5,84	2,2	2	1	1	1	0	Calvin cycle	Zoma_C_c22377_6	Ribulose bisphosphate carboxylase large chain
-65,6	5,67	9	9	1	1	1	0	Calvin cycle	tr|E0D9P3|E0D9P3_9LILI	Ribulose bisphosphate carboxylase large chain
-72,4	5,68	8,3	8	1	1	1	0	Calvin cycle	sp|P93936|RBL_WATAN	Ribulose bisphosphate carboxylase large chain; RuBisCO large subunit; EC 4.1.1.39; Flags: Fragment;
-95,9	5,49	42	64	9	26	**93**	37,6	chlorophyll	EG_Contig15_1	chlorophyll A-B binding protein (CAB), putative [Musa balbisiana]

-80,7	5,29	36	59	6	19	**39**	38,7	chlorophyll	EG_Contig99_6	chlorophyll A-B binding protein (CAB), putative [Musa acuminata]
-53	5,4	20	30	5	17	17	40,3	chlorophyll	EG_Contig27_6	chlorophyll A/B binding protein, putative [Ricinus communis] >gb|EEF42554.1| chlorophyll A/B binding protein, putative [Ricinus communis]
-28,6	4,67	12	12	2	4	**9**	0	chlorophyll	Pooc_Contig35_6	Chlorophyll a-b binding protein 13
-25,5	5,06	44	53	3	7	**7**	11,1	chlorophyll	Pooc_B_c272_6	Chlorophyll a-b binding protein CP29.1, chloroplastic
-9,2	3,92	6,8	10	1	2	2	21,8	chlorophyll	Pooc_B_c343_6	Magnesium-protoporphyrin IX monomethyl ester [oxidative] cyclase, chloroplastic
-46,6	5,27	4,6	5	1	1	**1**	0	chlorophyll	Pooc_Contig92_3	Chlorophyll a-b binding protein 40, chloroplastprecursor
-42,1	5,13	16	20	5	12	**22**	36,7	Glycolisis	tr|Q7FAH2|Q7FAH2_ORYSJ	Glyceraldehyde-3-phosphate dehydrogenase
-24,1	4,51	23	27	3	6	**14**	18,6	Glycolisis	tr|A4ZGB6|A4ZGB6_AGATE	Chloroplast glyceraldehyde-3-phosphate dehydrogenase B subunit
-74,9	5,38	7,6	8	3	7	**13**	0	Glycolisis	Zoma_B_i11172_5	Glyceraldehyde-3-phosphate dehydrogenase A, chloroplastic
-21,1	5,24	6	9	2	7	**13**	49	Glycolisis	Pooc_Contig14_1	Glyceraldehyde-3-phosphate dehydrogenase, cytosolic
-36,6	5,2	10	12	4	11	**13**	61,2	Glycolisis	Zoma_B_i13503_1	Phosphoglycerate kinase
-45,2	5,02	26	31	5	10	10	27,8	Glycolisis	Pooc_Contig109_2	Triosephosphate isomerase, cytosolic
-8,4	4,2	7	7	1	1	**9**	0	Glycolisis	tr|B4FTI5|B4FTI5_MAIZE	Fructose-bisphosphate aldolase
-13,3	4,54	12	15	2	6	**6**	25,1	Glycolisis	EG_Contig109_4	chloroplast glyceraldehyde-3-phosphate dehydrogenase, partial [Chlorokybus atmophyticus]
-42,5	5,23	5,4	5	2	3	**3**	0	Glycolisis	tr|Q9SNK3|Q9SNK3_ORYSJ	Glyceraldehyde-3-phosphate dehydrogenase B, chloroplast, putative, expressed
-76,5	5,49	5,4	5	1	2	**2**	0	Glycolisis	tr|H9B8E3|H9B8E3_MISSI	Glyceraldehyde-3-phosphate dehydrogenase-like protein
-15,1	4,58	6,2	6	1	1	1	0	Glycolisis	Zoma_B_i12119_2	hypothetical protein SORBIDRAFT_03g006130 [Sorghum bicolor] >gb|EES00320.1|
-29,3	5,02	14	25	4	13	13	24,7	Histone	Pooc_PC006G03_2	Histone H4
-22,9	5,11	22	38	3	12	12	16,6	Histone	tr|Q43724|Q43724_ASPOF	Histone H2B
-5,7	5,16	11	15	1	5	**5**	22,4	Histone	Pooc_PC008D12_1	PREDICTED: probable histone H2A.4 isoform 2 [Vitis vinifera]
-10,4	4,41	21	26	2	3	3	20,8	Histone	Zoma_Contig291_1	Histone H3.2
-21,4	4,9	6,2	10	1	2	2	25	Histone	Zoma_B_i11555_5	Histone H2B

-9,8	4,17	23	32	1	1	1	15,3	Histone	tr|F2CZQ5|F2CZQ5_HORVD	Histone H3
-12	4,73	3,4	5	2	5	**9**	80,1	HSP	sp|A2YWQ1|HSP81_ORYSI	Heat shock protein 81-1
-11,7	4,42	3,7	6	2	4	4	74	HSP	tr|Q2QV45|Q2QV45_ORYSJ	70 kDa heat shock protein
-9	4,15	4,5	6	2	3	**3**	70,5	HSP	sp|P11143|HSP70_MAIZE	Heat shock 70 kDa protein
-89,4	5,2	18	24	8	21	**21**	72,4	Mitochondrial	Zoma_B_i13224_2	ATP synthase subunit beta, mitochondrial
-19,4	4,34	7,2	9	3	5	**20**	59,1	Mitochondrial	sp|P19023|ATPBM_MAIZE	ATP synthase subunit beta, mitochondrial
-19,6	4,82	4,5	7	2	5	**14**	88,2	Mitochondrial	Zoma_C_c61233_6	ATP synthase subunit alpha mitochondrial
-24,2	4,82	12	16	3	8	8	35,2	Mitochondrial	sp|A6MMM0|CYF_DIOEL	Apocytochrome f
-12,7	4,47	15	25	2	4	**8**	24,2	Mitochondrial	sp|P05642|CYB6_MAIZE	Cytochrome b6
-19,2	4,62	12	16	3	6	**6**	25,1	Mitochondrial	tr|A8Y801|A8Y801_ZANAE	Cytochrome b6-f complex iron-sulfur subunit
-22,4	4,97	9,6	13	3	4	**6**	56,4	Mitochondrial	Zoma_B_i02521_4	Ferredoxin--NADP reductase, chloroplastic
-11,7	3,56	5,7	10	1	2	**10**	37	Peroxidase	Pooc_Contig281_1	Probable glutathione S-transferase
-5,6	4,49	5,3	6	1	3	3	26	Peroxidase	EG_Contig58_5	2-cys peroxiredoxin [Vigna radiata]
-7,7	4,25	6,3	9	1	3	3	31,4	Peroxidase	Pooc_Contig160_2	Peroxiredoxin-2B
-9,9	4,19	6	9	1	2	**2**	34,9	Peroxidase	Pooc_Contig136_3	Glutathione S-transferase 6, chloroplastic
-159	5,88	39	44	15	47	47	45,3	PS I	Pooc_Contig378_6	Oxygen-evolving enhancer protein 1
-50,4	5,19	27	52	6	18	18	29,4	PSI	Pooc_Contig240_3	Photosystem I reaction center subunit IV B, chloroplastic
-26,3	5,24	1,4	2	4	10	10	212	PSI	Zoma_B_i00191_2	photosystem I P700 chlorophyll A apoprotein A1 [Oryza sativa Indica Group]
-19,3	4,55	6,5	21	3	5	**9**	82,4	PSI	sp|A6MMK6|PSAB_DIOEL	Photosystem I P700 chlorophyll a apoprotein A2
-15,5	4,79	22	27	3	7	7	17,3	PSI	Pooc_Contig327_5	Photosystem I
-12,1	4,29	12	14	2	3	**3**	22	PSI	tr|Q84PB4|Q84PB4_ORYSJ	Chloroplast photosystem I reaction center subunit II-like protein
-68,3	5,23	16	44	7	14	**35**	54,9	PSII	tr|H6TGJ9|H6TGJ9_9LILI	Photosystem II CP47 protein
-45,7	5,4	16	39	5	19	**47**	51,8	PSII	tr|H2CPN3|H2CPN3_COLES	Photosystem II CP43 chlorophyll apoprotein;
-82,2	5,45	18	49	7	26	**45**	54,6	PSII	tr|A0ARD7|A0ARD7_SMIRO	Photosystem II CP47 chlorophyll apoprotein; Flags: Fragment;
-103	5,5	41	58	10	27	**30**	36,3	PSII	EG_Contig19_1	Oxygen-evolving enhancer protein 2, chloroplastic; photosystem II;
-75,3	5,3	25	52	7	18	**24**	39,6	PSII	sp|Q4FFP4|PSBD_ACOAM	Photosystem II D2 protein; PSII D2 protein; EC 1.10.3.9; Photosystem Q(A) protein;
-29,2	5,23	14	53	4	14	**18**	38,9	PSII	sp|Q3V554|PSBA_ACOCL	Photosystem Q(B) protein; EC 1.10.3.9; 32 kDa thylakoid membrane protein; Photosystem II protein D1; Flags: Precursor;

-35,3	4,84	5,3	12	4	10	**16**	158	PSII	Zoma_B_i08822_2	Photosystem II CP43 chlorophyll apoprotein
-39,2	4,96	21	35	4	12	12	30	PSII	Pooc_Contig333_3	Photosystem II 22 kDa protein, chloroplastic
-15,2	4,66	7,6	22	2	4	**6**	44,9	PSII	tr|H6TH78|H6TH78_9LILI	Photosystem II CP43
-12,9	4,42	5,7	7	2	7	**7**	93,9	Growth factor	tr|Q7XTK1|Q7XTK1_ORYSJ	Elongation factor
-5,8	4,2	6,1	8	1	3	3	30,6	stress	Pooc_Contig24_1	Universal stress protein A-like protein
-27,2	4,96	9,6	13	3	8	8	29,3	structural	Pooc_Contig341_3	60S ribosomal protein L35a-3
-16,6	4,89	14	21	3	8	**8**	37	Structural	Pooc_Contig338_6	PREDICTED: 20 kDa chaperonin, chloroplastic [Vitis vinifera]
-6,3	4,5	13	16	1	3	3	23,4	Structural	Pooc_PC039H04_3	Actin
-5,6	4,6	1,8	2	1	3	**3**	92,5	Growth factor	Zoma_B_i05359_2	Elongation factor TuB, chloroplastic
-7,6	4,02	7,6	20	1	1	**1**	33,5	Growth factor	Pooc_Contig188_1	Elongation factor 1-alpha
-80	5,49	17	26	7	20	**20**	42,7	uncharacterized	tr|F2D714|F2D714_HORVD	Predicted protein
-23	4,65	8,8	12	4	7	**11**	84,6	uncharacterized	tr|B8A1R8|B8A1R8_MAIZE	Putative uncharacterized protein
-32,6	4,74	34	76	4	10	**10**	22,3	uncharacterized	Pooc_Contig227_2	PREDICTED: uncharacterized protein LOC100262861 [Vitis vinifera]
-35,9	4,86	20	28	4	10	10	31	uncharacterized	EG_Contig45_6	uncharacterized protein LOC100808269
-26,2	4,76	5,9	9	3	8	**9**	76,6	uncharacterized	tr|F2CYQ8|F2CYQ8_HORVD	Predicted protein
-38,4	4,7	9,3	12	4	7	7	61	uncharacterized	tr|I1IW31|I1IW31_BRADI	Uncharacterized protein
-28,2	4,94	22	30	3	7	7	22,3	uncharacterized	EG_Contig71_4	unknown
-20	4,43	20	22	3	5	**5**	31,3	uncharacterized	EG_Contig98_4	conserved hypothetical protein [Ricinus communis] >gb|EEF43081.1|
-16,2	4,52	12	22	2	5	5	26,3	uncharacterized	Pooc_Contig308_2	unnamed protein product [Vitis vinifera]
-5,1	4,52	4,2	14	1	3	**3**	27,5	uncharacterized	Pooc_Contig217_2	PREDICTED: uncharacterized protein LOC100250168 [Vitis vinifera]
-6,5	4,08	4,7	5	1	3	3	39,7	uncharacterized	tr|I1I6Q9|I1I6Q9_BRADI	Uncharacterized protein
-16,1	4,38	13	21	1	1	**2**	28,1	uncharacterized	tr|F2E9F1|F2E9F1_HORVD	Predicted protein
-6,8	4,3	6,4	10	1	2	2	18,2	uncharacterized	tr|I1HWJ6|I1HWJ6_BRADI	Uncharacterized protein
-4,3	4,35	5,9	7	1	2	2	27,3	uncharacterized	Pooc_Contig88_5	Uncharacterized protein At4g01150, chloroplastic
-24,8	5,02	2,9	3	1	1	1	0	uncharacterized	tr|I1PWX1|I1PWX1_ORYGL	Uncharacterized protein
-7,3	4,27	5,8	9	2	2	2	45,2	vitamin	Zoma_Contig561_2	Thiazole biosynthetic enzyme, chloroplastic
-19,8	4,65	12	19	3	5	5	33	Flavonoids	Pooc_Contig89_5	Chalcone--flavonone isomerase
-13,6	4,7	4,4	8	1	3	1	38,5	Chlorophyll	EG_Contig11_1	type III chlorophyll a/b-binding protein [Lycoris aurea]
-28	4,58	8,3	15	3	3	1	55,1	ATP synthase	sp|A6MMJ2|ATPA_DIOEL	ATP synthase subunit alpha, chloroplastic
-23,7	4,75	3	3	1	3	1	0	ATP synthase	tr|H2F4D6|H2F4D6_9ASPA	ATP synthase subunit alpha, chloroplastic

-123	5,64	3	3	1	2	1	0	ATP synthase	tr|H2F4D9|H2F4D9_EUCGA	ATP synthase subunit alpha, chloroplastic
-44,9	5,05	7,4	12	4	9	1	88,2	Mitochondrial	Zoma_C_c61233_6	ATP synthase subunit alpha, mitochondrial
-12,6	4,06	2,8	3	1	1	1	0	ATP synthase	tr|H6SWX7|H6SWX7_9LILI	ATP synthase subunit beta
-34,8	4,76	3,2	3	1	1	1	0	ATP synthase	tr|Q4FGI4|Q4FGI4_TYPLA	ATP synthase subunit beta
-32,9	4,75	5	5	1	1	1	0	ATP synthase	tr|Q8WJG3|Q8WJG3_TACCH	ATP synthase subunit beta
-112	5,67	5	5	1	1	1	0	ATP synthase	tr|Q8WJG3|Q8WJG3_TACCH	ATP synthase subunit beta
-75,9	5,54	6,2	6	1	1	1	0	ATP synthase	tr|G1CZN3|G1CZN3_AGRST	ATP synthase subunit beta
-43,2	4,83	14	17	5	11	1	53,6	ATP synthase	tr|H2CPP4|H2CPP4_COLES	ATP synthase subunit beta, chloroplastic
-43	4,5	14	18	5	8	1	53,6	ATP synthase	sp|Q3V527|ATPB_ACOCL	ATP synthase subunit beta, chloroplastic
-189	5,89	4,2	4	1	4	1	0	ATP synthase	tr|H2CPP4|H2CPP4_COLES	ATP synthase subunit beta, chloroplastic
-175	5,86	5,6	6	1	2	1	0	ATP synthase	tr|Q8WJF3|Q8WJF3_9LILI	ATP synthase subunit beta, chloroplastic
-176	5,82	3,2	3	1	1	1	0	ATP synthase	tr|Q9BA75|Q9BA75_9LILI	ATP synthase subunit beta, chloroplastic
-169	5,84	4,3	4	1	1	1	0	ATP synthase	tr|Q9MTV4|Q9MTV4_9LILI	ATP synthase subunit beta, chloroplastic
-18	4,27	9	12	3	5	1	59,1	ATP synthase	sp|P19023|ATPBM_MAIZE	ATP synthase subunit beta, mitochondrial
-16,4	4,45	6,9	9	2	4	1	59,1	ATP synthase	sp|P19023|ATPBM_MAIZE	ATP synthase subunit beta, mitochondrial
-86	5,23	4,2	4	1	3	1	0	ATP synthase	sp|P19023|ATPBM_MAIZE	ATP synthase subunit beta, mitochondrial
-36,1	4,99	9	9	1	3	1	0	ATP synthase	Zoma_B_i12543_2	ATP synthase subunit beta, mitochondrial
-11,9	4,64	14	22	2	5	1	38,7	Chlorophyll	EG_Contig99_6	chlorophyll A-B binding protein (CAB), putative [Musa acuminata]
-9,7	4,35	14	22	2	4	1	38,7	Chlorophyll	EG_Contig99_6	chlorophyll A-B binding protein (CAB), putative [Musa acuminata]
-11,2	4,25	14	22	2	4	1	38,7	Chlorophyll	EG_Contig99_6	chlorophyll A-B binding protein (CAB), putative [Musa acuminata]
-12,9	4,69	6,9	11	2	4	1	38,7	Chlorophyll	EG_Contig99_6	chlorophyll A-B binding protein (CAB), putative [Musa acuminata]
-54,8	5,24	35	53	5	17	1	37,6	Chlorophyll	EG_Contig15_1	chlorophyll A-B binding protein (CAB), putative [Musa balbisiana]
-53,8	5,26	36	55	5	15	1	37,6	Chlorophyll	EG_Contig15_1	chlorophyll A-B binding protein (CAB), putative [Musa balbisiana]
-48,4	5,21	35	53	5	13	1	37,6	Chlorophyll	EG_Contig15_1	chlorophyll A-B binding protein (CAB), putative [Musa balbisiana]
-40,9	5,15	22	34	4	11	1	37,6	Chlorophyll	EG_Contig15_1	chlorophyll A-B binding protein (CAB), putative [Musa balbisiana]
-46,2	4,97	32	49	4	11	1	37,6	Chlorophyll	EG_Contig15_1	chlorophyll A-B binding protein (CAB), putative [Musa balbisiana]
-12,9	4,66	12	19	2	5	1	32,9	chlorophyll	Pooc_Contig35_6	Chlorophyll a-b binding protein 13, chloplastic
-22,2	4,84	15	17	2	5	1	18,6	Calvinin cycle	tr|A4ZGB6|A4ZGB6_AGATE	Chloroplast glyceraldehyde-3-phosphate dehydrogenase B subunit

-35,1	5,24	16	18	2	3	1	18,6	Calvinin cycle	tr|A4ZGB6|A4ZGB6_AGATE	Chloroplast glyceraldehyde-3-phosphate dehydrogenase B subunit
-7,7	4,29	8,9	11	2	3	1	33,7	Calvinin cycle	EG_Contig1_1...	chloroplast ribulose-1,5-bisphosphate carboxylase/oxygenase small subunit
-6,2	4,5	9,3	15	1	4	1	24,2	Mitochondrial	sp|P05642|CYB6_MAIZE	Cytochrome b6
-10,1	4,9	3	3	1	2	1	0	Mitochondrial	tr|Q8RVZ8|Q8RVZ8_WHEAT	Ferredoxin-NADP(H) oxidoreductase
-18,7	4,76	26	30	3	7	1	23,5	Glycolisis	Pooc_PC035C04_2	Fructose-bisphosphate aldolase, chloroplastic
-10,6	4,34	7	7	1	1	1	0	Glycolisis	sp|Q40677|ALFC_ORYSJ	Fructose-bisphosphate aldolase, chloroplastic
-32,2	5,1	11	11	3	7	1	0	Glycolisis	Pooc_PC053G11_2	Glyceraldehyde-3-phosphate dehydrogenase
-34,7	5,23	5,4	5	1	3	1	0	Glycolisis	tr|Q5PY03|Q5PY03_MUSAC	Glyceraldehyde-3-phosphate dehydrogenase
-23,1	4,82	10	15	3	6	1	42,8	Glycolisis	sp|P09315|G3PA_MAIZE	Glyceraldehyde-3-phosphate dehydrogenase A, chloroplastic
-41,2	5,33	5,3	5	2	4	1	0	Glycolisis	Pooc_Contig14_2	Glyceraldehyde-3-phosphate dehydrogenase, cytosolic
-32	5,25	1,7	2	1	2	1	0	Glycolisis	Zoma_Contig14_1	Glyceraldehyde-3-phosphate dehydrogenase, cytosolic
-12,1	4,39	3,4	5	2	4	1	80,1	HSP	sp|A2YWQ1|HSP81_ORYSI	Heat shock protein 81-1
-21,9	4,61	1,2	1	1	1	1	0	amino acid biosyn	tr|Q8W0Q7|Q8W0Q7_SORBI	Methionine synthase protein;
-21,5	4,99	3,5	4	1	2	1	0	Glycolisis	tr|Q1ENY9|Q1ENY9_MUSAC	Phosphoglycerate kinase
-12,8	4,2	3,8	12	2	4	1	82,2	PSI	sp|Q3V535|PSAB_ACOCL	Photosystem I P700 chlorophyll a apoprotein A2
-13,9	4,63	3,1	3	1	2	1	0	PSII	tr|H6TH58|H6TH58_9LILI	Photosystem II CP43
-43,9	5,31	1	2	1	3	1	158	PSII	Zoma_B_i08822_2	Photosystem II CP43 chlorophyll apoprotein
-23,9	5,03	1	2	1	3	1	158	PSII	Zoma_B_i08822_2	Photosystem II CP43 chlorophyll apoprotein
-22,7	5,3	9,3	23	3	11	1	51,8	PSII	tr|H2CPN3|H2CPN3_COLES	Photosystem II CP43 chlorophyll apoprotein;
-24,4	5,13	9,3	23	3	9	1	51,8	PSII	tr|H2CPN3|H2CPN3_COLES	Photosystem II CP43 chlorophyll apoprotein;
-34,9	4,88	2,7	3	1	3	1	0	PSII	tr|H2CPN3|H2CPN3_COLES	Photosystem II CP43 chlorophyll apoprotein;
-80,7	5,37	3,7	4	2	4	1	0	PSII	tr|H2CPH7|H2CPH7_COLES	Photosystem II CP47 chlorophyll apoprotein;
-47,8	4,93	1,8	2	1	1	1	0	PSII	tr|H2CPH7|H2CPH7_COLES	Photosystem II CP47 chlorophyll apoprotein;
-58,5	5,01	12	34	5	14	1	54,6	PSII	tr|A0ARD7|A0ARD7_SMIRO	Photosystem II CP47 chlorophyll apoprotein; Flags: Fragment;
-50,5	5,06	4	4	1	3	1	0	PSII	tr|A0ARD8|A0ARD8_9LILI	Photosystem II CP47 chlorophyll apoprotein; Flags: Fragment;
-65,7	5,2	4	4	1	2	1	0	PSII	tr|A0ARD7|A0ARD7_SMIRO	Photosystem II CP47 chlorophyll apoprotein; Flags: Fragment;
-55,8	4,99	12	33	5	13	1	54,9	PSII	tr|H6TGJ9|H6TGJ9_9LILI	Photosystem II CP47 protein
-78,4	5,39	3,2	3	1	3	1	0	PSII	tr|H6TGJ9|H6TGJ9_9LILI	Photosystem II CP47 protein

-53	4,94	3,2	3	1	3	1	0	PSII	tr|H6TGJ9|H6TGJ9_9LILI	Photosystem II CP47 protein
-60,8	5,13	1,8	2	1	2	1	0	PSII	tr|H6TGL1|H6TGL1_9LILI	Photosystem II CP47 protein
-22,6	4,44	12	25	3	4	1	39,6	PSII	sp|Q4FFP4|PSBD_ACOAM	Photosystem II D2 protein; PSII D2 protein; EC 1.10.3.9; Photosystem Q(A) protein;
-10,4	4	7,1	15	2	2	1	39,6	PSII	sp|Q4FFP4|PSBD_ACOAM	Photosystem II D2 protein; PSII D2 protein; EC 1.10.3.9; Photosystem Q(A) protein;
-8,9	4,44	6,2	23	2	4	1	38,9	PSII	sp|Q3V554|PSBA_ACOCL	Photosystem Q(B) protein; EC 1.10.3.9; 32 kDa thylakoid membrane protein; Photosystem II protein D1; Flags: Precursor;
-10,7	4,14	2,8	4	1	1	1	76,6	uncharacterized	tr|F2CYQ8|F2CYQ8_HORVD	Predicted protein
-24,7	4,58	13	13	1	1	1	0	uncharacterized	tr|F2E9F1|F2E9F1_HORVD	Predicted protein
-16,5	4,69	10	18	2	8	1	37		Pooc_Contig281_1	Probable glutathione S-transferase GSTU6
-18,2	4,53	7,8	8	2	3	1	0	uncharacterized	tr|B7ZZZ2|B7ZZZ2_MAIZE	Putative uncharacterized protein
-20,7	4,59	1,3	1	1	1	1	0	uncharacterized	tr|B8AR75|B8AR75_ORYSI	Putative uncharacterized protein
-78,3	5,04	24	45	10	20	1	44	Calvinin cycle	gi|2734972|gb|AAB93814.1|	rbcL , ribulose-1,5-bisphosphate carboxylase/oxygenase large subunit, partial (chloroplast) [Posidonia oceanica].
-32,6	4,82	9,4	18	1	2	1	44	Calvinin cycle	gi|2734972|gb|AAB93814.1|	rbcL , ribulose-1,5-bisphosphate carboxylase/oxygenase large subunit, partial (chloroplast) [Posidonia oceanica].
-118	5,5	9,4	9	1	1	1	0	Calvinin cycle	gi|2734972|gb|AAB93814.1|	rbcL , ribulose-1,5-bisphosphate carboxylase/oxygenase large subunit, partial (chloroplast) [Posidonia oceanica].
-9,9	4,13	14	20	2	3	1	36,3	PSII	EG_Contig19_1	Oxygen-evolving enhancer protein 2, chloroplastic , photosystem II oxygen evolving complex protein 2 precursor
-74,8	5,49	2,5	3	1	1	1	0	Calvinin cycle	sp|P34767|RBL_ALIPL	Ribulose bisphosphate carboxylase large chain
-40,2	4,84	1,5	1	1	1	1	0	Calvinin cycle	tr|Q9BA33|Q9BA33_BALSE	Ribulose bisphosphate carboxylase large subunit
-22	4,44	8,1	8	1	1	1	0	Calvinin cycle	tr|B0B774|B0B774_9POAL	Ribulose-1,5-bisphosphate carboxylase/oxygenase large subunit
-78,6	5,52	3,9	4	1	1	1	0	Calvinin cycle	tr|B5SW32|B5SW32_9POAL	Ribulose-1,5-bisphosphate carboxylase/oxygenase large subunit
-49,7	5,38	3,6	4	1	1	1	0	Calvinin cycle	tr|E5G0I3|E5G0I3_9ASPA	Ribulose-1,5-bisphosphate carboxylase/oxygenase large subunit
-47,6	5,36	3,6	4	1	1	1	0	Calvinin cycle	tr|Q6VW18|Q6VW18_9ASPA	Ribulose-1,5-bisphosphate carboxylase/oxygenase large subunit

	-42,4	5	11	24	5	11	1	51,4	Calvinin cycle	tr|B5WX62|B5WX62_9ARAE	Ribulose-biphosphate carboxylase
	-121	5,58	4,5	5	2	5	1	0	Calvinin cycle	tr|B5WX62|B5WX62_9ARAE	Ribulose-biphosphate carboxylase
	-34	4,95	3	3	1	4	1	0	Calvinin cycle	tr|B5WX64|B5WX64_9ARAE	Ribulose-biphosphate carboxylase
	-77,4	5,04	2,6	6	1	3	1	51,4	Calvinin cycle	tr|B5WX89|B5WX89_9ARAE	Ribulose-biphosphate carboxylase
	-68,2	5,07	2,2	2	1	3	1	0	Calvinin cycle	tr|B5WX62|B5WX62_9ARAE	Ribulose-biphosphate carboxylase
	-145	5,87	2,6	3	1	3	1	0	Calvinin cycle	tr|B5WX89|B5WX89_9ARAE	Ribulose-biphosphate carboxylase
	-123	5,94	2,2	2	1	3	1	0	Calvinin cycle	tr|B5WX62|B5WX62_9ARAE	Ribulose-biphosphate carboxylase
	-55,8	4,79	14	19	7	13	1	77,6	Calvinin cycle	Zoma_B_i13386_5	RuBisCO large subunit-binding protein subunit beta, chloroplastic
						###	##				
13:00 h, 20 m depth	log(e)	log(I)	% (measured)	% (corrected)	unique	total parz	**total**	Mr	metabolism	Accession	Description
	-111	5,81	51	60	11	55		29	Aldolase	Pooc_Contig48_2	OSIGBa0142I02-OSIGBa0101B20.20 [Oryza sativa Indica Group] >gb|EAZ31829.1|
	-111	5,54	45	54	10	38		28,9	Alkaloids	Pooc_Contig132_3	S-norcoclaurine synthase OS=Thalict…
	-10,5	4,19	10	12	2	4		28,9	Alkaloids	Pooc_Contig132_3	S-norcoclaurine synthase OS=Thalict…
	-6,2	3,91	12	14	1	1		28,9	Alkaloids	Pooc_Contig132_3	S-norcoclaurine synthase OS=Thalict…
	-46,7	5,18	12	17	6	16		84,4	aminoacid biosyn	tr|B6UF55|B6UF55_MAIZE	5-methyltetrahydropteroyltriglutamate--homocysteine methyltransferase
	-35,1	5,02	2,3	2	1	1		0	aminoacid biosyn	Zoma_B_i01703_4	5-methyltetrahydropteroyltriglutamate--homocysteine methyltransferase
	-18,5	4,65	5,3	7	4	7		83,7	aminoacid biosyn	tr|Q8W0Q7|Q8W0Q7_SORBI	Methionine synthase protein;
	-46,5	5,14	1,2	1	1	2		0	aminoacid biosyn	tr|Q8W0Q7|Q8W0Q7_SORBI	Methionine synthase protein;
	-18,3	4,1	3,3	5	1	3		63,9	aminoacid biosyn	tr|Q7XMP6|Q7XMP6_ORYSJ	OSJNBb0059K02.15 protein
	-44,3	5,06	27	40	5	14		23,1	aminoacid biosyn	Pooc_PC028C07_2	Peptidyl-prolyl cis-trans isomerase
	-7,1	4,39	7,6	14	1	4		18,3	aminoacid biosyn	sp|P21569|CYPH_MAIZE	Peptidyl-prolyl cis-trans isomerase
	-62,2	5,43	0,8	1	1	2		0	ATP synthase	Zoma_B_i02363_1	ATP synthase CF1 alpha chain [Phoenix dactylifera]
	-96,3	5,67	23	41	10	27		55,1	ATP synthase	sp|A6MMJ2|ATPA_DIOEL	ATP synthase subunit alpha, chloroplastic
	-96	5,71	3	3	1	3		0	ATP synthase	tr|H2F4D9|H2F4D9_EUCGA	ATP synthase subunit alpha, chloroplastic
	-190	5,88	61	76	16	44		45,4	ATP synthase	tr|H6THA9|H6THA9_9LILI	ATP synthase subunit beta
	-181	5,89	5,5	5	2	4		0	ATP synthase	tr|G8A3N5|G8A3N5_9LILI	ATP synthase subunit beta
	-155	5,84	5,4	5	1	3		0	ATP synthase	tr|Q8WJH1|Q8WJH1_9LILI	ATP synthase subunit beta
	-151	5,81	3,3	3	1	1		0	ATP synthase	tr|Q95FJ9|Q95FJ9_SPAAM	ATP synthase subunit beta

-108	5,7	5	5	1	1		0	ATP synthase	tr|Q8WJG3|Q8WJG3_TACCH	ATP synthase subunit beta
-15,5	4,47	5,6	7	2	5		53,6	ATP synthase	sp|Q3V527|ATPB_ACOCL	ATP synthase subunit beta, chloroplastic
-13	4,99	6,3	7	2	6		49,1	ATP synthase	tr|Q7XN85|Q7XN85_ORYSJ	OSJNBa0011F23.7 protein
-11,1	4,33	7	9	2	2		61,9	ATP Synthase	sp|P49087|VATA_MAIZE	V-type proton ATPase catalytic subunit A
-12,7	4,41	5,5	8	2	4		54	ATP Synthase	sp|Q40078|VATB1_HORVU	V-type proton ATPase subunit B 1
-42,5	5,23	20	26	5	16		33,7	Calvin cycle	EG_Contig1_1...	chloroplast ribulose-1,5-bisphosphate carboxylase/oxygenase small subunit [Musa acuminata AAA Group]
-35,1	4,94	5,3	5	2	4		0	Calvin cycle	tr|Q7X9A7|Q7X9A7_ORYSJ	Putative rubisco subunit binding-protein alpha subunit (60 kDa chaperonin alpha subunit)
-131	5,71	38	71	14	37		44	Calvin cycle	gi|2734972|gb|AAB93814.1|	rbcL , ribulose-1,5-bisphosphate carboxylase/oxygenase large subunit, partial (chloroplast) [Posidonia oceanica].
-68,2	5,07	24	45	8	17		44	Calvin cycle	gi|2734972|gb|AAB93814.1|	rbcL , ribulose-1,5-bisphosphate carboxylase/oxygenase large subunit, partial (chloroplast) [Posidonia oceanica].
-45,3	4,94	22	41	6	10		44	Calvin cycle	gi|2734972|gb|AAB93814.1|	rbcL , ribulose-1,5-bisphosphate carboxylase/oxygenase large subunit, partial (chloroplast) [Posidonia oceanica].
-14,2	4,24	14	26	2	4		44	Calvin cycle	gi|2734972|gb|AAB93814.1|	rbcL , ribulose-1,5-bisphosphate carboxylase/oxygenase large subunit, partial (chloroplast) [Posidonia oceanica].
-71,6	5,07	9,4	9	1	2		0	Calvin cycle	gi|2734972|gb|AAB93814.1|	rbcL , ribulose-1,5-bisphosphate carboxylase/oxygenase large subunit, partial (chloroplast) [Posidonia oceanica].
-51,6	5,44	2,6	3	1	1		0	Calvin cycle	tr|Q95CD8|Q95CD8_9LILI	Ribulose 1,5-bisphosphate carboxylase large subunit
-25,8	4,64	4,6	5	1	1		0	Calvin cycle	sp|P34767|RBL_ALIPL	Ribulose bisphosphate carboxylase large chain
-8,9	4,54	7,8	17	1	1		52,6	Calvin cycle	tr|H2F5B1|H2F5B1_9ASPA	Ribulose bisphosphate carboxylase large chain
-92,7	5,6	1,7	2	1	1		0	Calvin cycle	tr|Q9MU73|Q9MU73_9LILI	Ribulose bisphosphate carboxylase large chain
-57,8	5,46	3,8	4	1	1		0	Calvin cycle	tr|D6MYJ6|D6MYJ6_9ARAE	Ribulose bisphosphate carboxylase large chain
-56,1	5,57	9	9	1	1		0	Calvin cycle	tr|E0D9P3|E0D9P3_9LILI	Ribulose bisphosphate carboxylase large chain
-55,8	5,42	4,6	5	1	1		0	Calvin cycle	sp|P34767|RBL_ALIPL	Ribulose bisphosphate carboxylase large chain
-43,9	5,41	1,5	1	1	1		0	Calvin cycle	tr|Q9BA33|Q9BA33_BALSE	Ribulose bisphosphate carboxylase large subunit
-27,8	5,05	2,3	2	1	3		0	Calvin cycle	tr|Q8WH35|Q8WH35_9ASPA	Ribulose-1,5-biphosphate-carboxylase

-10,9	4,5	4,1	9	1	3		49	Calvin cycle	tr|C6G4U0|C6G4U0_9ASPA	Ribulose-1,5-bisphosphate carboxylase/oxygenase large subunit
-6,8	4,22	4,1	9	1	1		49	Calvin cycle	tr|C6G4U0|C6G4U0_9ASPA	Ribulose-1,5-bisphosphate carboxylase/oxygenase large subunit
-16	4,71	4,1	9	1	1		49	Calvin cycle	tr|C6G4U0|C6G4U0_9ASPA	Ribulose-1,5-bisphosphate carboxylase/oxygenase large subunit
-74	5,25	17	37	9	18		51,3	Calvin cycle	tr|B5WX64|B5WX64_9ARAE	Ribulose-biphosphate carboxylase
-67,8	5,26	4,5	5	2	5		0	Calvin cycle	tr|B5WX64|B5WX64_9ARAE	Ribulose-biphosphate carboxylase
-73,8	5,18	3,9	4	2	4		0	Calvin cycle	tr|B5WX89|B5WX89_9ARAE	Ribulose-biphosphate carboxylase
-101	5,83	3	3	2	4		0	Calvin cycle	tr|B5WX62|B5WX62_9ARAE	Ribulose-biphosphate carboxylase
-68,2	5,18	2,6	6	1	3		51,4	Calvin cycle	tr|B5WX89|B5WX89_9ARAE	Ribulose-biphosphate carboxylase
-111	5,73	2,6	3	1	3		0	Calvin cycle	tr|B5WX89|B5WX89_9ARAE	Ribulose-biphosphate carboxylase
-58,3	5,59	3	3	1	3		0	Calvin cycle	tr|Q9MRC5|Q9MRC5_9POAL	Ribulose-bisphosphate carboxylase large subunit
-48,5	4,88	9,4	14	5	11		72,6	Calvin cycle	Zoma_B_i13574_3	RuBisCO large subunit-binding protein subunit alpha, chloroplastic
-35,3	4,96	3,2	4	1	3		77,6	Calvin cycle	Zoma_B_i13386_5	RuBisCO large subunit-binding protein subunit beta, chloroplastic
-12,4	4,59	1,3	1	1	3		0	Calvin cycle	Zoma_B_i14449_4	Transketolase, chloroplastic
-29,6	4,62	18	26	4	10		40,3	chlorophyll	EG_Contig27_6	chlorophyll A/B binding protein, putative [Ricinus communis] >gb|EEF42554.1| chlorophyll A/B binding protein, putative [Ricinus communis]
-14,3	4,42	16	26	3	5		38,7	chlorophyll	EG_Contig99_6	chlorophyll A-B binding protein (CAB), putative [Musa acuminata]
-16,8	4,39	16	26	3	4		38,7	chlorophyll	EG_Contig99_6	chlorophyll A-B binding protein (CAB), putative [Musa acuminata]
-16,2	4,25	16	26	3	4		38,7	chlorophyll	EG_Contig99_6	chlorophyll A-B binding protein (CAB), putative [Musa acuminata]
-8,7	3,98	14	22	2	3		38,7	chlorophyll	EG_Contig99_6	chlorophyll A-B binding protein (CAB), putative [Musa acuminata]
-49	4,95	35	53	5	12		37,6	chlorophyll	EG_Contig15_1	chlorophyll A-B binding protein (CAB), putative [Musa balbisiana]
-29	4,67	32	49	4	7		37,6	chlorophyll	EG_Contig15_1	chlorophyll A-B binding protein (CAB), putative [Musa balbisiana]
-24,4	4,74	22	34	3	6		37,6	chlorophyll	EG_Contig15_1	chlorophyll A-B binding protein (CAB), putative [Musa balbisiana]
-16,4	4,81	18	27	2	5		37,6	chlorophyll	EG_Contig15_1	chlorophyll A-B binding protein (CAB), putative [Musa balbisiana]
-20	4,34	22	34	3	5		37,6	chlorophyll	EG_Contig15_1	chlorophyll A-B binding protein (CAB), putative [Musa balbisiana]
-12,9	4,42	14	22	2	5		37,6	chlorophyll	EG_Contig15_1	chlorophyll A-B binding protein (CAB), putative

										[Musa balbisiana]
-22,6	4,99	26	41	3	6		21,4	Glycoliis	Pooc_PC016D03_2	Fructose-bisphosphate aldolase cytoplasmic isozyme
-29,8	5,19	16	18	3	5		18,6	Glycolisi	tr|A4ZGB6|A4ZGB6_AGATE	Chloroplast glyceraldehyde-3-phosphate dehydrogenase B subunit
-20,5	5,13	5,2	5	1	3		0	Glycolisi	EG_Contig109_4	chloroplast glyceraldehyde-3-phosphate dehydrogenase, partial [Chlorokybus atmophyticus]
-16,9	4,61	5,6	6	2	3		0	Glycolisis	tr|B3TLY1|B3TLY1_ELAGV	Fructose-bisphosphate aldolase
-14,7	4,92	7	8	2	3		47,9	Glycolisis	sp|Q42971|ENO_ORYSJ	Enolase
-11,6	4,53	20	23	2	4		23,5	Glycolisis	Pooc_PC035C04_2	Fructose-bisphosphate aldolase
-24,7	4,89	4,2	5	1	1		42,3	Glycolisis	tr|Q1EPF8|Q1EPF8_MUSAC	Phosphoglycerate kinase
-10,6	4,75	3,5	4	1	1		0	Glycolisis	tr|Q1ENY9|Q1ENY9_MUSAC	Phosphoglycerate kinase
-33,8	5,24	11	13	4	10		61,2	Glycolisis	Zoma_B_i13503_1	Phosphoglycerate kinase, chloroplastic
-8,7	4,17	4,6	6	1	2		57,4	Glycolisis	tr|Q2QXR8|Q2QXR8_ORYSJ	Pyruvate kinase
-44,2	5,58	27	35	5	19		20,8	Glycolysis	tr|C4B8E5|C4B8E5_TULGE	Glyceraldehyde-3-phosphate dehydrogenase
-22	5,05	11	11	2	6		0	Glycolysis	Pooc_PC053G11_2	Glyceraldehyde-3-phosphate dehydrogenase
-38,2	5,3	2,4	2	1	3		0	Glycolysis	tr|Q7FAH2|Q7FAH2_ORYSJ	Glyceraldehyde-3-phosphate dehydrogenase
-37	5,5	7,8	8	3	6		0	Glycolysis	Pooc_Contig14_2	Glyceraldehyde-3-phosphate dehydrogenase, cytosolic
-17,3	5,13	6	9	2	6		49	Glycolysis	Pooc_Contig14_1	Glyceraldehyde-3-phosphate dehydrogenase, cytosolic
-21,3	5,45	1,7	2	1	3		0	Glycolysis	Zoma_Contig14_1	Glyceraldehyde-3-phosphate dehydrogenase, cytosolic
-7	4,1	5,1	7	2	2		48,9	Glycolysis	Pooc_Contig14_2	Glyceraldehyde-3-phosphate dehydrogenase, cytosolic
-54,8	5,44	23	35	6	17		33,6	Glycolysis	tr|H9B8E3|H9B8E3_MISSI	Glyceraldehyde-3-phosphate dehydrogenase-like protein
-7,9	4,23	2,6	3	1	5		93,9	Growth factor	tr|Q7XTK1|Q7XTK1_ORYSJ	Elongation factor
-10,8	4,91	7,4	10	2	6		49,4	Growth factor	tr|Q4TUC4|Q4TUC4_MUSAC	Elongation factor 1-alpha
-8,7	4,37	7,4	10	2	3		49,4	Growth factor	tr|Q4TUC4|Q4TUC4_MUSAC	Elongation factor 1-alpha
-7,6	4,72	7,6	20	1	3		33,5	Growth factor	Pooc_Contig188_1	Elongation factor 1-alpha
-10,5	4,4	5,7	8	1	3		31	Growth factor	EG_Contig45_6	uncharacterized protein LOC100808269
-10	4,93	20	58	2	7		16,1	Histone	sp|P02277|H2A3_WHEAT	Histone H2A.2.2
-22,4	5,19	22	38	3	14		16,6	Histone	tr|Q43724|Q43724_ASPOF	Histone H2B
-12,9	4,21	21	26	2	2		20,8	Histone	Zoma_Contig291_1	Histone H3
-8,9	4,29	23	23	1	2		0	Histone	tr|F2CZQ5|F2CZQ5_HORVD	Histone H3

-7,9	4,47	8,8	16	2	5		24,7	Histone	Pooc_PC006G03_2	Histone H4
-21,4	4,84	3,7	6	2	6		74	HSP	tr|Q2QV45|Q2QV45_ORYSJ	70 kDa heat shock protein
-54,5	5,1	10	13	6	13		70,5	HSP	sp|P11143|HSP70_MAIZE	Heat shock 70 kDa protein
-7,8	4,13	0,7	1	1	3		258	Lipid metab	sp|B9FK36|ACC2_ORYSJ	Acetyl-CoA carboxylase 2
-6,2	4,36	2,5	3	1	3		66	Lipid metab	sp|Q93VT8|ACLB1_ORYSJ	ATP-citrate synthase beta chain protein 1
-44,7	5,26	7,4	12	4	12		88,2	Mitochondrial	Zoma_C_c61233_6	ATP synthase subunit alpha, mitochondrial
-64,9	5,35	13	17	6	18		72,4	Mitochondrial	Zoma_B_i13224_2	ATP synthase subunit beta, mitochondrial
-55,3	5,3	11	14	5	13		72,4	Mitochondrial	Zoma_B_i13224_2	ATP synthase subunit beta, mitochondrial
-62,1	5,33	4,2	4	1	3		0	Mitochondrial	sp|P19023|ATPBM_MAIZE	ATP synthase subunit beta, mitochondrial
-23,2	4,91	9	9	1	3		0	Mitochondrial	Zoma_B_i12543_2	ATP synthase subunit beta, mitochondrial
-50,9	5,34	4,2	4	1	3		0	Mitochondrial	sp|P19023|ATPBM_MAIZE	ATP synthase subunit beta, mitochondrial
-22,1	4,98	9	9	1	1		0	Mitochondrial	Zoma_B_i12543_2	ATP synthase subunit beta, mitochondrial
-13,8	4,96	6,1	9	2	5		52,2	peroxidase	Zoma_B_i12464_1	GDP-mannose 3,5-epimerase 1
-14,1	4,32	25	39	2	4		17,4	peroxidase	Pooc_B_c362_3	polyphenol oxidase [Prunus salicina var. cordata]
-11,4	3,91	5,7	10	1	4		37	peroxidase	Pooc_Contig281_1	Probable glutathione S-transferase GSTU6
-10,7	3,9	5,7	10	1	3		37	peroxidase	Pooc_Contig281_1	Probable glutathione S-transferase GSTU6
-10,8	3,77	5,7	10	1	2		37	peroxidase	Pooc_Contig281_1	Probable glutathione S-transferase GSTU6
-45	4,83	18	20	6	18		45,3	PSI	EG_Contig46_1	Full=Oxygen-evolving enhancer protein 1, chloroplastic
-17,1	5,11	1,5	3	2	8		83,1	PSI	sp|A1EA08|PSAA_AGRST	Photosystem I P700 chlorophyll a apoprotein A1
-18,5	4,47	1,7	3	3	4		241	PSI	Zoma_C_c64621_5	Photosystem I P700 chlorophyll a apoprotein A1
-14,5	4,48	3,8	12	2	6		82,2	PSI	sp|Q3V535|PSAB_ACOCL	Photosystem I P700 chlorophyll a apoprotein A2
-29	4,71	27	52	4	11		29,4	PSI	Pooc_Contig240_3	Photosystem I reaction center subunit IV B, chloroplastic
-69,5	5,17	35	49	7	19		36,3	PSI	EG_Contig19_1	Oxygen-evolving enhancer protein 2, chloroplastic; photosystem II oxygen evolving complex protein 2 precursor
-9,2	4,19	6	10	1	3		30	PSII	Pooc_Contig333_3	Photosystem II 22 kDa protein, chloroplastic
-46,9	5,3	6,3	14	5	15		158	PSII	Zoma_B_i08822_2	Photosystem II CP43 chlorophyll apoprotein
-29,6	5,27	3,3	7	4	12		158	PSII	Zoma_B_i08822_2	Photosystem II CP43 chlorophyll apoprotein
-30,9	5,1	5,3	12	4	11		158	PSII	Zoma_B_i08822_2	Photosystem II CP43 chlorophyll apoprotein
-35,6	5,29	16	38	4	13		51,8	PSII	tr|H2CPN3|H2CPN3_COLES	Photosystem II CP43 chlorophyll apoprotein;
-46,1	5,35	2,7	7	1	4		51,8	PSII	tr|H2CPN3|H2CPN3_COLES	Photosystem II CP43 chlorophyll apoprotein;

-29,6	5,14	2,7	7	1	3		51,8	PSII	tr|H2CPN3|H2CPN3_COLES	Photosystem II CP43 chlorophyll apoprotein;
-28,4	5,37	2,7	7	1	3		51,8	PSII	tr|H2CPN3|H2CPN3_COLES	Photosystem II CP43 chlorophyll apoprotein;
-44,7	5,1	12	33	5	12		56,1	PSII	tr|H6T014|H6T014_LILSU	Photosystem II CP47 chlorophyll apoprotein
-39,1	5,15	3,2	3	1	1		0	PSII	tr|Q67I20|Q67I20_9ASPA	Photosystem II CP47 chlorophyll apoprotein
-108	5,31	3,7	4	2	4		0	PSII	tr|H2CPH7|H2CPH7_COLES	Photosystem II CP47 chlorophyll apoprotein;
-43,3	4,9	1,8	2	1	3		0	PSII	tr|H2CPH7|H2CPH7_COLES	Photosystem II CP47 chlorophyll apoprotein;
-61,4	5,17	1,8	2	1	2		0	PSII	tr|H2CPH7|H2CPH7_COLES	Photosystem II CP47 chlorophyll apoprotein;
-107	5,41	4	4	1	5		0	PSII	tr|A0ARD7|A0ARD7_SMIRO	Photosystem II CP47 chlorophyll apoprotein; Flags: Fragment;
-45,7	5,3	4	4	1	4		0	PSII	tr|A0ARD7|A0ARD7_SMIRO	Photosystem II CP47 chlorophyll apoprotein; Flags: Fragment;
-62	5,17	4	4	1	1		0	PSII	tr|A0ARD8|A0ARD8_9LILI	Photosystem II CP47 chlorophyll apoprotein; Flags: Fragment;
-113	5,35	20	55	8	20		54,9	PSII	tr|H6TGJ9|H6TGJ9_9LILI	Photosystem II CP47 protein
-68,8	5,25	14	40	6	16		54,9	PSII	tr|H6TGJ9|H6TGJ9_9LILI	Photosystem II CP47 protein
-49,1	5,22	11	31	5	12		54,9	PSII	tr|H6TGJ9|H6TGJ9_9LILI	Photosystem II CP47 protein
-43,2	4,93	3,2	9	1	2		54,9	PSII	tr|H6TGJ9|H6TGJ9_9LILI	Photosystem II CP47 protein
-42,8	5,12	1,8	2	1	1		0	PSII	tr|H6TGL1|H6TGL1_9LILI	Photosystem II CP47 protein
-7,4	4,35	3,4	7	1	3		39,6	PSII	sp|Q4FFP4|PSBD_ACOAM	Photosystem II D2 protein; PSII D2 protein; EC 1.10.3.9; Photosystem Q(A) protein;
-26,8	4,81	5,9	6	1	2		0	PSII	sp|Q4FFP4|PSBD_ACOAM	Photosystem II D2 protein; PSII D2 protein; EC 1.10.3.9; Photosystem Q(A) protein;
-5	3,59	3,4	7	1	2		39,6	PSII	sp|Q4FFP4|PSBD_ACOAM	Photosystem II D2 protein; PSII D2 protein; EC 1.10.3.9; Photosystem Q(A) protein;
-8,1	4,65	6,2	23	2	5		38,9	PSII	sp|Q3V554|PSBA_ACOCL	Photosystem Q(B) protein; EC 1.10.3.9; 32 kDa thylakoid membrane protein; Photosystem II protein D1; Flags: Precursor;
-45,2	4,94	21	23	5	8		39,1	structural	tr|H9B635|H9B635_SEDJA	Actin
-40,1	4,88	3,2	3	1	1		0	structural	sp|A2XLF2|ACT1_ORYSI	Actin-1
-46,4	5,09	12	15	5	11		64	structural	tr|Q9LWT6|Q9LWT6_ORYSJ	Putative chaperonin 60 beta
-17,4	4,77	4,4	6	2	4		76,6	uncharacterized	tr|F2CYQ8|F2CYQ8_HORVD	Predicted protein
-6,7	4,02	2,8	4	1	1		76,6	uncharacterized	tr|F2CYQ8|F2CYQ8_HORVD	Predicted protein
-12,1	4,11	4,4	4	1	1		0	uncharacterized	tr|B7ZZZ2|B7ZZZ2_MAIZE	Putative uncharacterized protein
-56,1	5,21	12	16	7	16		80,3	uncharacterized	tr|I1I8C1|I1I8C1_BRADI	Uncharacterized protein
-24,9	4,6	7,5	10	3	8		93,7	uncharacterized	tr|I1HPV9|I1HPV9_BRADI	Uncharacterized protein

	-26,9	4,63	4,3	9	2	4		54,7	uncharacterized	tr|I1H3A2|I1H3A2_BRADI	Uncharacterized protein
	-9,5	3,99	4,7	5	1	2		39,7	uncharacterized	tr|I1I6Q9|I1I6Q9_BRADI	Uncharacterized protein
	-6,4	3,45	4,5	8	1	1		60,1	uncharacterized	tr|I1HBG2|I1HBG2_BRADI	Uncharacterized protein
	-7,9	4,36	8,2	11	1	3		22,3	uncharacterized	EG_Contig71_4	unknown [Lotus japonicus]
						###					
13:00 h, 30 m depth	log(e)	log(I)	% (measured)	% (corrected)	unique	total parz	**total**	Mr	metabolism	Accession	Description
	-65,1	5,23	0,8	1	1	2	**2**	0	ATP Synthase	Zoma_B_i02363_1	ATP synthase CF1 alpha chain [Phoenix dactylifera] >gb|ADD63159.1|
	-89,3	5,43	19	33	9	32	**34**	55,3	ATP Synthase	tr|H2F4C9|H2F4C9_9ASPA	ATP synthase subunit alpha, chloroplastic
	-86,2	5,42	2	2	1	2		0	ATP Synthase	sp|A6MMJ2|ATPA_DIOEL	ATP synthase subunit alpha, chloroplastic
	-10,5	4,17	4,5	7	2	3	**3**	88,2	ATP Synthase	Zoma_C_c61233_6	ATP synthase subunit alpha, mitochondrial
	-58,3	4,99	17	22	6	16	**22**	53,7	ATP Synthase	tr|Q4FGI4|Q4FGI4_TYPLA	ATP synthase subunit beta
	-92,3	5,22	5,1	5	1	5		0	ATP Synthase	tr|O24345|O24345_SORBI	ATP synthase subunit beta
	-54,3	4,94	2,6	3	1	1		0	ATP Synthase	tr|H2CPP4|H2CPP4_COLES	ATP synthase subunit beta, chloroplastic
	-93,7	5,2	19	25	9	23	**24**	72,4	ATP Synthase	Zoma_B_i13224_2	ATP synthase subunit beta, mitochondrial
	-44,2	4,87	9	9	1	1		0	ATP Synthase	Zoma_B_i12543_2	ATP synthase subunit beta, mitochondrial
	-21,2	4,71	28	42	3	7	**20**	37,6	Chlorophyll	EG_Contig15_1	chlorophyll A-B binding protein (CAB), putative [Musa balbisiana]
	-34,9	4,52	32	49	4	7		37,6	Chlorophyll	EG_Contig15_1	chlorophyll A-B binding protein (CAB), putative [Musa balbisiana]
	-21	4,48	22	34	3	6		37,6	Chlorophyll	EG_Contig15_1	chlorophyll A-B binding protein (CAB), putative [Musa balbisiana]
	-7,7	3,85	2,9	4	1	1	**1**	48,9	Glycolisis	Pooc_Contig14_2	Glyceraldehyde-3-phosphate dehydrogenase, cytosolic
	-18,8	4,57	5,4	7	3	5	**5**	80,1	HSP	sp|A2YWQ1|HSP81_ORYSI	Heat shock protein 81-1
	-10,7	4,11	3,3	5	1	4	**4**	63,9	aminoacid biosyn	tr|Q7XMP6|Q7XMP6_ORYSJ	OSJNBb0059K02.15 protein
	-14,9	4,68	1,5	3	2	5	**6**	83,1	PSI	sp|A1EA08|PSAA_AGRST	Photosystem I P700 chlorophyll a apoprotein A1
	-18,3	4,19	0,4	0	1	1		0	PSI	Zoma_C_c64621_5	Photosystem I P700 chlorophyll a apoprotein A1
	-19,9	4,32	6,5	21	3	5	**6**	82,4	PSI	sp|A6MMK6|PSAB_DIOEL	Photosystem I P700 chlorophyll a apoprotein A2
	-18,7	4,29	2,7	3	1	1		0	PSI	sp|Q6ENH5|PSAB_ORYNI	Photosystem I P700 chlorophyll a apoprotein A2
	-22,3	4,94	3,2	7	3	11	**24**	158	PSII	Zoma_B_i08822_2	Photosystem II CP43 chlorophyll apoprotein
	-22,2	4,82	3,2	7	3	10		158	PSII	Zoma_B_i08822_2	Photosystem II CP43 chlorophyll apoprotein

-26,3	5,02	1	1	1	3		0	PSII	Zoma_B_i08822_2	Photosystem II CP43 chlorophyll apoprotein
-28,7	5,11	9,3	23	3	14	**15**	51,8	PSII	tr|H2CPN3|H2CPN3_COLES	Photosystem II CP43 chlorophyll apoprotein;
-20	4,77	2,7	3	1	1		0	PSII	tr|H2CPN3|H2CPN3_COLES	Photosystem II CP43 chlorophyll apoprotein;
-12,1	4,03	3,9	11	2	3	**9**	56	PSII	sp|A9LYC6|PSBB_ACOAM	Photosystem II CP47 chlorophyll apoprotein
-73,2	5,18	4	4	1	6		0	PSII	tr|A0ARD7|A0ARD7_SMIRO	Photosystem II CP47 chlorophyll apoprotein; Flags: Fragment;
-78,1	5,11	17	48	7	20	**23**	54,9	PSII	tr|H6TGJ9|H6TGJ9_9LILI	Photosystem II CP47 protein
-27,9	4,94	9,6	30	3	12	**12**	45,4	PSII	tr|A0ARD0|A0ARD0_9LILI	Photosystem II CP47 protein
-24,5	4,55	3,2	9	1	2		54,9	PSII	tr|H6TGJ9|H6TGJ9_9LILI	Photosystem II CP47 protein
-69,1	4,98	1,8	2	1	1		0	PSII	tr|H6TGH1|H6TGH1_9LILI	Photosystem II CP47 protein
-14,4	4,38	9,3	20	2	4	**4**	39,6	PSII	sp|Q4FFP4|PSBD_ACOAM	Photosystem II D2 protein; PSII D2 protein; EC 1.10.3.9; Photosystem Q(A) protein;
-7,8	4,35	2,8	4	1	3	**3**	76,6	uncharacterized	tr|F2CYQ8|F2CYQ8_HORVD	Predicted protein
-21,1	4,15	8	10	3	3	**3**	64	structural	tr|Q9LWT6|Q9LWT6_ORYSJ	Putative chaperonin 60 beta
-64,5	5	27	51	8	17	**24**	44	Calvin cycle	gi|2734972|gb|AAB93814.1|	rbcL , ribulose-1,5-bisphosphate carboxylase/oxygenase large subunit, partial (chloroplast) [Posidonia oceanica].
-17,6	4,56	8,1	15	3	5		44	Calvin cycle	gi|2734972|gb|AAB93814.1|	rbcL , ribulose-1,5-bisphosphate carboxylase/oxygenase large subunit, partial (chloroplast) [Posidonia oceanica].
-61,5	4,97	9,4	18	1	2		44	Calvin cycle	gi|2734972|gb|AAB93814.1|	rbcL , ribulose-1,5-bisphosphate carboxylase/oxygenase large subunit, partial (chloroplast) [Posidonia oceanica].
-42,9	4,85	2,2	2	1	2	**4**	0	Calvin cycle	Zoma_C_c22377_6	Ribulose bisphosphate carboxylase large chain
-24,5	4,51	4,6	11	1	1		43,9	Calvin cycle	sp|P34767|RBL_ALIPL	Ribulose bisphosphate carboxylase large chain
-64,6	5	2,2	2	1	1		0	Calvin cycle	Zoma_C_c22377_6	Ribulose bisphosphate carboxylase large chain
-16,2	4,6	2,3	2	1	1	**2**	0	Calvin cycle	tr|Q8WH35|Q8WH35_9ASPA	Ribulose-1,5-biphosphate-carboxylase
-7,8	3,99	4,1	9	1	1		49	Calvin cycle	tr|C6G4U0|C6G4U0_9ASPA	Ribulose-1,5-bisphosphate carboxylase/oxygenase large subunit
-67,8	5,03	18	39	8	20	**26**	51,3	Calvin cycle	tr|B5WX64|B5WX64_9ARAE	Ribulose-biphosphate carboxylase
-61	5,1	4,5	5	2	3		0	Calvin cycle	tr|B5WX62|B5WX62_9ARAE	Ribulose-biphosphate carboxylase
-66,7	5,11	3,9	4	1	3		0	Calvin cycle	tr|B5WX62|B5WX62_9ARAE	Ribulose-biphosphate carboxylase
-11,9	4,48	16	20	2	6	**9**	28,9	Alkaloids	Pooc_Contig132_3	S-norcoclaurine synthase OS=Thalict…
-10,6	4,06	16	20	2	3		28,9	Alkaloids	Pooc_Contig132_3	S-norcoclaurine synthase OS=Thalict…

-11	3,86	5,3	8	2	2	**2**	54	ATP Synthase	sp|Q40078|VATB1_HORVU	V-type proton ATPase subunit B 1
					287					

Works submitted to Marine Ecology

Responses of Mediterranean *Cymodocea nodosa seagrass* to hypersaline stress at physiological and molecular levels.

Amalia Piro[1], Antonia Spadafora[1], Ilia Anna Serra[1], Ruiz J.M.[2] and Mazzuca S.[1,2]

[1] Doctorate School of Life Science, Università della Calabria, Rende, Italy; [2] Department of Chemistry and Technology, Università della Calabria, Rende, Italy; [3] Spanish Institute of Oceanography, 30740 Murcia, Spain.

Purification of intact chloroplasts from marine plant *Posidonia oceanica* suitable for organelle proteomics.

Amalia Piro [1], Ilia Anna Serra[2], Antonia Spadafora [2], Monica Cardilio[3], Linda Bianco[4], Gaetano Perrotta[4], Silvia Mazzuca [2]

[1] Doctorate School of Life Science, Università della Calabria, Rende, Italy; [2] Department of Chemistry and Technology, Università della Calabria, Rende, Italy; [3]A.S. Diving Center Paolano, Lungomare Nord, Paola, Italy; [4]Italian National Agency for New Technologies, Energy and Sustainable Economic Development (ENEA), TRISAIA Research Center, Rotondella (Matera), Italy